Hydrographic Observations at the Woods Hole Oceanographic Institution (WHOI) Hawaii Ocean Timeseries (HOT) Site (WHOTS): 2004 - 2006

Fernando Santiago-Mandujano, Paul Lethaby, Roger Lukas, Jefrey Snyder Robert Weller, Albert Plueddemann, Jeffrey Lord, Sean Whelan, Paul Bouchard, and Nan Galbraith

Data Report # 1

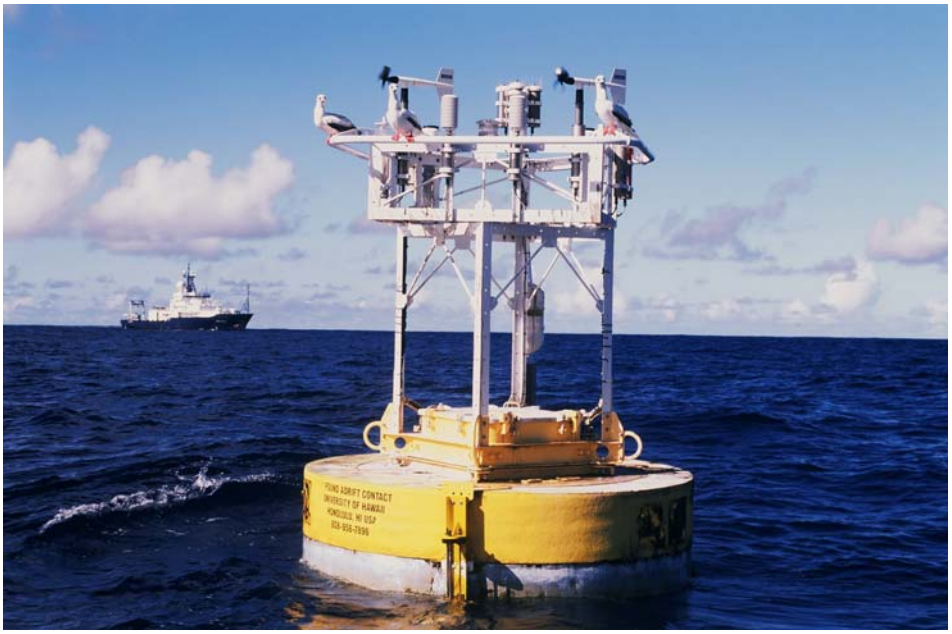

Draft 2.4

SCHOOL OF OCEAN AND EARTH SCIENCE AND TECHNOLOGY
UNIVERSITY OF HAWAI'I AT MĀNOA
SOEST Publication #

Acknowledgments

Many people participated in the WHOTS mooring deployment/recovery cruises. They are listed in Table 2.1. We gratefully acknowledge their contributions and support. Thanks are due to all the personnel of the Upper Ocean Processes Group (UOP) at WHOI who prepared the WHOTS buoy's instrumentation and mooring; to Jerome Aucan, Mark Valenciano, John Yeh, and Brandon Shima for their technical assistance with the moored and shipboard instrumentation; to Nancy Paquin for her excellent project support, and to Kellie Terada, and Matthew Markley for their shore-based support. Special thanks are due to Jules Hummon for processing the shipboard ADCP data. Thanks also to Mark Merrifield for providing the Waimea Bay wave data from the Datawell directional buoy, and to Lara Hutto for processing the NGVM data. We gratefully acknowledge the support from Nordeen Larson and colleagues at Sea-Bird for helping us maintain the quality of the CTD data. We would also like to thank the captains and crew of the R/V *Ka'imikai-O-Kanaloa*, R/V *Melville*, and R/V *Roger Revelle* and especially the University of Hawaii Marine Center staff for their efforts. The WHOTS Ocean Reference Station mooring is funded by the National Oceanic and Atmospheric Administration (NOAA) through the Cooperative Institute for Climate and Ocean Research (CICOR) under Grant No. NA17RJ1223 to the Woods Hole Oceanographic Institution. Support for preparation and processing of subsurface instrumentation at WHOI is via a subcontract from the UH NSF project.

Table of Contents

List of Figures

1. Introduction.

In 2003, Robert Weller (Woods Hole Oceanographic Institution [WHOI]), Albert Plueddemann (WHOI) and Roger Lukas (University of Hawaii [UH]) proposed to establish a long-term surface mooring at the Hawaii Ocean Time-series (HOT) Station ALOHA (22°45'N, 158°W) to provide sustained, high-quality air-sea fluxes and the associated upper ocean response as a coordinated part of the HOT program, and as an element of the array of global ocean reference stations supported by the National Oceanic and Atmospheric Administration's (NOAA) Office of Climate Observation.

With support from the NOAA and the National Science Foundation (NSF), the WHOI HOT Site (WHOTS) surface mooring has been maintained at Station ALOHA since August 2004. The objective of this project is to provide long-term, high-quality air-sea fluxes as a coordinated part of the HOT program and contribute to the goals of observing heat, fresh water and chemical fluxes at a site representative of the oligotrophic North Pacific Ocean. The approach is to maintain a surface mooring outfitted for meteorological and oceanographic measurements at a site near Station ALOHA by successive mooring turnarounds. These observations will be used to investigate air sea interaction processes related to climate variability.

The mooring system is described in the mooring deployment/recovery cruise reports (Plueddemann et al., 2006; Whelan et al., 2007). Briefly, a Surlyn foam surface buoy is equipped with meteorological instrumentation including two complete Air-Sea Interaction Meteorological (ASIMET) systems, measuring air and sea surface temperatures, relative humidity, barometric pressure, wind speed and direction, incoming shortwave and longwave radiation, and precipitation. Complete surface meteorological measurements are recorded every minute, as required to compute air-sea fluxes of heat, freshwater and momentum. Each ASIMET system also transmits hourly averages of the surface meteorological variables via the Argos satellite system. The mooring line is instrumented in order to collect time series of upper ocean temperatures, velocities, and salinities coincident with the surface forcing record. This includes vector measuring current meters, conductivity, salinity and temperature recorders, and an Acoustic Doppler current profiler (ADCP). See the mooring diagram in Figure 1-1.

The subsurface instrumentation is located to resolve the temporal variations of shear and stratification in the upper pycnocline to support study of mixed layer entrainment. Experience with moored profiler measurements near Hawaii suggests that Richardson number estimates over 10 m scales are adequate. Salinity is clearly important to the stratification, as salt-stratified barrier layers are observed at HOT (Lukas, 2003) and in the region (Kara et al., 2000), so we use Sea-Bird SeaCATs and MicroCATs with vertical separation ranging from 5-20 m to measure temperature and salinity. We use an RDI ADCP to obtain current profiles across the entrainment zone and into the mixed layer. As our emphasis is on the entrainment of upper pycnocline waters, the ADCP is in an upward-looking configuration at 126 m, using 4 m bins. To provide near-surface velocity (where the ADCP estimates would not be reliable) we deploy two Next Generation Vector Measuring Current Meters (NGVM). The nominal mooring design is a balance between resolving extremes versus typical annual cycling of the mixed layer (see Figure 1-3).

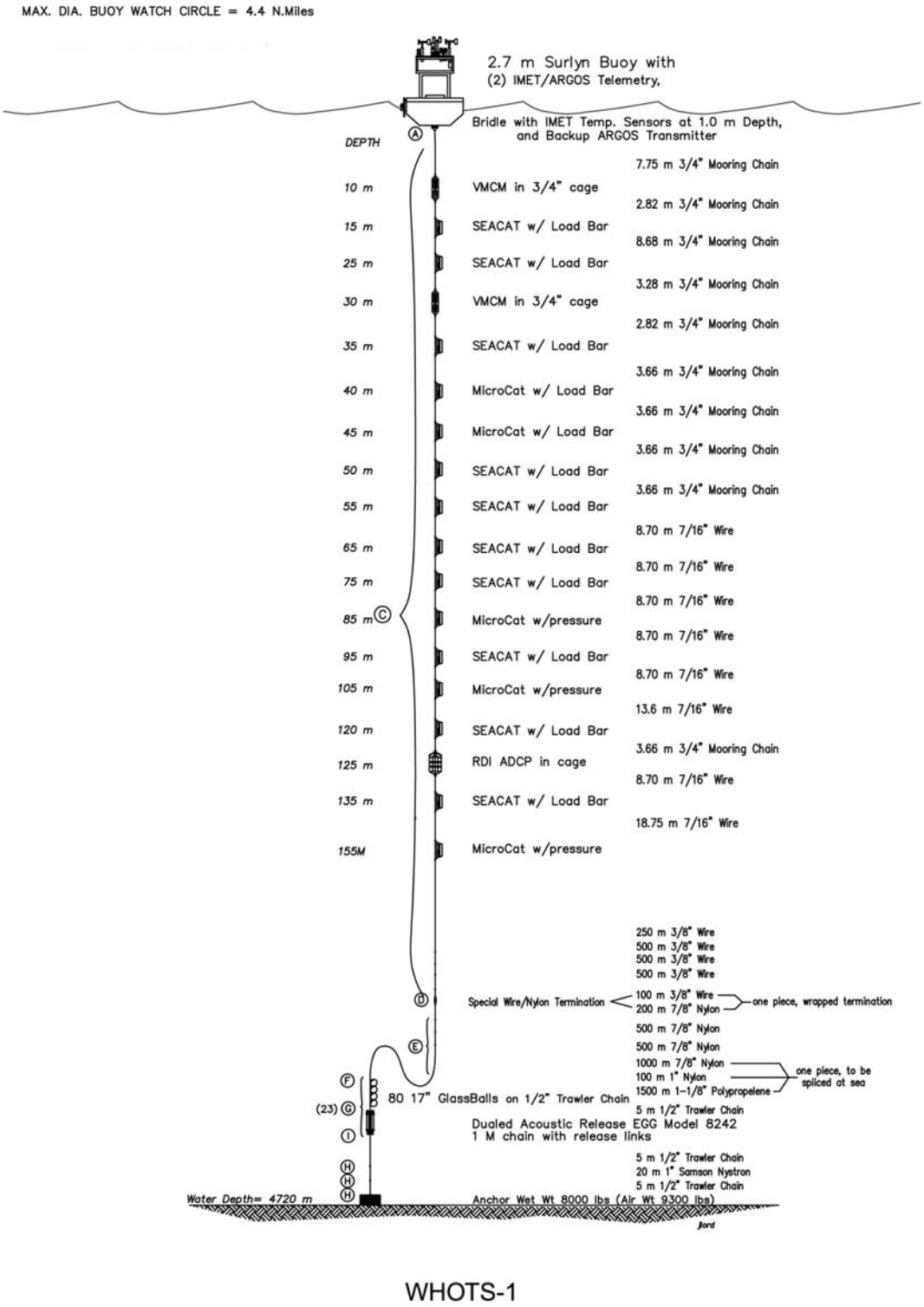

Figure 1-1 WHOTS-1 mooring design.

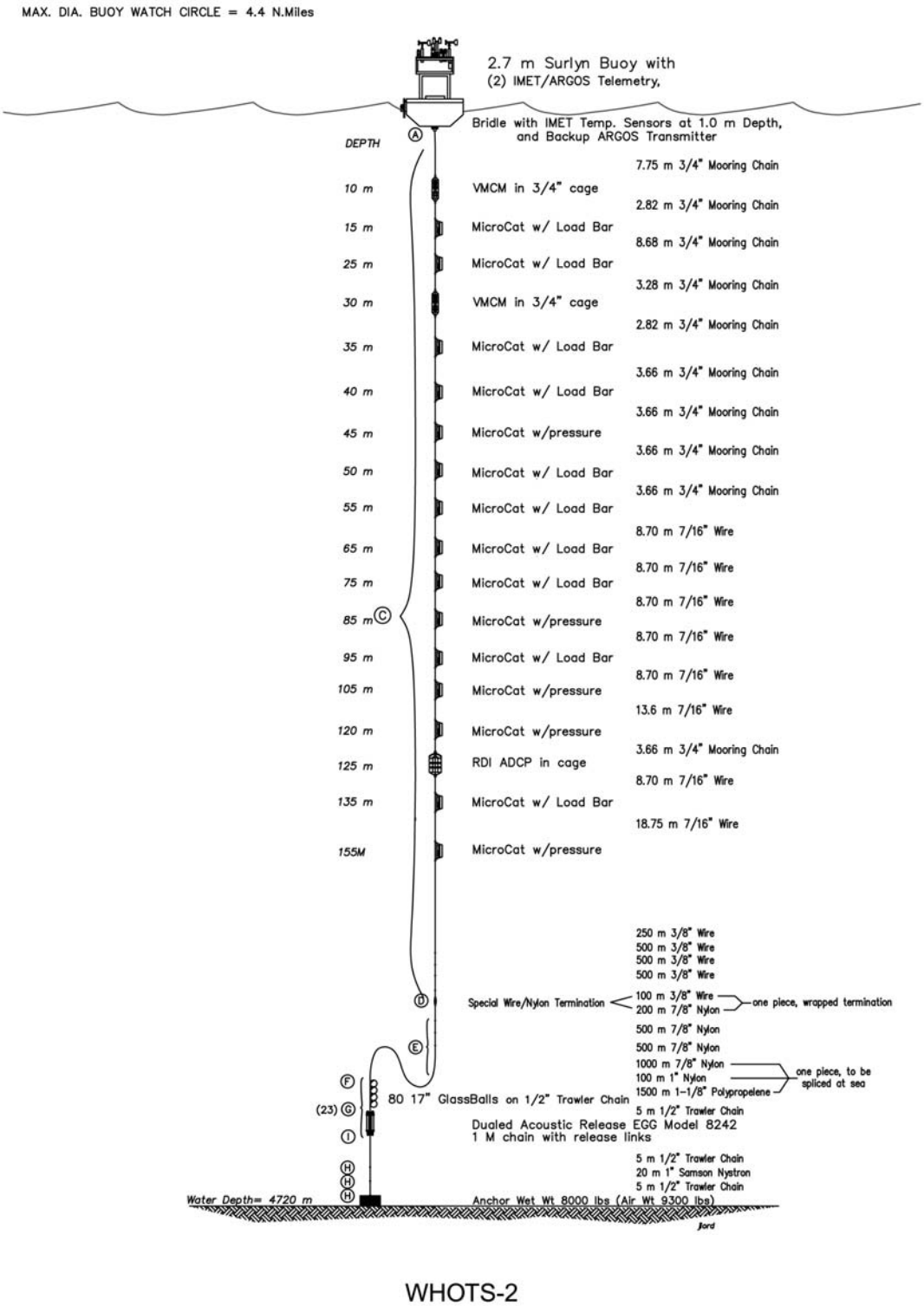

Figure 1-2. WHOTS-2 mooring design.

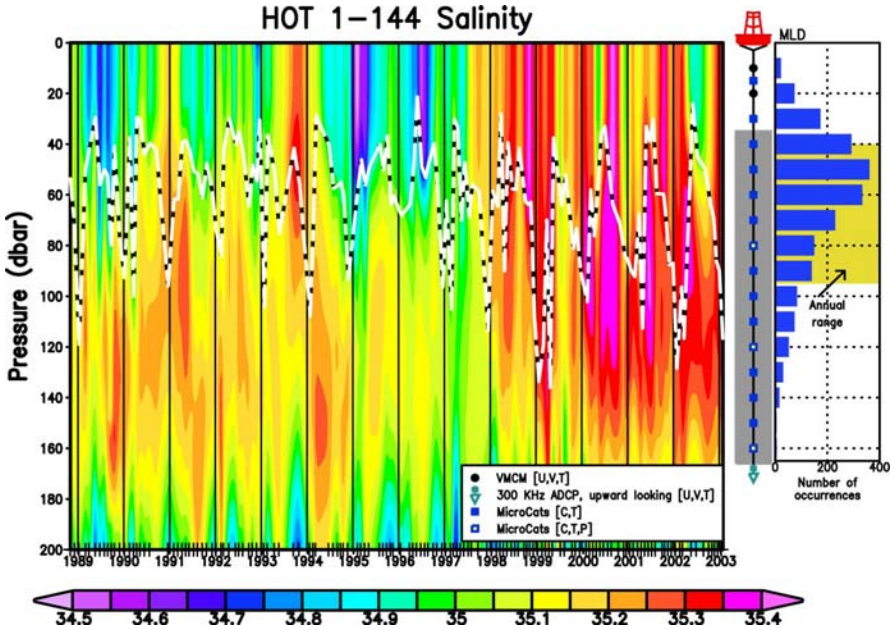

Figure 1-3. Salinity observed in the upper 200 m at ALOHA. Dashed line is the cruise-averaged mixed layer depth (MLD) determined (by vertical density change) from multiple CTD casts. Histogram along right side shows the MLD distribution for all HOT CTD casts, with t the average annual range indicated, corresponding to the pressure scale on the left. The proposed distribution of instrumentation (see legend) on the surface mooring is indicated; the gray area is the coverage of the ADCP current profile measurements. Timing of HOT cruises is indicated by tick marks along the time axis.

The first WHOTS mooring (WHOTS-1 mooring) was deployed in August 2004 aboard the UH R/V *Ka'imikai-O-Kanaloa*, and it was recovered in July 2005 during an 8-day cruise (WHOTS-2 cruise) aboard the Scripps Institution of Oceanography (SIO) R/V *Melville*. The second mooring (WHOTS-2 mooring) was deployed during the WHOTS-2 cruise, and it was recovered in June 2006 during a 7-day cruise (WHOTS-3 cruise) aboard the SIO R/V *Roger Revelle*. A third mooring was deployed during the WHOTS-3 cruise, to be recovered in June 2007.

This report documents and describes the oceanographic observations made on the first two WHOTS moorings during a period of nearly one year each, and from shipboard during the two cruises when the moorings were deployed and recovered. Sections 2 and 3, respectively, include a detailed description of the cruises and the moorings. Sampling and processing procedures of the hydrographic casts, thermosalinograph, and shipboard ADCP data collected during cruises are in Section 4. Section 5 includes the processing procedures for the data collected by the moored instruments: SeaCATs, MicroCATs, NGVMs, and moored ADCP. Plots of the resulting data and a preliminary analysis are included in Section 6.

2. Description of WHOTS deployment cruises

A. WHOTS-1 Cruise

The Woods Hole Oceanographic Institution Upper Ocean Processes Group (WHOI/UOP), with the assistance of the UH group conducted the first deployment of the WHOTS mooring on board the R/V *Ka'imikai-O-Kanaloa* during the WHOTS-1 cruise between 10 and 13 August 2004. No hydrographic observations were made during this cruise. The scientific personnel that participated during the cruise are listed in Table 2.1

Table 2.1 Scientific personnel on R/V Ka'imikai-O-Kanaloa *during the WHOTS-1 cruise, on the R/V* Melville *during the WHOTS-2 cruise, and on the R/V* Roger Revelle *during the WHOTS-3 cruise.*

Cruise	**Name**	**Title or function**	**Affiliation**
WHOTS-1	Bouchard, Paul	Senior Engineering Assistant	WHOI
	Dunn, Jim	Engineering Assistant	WHOI
	Foreman, Gabe	Marine Technician	UH/STAG[1]
	Gravatt, Dave	Marine Technician	UH/STAG
	Lord, Jeff	Senior Engineering Assistant	WHOI
	Lukas, Roger	Professor/PI	UH
	Snyder, Jefrey	Marine Electronic's Technician	UH
	Weller, Robert	Chief Scientist	WHOI
WHOTS-2	Aucan, Jerome	Graduate Student	UH
	Bouchard, Paul	Senior Engineering Assistant	WHOI
	Lethaby, Paul	Research Associate	UH
	Lord, Jeff	Senior Engineering Assistant	WHOI
	Lukas, Roger	Professor/PI	UH
	McAndrew, Patricia	Graduate Student	UH/BEACH[2]
	Plueddemann, Albert	Chief Scientist/PI	WHOI
	Sadler, Daniel	Research Associate	UH/BEACH
	S-Mandujano, Fernando	Research Associate	UH
	Valenciano, Mark	Marine Electronic's Technician	UH
	Walsh, Alex		E-Paint Co.
	Ward, Jillian	Graduate Student	UH
	Weller, Robert	Senior Scientist/PI	WHOI
WHOTS-3	Aucan, Jerome	Graduate Student	UH
	Bradley, Edward	Senior Scientist	CSIRO
	Burman, Scott	Volunteer	
	Griffiths, Diana	Teacher-at-Sea	NOAA
	Lethaby, Paul	Research Associate	UH
	Lord, Jeff	Senior Engineering Assistant	WHOI

[1] Shipboard Technical Assistance Group
[2] Biogeochemical Ecological Assessment of Complex Habitats group

Cruise	Name	Title or function	Affiliation
	Lukas, Roger	Professor/PI	UH
	Shima, Brandon	Undergraduate Student	UH
	Smith, Theresa		NOAA
	Snyder, Jefrey	Marine Electronic's Technician	UH
	Weller, Robert	Chief Scientist/PI	WHOI
	Whelan, Sean	Engineer Assistant	WHOI
	Yeh, John	Graduate Student	UH

B. WHOTS-2 Cruise

The WHOI/UOP Group conducted the mooring turnaround operations during the WHOTS-2 cruise between 23 and 30 July 2005. The shipboard oceanographic observations during the cruise were conducted by the UH group. A complete description of these operations is available in the WHOTS-2 cruise report (Plueddemann *et al*., 2006).

The R/V *Melville* was used to recover the WHOTS-1 mooring on 25 July, and the WHOTS-2 mooring was deployed on 28 July at approximately 22° 46' N, 157° 54' W in 4695 m of water. A Sea-Bird CTD (conductivity, temperature and depth) system was used to measure T, S, and O_2 profiles to survey an eddy located near the site (stations 1 through 13), and a series of six CTD stations were occupied during the return trip to Honolulu (stations 14 through 19, Figure 6-1). The time, location, and maximum CTD pressure for each of the profiles are listed in Table 2.2.

CTD casts were made at stations 1 and 2 near the WHOTS-1 mooring for comparison with subsurface instruments before recovery, and at stations 12 and 13 near the WHOTS-2 mooring after deployment. The cast at station 8 was made after the WHOTS-1 recovery, with four MicroCATs (SN 2451, 2965, 3381, and 3382) attached to the rosette package, to provide a cross-calibration between the CTD and the recovered MicroCATs before redeployment. This cast included four approximately ten-minute long stops at selected depths to provide stable conditions for the calibration

Between two and five salinity samples were taken from each cast to calibrate the conductivity sensors used for the CTD profiling. Dissolved oxygen samples (4 and 8 per cast) were also taken from eleven casts for calibration of the CTD oxygen sensors. .

Table 2.2 CTD stations occupied during the WHOTS-2 Deployment cruise

Station	Date	Time (GMT)	Location	Maximum pressure (dbar)
1	7/24/05	22:25	22° 47.10' N, 157° 55.64' W	202
2	7/25/05	03:55	22° 47.46' N, 157° 54.44' W	1020
4	7/26/05	07:20	22° 22.49' N, 157° 30.00' W	1020
5	7/26/05	10:55	22° 27.29' N, 157° 39.28' W	1020
6	7/26/05	14:23	22° 33.04' N, 157° 48.55' W	1020
7	7/26/05	17:56	22° 35.66' N, 157° 53.09' W	1020
8	7/26/05	21:46	22° 38.40' N, 157° 57.89' W	1020

9	7/27/05	00:54	22° 41.64' N, 158° 03.60' W	1020
10	7/27/05	04:25	22° 45.01' N, 158° 09.55' W	1020
11	7/27/05	07:48	22° 50.20' N, 158° 18.69' W	1020
12	7/28/05	21:57	22° 47.09' N, 157° 55.61' W	1020
13	7/29/05	03:53	22° 46.01' N, 157° 54.62' W	200
14	7/29/05	15:23	22° 40.00' N, 158° 00.00' W	1020
15	7/29/05	18:09	22° 29.99' N, 158° 00.05' W	1020
16	7/29/05	22:32	22° 29.99' N, 157° 30.12' W	1020
17	7/30/05	02:35	22° 20.01' N, 158° 00.15' W	1024
18	7/30/05	05:55	22° 10.00' N, 158° 00.03' W	1030
19	7/30/05	08:28	22° 00.02' N, 158° 00.02' W	1020

In addition, continuous acoustic Doppler current profiler (ADCP) and near surface thermosalinograph (TSG) data were obtained while underway.

The R/V *Melville* was equipped with an RD Instruments Narrow Band 150 kHz ADCP and an RD Instruments Ocean Surveyor 75 kHz ADCP. Configurations for each system are shown in Table 2.3. The two systems used input from the gyro compass and a Trimble 4000AX GPS receiver to establish the heading and attitude of the ship while an Ashtech ADU-II 3DF system archived attitude data for use in post-processing.

Table 2.3 Configuration of the RD Instruments Narrow Band 150 kHz ADCP and the Ocean Surveyor 75kHz ADCP on board the R/V Melville during the WHOTS-2 deployment cruise.

	NB150	**OS75**
Sample interval (s)	300	300
Number of bins	70	60
Bin Length (m)	8	16
Pulse Length (m)	8	16
Transducer depth (m)	5	5
Blanking length (m)	4	8

The TSG observations were made by the ship's underway uncontaminated seawater system, drawing water from a nominal depth of 4 meters with a sampling interval of 30 seconds. The data were acquired continuously during the WHOTS-2 cruise, with salt calibration samples taken roughly twice per day from an outlet in the flowthrough system located less than 0.5 m from the TSG. In addition, the temperature and salinity records were checked against the CTD station data.

The scientific personnel that participated during the WHOTS-2 deployment cruise are listed in Table 2.1.

C. WHOTS-3 Cruise

The WHOI/UOP group conducted the mooring turnaround operations during the WHOTS-3 deployment cruise between 22 and 29 June, 2006. The shipboard oceanographic observations during the cruise were conducted by the UH group. A complete description of these operations is available in the WHOTS-3 cruise report (Whelan et al., 2007).

The R/V *Roger Revelle* was used to recover the WHOTS-2 mooring on 24 June, and the new WHOTS-3 mooring was deployed on 26 June. The ship provided CTD and water sampling equipment, including a Sea-Bird CTD sampling at 24 Hz, with pressure, dual temperature and dual conductivity sensors. Sea-Bird temperature and conductivity sensors used by UH routinely as part of the Hawaii Ocean Time-series were used to allow the data to be more easily tied into the HOT CTD dataset. The CTD was installed inside a twelve-place rosette with 12-liter Bullister-type sampling bottles.

A total of 16 CTD profiles were obtained. Two series of CTD casts were made to obtain profiles for comparison with subsurface instruments on the WHOTS-2 mooring before recovery (station 50, casts 1 through 7), and with those on the WHOTS-3 mooring after deployment (station 50, casts 8 through 14). The comparison series consisted of casts to at least 200 m every two hours for twelve hours (roughly one semidiurnal tidal cycle). In addition, three 1000 m CTD profiles were made to provide a cross-calibration between the CTD and the SBE-37 MicroCATs that were recovered from the WHOTS-2 mooring (station 2, casts 1 and 2, and station 50, cast 8). These casts included four approximately ten-minute long stops at four selected depths to provide stable conditions for the cross-calibration. Table 2.4 provides summary information for the CTD stations.

Water samples were taken from all casts for salinity analysis to calibrate the conductivity sensors used for the CTD profiling. Four samples were taken from 1000 m casts and two samples from the 200 m casts. Also, water samples were drawn from the flowthrough system located in the bow thruster room, less than 3 m from the shipboard Sea-Bird thermosalinograph system for post-calibration of that dataset.

Station numbers were assigned the standard HOT notation. Station 2 refers to profiles taken within a six-mile radius of 22°45'N, 158°W. Station 50 is used to refer to profiles taken close to the WHOTS buoy (within a km) for comparison.

Table 2.4 CTD stations occupied during the WHOTS-3 deployment cruise. Note that numbering of stations follows the HOT conventions.

Station/cast	Date	Time (GMT)	Location	Maximum pressure (dbar)
50/1	6/23/06	21:21	22° 47.875' N, 157° 55.057' W	1020
50/2	6/23/06	23:07	22° 47.875' N, 157° 55.055' W	210
50/3	6/24/06	00:59	22° 47.802' N, 157° 54.678' W	210

50/4	6/24/06	03:03	22° 47.820' N, 157° 54.630' W	210
50/5	6/24/06	05:00	22° 47.842' N, 157° 54.439' W	210
50/6	6/24/06	06:58	22° 47.824' N, 157° 54.339' W	210
50/7	6/24/06	08:57	22° 47.791' N, 157° 54.220' W	210
2/1	6/25/06	19:30	22° 50.498' N, 157° 58.994' W	1020
2/2	6/25/06	22:30	22° 50.972' N, 157° 58.939' W	1020
50/8	6/27/06	18:31	22° 47.514' N, 157° 55.617' W	1020
50/9	6/27/06	20:32	22° 47.516' N, 157° 55.664' W	210
50/10	6/27/06	22:29	22° 47.512' N, 157° 55.385' W	210
50/11	6/28/06	00:31	22° 47.544' N, 157° 55.368' W	210
50/12	6/28/06	02:30	22° 47.575' N, 157° 55.671' W	210
50/13	6/28/06	04:30	22° 47.661' N, 157° 55.388' W	210
50/14	6/28/06	06:29	22° 47.870' N, 157° 55.028' W	210

In addition to CTD profiles, continuous ADCP and near-surface TSG data were obtained while underway.

The R/V *Roger Revelle* was equipped with an RD Instruments Narrow Band 150 kHz ADCP. The setup configuration is shown in Table 2.5. Position information was provided by a gyro compass and an Ashtech ADU-II 3DF GPS receiver.

Table 2.5 Configuration of the RD Instruments Narrow Band 150 kHz ADCP used during the WHOTS-3 cruise onboard the R/V Roger Revelle.

	NB150
Sample interval (s)	300
Number of bins	70
Bin Length (m)	8
Pulse Length (m)	8
Transducer depth (m)	5
Blanking length (m)	4

The TSG observations were made by the ship's underway uncontaminated seawater system, drawing water from a nominal depth of 5.7 m with a sampling interval of 10 seconds. The data were acquired continuously during the WHOTS-3 cruise with salinity calibration samples taken 6 times per day. In addition, the temperature and salinity records were compared with the CTD station data.

The scientific personnel that participated during the WHOTS-3 deployment cruise are listed in Table 2.1.

3. Description of WHOTS Moorings

A. Deployment 1

The WHOTS-1 mooring, deployed on 13 August 2004 from the UH's R/V *Ka imikai- O-Kanoloa* (KOK), was outfitted with a full suite of ASIMET sensors on the buoy and subsurface instruments from 10 to 155 m depth (Figure 1-1). The WHOTS-1 recovery on 25 July 2005 resulted in 347 days on station.

An internally-logging Sea-Bird SBE-39 temperature sensor was housed in a foam collar and mounted on the outside face of the buoy hull. Vertical rails allowed the foam to move up and down with the waves, so that the sensor measured the sea surface temperature (SST) within the upper 10-20 cm of the water column. This floating SST sensor operated for the full deployment and showed temperatures that agreed well with the ASIMET SST measured beneath the buoy hull at 1 m depth.

Two SBE-37 MicroCATs were mounted beneath the buoy hull, for near-surface measurements of temperature and conductivity.

An internally-logging Seimac Global Positioning System (GPS) unit was included in the buoy, to monitor buoy position at 10 minute intervals. Unfortunately, this sensor did not perform well. Data gaps of tens of minutes to several hours were found, occasional wild points were evident, and data logging stopped completely after only 32 days. Reasons for the failure are still being investigated.

Instrumentation provided by UH for the WHOTS-1 mooring included ten Sea-Bird SBE-16 SeaCATs, five SBE-37 MicroCATs and an RD Instruments 300 kHz ADCP. The SeaCATs and MicroCATs measured temperature and conductivity; three of the MicroCATs also measured pressure. WHOI provided two NGVMs and all required subsurface mooring hardware via a subcontract with UH. *Table 3.1* provides a listing of the WHOTS-1 MicroCATs and SeaCATs at their nominal depths on the mooring, along with serial numbers, sampling rates and other pertinent information. This table also includes the Sea-Bird temperature and conductivity sensors installed on the buoy.

The RDI 300 kHz Workhorse Sentinel ADCP, SN 4891, with an additional external battery pack, was deployed at 125 m with transducers facing upwards. The instrument was set to ping at 4-second intervals for 160 seconds every 10 minutes. This burst sampling was designed to minimize aliasing by occasional large ocean swell orbital motions. Bin size was set for 4 m. The total number of ensemble records was 50,414. The first ensemble was at 8/10/2004 00:00:00Z, and the last was at 7/26/2005 02:10:00Z. This instrument also measured temperature.

The two NGVMs, SN 012 and 019 were deployed at 10 m and 30 m depth respectively. The instruments were prepared for deployment by the WHOI/UOP group and set to sample at 1-minute intervals. These instruments also measured temperature.

Table 3.1 WHOTS-1 MicroCAT / SeaCAT Deployment Information. All times stated are in GMT. Serial numbers starting with 16 are Sea-Bird SeaCATs; those starting with 37 are MicroCATs, the one starting with 39 is the Sea-Bird temperature sensor.

Depth (m)	Sea-Bird Serial #	Param-eters	Sample Int (seconds)	Time Logging Started	Time in the water
0	39-1447	T	300	8/4/2004 01:00	8/12/2004 19:56
1	37SM485-3601	C, T	300	8/4/2004 01:00	8/12/2004 19:56
1	37SM485-3602	C, T	300	8/4/2004 01:00	8/12/2004 19:56
15	163452-0801	C, T	600	8/8/2004 00:00	8/12/2004 18:32
25	165807-1085	C, T	600	8/8/2004 00:00	8/12/2004 18:25
35	165807-1087	C, T	600	8/8/2004 00:00	8/12/2004 18:19
40	37SM31486-3381	C, T	150	8/8/2004 00:00	8/12/2004 18:14
45	37SM31486-3382	C, T	150	8/8/2004 00:00	8/12/2004 18:13
50	165807-1088	C, T	600	8/8/2004 00:00	8/12/2004 18:09
55	165807-1090	C, T	600	8/8/2004 00:00	8/12/2004 18:09
65	165807-1092	C, T	600	8/8/2004 00:00	8/12/2004 20:14
75	165807-1095	C, T	600	8/8/2004 00:00	8/12/2004 20:19
85	37SM31486-2451	C, T, P	180	8/8/2004 00:00	8/12/2004 20:22
95	165807-1097	C, T	600	8/8/2004 00:00	8/12/2004 20:27
105	37SM31486-2769	C, T, P	180	8/8/2004 00:00	8/12/2004 20:32
120	165807-1099	C, T	600	8/8/2004 00:00	8/12/2004 20:36
135	165807-1100	C, T	600	8/8/2004 00:00	8/12/2004 20:46
155	37SM31486-2965	C, T, P	180	8/8/2004 00:00	8/12/2004 20:51

All WHOTS-1 instruments were successfully recovered as shown in Table 3.2. All instruments provided full data return except the shallow NGVM; the battery was depleted after about 8 months of sampling. After recovery and before the data logging was stopped, the SeaCATs and MicroCATs from levels below 1 m were placed in a cold fresh water bath to create a spike in the data, to check for any malfunction of the internal clock (Table 3.2)

The data from the upward-looking ADCP at 125 m appeared to be of high quality, except that acoustic returns from the upper 50 m of the water column were intermittent, apparently due to very low levels of scattering material near the surface. Diurnal migration of plankton often allowed good data returns to near the surface at night.

Table 3.2 WHOTS-1 MicroCAT / SeaCAT Recovery Information. All times stated are in GMT.

Depth (m)	Sea-Bird Serial #	Time out of water	Time of cold water spike	Time Logging Stopped	Samples Logged	Data Quality
0	39-1447	7/26/2005 00:15	NA	7/26/2005 15:30:00	102702	Good
1	37SM485-3601	7/26/2005 00:15	NA	7/26/2005 17:55:04	102731	Good
1	37SM485-3602	7/26/2005 00:15	NA	7/26/2005 15:20:04	102700	Good
15	163452-0801	7/26/2005 00:44	7/26/2005 03:11:20	7/28/2005 00:58:00	50982	Good
25	165807-1085	7/26/2005 00:50	7/26/2005 03:11:20	7/27/2005 22:50:00	50970	Good
35	165807-1087	7/26/2005 00:58	7/26/2005 03:11:20	7/27/2005 23:20:00	50972	Good
40	37SM31486-3381	7/26/2005 01:00	7/26/2005 01:35:58	7/26/2005 03:00:00	202872	Good
45	37SM31486-3382	7/26/2005 01:05	7/26/2005 01:35:58	7/26/2005 03:03:00	202825	Good
50	165807-1088	7/26/2005 01:09	7/26/2005 03:11:20	7/28/2005 00:27:00	50979	Good
55	165807-1090	7/25/2005 23:28	7/26/2005 01:34:30	7/27/2005 18:27:00	50943	Good
65	165807-1092	7/25/2005 23:24	7/26/2005 01:34:30	7/27/2005 21:22:00	50961	Good
75	165807-1095	7/25/2005 23:21	7/26/2005 01:34:30	7/27/2005 22:18:00	50966	Good
85	37SM31486-2451	7/25/2005 23:17	7/26/2005 01:35:58	7/26/2005 02:46:00	169014	Good

95	165807-1097	7/25/2005 23:11	7/26/2005 01:34:30	7/27/2005 20:16:00	50954	Good
105	37SM31486-2769	7/25/2005 23:08	7/26/2005 01:35:58	7/26/2005 02:31:00	169010	Good
120	165807-1099	7/25/2005 22:59	7/26/2005 01:34:30	7/27/2005 23:50:00	50976	Good
135	165807-1100	7/25/2005 22:55	7/26/2005 01:34:30	7/27/2005 20:52:00	50958	Good
155	37SM31486-2965	7/25/2005 22:47	7/26/2005 01:35:58	7/26/2005 05:12:00	169062	Good

B. Deployment 2

The WHOTS-2 mooring was deployed on 28 July 2005 from the R/V *Melville* at approximately 22° 46' N, 157° 54' W in 4695 m of water. The buoy was outfitted with two independent ASIMET systems to provide redundancy. Each system included six sensor modules attached to the upper section of the two-part aluminum tower at a height of about 3 m above the water line, and a data logger mounted in the buoy well. An Iridium modem subsystem was added to the ASIMET logger as a supplemental means of transmitting meteorological data. The tower also contained a radar reflector, a marine lantern, and two independent Argos satellite transmission systems that provided continuous monitoring of buoy position. For WHOTS-2, a self-contained GPS receiver was also deployed on the buoy tower. Sea surface temperature and salinity were measured by two Sea-Bird MicroCATs bolted to the underside of the buoy hull and cabled to the loggers through an access tube through the buoy foam. An internally-logging Sea-Bird SBE-39 temperature sensor was housed in a foam collar and mounted on the outside face of the buoy hull. Vertical rails allowed the foam to move up and down with the waves, so that the sensor measured the sea surface temperature (SST) within the upper 10-20 cm of the water column.

The mooring was outfitted with subsurface instruments from 10 to 155 m depth consisting of fifteen conductivity-temperature (C-T) sensors, two NGVMs and an ADCP. The mooring design (Figure 1-2) was nearly identical to that of WHOTS-1, the principal difference being the use of MicroCATs for temperature and conductivity measurements in all the levels. The WHOTS-2 recovery on 24 June 2006 resulted in 331 days on station.

UH provided twelve new MicroCATs for the WHOTS-2 mooring deployment. Three of the MicroCATs deployed on WHOTS-1 were turned around at sea and redeployed. This involved cleaning the instruments, downloading data, verifying data quality, calibrating against the CTD (see Section 2B), and installing new batteries and anti-fouling. Table 3.3 gives summary information for the MicroCATs deployed on WHOTS-2. The RDI 300 khz ADCP was also turned around and redeployed. This involved cleaning the instrument, downloading data, verifying data quality, changing batteries, reprogramming and attaching new sacrificial zinc anodes. WHOI/UOP provided two refurbished NGVMs for WHOTS-2.

Before deployment, the MicroCATs from levels below 2 m were dunked in a cold freshwater bath to generate a spike in the data to be used for synchronization of their internal clocks (Table 3.3).

The ADCP, SN 4891, was deployed at 125 m with transducers facing upwards. The instrument was set to ping every 15 seconds, ensemble averaged every 10 minutes. This default setting did not result in burst sampling as was done for the WHOTS-1 mooring record. Bin size was set for

4 m. The total number of ensemble records was 48,092. The first ensemble was at 7/27/2005 03:50:00Z, and the last was at 6/26/2006 03:00:00Z. This instrument also measured temperature.

The two NGVMs, SN 066 and 068 were deployed at 10 m and 30 m depth respectively. The instruments were prepared for deployment by the WHOI/UOP group and set to record at 1-minute intervals. These instruments also measured temperature.

Table 3.3 WHOTS-2 Mooring - MicroCAT Deployment Information. All times stated are in GMT.

Depth (meters)	Sea-Bird Serial #	Parameters	Sample Interval (seconds)	Navg	Time Logging Started	Cold Spike Time	Time in the water
0	39-1446	T	300		7/16/2005 01:00	NA	7/27/2005 19:10
1.5	37SM485-1836	C, T	60		7/15/2005 22:00	NA	7/27/2005 18:50
1.5	37SM485-3604	C, T	60		7/15/2005 22:00	NA	7/27/2005 18:50
15	37SM31486-3382	C, T	150	2	7/27/2005 6:00	06:31:00 - 07:03:30	7/27/2005 18:31
25	37SM31486-3621	C, T	150	2	7/27/2005 6:00	06:31:00 - 07:03:30	7/27/2005 18:27
35	37SM31486-3620	C, T	150	2	7/27/2005 6:00	06:31:00 - 07:03:30	7/27/2005 18:20
40	37SM31486-3632	C, T	150	2	7/27/2005 6:00	06:31:00 - 07:03:30	7/27/2005 18:18
45	37SM31486-2965	C, T, P	180	1	7/27/2005 6:00	06:31:00 - 07:03:30	7/27/2005 18:16
50	37SM31486-3633	C, T	150	2	7/27/2005 6:00	06:31:00 - 07:03:30	7/27/2005 18:13
55	37SM31486-3619	C, T	150	2	7/27/2005 6:00	06:31:00 - 07:03:30	7/27/2005 19:13
65	37SM31486-3791	C, T	150	2	7/27/2005 6:00	06:31:00 - 07:03:30	7/27/2005 19:17
75	37SM31486-3618	C, T	150	2	7/27/2005 6:00	06:31:00 - 07:03:30	7/27/2005 19:21
85	37SM31486-3670	C, T, P	180	1	7/27/2005 6:00	06:31:00 - 07:03:30	7/27/2005 19:24
95	37SM31486-3617	C, T	150	2	7/27/2005 6:00	06:31:00 - 07:03:30	7/27/2005 19:26
105	37SM31486-3669	C, T, P	180	1	7/27/2005 6:00	06:31:00 - 07:03:30	7/27/2005 19:29
120	37SM31486-2451	C, T, P	180	1	7/27/2005 6:00	06:31:00 - 07:03:30	7/27/2005 19:34
135	37SM31486-3634	C, T	150	2	7/27/2005 6:00	06:31:00 - 07:03:30	7/27/2005 19:42
155	37SM31486-3668	C, T, P	180	1	7/27/2005 6:00	06:31:00 - 07:03:30	7/27/2005 19:46

All WHOTS-2 instruments were successfully recovered as shown in Table 3.4. All instruments provided full data return, except for one of the near-surface MicroCATs (SN 1836), which stopped working after less than three months of sampling. After recovery and before the data logging was stopped, the MicroCATs from levels below 2 m were dumped in a cold freshwater bath to create a spike in the data to check for any malfunction of the internal clock (Table 3.4)

The data from the upward-looking ADCP at 125 m appeared to be of high quality also, except that acoustic returns from the upper 50 m of the water column are intermittent, due to very low levels of scattering material near the surface. Diurnal migration of plankton often allowed good data returns to near the surface at night, however. A seasonal variation of good returns from the upper water column is also apparent.

Table 3.4 WHOTS-2 Mooring - MicroCAT Recovery Information. All times stated are in GMT

Depth (meters)	Seabird Serial #	Time out of water	Time of cold spike	Time Logging Stopped	Samples Logged	Data Quality
0	39-1446	6/24/2006 18:50	NA	6/25/2006 01:50:00	99083	Good
1.5	37SM485-1836	6/24/2006 18:50	NA	9/16/2005 19:50:00	18119	Incomplete
1.5	37SM485-3604	6/24/2006 18:50	NA	6/25/2006 01:50:00	477648	Good
15	37SM31486-3382	6/24/2006 19:56	6/24/2006 22:13:00	6/24/2006 23:50:30	191660	Good
25	37SM31486-3621	6/24/2006 20:02	6/24/2006 22:13:00	6/24/2006 23:54:15	191660	Good
35	37SM31486-3620	6/24/2006 20:05	6/24/2006 22:13:00	6/24/2006 23:55:00	191663	Good
40	37SM31486-3632	6/24/2006 20:10	6/24/2006 22:53:00	6/25/2006 04:03:30	191761	Good
45	37SM31486-2965	6/24/2006 20:14	6/24/2006 22:53:00	6/25/2006 03:57:30	159799	Good
50	37SM31486-3633	6/24/2006 20:17	6/24/2006 22:53:00	6/25/2006 03:55:00	191758	Good
55	37SM31486-3619	6/24/2006 20:19	6/24/2006 22:53:00	6/25/2006 04:08:00	191763	Good
65	37SM31486-3791	6/24/2006 20:26	6/24/2006 22:13:00	6/24/2006 23:52:15	191661	Good
75	37SM31486-3618	6/24/2006 20:31	6/24/2006 22:13:00	6/24/2006 23:52:30	191662	Good
85	37SM31486-3670	6/24/2006 20:35	6/24/2006 22:53:00	6/25/2006 07:30:15	159870	Good
95	37SM31486-3617	6/24/2006 20:40	6/24/2006 22:53:00	6/25/2006 04:02:00	191761	Good
105	37SM31486-3669	6/24/2006 20:43	6/24/2006 22:53:00	6/25/2006 04:00:00	159800	Good
120	37SM31486-2451	6/24/2006 20:50	6/24/2006 22:13:00	6/24/2006 23:54:15	159718	Good
135	37SM31486-3634	6/24/2006 20:59	6/24/2006 22:13:00	6/25/2006 07:29:30	191844	Good
155	37SM31486-3668	6/24/2006 21:04	6/24/2006 22:53:00	6/25/2006 03:53:12	159191	Good

4. WHOTS-2 and -3 deployment cruise shipboard observations

The profile observations made during WHOTS cruises were obtained with a Sea-Bird CTD (conductivity, temperature and depth) instrument with duplicate temperature and conductivity sensors (and oxygen during WHOTS-2). Measurements were made to better than 0.01°C in temperature, 0.01 for salinity, and 1.5 µmol/kg in dissolved oxygen below 5 m. In addition, the R/V *Melville* and the R/V *Roger Revelle* came equipped with a thermosalinograph which provided a continuous, high-resolution depiction of temperature and salinity of the near-surface layer. Horizontal currents over the depth range of 20-300 m were measured from the shipboard 150 kHz ADCP with a vertical resolution of 8 m, and over the depth range of 40-800 m by the 75 kHz ADCP with a vertical resolution of 16 m.

A. Conductivity, Temperature and Depth (CTD) profiling

Continuous measurements of temperature, conductivity and pressure were made with the UH Sea-Bird SBE-911+ CTD package (S/N 92859) during the WHOTS-2 cruise, and with the R/V *Roger Revelle*'s SBE-911+ CTD (S/N 09P37218-0777) during WHOTS-3. Each CTD was equipped with an internal Digiquartz pressure sensor and two pairs of external temperature and conductivity sensors. Each of the temperature-conductivity sensor pairs used a Sea-Bird TC duct which circulated seawater through independent pump and plumbing installations. During WHOTS-2, the CTD configuration also included two oxygen sensors, installed in the plumbing

for each sensor set; and one unplumbed Seapoint fluorometer. In both cruises, the CTD was mounted in a vertical position in the lower part of a Rosette sampler, with the sensors' water intakes located at the bottom of the Rosette. WHOTS-2 used a 24-place Rosette, and WHOTS-3 used a 12-place Rosette.

The package was deployed on a conducting cable, which allowed for real-time data acquisition and display. The deployment procedure consisted in lowering the package to 10-15 dbar and waiting until the CTD pumps started operating. The CTD was then raised until the sensors were close to the surface to begin the CTD cast. The time and position of each cast was obtained via a GPS connection to the CTD deck box. Sampling bottles were 12-l Bullister type during WHOTS-2, and 5-liter Niskin bottles during WHOTS-3. Between two and five salinity samples were taken on each cast for calibration of the conductivity sensors. Between 4 and 8 samples were taken during 11 casts in WHOTS-2 to measure dissolved oxygen for calibration of the oxygen sensors.

1. Data acquisition and processing.

CTD data were acquired at the instrument's highest sampling rate of 24 samples per second. Digital data were stored on a laptop computer and, for redundancy, the analog signal was recorded on VHS video tapes.

Figure 4-1 shows a flowchart of the CTD data processing. The raw CTD data were first converted from frequencies to engineering units using nominal sensor calibrations and then screened for spikes or missing data using a 9-point median filter. After screening, the correct alignment of temperature and conductivity time-series was computed since the lag between temperature and conductivity depends on the relative position of the sensors. Both T-C pairs were also aligned with each other by cross-correlating the two temperature sensors. Conductivity measurement were corrected for thermal inertia of the glass conductivity cell as explained below, and the data were averaged to half-second values; salinity was then computed. Details of these procedures are described in the following sections. Spikes in the data occur when the CTD samples the disturbed water of its wake. Therefore, samples from the downcast were rejected when the CTD was moving upward or when its acceleration exceeded 0.5 m s^{-2} in magnitude. The data were subsequently averaged into 2-dbar pressure bins after calibrating the CTD conductivity with the bottle salinities, and after calibrating the CTD oxygen with the dissolved oxygen samples for the WHOTS-2 data.

The data were additionally screened by comparing the T-C sensor pairs. These differences permitted identification of problems with the sensors. The data from only one T-C pair, whichever was deemed most reliable, is reported here. Only data from the downcast are reported, as upcast data are contaminated by rosette wake effects.

Temperature is reported in the ITS-90 scale. Salinity and all derived units were calculated using the UNESCO (1981) routines; salinity is reported in the practical salinity scale (PSS-78).

2. CTD sensor calibration and corrections

Pressure

The pressure calibration strategy for CTD pressure transducer SN 51412 used during WHOTS-2 employed a high-quality quartz pressure transducer as a transfer standard. Periodic recalibrations of this lab standard were performed with a primary pressure standard. Pressure transducer SN 88907 used during WHOTS-3 was calibrated on 19 April 2005. The only corrections applied to the CTD pressures were a constant offset determined at the time that the CTD first enters the water on each cast. In addition, a span correction determined from bench tests on the sensor against the transfer standard was applied for sensor SN 51412.

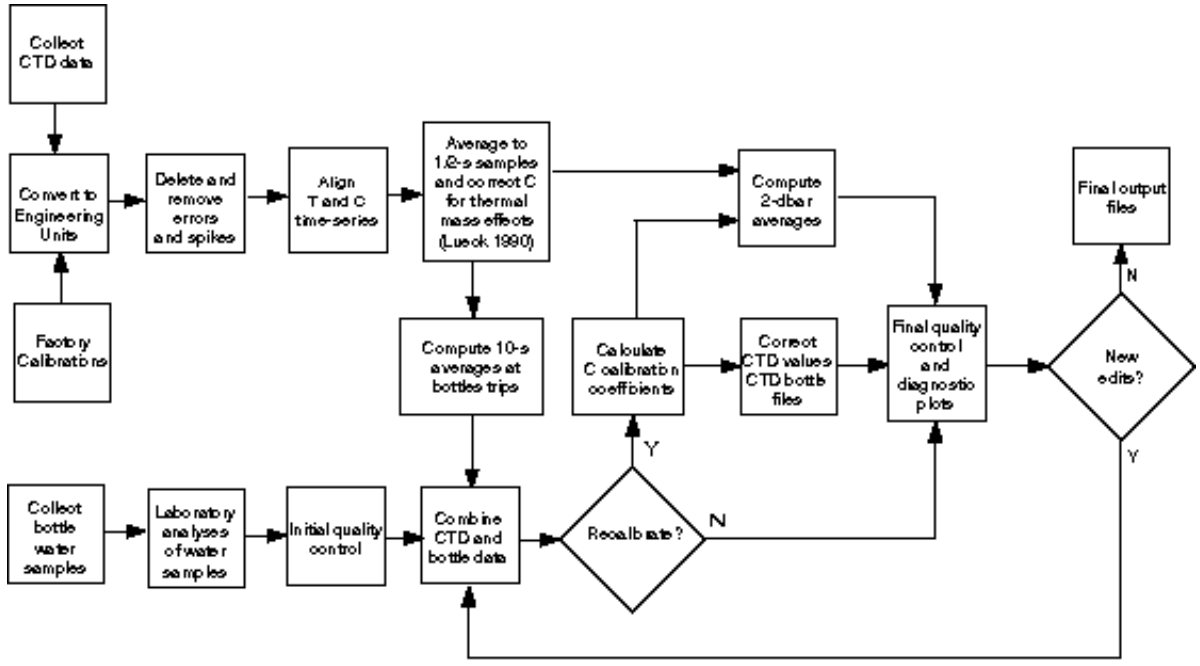

Figure 4-1 Flowchart of CTD data processing

Transfer Standard Calibration

The transfer standard is a Paroscientific Model 760 pressure gauge equipped with a 10,000 PSI transducer. This instrument was purchased in March 1988, and was originally calibrated against a primary standard. Subsequent recalibrations have been performed every 2.5 years on average either at the Northwest Regional Calibration Center or at the SIO. The latest calibrations were conducted at the SIO in April 1999, May 2001, May 2003, and July 2005.

CTD Pressure Transducer SN 51412 Bench Tests

CTD pressure transducer bench tests were done using an Ametek T-100 pump and a manifold to apply pressure simultaneously to the CTD pressure transducer and to the transfer standard. All these tests generated calibration data at six pressure levels between 0 and 4500 dbar, for both increasing and decreasing pressures. Pressure sensor #51412 was used during the WHOTS-2 cruise. The results of the bench tests on this sensor from 1998 until 2005 are shown in Table 4.1. The 0 dbar offset has remained relatively constant at slightly more than 1 dbar. A correction was applied for this offset during the cruise. (A more accurate offset was later determined for the time that the CTD first enters the water on each cast). The 0-4500 dbar span has also remained relatively constant; a span correction of 0.47 dbar/4500 dbar was applied for all the WHOTS-2 casts. The sensor hysteresis has remained relatively small and constant.

Table 4.1 CTD pressure sensor #51412 calibrations against the transfer standard

Calibration Date	Offset @ 0 dbar	0-4500 dbar offset	Hysteresis
16 February 2005	1.35	0.75	0.15
4 July 2004	1.16	0.64	0.15
10 February 2004	1.28	0.53	0.1
29 July 2003	1.25	0.55	0.1
5 February 2003	1.15	0.55	0.1
17 July 2002	1.2	0.5	0.1
31 January 2002	1.2	0.5	0.2
29 June 2001	1.14	0.5	0.1
5 February 2001	1.1	0.56	0.03
16 August 2000	1.05	0.6	0.05
14 January 2000	1.1	0.55	0.05
25 June 1999	1.0	0.47	0.05
26 January 1999	0.95	0.55	0.05
14 September 1998	1.25	0.55	0.05

Temperature

Four Sea-Bird SBE-3-Plus temperature transducers (#2700, #2242, #2454, and #4448) were used during WHOTS-2 and -3, and were calibrated at Sea-Bird before and after each cruise to an accuracy better than 0.5×10^{-3}°C. Calibration coefficients obtained at Sea-Bird are listed in Table 4.2. These coefficients were used in the following formula that gives the temperature (in °C) as a function of the frequency signal (f):

$$Temperature = 1/\{a+b[ln(fo/f)]+c[ln^2(fo/f)+d[ln^3(fo/f]\}-273.15$$

For each sensor, we calculated the 0-30°C average offset for each calibration relative to the oldest one, and applied a linear fit to these offsets. A single baseline calibration was chosen and a temperature-independent offset relative to the baseline calibration was applied to the data to

remove the temporal trend due to the sensor drift. The maximum drift correction for WHOTS cruises was less than 0.2 x 10^{-3}°C. The baseline calibration was selected as the one for which the trend-corrected average from 0-5°C was nearest to the ensemble mean of these averages.

Table 4.2 Calibration coefficients for Sea-Bird temperature sensors. RMS residuals from calibration give an indication of calibration quality.

SN	*Date yymmdd*	*f0*	*a*	*b*	*c*	*d*	*RMS (m°C)*
2242	051020	2997.330	3.68121751e-03	6.02947539e-04	1.62210189e-05	2.17306310e-06	0.08
2242	050827	2997.339	3.68121605e-03	6.02951279e-04	1.62284970e-05	2.17573971e-06	0.07
2242	050706	2997.345	3.68121499e-03	6.02953872e-04	1.62600888e-05	2.21086408e-06	0.06
2242	050406	2997.376	3.68121221e-03	6.02941351e-04	1.62151004e-05	2.17196077e-06	0.09
2242	050111	2997.35	3.68121134E-03	6.02950170E-04	1.62337733E-05	2.17899661E-06	0.07
2242	041111	2997.35	3.68121113E-03	6.02952691E-04	1.62557770E-05	2.20464599E-06	0.07
2242	040902	2997.34	3.68121142E-03	6.02944339E-04	1.62325783E-05	2.18293451E-06	0.07
2242	040626	2997.35	3.68121105E-03	6.02955276E-04	1.62397550E-05	2.18086509E-06	0.06
2242	040401	2997.34	3.68121397E-03	6.02939174E-04	1.62163129E-05	2.17593757E-06	0.08
2242	040206	2997.36	3.68121397E-03	6.02950385E-04	1.62469288E-05	2.20053454E-06	0.08
2242	031125	2997.37	3.68121243e-03	6.02953206e-04	1.62706534e-05	2.22800165e-06	0.07
2242	030903	2997.39	3.68120697e-03	6.02936404e-04	1.62230847e-05	2.18328156e-06	0.09
2242	030801	2997.38	3.68120804e-03	6.02930569e-04	1.62081910e-05	2.17099531e-06	0.07
2242	030701	2997.38	3.68120849e-03	6.02929736e-04	1.62083321e-05	2.17299481e-06	0.09
2242	030506	2997.38	3.68120883e-03	6.02925362e-04	1.62039894e-05	2.17125544e-06	0.07
2242	030410	2997.39	3.68120958e-03	6.02928552e-04	1.61962650e-05	2.15700218e-06	0.07
2242	030319	2997.39	3.68120952e-03	6.02930555e-04	1.62131526e-05	2.17534168e-06	0.07
2454	060801	2885.730	3.68121424e-03	6.02175648e-04	1.67513098e-05	2.36269660e-06	0.03
2454	060415	2885.752	3.68121439e-03	6.02187499e-04	1.67547819e-05	2.35423435e-06	0.07
2454	051020	2885.746	3.68121819e-03	6.02183987e-04	1.67711663e-05	2.38731519e-06	0.06
2454	050827	2885.744	3.68121676e-03	6.02187449e-04	1.67885159e-05	2.40097525e-06	0.05
2454	050706	2885.742	3.68121551e-03	6.02184381e-04	1.67859182e-05	2.39915470e-06	0.05
2454	050407	2885.757	3.68121334e-03	6.02186285e-04	1.67971302e-05	2.40912421e-06	0.07
2454	050111	2885.74	3.68121209E-03	6.02189593E-04	1.68073225E-05	2.41468487E-06	0.07
2454	041111	2885.73	3.68121193E-03	6.02184316E-04	1.68016426E-05	2.41392105E-06	0.06
2700	051020	2972.602	3.68121843e-03	6.04815410e-04	1.65540507e-05	2.38074221e-06	0.06
2700	050831	2972.602	3.68121687e-03	6.04816716e-04	1.65592394e-05	2.38239620e-06	0.04
2700	050706	2972.613	3.68121552e-03	6.04817663e-04	1.65641164e-05	2.38432603e-06	0.05
2700	050406	2972.639	3.68121334e-03	6.04819001e-04	1.65681867e-05	2.39213354e-06	0.08
2700	050111	2972.6	3.68121232E-03	6.04822192E-04	1.65825571E-05	2.39934333E-06	0.08
2700	041111	2972.6	3.68121197E-03	6.04821651E-04	1.65899272E-05	2.40900872E-06	0.06
2700	040902	2972.58	3.68121238E-03	6.04814992E-04	1.65732011E-05	2.39156477E-06	0.09
2700	040626	2972.56	3.68121206E-03	6.04791567E-04	1.65117055E-05	2.34596117E-06	0.07
2700	040401	2972.57	3.68121493E-03	6.04810471E-04	1.65672157E-05	2.39636770E-06	0.08
2700	040206	2972.58	3.68121481E-03	6.04821743E-04	1.65970248E-05	2.41924836E-06	0.08
2700	031125	2972.59	3.68121336e-03	6.04818783e-04	1.65997732e-05	2.43503194e-06	0.06
2700	030903	2972.59	3.68120806e-03	6.04805757e-04	1.65648723e-05	2.39236639e-06	0.07
2700	030801	2972.58	3.68120899e-03	6.04812762e-04	1.65905717e-05	2.41626696e-06	0.06
2700	030701	2972.58	3.68120955e-03	6.04807049e-04	1.65701857e-05	2.39919052e-06	0.08
2700	030506	2972.58	3.68120985e-03	6.04804333e-04	1.65669101e-05	2.39844428e-06	0.09
2700	030410	2972.58	3.68121066e-03	6.04800286e-04	1.65305956e-05	2.35650390e-06	0.07
2700	030319	2972.58	3.68121081e-03	6.04807178e-04	1.65611632e-05	2.38338921e-06	0.07
2700	030130	2972.59	3.68121221e-03	6.04801751e-04	1.65234207e-05	2.34737465e-06	0.08
2700	030104	2972.57	3.68121204e-03	6.04801026e-04	1.65408098e-05	2.36946200e-06	0.07
4448	060801	2872.314	3.68121418e-03	5.97049695e-04	1.49291789e-05	1.70648232e-06	0.03
4448	060415	2872.310	3.68121431e-03	5.97077412e-04	1.50501277e-05	1.81399552e-06	0.06
4448	051110	2872.337	3.68121770e-03	5.97041275e-04	1.49263547e-05	1.72296669e-06	0.01

A small residual pressure effect on the temperature sensors documented in Tupas et al. (1997) has been removed from measurements obtained with our sensors. Another correction to our

temperature measurements was for the viscous heating of the sensor tip due to the water flow past it (Larson and Pederson, 1996). This correction is thoroughly documented in Tupas et al. (1997).

Dual sensors were used during all casts of the WHOTS-2 and -3 cruises. Sensors #2700 and #2242 were used during WHOTS-2; and sensors #2454 and #4448 were used during WHOTS-3. The temperature differences between sensor pairs were calculated for each cast to evaluate the quality of the data, and to identify possible problems with the sensors. All sensors performed correctly during the cruises, showing temperature differences within expected values. The mean temperature difference in the water column was typically less than 2 x 10^{-3} °C in the 1000 m casts, with a standard deviation of less than 0.5 x 10^{-3} °C below 500 dbar. The largest variability in temperature difference between sensor pairs was observed in the thermocline, where the standard deviation reached nearly 1 x 10^{-2} °C. These differences are not unexpected, since each sensor has independent water intakes it is possible that when the CTD passes through this steep gradient region each sensor measures water from slightly different levels, yielding significant temperature differences.

Temperature sensor #2700

This sensor was used during the WHOTS-2 cruise. The calibrations between January 2003 and October 2005 were used to calculate the sensor drift and the drift corrections. A linear fit to the 0-30°C average offset from each calibration relative to 11 January 2005 gave an intercept of 1.51 x 10^{-4} °C with a slope of -6.54 X 10^{-7} ^{o}C day^{-1}. The RMS deviation of the offsets from this fit was 1.8 x 10^{-4} °C. The 20 October 2005 calibration showed a small deviation from the 0-5°C ensemble mean of all the calibrations (all corrected for linear drift to the cruise date, July 26, 2005) and was used as a baseline. A drift correction was obtained using this baseline calibration (Table 4.3). This correction is less than 0.1 x 10^{-3} °C and deemed insignificant.

Temperature sensor #2242

This sensor was also used during the WHOTS-2 cruise. The calibrations between March 2003 and October 2005 were used to calculate the sensor drift and the drift corrections. A linear fit to the 0-30°C average offset from each calibration relative to 11 January 2005 gave an intercept of 2.29 x 10^{-4} °C with a slope of -6.56 X 10^{-7} ^{o}C day^{-1}. The RMS deviation of the offsets from this fit was 2.0 x 10^{-4} °C. The 6 July 2005 calibration showed a small deviation from the 0-5°C ensemble mean of all the calibrations (all corrected for linear drift to the cruise date, July 26, 2005) and was used as a baseline. A drift correction was obtained using this baseline calibration (Table 4.3). This correction is less than 0.1 x 10^{-3} °C and deemed insignificant.

Temperature sensor #2454

This sensor was used during the WHOTS-3 cruise. The calibrations between November 2004 and August 2006 were used to calculate the sensor drift and the drift corrections. A linear fit to the 0-30°C average offset from each calibration relative to 15 April 2006 gave an intercept of -8.28 x 10^{-5} °C with a slope of -1.11 X 10^{-7} ^{o} C day^{-1}. The RMS deviation of the offsets from this fit was 2.0 x 10^{-4} °C. The 1 August 2006 calibration showed a small deviation from the 0-5°C

ensemble mean of all the calibrations (all corrected for linear drift to the cruise date, June 26, 2006) and was used as a baseline. A drift correction was obtained using this baseline calibration (Table 4.3). This correction is less than 0.1 x 10^{-3} °C and deemed insignificant.

Temperature sensor #4448

This sensor was also used during the WHOTS-3 cruise. The calibrations between November 2005 and August 2006 were used to calculate the sensor drift and the drift corrections. A linear fit to the 0-30°C average offset from each calibration relative to 15 April 2006 gave an intercept of -1.86 x 10^{-4} °C with a slope of -3.13 X 10^{-6} °C day^{-1}. The RMS deviation of the offsets from this fit was 1.3 x 10^{-4} °C. The 1 August 2006 calibration showed a small deviation from the 0-5°C ensemble mean of all the calibrations (all corrected for linear drift to the cruise date, June 26, 2006) and was used as a baseline. A drift correction was obtained using this baseline calibration (Table 4.3). This correction is 0.11 x 10^{-3} °C and deemed insignificant.

Table 4.3 Temperature (T) and Conductivity (C) sensors used during the WHOTS cruises, including temperature drift correction and the thermal inertia parameter (alpha). Dual temperature and conductivity sensors were used during both cruises. The data reported here are from the sensors marked with (*).

Cruise	T-sensor #	T-correction (m°C)	C-sensor #	alpha
WHOTS-2	2700 (*)	0.056	2725 (*)	0.020
WHOTS-2	2242	0.013	2541	0.020
WHOTS-3	2454 (*)	0.005	2959 (*)	0.028
WHOTS-3	4448	-0.113	3162	0.028

Conductivity

Four Sea-Bird SBE 4C conductivity sensors (#2725, #2541, #2959, and #3162) were used during the WHOTS cruises. Dual sensors were used during all the cruise casts. As mentioned earlier, only the data from the most reliable sensor (and its corresponding temperature sensor pair, as shown in Table 4.3) are reported here.

Sensor #2725 was calibrated at Sea-Bird in November 2004, sensor #2541 was calibrated in January 2005, sensors #2959 and #3162 were calibrated in May 2006. The nominal conductivity calibrations were used for data acquisition. Final calibration was determined empirically from salinities of discrete water samples acquired during each cast. Prior to empirical calibration, conductivity was corrected for thermal inertia of the glass conductivity cell using the recursive filter given by Lueck (1990) and Lueck and Picklo (1990). Sensor parameters alpha and beta, which characterize the initial magnitude of the thermal effect and its relaxation time, are needed for this correction. As recommended by Lueck (personal communication, 1990), beta was set to 0.1 s^{-1}, but alpha was calculated for each sensor to close the spread between the down- and up-cast *T-S* curves (Table 4.3).

Salinity samples were collected at selected depths during each cast and measured with a salinometer (Sect. 4.B.1). The nominally calibrated CTD salinity trace was used to identify questionable samples. Salinity samples were later quality controlled and flagged by comparing them against the empirically calibrated CTD salinities.

Calibration of each conductivity sensor was performed empirically by comparing its nominally calibrated output against the calculated conductivity values obtained from the water sample salinities, using the pressure and temperature of the CTD at the time of bottle closure. An initial estimate of bias (*b0*) and slope (*b1*) corrections to the nominal calibration were determined from a linear least squares fit to the ensemble of CTD-bottle conductivity differences as a function of conductivity, from all casts during the sensor use. This calibration was then used to identify suspect water samples. These samples were deleted from the analysis, and the calibration was repeated. Conductivity calibration coefficients for the sensors used during WHOTS cruises are given in Table 4.4.

Table 4.4 CTD Conductivity calibration coefficients obtained from comparison against bottle salinities.

Cruise	Sensor #	b0	b1
WHOTS-2	2725	0.000183	0.000016
WHOTS-2	2541	0.000186	0.000032
WHOTS-3	2959	0.000450	-0.000067
WHOTS-3	3162	0.000395	-0.000093

The final step of the calibration was to perform a profile-dependent bias correction, to allow for a drift of the conductivity cell with time during each cruise, or for sudden offsets due to fouling. This offset was determined by taking the median value of CTD-bottle salinity differences for each profile. No offset corrections were necessary for any of the WHOTS cruises casts.

The quality of the conductivity calibration is illustrated by Figure 4-2, which shows the differences between the corrected CTD salinities and the bottle salinities as a function of pressure for the WHOTS-2 and -3 cruises. Table 4.5 gives the mean and standard deviations for the final calibrated CTD minus water sample salinities.

Table 4.5 CTD-Bottle salinity comparison for each sensor.

		0 to 1200 dbar		500 to 1200 dbar	
Cruise	Sensor #	Mean	Standard Deviation	Mean	Standard Deviation
WHOTS-2	2725	0.0000	0.0011	-0.0003	0.0011
WHOTS-2	2541	0.0000	0.0011	0.0000	0.0010
WHOTS-3	2959	0.0000	0.0013	0.0002	0.0008
WHOTS-3	3162	0.0000	0.0014	0.0000	0.0009

Salinity differences between sensor sets were calculated the same way as for the temperature in order to identify problems with any of the sensors. These differences show a behavior similar to the temperature differences in the thermocline region. Maximum absolute salinity differences of about 9×10^{-3} were observed at 100 dbar, decreasing to less than 2×10^{-3} below 200 dbar. This

behavior is due to a combination of the residual temperature effect on the temperature sensors described in the previous section, and an additional residual temperature effect on the conductivity sensors (N. Larson personal communication, 1999). The temperature effect on the conductivity sensors is similar to that described for the temperature sensors, and affects the conductivity measurements when the sensor passes through intense temperature gradients.

The largest variability in the salinity difference between sensors was observed in the halocline, with standard deviations of up to 1 x 10^{-2} between 50 and 100 dbar.

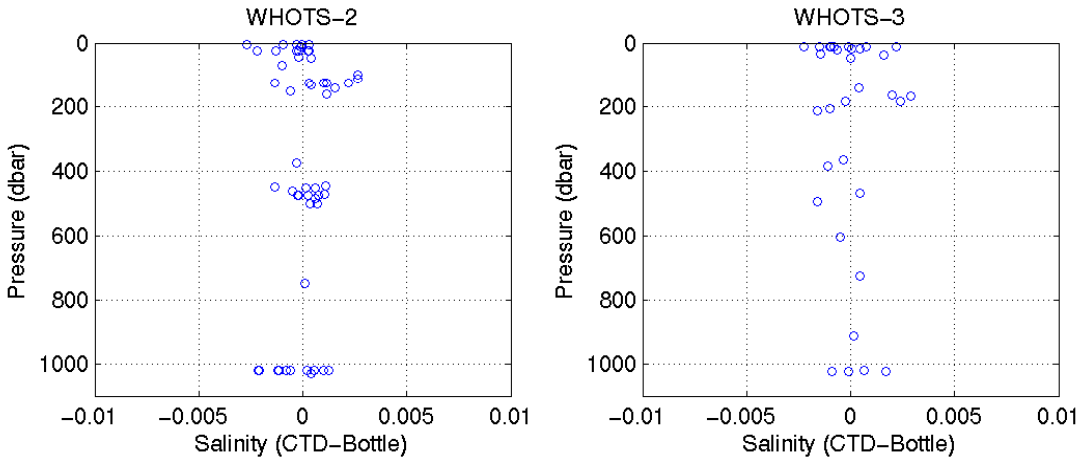

Figure 4-2 Difference between calibrated CTD salinities and bottle salinities for all the casts during WHOTS-2 and –3 deployment cruises.

Oxygen

During the WHOTS-2 deployment cruise two Sea-Bird SBE-43 oxygen sensors were used: #43325, and #43134. No oxygen sensors were used during the WHOTS-3 cruise. Sensor #43325 was calibrated on 26 July 2004, and sensor #43134 was calibrated on 4 June 2005. Water bottle oxygen data were screened and the oxygen sensors were empirically calibrated. The analysis of water bottle samples is described in Section 4.B.2. The calibration procedure follows Owens and Millard (1985), and consists of fitting a nonlinear equation to the CTD oxygen current. The bottle values of dissolved oxygen and the downcast CTD observations at the potential density of each bottle trip were grouped together for each cruise to find the best set of parameters with a non-linear least squares algorithm.

Table 4.6 shows the mean and standard deviation for the calibrated CTD oxygen minus water sample residuals for WHOTS-2 cruise. Dual sensors were used during the cruise, but only the sensor whose data were deemed more reliable is reported.

Table 4.6 CTD-Bottle dissolved oxygen comparison for each sensor during WHOTS-2 cruise. The units are µmol kg^{-1}. No oxygen data were collected during cruise WHOTS-3. The data reported here are from the sensor marked with (*).

		0 to 1200 dbar		500 to 1200 dbar	
Cruise	Sensor #	Mean	Standard Deviation	Mean	Standard Deviation
WHOTS-2	43325 (*)	-0.008	1.05	0.146	0.80
WHOTS-2	43134	-0.008	0.66	-0.018	0.65

B. Water samples

1. Salinity

Salinity samples were collected in 250 ml glass bottles during WHOTS-2 and -3. Samples from WHOTS-2 were stored and measured after the cruise in the laboratory at the UH using a Guildline Autosal 8400B. Samples from WHOTS-3 were measured during the cruise using the same Autosal. IAPSO[3] [P J1] standard seawater samples were measured to standardize the Autosal, and samples from a large batch of "secondary standard" (substandard) seawater were measured after every 24 bottle samples of each cruise to detect drift in the Autosal. Standard deviations of the secondary standard measurements were less than ± 0.001 for WHOTS-2 and -3 cruises (Table 4.7).

The substandard water was collected during HOT cruises from 1000 m at station ALOHA and drained into a 50-liter Nalgene plastic carboy. In the laboratory, the water was then thoroughly mixed in a glass carboy for 20 minutes, after which a 2-inch protective layer of white oil was added on top to deter evaporation. The substandard water was allowed to stand for approximately three days before it was used, and was stored in the same temperature controlled room as the Autosal, protecting it from the light with black plastic bags to prevent algae growth. Substandard seawater batches #37 and #39 were prepared on 29 June 2005, and 7 April 2006, respectively and used for WHOTS-2 and -3 samples respectively. During the WHOTS-3 cruise substandard water was decanted from the carboy into 250 ml sample bottles for ease of transit. The top of the bottle and the thimble were thoroughly dried before being tightly capped to prevent water from being trapped between the cap or thimble and the bottle's mouth. It has been observed that residual water trapped in this way increases its salinity due to evaporation, and it can leak into the sample when the bottle is opened for measuring.

Salinity samples from the WHOTS-3 cruise were measured together with samples from a previous HOT cruise (HOT-182, 12-16 June 2006). The substandard statistics in Table 4.7 include all the substandard samples measured.

Table 4.7 Precision of salinity measurements using secondary lab standards.

Cruise	Mean Salinity +/- SD	# Samples	Substandard Batch #	IAPSO Batch #
WHOTS-2	34.4765 +/- 0.00045	8	37	P143

[3] International Association for Physical Sciences of the Ocean

Cruise	Mean Salinity +/- SD	# Samples	Substandard Batch #	IAPSO Batch #
WHOTS-3	34.4668 +/- 0.00030	13	39	P145

2. Dissolved Oxygen

Dissolved oxygen samples during the WHOTS-2 cruise were collected and analyzed using a computer-controlled potentiometric end-point titration procedure as described in Tupas et al. (1997). Using a calibrated digital thermistor, we measured the temperature of the seawater sample at the time the iodine flask was filled. This was done to evaluate the magnitude of sample temperature error that affects the calculation of oxygen concentrations in units of μmol kg^{-1}.

Since the measuring procedures were the same as those used during HOT cruises, the precision of the Winkler titration method was estimated using all the HOT cruise data during 2005 (Fujieki et al., 2006). The pooled annual mean per cent coefficient of variation (%CV = 100 standard deviation/mean) of our oxygen analyses in 2005 was 0.16 %, which was calculated by averaging the mean %CV of N-triplicate samples on each cruise.

C. Thermosalinograph data acquisition and processing

1. WHOTS-2 Deployment Cruise

Near-surface temperature and salinity data for the WHOTS-2 cruise were acquired through the use of a thermosalinograph system aboard the R/V *Melville*. The seawater intake was situated approximately 4 m below the sea surface in the bow thruster room. A SBE-45 thermosalinograph, #0067 last calibrated 17 November 2004, was situated in the ship's analytical lab located roughly at midships. There was no external temperature sensor installed on the seawater intake. There were 2 hull mounted temperature sensors situated beneath the bulbus bow at a similar depth to the seawater intake. Also there was an auxiliary temperature sensor, Omega ON-403-PP, installed next to the SBE-45 in the analytical lab.

Data were acquired every 30 seconds for the duration of the cruise and salinity samples were taken roughly every 12 hours throughout the cruise for calibration from an outlet in the flowthrough system located next to the SBE-45.

Temperature Calibration

The hull mounted temperature sensors have no calibration available, and were considered to be not of high enough quality when compared with the 4 dbar CTD temperature data. With a stated accuracy of ±0.02°C the auxiliary temperature sensor ON-403-PP was also not of high enough quality. Data from these sensors were not used for this report; rather data from the SBE-45 temperature sensor were used instead as a measure of the intake seawater temperature, with an offset correction applied after comparing it with the 4 dbar CTD temperature data.

Nominal Conductivity Calibration

Sea-Bird conductivity sensor 0067 was calibrated at Sea-Bird on 17 November 2004. All conductivity data from the thermosalinograph were calibrated with coefficients obtained from this calibration. However, all the final salinity data reported here were calibrated against bottle data as explained below.

Data Processing

Daily files containing air, water and navigation data recorded every 30 seconds were concatenated and the relevant fields output in a format similar to that used from the HOT cruises aboard the R/V *Kilo Moana* or R/V *Ka'imikai-O-Kanaloa.* The data were then screened for gross errors, with upper and lower bounds of 18 °C and 35 °C for temperature and 3 Siemens m^{-1} and 6 Siemens m^{-1} for conductivity. There were 8 points outside the valid temperature range and no gross errors detected in conductivity.

A 5-point running median filter was used to detect one- or two-point temperature and conductivity glitches in the thermosalinograph data. Glitches in temperature and conductivity detected by the 5-point median filter were immediately replaced by the median. Threshold values of 0.3°C for temperature and 0.1 Siemens m^{-1} for conductivity were used for the median filter. Three temperature points and fourteen conductivity points were replaced after running the median filter. A 3-point triangular running mean filter was used to smooth the temperature and conductivity data after passing the glitch detection.

The thermosalinograph aboard the R/V *Melville* was set to record data every 30 seconds, but occasionally, due to an error in the acquisition software rounding routine, a record is written at a longer interval. There were 1509 timing errors in total, all between 30-32 seconds.

Data were manually flagged to remove contamination by the introduction of bubbles to the flowthrough system during rough conditions. Of a total of 22260 data points, 3624 points were flagged as bad in both temperature and conductivity and 137 points were flagged bad in conductivity only.

Bottle Salinity and CTD Salinity Comparisons

The thermosalinograph salinity was calibrated by comparing it to bottle salinity samples drawn from a water intake next to the thermosalinograph. Fourteen salinity samples were collected and analyzed as described in Section 4.B.1. The comparison was made in conductivity in order to eliminate the effects of temperature. The conductivity of the bottle was computed using the salinity of the bottle, thermosalinograph temperature and a pressure of 10 dbar, which includes the pressure of the pump.

Salinity samples were drawn from the flowthrough system less than 0.5 m from the SBE-45 and consequently there should be virtually no delay between when the water passes through the thermosalinograph and it being sampled. A 90 second average centered on the sample draw time was chosen for processing purposes.

The CTD salinity data at 4 dbar were compared with the thermosalinograph conductivity. Using the thermosalinograph temperature data and a pressure of 10 dbar the CTD conductivity was calculated for the 19 casts conducted while the thermosalinograph was running.

One salinity sample, bottle #1, and three CTD casts, 1, 8, and 9 were excluded from the thermosalinograph processing as they were obvious outliers. The SBE-45 conductivity sensor was found to have drifted over the duration of the cruise by an equivalent salinity of 1.07×10^{-3} Sm^{-1} day^{-1}. The reason for this drift is unknown.

A cubic spline was fit to the time series of the differences between the bottle and thermosalinograph conductivity and a correction was obtained for the thermosalinograph conductivities. Salinity was calculated using these corrected conductivities, the thermosalinograph temperatures and the water pressure. After correction, the mean difference between the bottle and thermosalinograph salinities was 0.000 with a standard deviation of 0.001. The mean CTD/thermosalinograph difference was -0.002 with a standard deviation of 0.0014.

CTD Temperature Comparisons

There were 19 CTD casts conducted during the WHOTS-2 cruise. The 4 dbar CTD temperature data were compared to the thermosalinograph. Temperatures recorded by the hull mounted temperature sensors were consistently lower than the 4 dbar CTD data with an approximate mean difference of 0.3°C and were considered not good enough due to the lack of calibration history. The SBE-45 temperature data were used as a measure of the water temperature with an offset correction of 0.064 °C derived from the 4 dbar CTD temperature comparisons. Temperature data for the whole record were subsequently flagged as uncalibrated data.

2. WHOTS-3 Deployment Cruise

Near-surface temperature and salinity data for the WHOTS-3 cruise were acquired through the use of a thermosalinograph system aboard the R/V *Roger Revelle*. The seawater intake was situated approximately 5 m below the sea surface in the bow thruster room. A SBE-45 thermosalinograph, #0082 was also situated in the bow thruster room. There was no external temperature sensor installed on the seawater intake.

Data were acquired every 30 seconds for the duration of the cruise and salinity samples were taken periodically throughout the cruise for calibration from an outlet in the flowthrough system located less than 3 m from the SBE-45.

Temperature Calibration

Data from the SBE-45 temperature sensor were used as a measure of the intake seawater temperature, with an offset correction applied after comparing it with the 6 dbar CTD temperature data. This sensor was last calibrated at Sea-Bird on 7 June 2006.

Nominal Conductivity Calibration

Sea-Bird conductivity sensor #0082 was calibrated at Sea-Bird on 7 June 2006. All conductivity data from the thermosalinograph were calibrated with coefficients obtained from this calibration. However, all the final salinity data reported here were calibrated against bottle data as explained below.

Data Processing

Daily files containing air, water and navigation data recorded every 30 seconds were concatenated and the relevant fields output in a format similar to that used in thermosalinograph data collected during HOT cruises. The data were then screened for gross errors, with upper and lower bounds of 18 °C and 35 °C for temperature and 3 Siemens m^{-1} and 6 Siemens m^{-1} for conductivity. There were no points outside the valid temperature and conductivity ranges and no gross errors detected.

A 5-point running median filter was used to detect one or two point temperature and conductivity glitches in the thermosalinograph data. Glitches in temperature and conductivity detected by the 5-point median filter were immediately replaced by the median. Threshold values of 0.3 °C for temperature and 0.1 Siemens m^{-1} for conductivity were used for the median filter. No points were replaced after running the median filter. A 3-point triangular running mean filter was used to smooth the temperature and conductivity data after passing the glitch detection.

The thermosalinograph aboard the R/V *Roger Revelle* was set to record data every 30 seconds, but occasionally, due to an error in the acquisition software rounding routine, a record is written at a longer interval. There were 1750 timing errors in total, most of them between 30-32 seconds.

Data were visually scanned to flag glitches probably caused by contamination due to the introduction of bubbles to the flowthrough system during rough conditions. Of a total of 18940 data points, 6 conductivity data points were flagged as bad.

Bottle Salinity and CTD Salinity Comparisons

The thermosalinograph salinity was calibrated by comparing it to bottle salinity samples drawn from a water intake next to the thermosalinograph. Thirteen salinity samples were collected and

analyzed as described in Section 4.B.1. The comparison was made in conductivity in order to eliminate the effects of temperature. The conductivity of the bottle was computed using the salinity of the bottle, thermosalinograph temperature and a pressure of 6 dbar, which includes the pressure of the pump.

Salinity samples were drawn from the flowthrough system, located less than 3 m from the SBE-45 and consequently there should be virtually no delay between when the water passes through the thermosalinograph and it being sampled. A 90 second average centered on the sample draw time was chosen for processing purposes.

The CTD salinity data at 6 dbar was used to compare with the thermosalinograph conductivity. Using the thermosalinograph temperature data and a pressure of 6 dbar the CTD conductivity was calculated for the 16 casts conducted while the thermosalinograph was running. One CTD cast (station 2 cast 1) was excluded from the processing as it was an obvious outlier. The SBE-45 conductivity sensor had a mean offset of 2 $x10^{-3}$ Sm^{-1} with respect to the CTD data, and drifted at a rate of $1.14x10^{-4}$ Sm^{-1} day^{-1} over the duration of the cruise. The reason for this drift is unknown.

A cubic spline was fit to the time series of the differences between the bottle and thermosalinograph conductivity and a correction was obtained for the thermosalinograph conductivities. Salinity was calculated using these corrected conductivities, the thermosalinograph temperatures, and 6-dbar pressure. After correction, the mean difference between the bottle and thermosalinograph salinities was 0.0000 with a standard deviation of 0.001. The mean CTD - thermosalinograph difference was -0.002 with a standard deviation of 0.001.

CTD Temperature Comparisons

There were 16 CTD casts conducted during the WHOTS-3 cruise. The 6 dbar CTD temperature data were used to compare with the thermosalinograph. Since there was no remote temperature sensor in the seawater intake during this cruise, the SBE-45 temperature data were used as a measure of the water temperature with an offset correction of -0.242 °C derived from the 6 dbar CTD temperature comparisons. Temperature data for the whole record were subsequently flagged as uncalibrated data.

D. Shipboard ADCP

1. WHOTS-2 Deployment Cruise

Currents measured by the Narrow Band 150 kHz ADCP and the Ocean Surveyor 75 kHz ADCP were processed by the using the CODAS ADCP processing suite by J. Hummon. Horizontal velocity data, latitude and longitude were processed with 5 minute ensemble averages and 8 m depth resolution, and 5 min ensemble averages and 16 m depth resolution for the NB150 and OS75 ADCPs respectively. In the final datasets there was a discrepancy between the time and

position of the ship as recorded by each ADCP system. Upon consultation with J. Hummon it was found that the CODAS software does not cross reference time from each ADCP which is set locally by the acquisition computer on board the ship. Time from the NB150 was 5 integer days slow and this was corrected for. The OS75 operated continuously throughout the cruise but data from the NB150 stops approximately 17 hours before the ship returned to port. This coincides with the arrival at Station 16, a reoccupation of eddy center on the return leg of the cruise (see Figure 6-1). The times of the datasets from the NB150 and the OS75 are shown in Table 4.8.

Table 4.8 ADCP record times (UTC) for the Narrow Band 150 kHz and the Ocean Surveyor 75 kHz ADCP during the WHOTS-2 cruise.

WHOTS-2	**NB150***	**OS75**
File beginning time	24-Jul-2005 02:20	24-Jul-2005 02:45
File ending time	30-Jul-2005 00:02	30-Jul-2005 17:42

* Adjusted time

2. WHOTS-3 Deployment Cruise

ADCP Data from the R/V *Roger Revelle* were acquired and processed in real time with CODAS software. Post processing of the data has not been completed at the time of writing this report. The ADCP was initially configured as tabulated in Table 2.5 but the dataset used had ensemble averages of 15 minutes and not the original 5 minutes. It is not clear why there is this inconsistency with the data and the metadata. The ADCP operated for the entirety of the cruise and the file start and end times are shown in Table 4.9.

Table 4.9 ADCP record times (UTC) for the Narrow Band 150 kHz ADCP during the WHOTS-3 cruise.

WHOTS-3	**NB150**
File beginning time	23-Jun-2006 03:00
File ending time	29-Jun-2006 17:47

5. Moored Instrument Observations.

A. SeaCAT and MicroCAT data processing procedures

The SeaCAT's and MicroCAT's temperature, conductivity and pressure sensors (when available) were calibrated at Sea-Bird prior to their respective deployments on the dates shown in Table 5.1. The internally recorded data from each instrument were retrieved on board of the ship

after the mooring recovery, and the nominally calibrated data were plotted for a visual assessment of the data quality. The data processing included checking the internal clock data, pressure sensor drift correction, temperature sensor stability, and conductivity calibration against CTD data from casts conducted near the mooring during HOT cruises. The detailed processing procedures are described in this section.

Table 5.1 WHOTS-1 and -2 MicroCAT / SeaCAT temperature sensor calibration dates, and sensor drift during deployments.

Sea-Bird Serial	**Pre-deployment calibration**	**Post-recovery calibration**	**Total Temperature drift during WHOTS deployment (m^{o}C)**	
			1	**2**
39-1447	6/8/2004	Not Calibrated	-	
37SM485-3601	4/21/2004	3/3/2006	0.42	
37SM485-3602	4/21/2004	3/3/2006	0.58	
163452-0801	9/29/2003	8/16/2005	1.25	
165807-1085	7/13/2004	8/16/2005	0.06	
165807-1087	9/29/2003	8/16/2005	0.35	
165807-1088	9/29/2003	8/16/2005	0.54	
165807-1090	10/2/2003	8/16/2005	0.70	
165807-1092	10/2/2003	8/17/2005	1.18	
165807-1095	9/29/2003	8/17/2005	0.85	
165807-1097	5/28/2004	8/17/2005	0.29	
165807-1099	10/7/2003	8/17/2005	0.23	
165807-1100	10/5/2003	8/17/2005	2.31	
37SM31486-2451	2/24/2004	8/18/2006	0.84	0.80
37SM31486-2769	2/25/2004	8/10/2005	1.71	1.63
37SM31486-2965	2/25/2004	8/18/2006	2.09	1.99
37SM31486-3381	2/25/2004	8/10/2005	-0.18	-0.17
39-1446	5/12/2004	1/24/2007		-0.32

37SM485-1836	8/28/2004	1/25/2007		0.11
37SM485-3604	8/28/2004	1/25/2007		0.12
37SM31486-3618	6/10/2004	8/17/2006		1.18
37SM31486-3617	6/10/2004	8/18/2006		0.36
37SM31486-3619	6/10/2004	8/17/2006		1.00
37SM31486-3620	6/10/2004	8/17/2006		0.36
37SM31486-3621	6/10/2004	8/17/2006		1.18

1. Internal Clock Check and Missing Samples

After each recovery and before the data logging was stopped, the SeaCATs and MicroCATs were placed in a cold freshwater bath to create a spike in the data, to check for any problem in the internal clocks, and for any missing samples (Table 3.2 and Table 3.4). In addition, the MicroCATs used in the second deployment were also placed in a cold freshwater bath before deployment to create a spike in the data (Table 3.3). The cold freshwater spike was detected in the sensor's data by a sudden decrease in temperature and salinity. For all the instruments, the clock time of this event matched correctly the time of the spike (within the sampling interval of each instrument). No missing samples were detected for any of the instruments.

2. Pressure Drift Correction and Pressure Variability

Some of the MicroCATs used in the moorings were outfitted with pressure sensors (*Table 3.1* and Table 3.2). A bias was detected in the pressure sensors by comparing the on-deck pressure readings before deployment and after recovery. Table 5.2 shows the magnitude of the bias for each of the sensors before and after deployment. To correct for this offset, a linear fit between the initial and final on-deck pressure offset as a function of time was obtained, and subtracted from each sensor. Figure 5-1 and Figure 5-2 and show the linearly corrected pressures measured by the MicroCATs during each of the deployments. For all the sensors, the mean difference from the nominal instrument pressure (based on the deployed depth) was less than 1 dbar. The standard deviation of the pressure for the duration of the record was also less than 1 dbar for all sensors, with the deeper sensors showing a larger standard deviation. The range of variability for all sensors was about ± 3 dbar, with some few extreme cases when the variability was of up to 5 dbar.

The causes of pressure variability can be several, including density variations; horizontal dynamic pressure (not only due to the currents, but also due to the motion of the mooring); mooring position, etc. The effect of the mooring position on the pressure measured by the

sensors can be observed in Figure 5-3 and Figure 5-4 respectively for each of the deployments. These figures show the distance between the buoy and its anchor (calculated from the buoy's Argos positions), as a function of pressure for each of the instruments. The red line in the plot is a quadratic fit to the median pressure calculated every 0.2 km distance bins. For the deep instruments, these plots show a decrease in pressure of up to 1 dbar as the distance from the anchor increases. This pressure decrease is caused by the rising of the instruments when the mooring line deviates from its vertical position as it is being pulled by the anchor, and it is more noticeable for the sensors located deeper in the line.

Table 5.2 Pressure bias of MicroCATs with pressure sensor.

Deployment	Depth (m)	Sea-Bird Serial #	Bias before deployment (dbar)	Bias after recovery (dbar)
WHOTS-1	85	37SM31486-2451	-0.1	-2.5
WHOTS-1	105	37SM31486-2769	0.05	0.05
WHOTS-1	155	37SM31486-2965	0.04	-1.9
WHOTS-2	45	37SM31486-2965	-1.7	-2.0
WHOTS-2	85	37SM31486-3670	0.02	-0.3
WHOTS-2	105	37SM31486-3669	0.04	0.2
WHOTS-2	120	37SM31486-2451	-2.25	-4.4
WHOTS-2	155	37SM31486-3668	0.06	-0.05

A measure of the relative instrument vertical displacements with respect to each other is given by the differences between the sensor's pressures. Figure 5-5 through Figure 5-8 show these differences for all the possible sensor pair combinations for each deployment. Scatter plots of the pressure between these same pairs of sensors give an indication of the relation between the sensors' vertical displacements (Figure 5-9 through Figure 5-11). Surprisingly only two sensor pairs during the WHOTS-2 deployment: 85-45 m, and 155-105 m (Figure 5-10 and Figure 5-11 showed a noticeable pressure correlation. In addition, it is evident from the pressure difference plots (Figure 5-6 and Figure 5-8) that this correspondence happened mostly during the second half of the deployment, when the pressure differences for both pairs were nearly constant. Other sensor pairs during WHOTS-2 also showed instances when the pressure differences were nearly constant, such as 155-45 m around day 590 (Figure 5-6), and 155-120 m near day 610 (Figure 5-8), although these instances were very short lived.

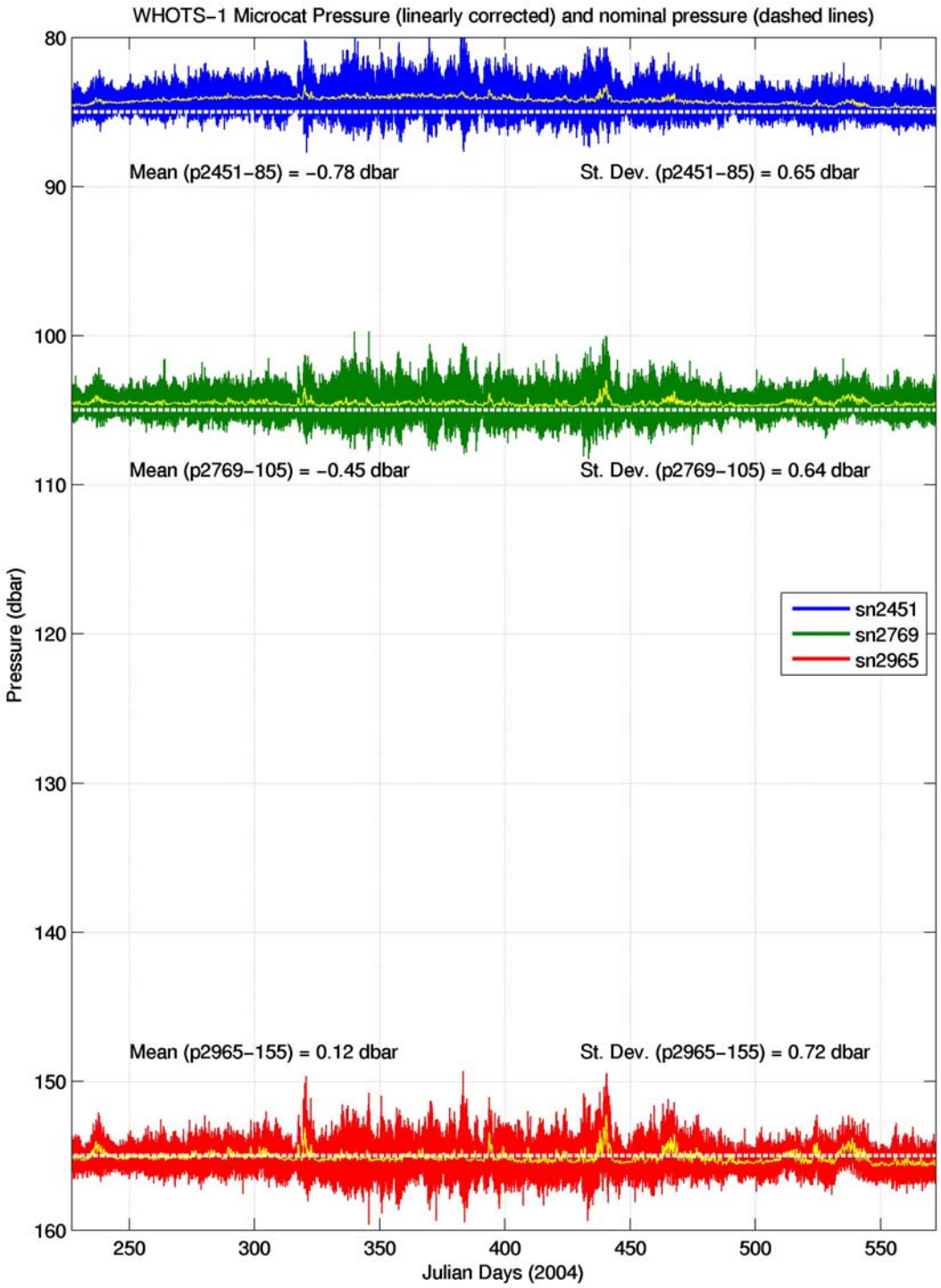

Figure 5-1. Linearly corrected pressures from MicroCATs during WHOTS-1 deployment. The yellow line is a 5-hour running mean. The horizontal dashed line is the sensor's nominal pressure, based on deployed depth.

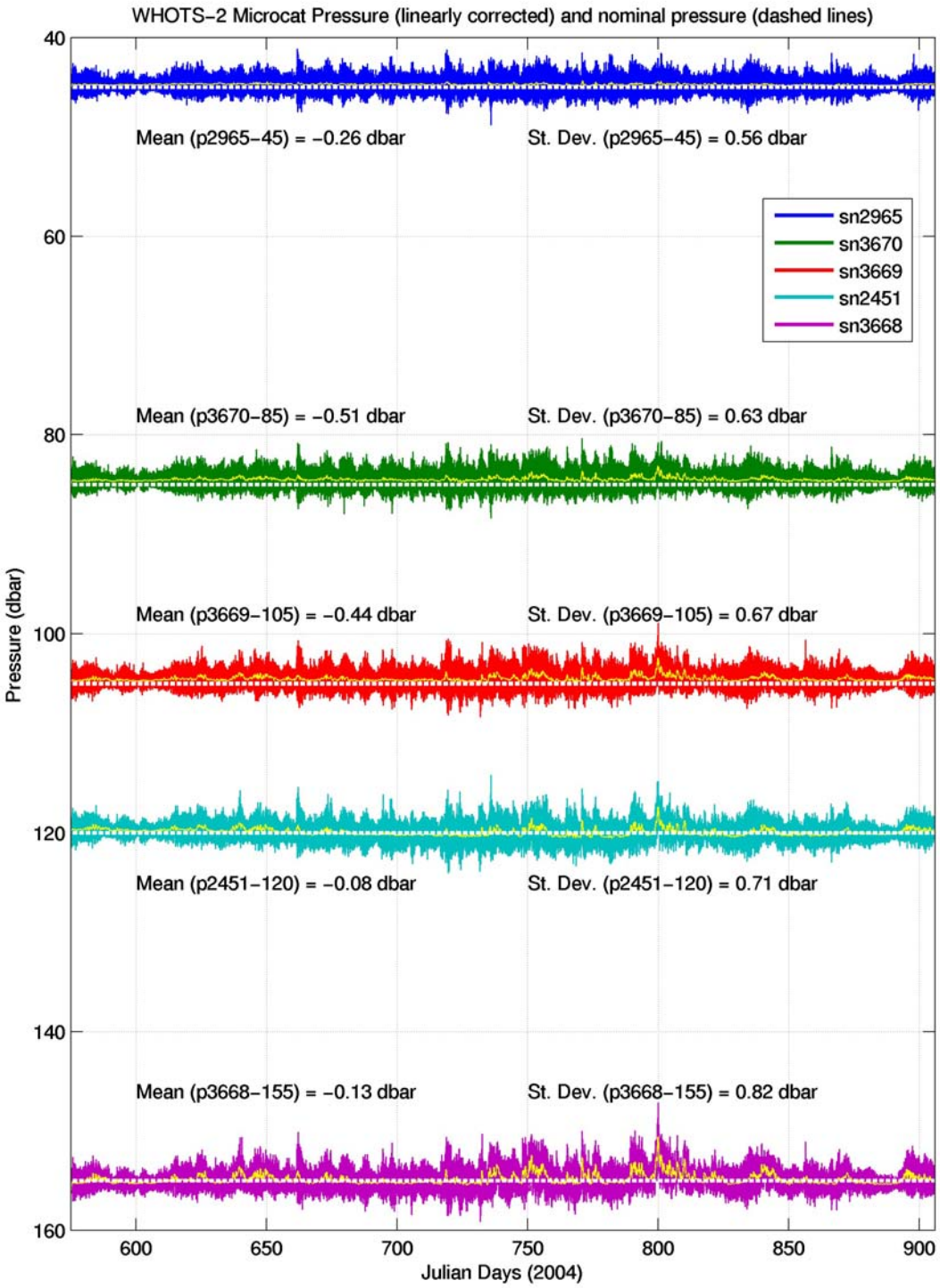

Figure 5-2. Same as Figure 5.1 but for WHOTS-2 deployment.

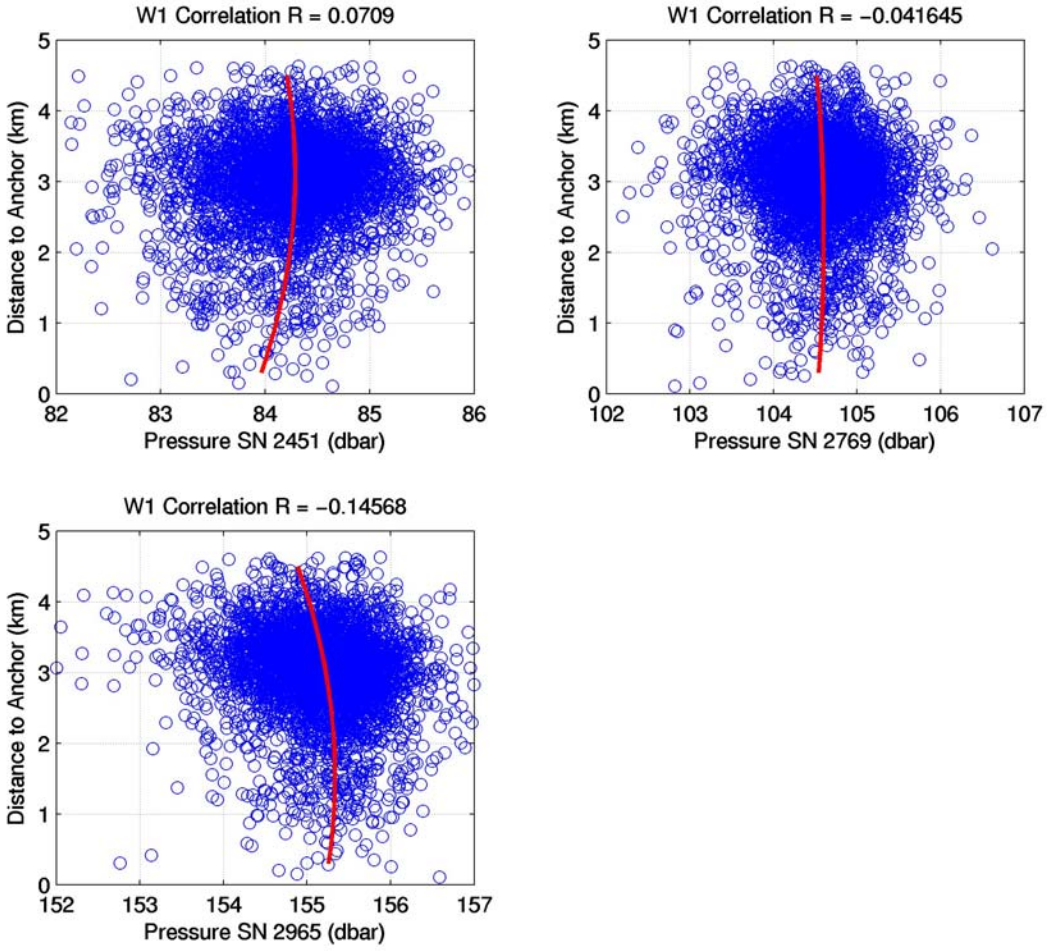

Figure 5-3. Scatter plots of the distance of the buoy to its anchor as a function of the pressure measured by each of the MicroCATs during WHOTS-1 (blue circles). The red line is a quadratic fit to the median pressure at each distance bin, for 0.2 km bins.

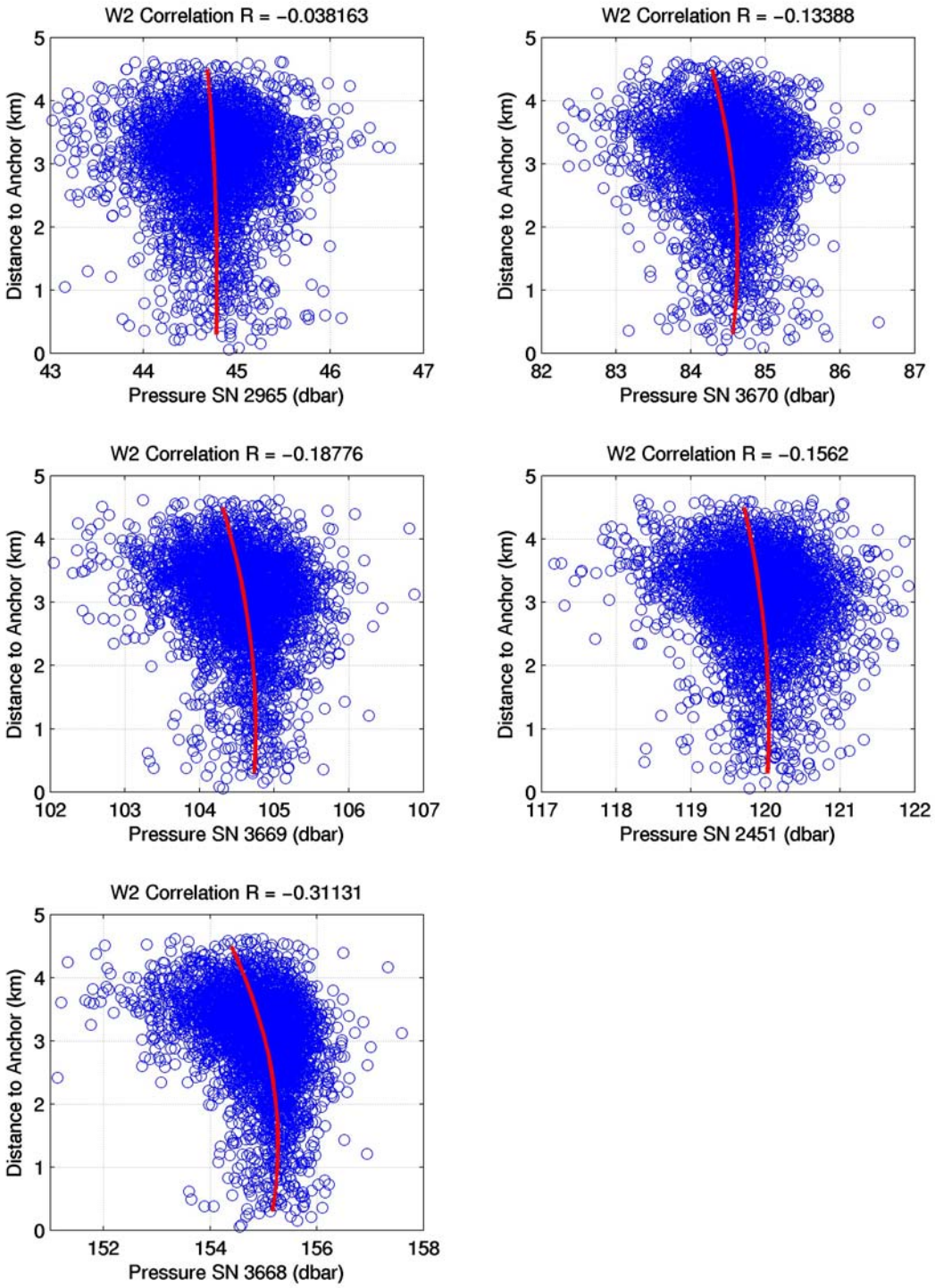

Figure 5-4. Same as Figure 5.3, but for the WHOTS-2 deployment.

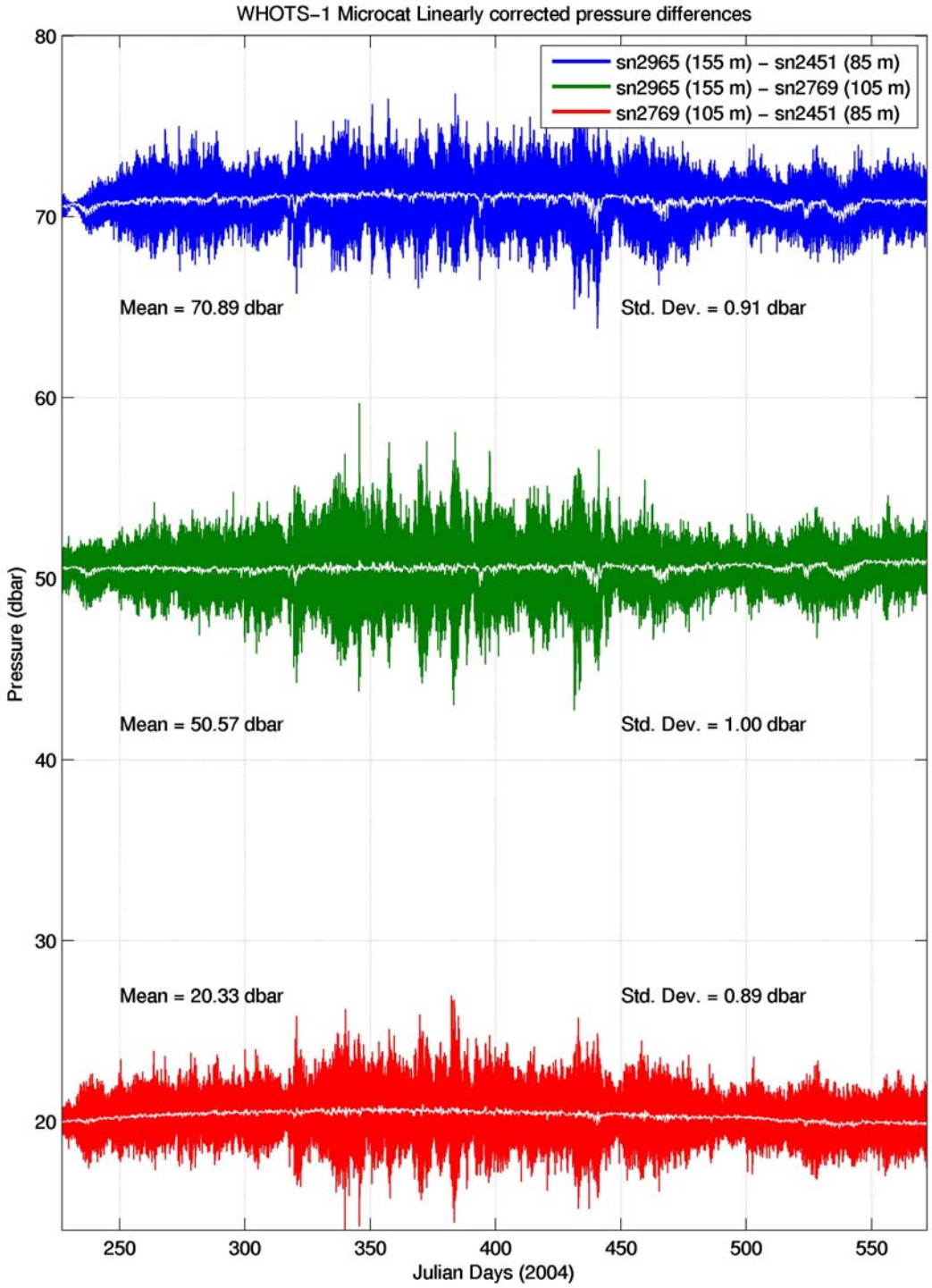

Figure 5-5. Pressure differences between MicroCATs with pressure sensors during WHOTS-1 deployment. The white line is a 5-hour running mean of the differences.

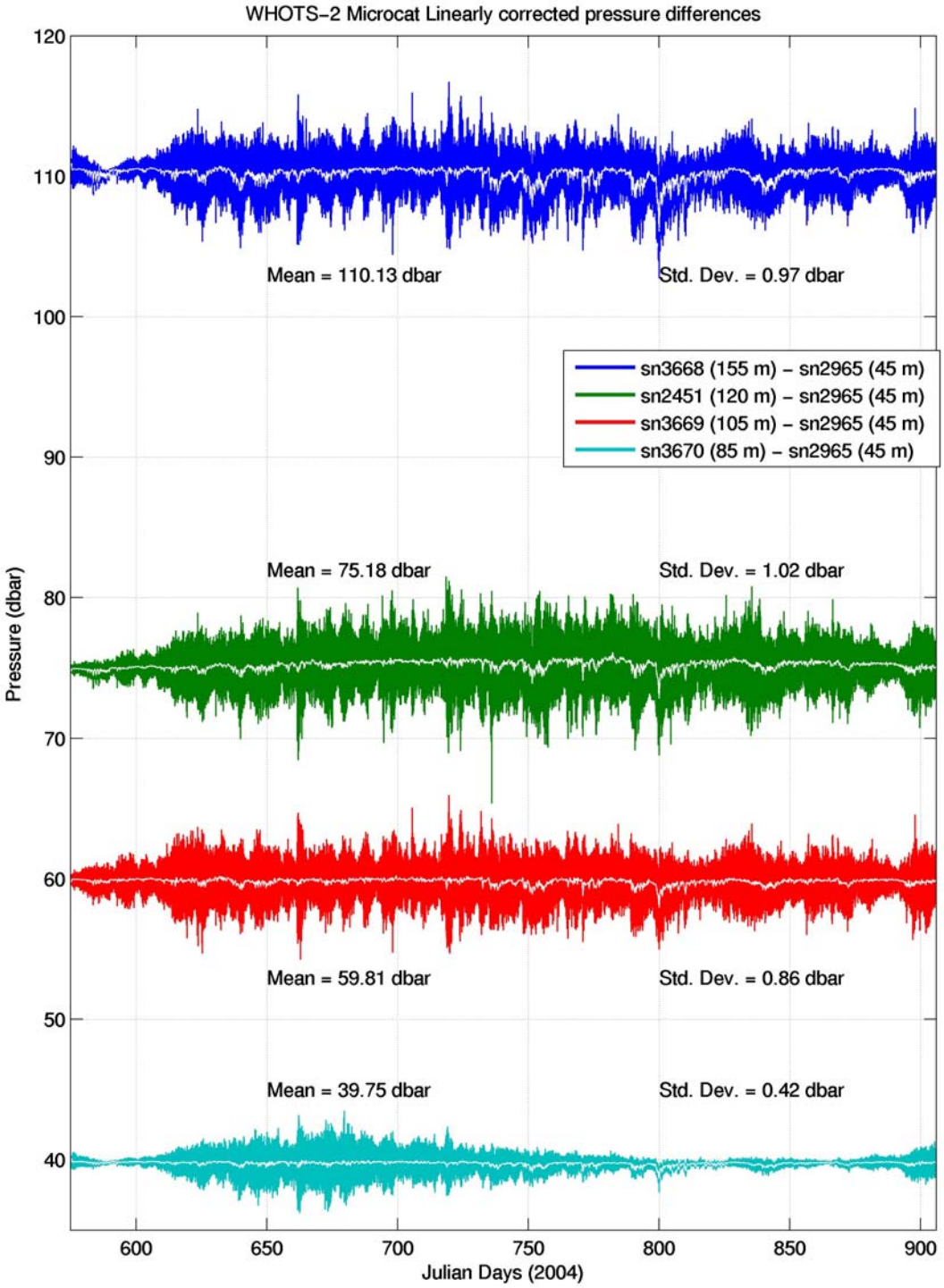

Figure 5-6 Same as in Figure 5.5 but for WHOTS-2 deployment.

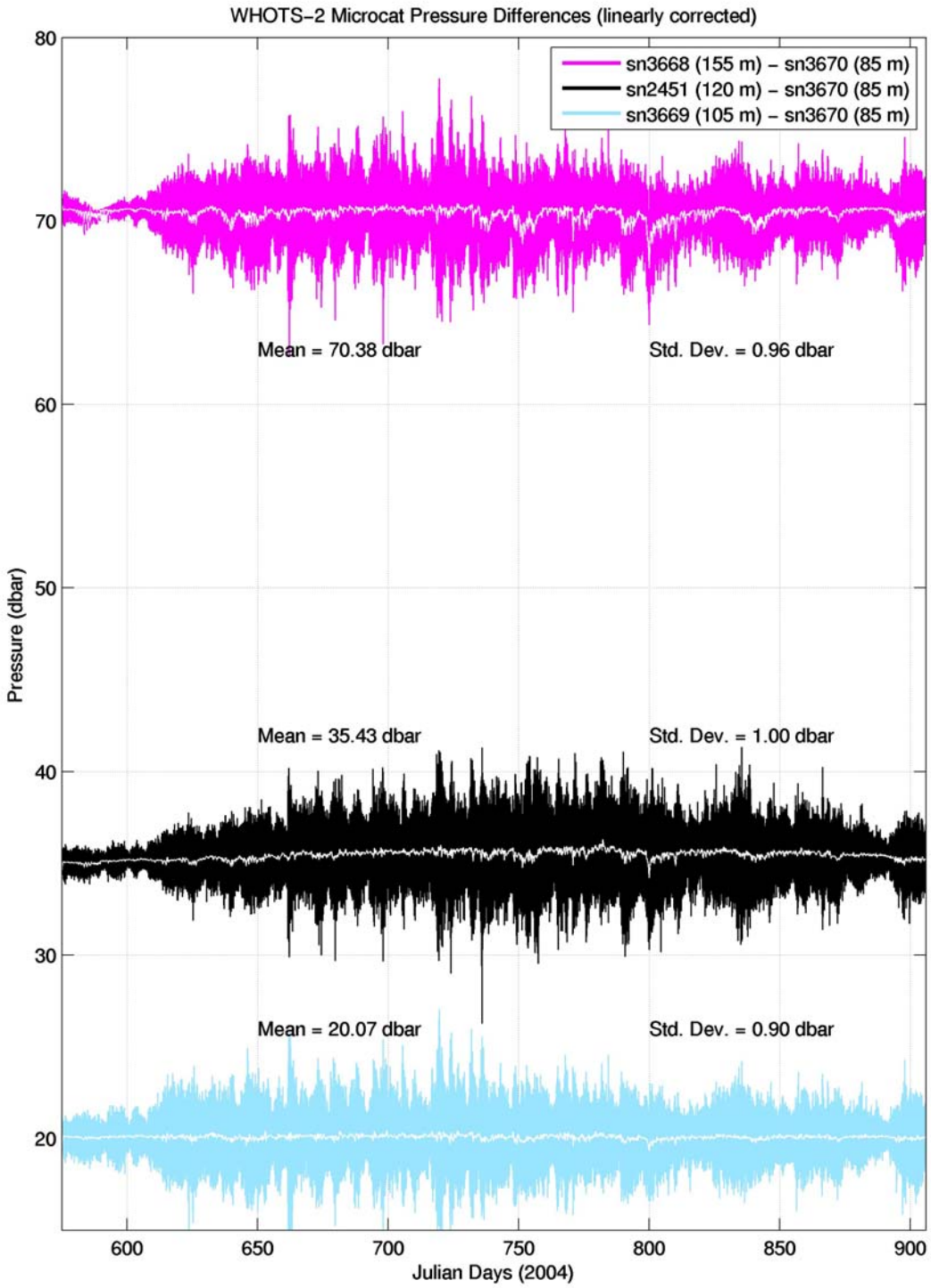

Figure 5-7 (Contd. from Fig. 5.6.)

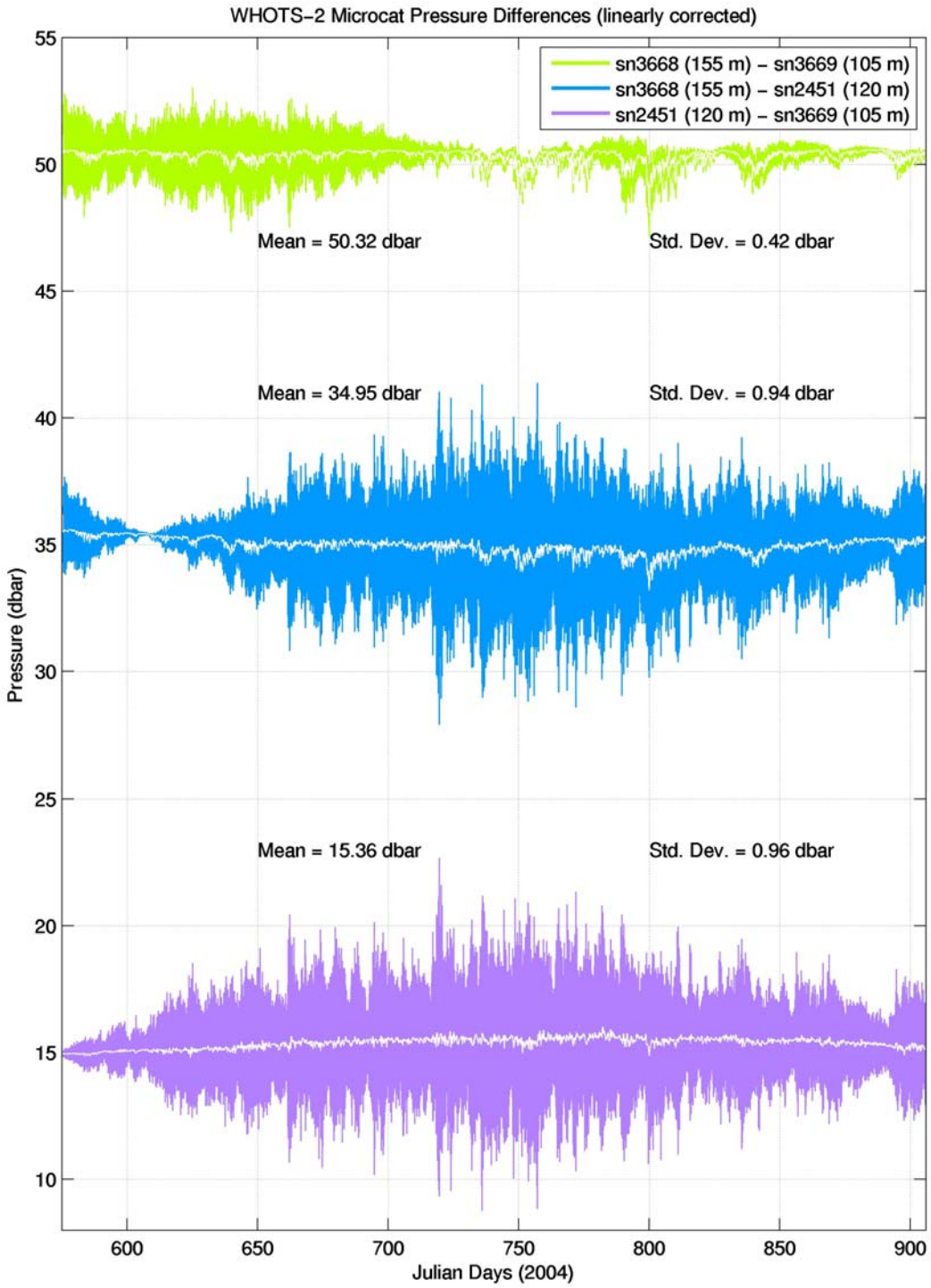

Figure 5-8 (Contd. from Fig. 5.6)

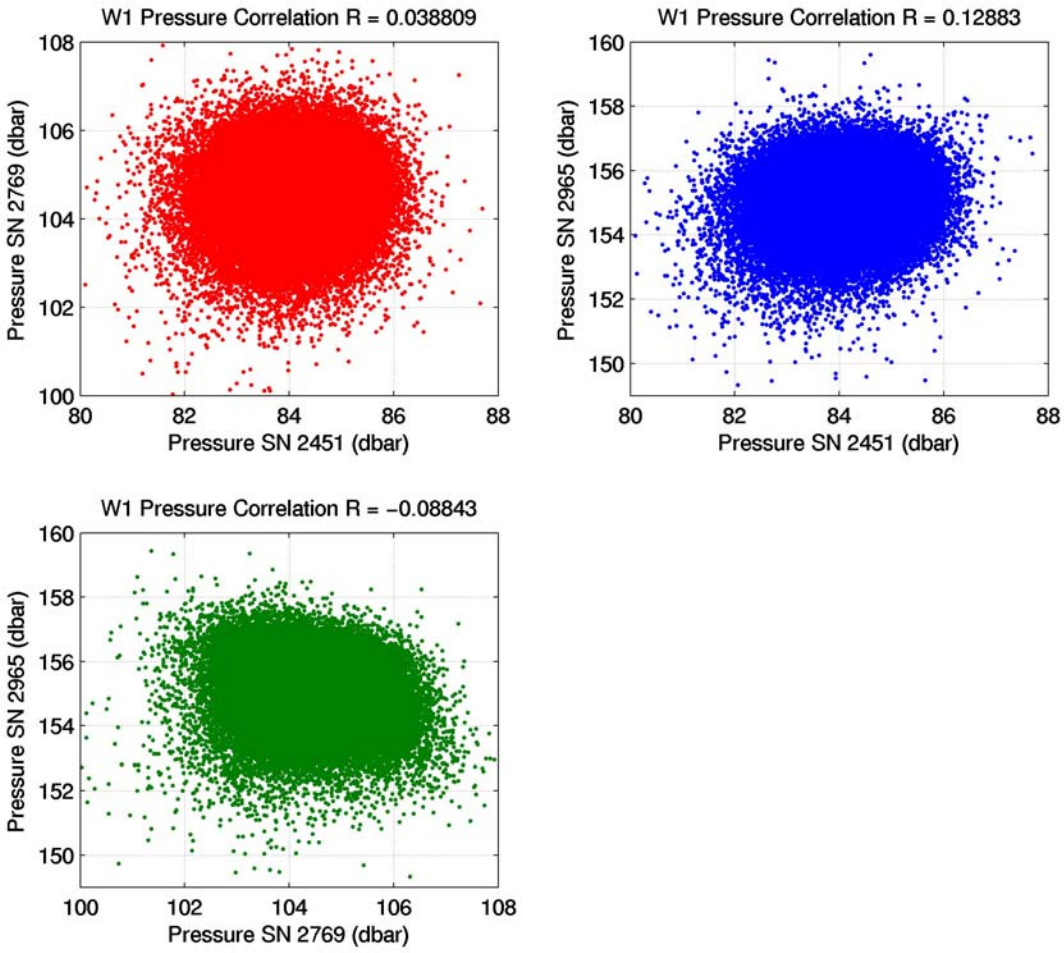

Figure 5-9. Scatter plot of pressure between MicroCATs during WHOTS-1 deployment. The combinations correspond to those in Figure 5.5.

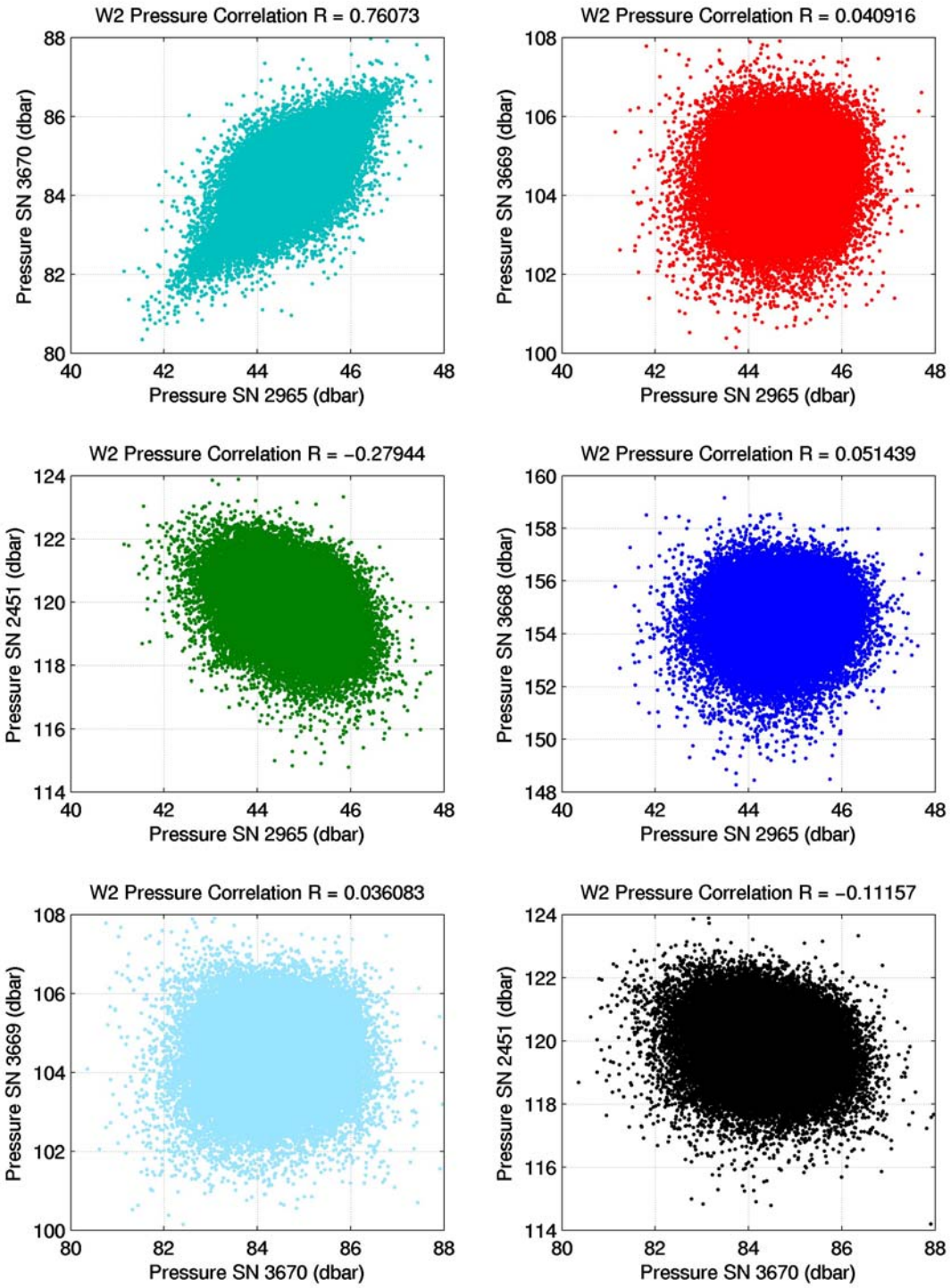

Figure 5-10. Same as in Figure 5.9, but for WHOTS-2 deployment. The sensor combinations correspond to those in Figures 5.6 through 5.8.

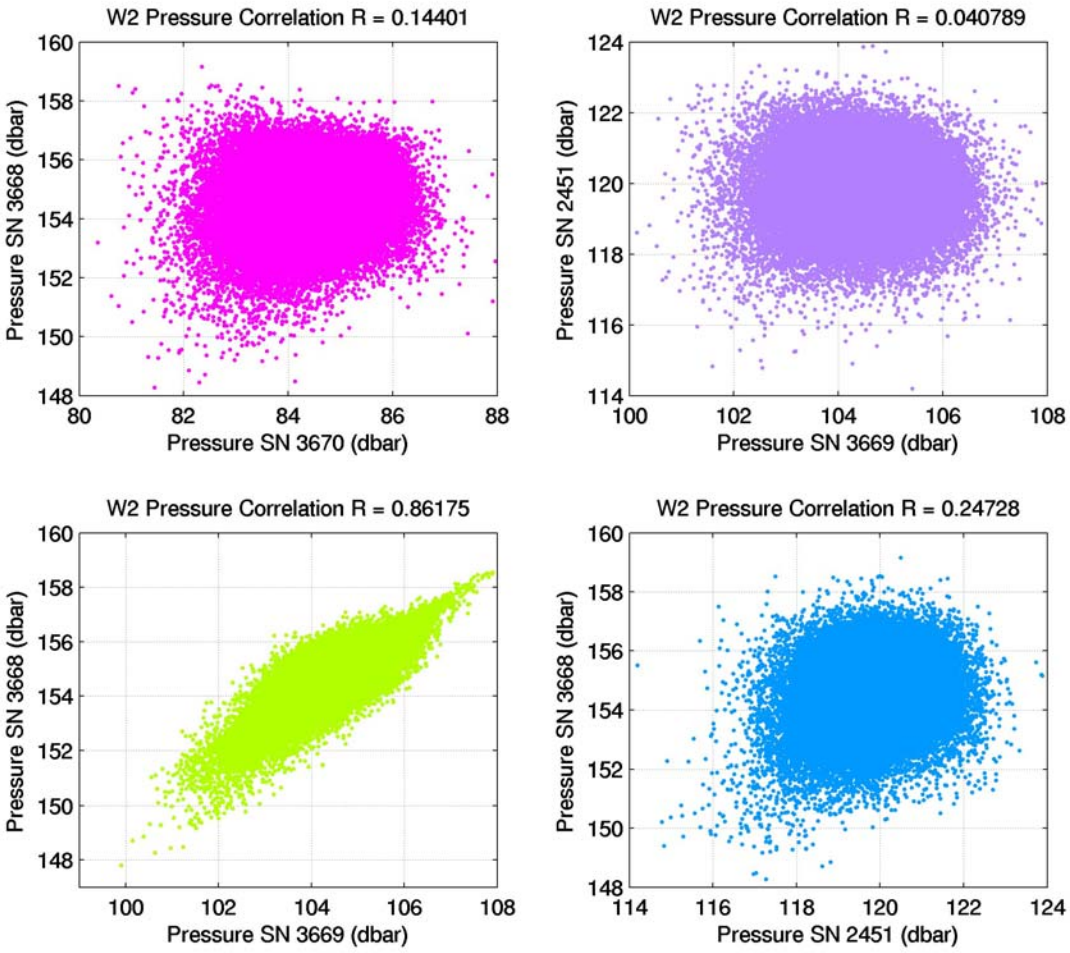

Figure 5-11. (Contd. from Figure 5.10)

3. Temperature Sensor Stability

The SeaCAT and MicroCAT temperature sensors were calibrated at Sea-Bird before and after each deployment, except for four instruments that were re-deployed for WHOTS-2 (see Table 5.1). Sea-Bird's evaluation of each sensor's drift was used to calculate the temperature offset for the duration of the deployment (Table 5.1). These values turned out to be insignificant (not higher than 0.0025 °C for all sensors), and no correction was applied to the data. Comparisons between the CTD and SeaCAT/MicroCAT data from casts conducted near the mooring during HOT cruises confirmed that the temperature drift of the moored instruments was insignificant.

A temperature comparison between the two MicroCATs installed below the buoy during WHOTS-1 show the stability of the sensors for the duration of the deployment (Figure 5-20, upper panel).

A temperature comparison between one of the WHOTS-1 near-surface MicroCATs (SN 3602) and the surface temperature sensor (SN 1447) is shown in Figure 5-12. A similar comparison between the near-surface MicroCAT SN 3604 and the surface temperature sensor (SN 1446) during WHOTS-2 is shown in Figure 5-13. Both comparisons show a mean surface temperature 0.007 °C lower than the near-surface temperature. In addition, the plots show various instances of large negative values of up to between -0.2 and -0.4 °C. These differences are caused by a decrease in the surface temperature. With the wave and buoy motions and wave breaking, the surface sensor may have measured temperatures from many different depths, including above the surface. Measuring the air temperature often enough could have biased the low temperatures registered by this sensor.

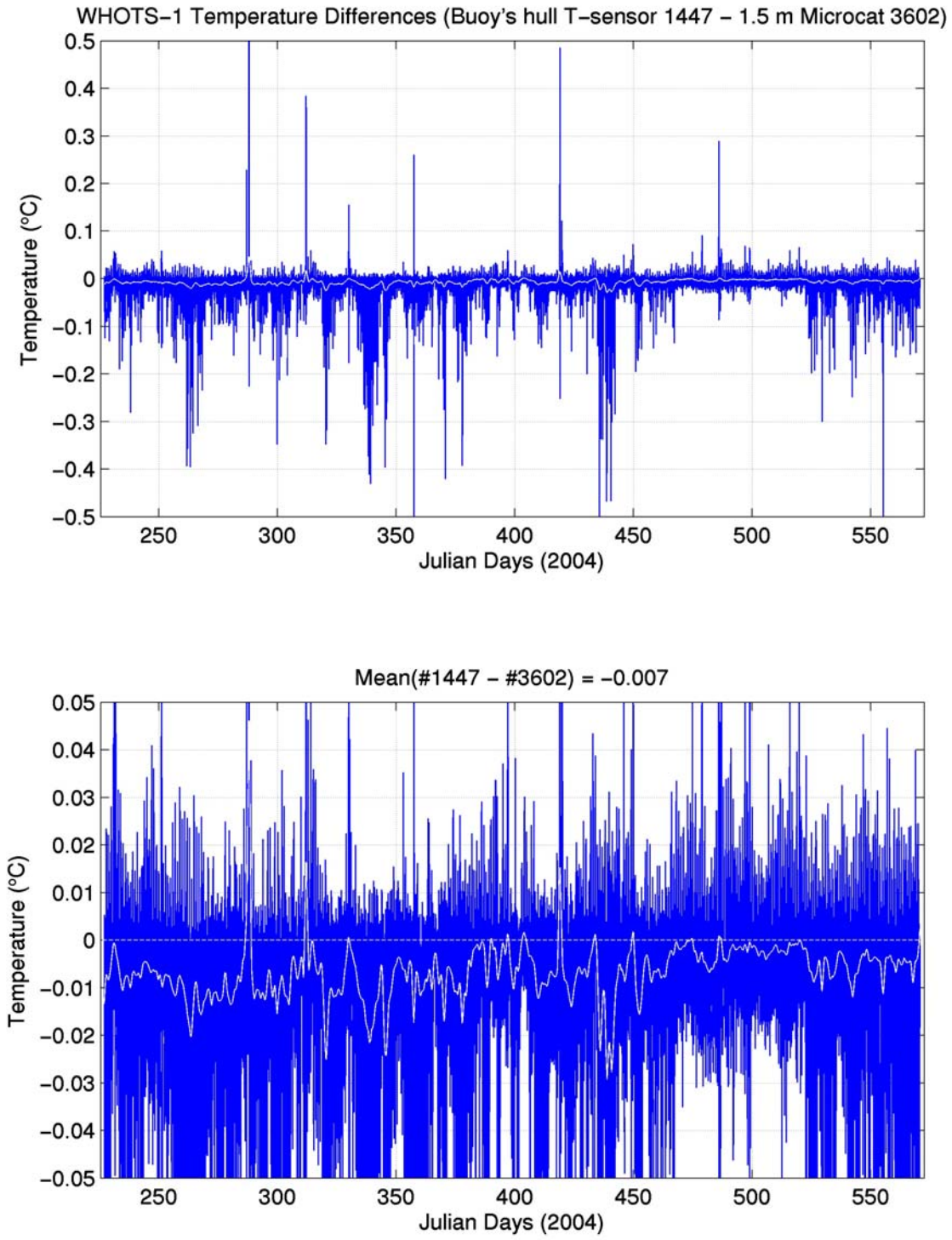

Figure 5-12. Temperature difference between MicroCAT SN 3602 at 1.5 m, and surface temperature sensor SN 1447 during WHOTS-1 deployment (upper panel). The lower panel is a closer look at the same differences. The white line is a 24-hour running mean of the differences.

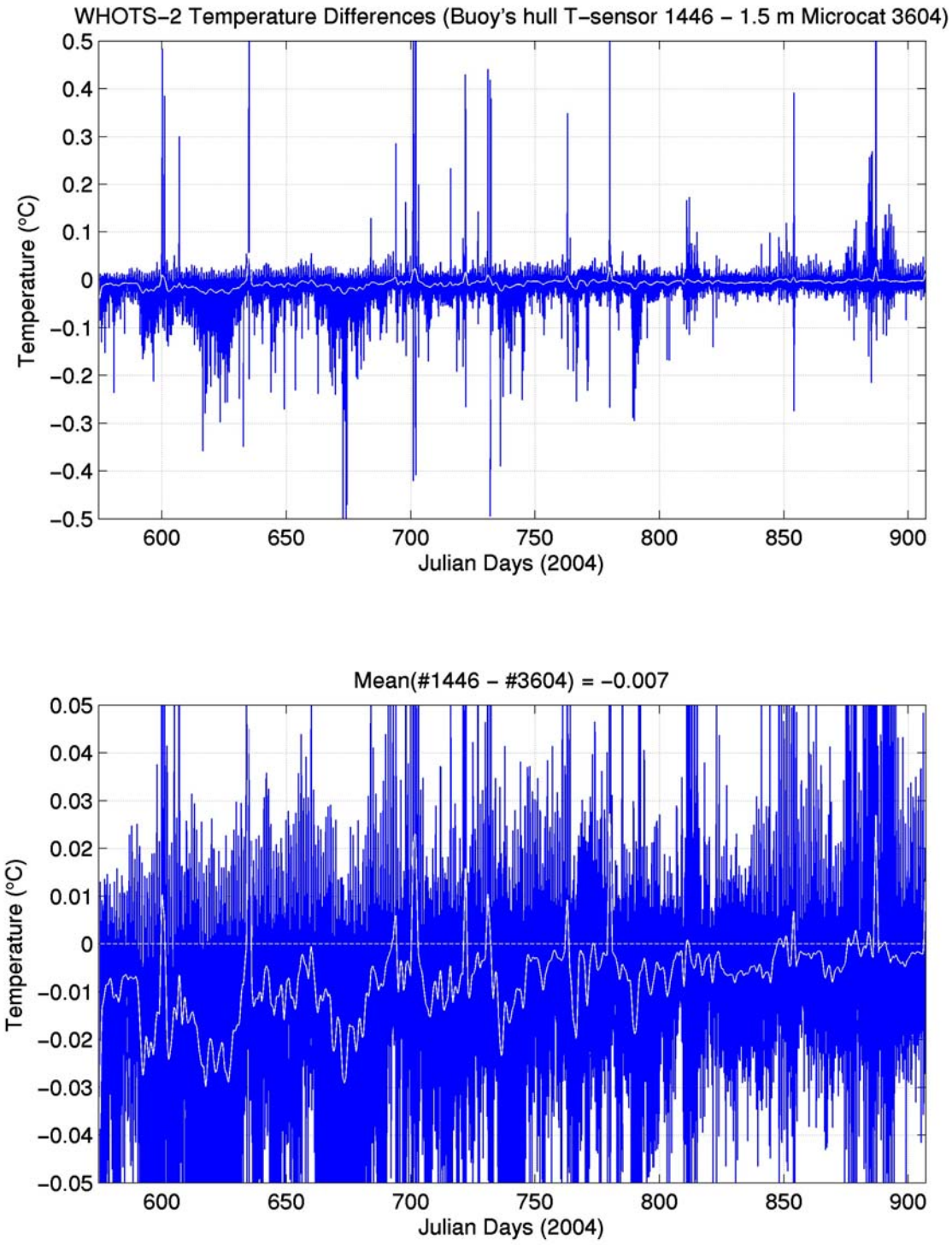

Figure 5-13. Temperature difference between MicroCAT SN 3604 at 1.5 m, and surface temperature sensor SN 1446 during WHOTS-2 deployment (upper panel). The lower panel is a closer look at the same differences. The white line is a 24-hour running mean of the differences.

In addition to the temperature sensors in the Sea-Bird instruments, there were additional temperature sensors in the NGVMs (at 10 and 30 m), and in the ADCP (at 125 m). In order to evaluate the quality of the temperatures from these sensors, comparisons with the temperatures from adjacent SeaCATs or MicroCATs were conducted. First we will show these comparisons for the WHOTS-1 deployment, and the WHOTS-2 comparisons follow.

WHOTS-1 NGVM and ADCP Temperature sensors stability

The upper panel of Figure 5-14 shows the difference between the 10-m NGVM and the 15-m SeaCAT temperatures during WHOTS-1. Also shown for comparison in the lower panel of the figure are the differences between SeaCAT temperatures at 15 and 25 m. The NGVM stopped recording early during the deployment as indicated earlier in this report, in addition the plot shows a temperature offset of nearly 0.1 °C. This offset is due to the NGVM and not to the 15-m SeaCat temperatures, since the differences between the 15 and the 25-m SeaCATs do not show a similar offset. In addition, the NGVM temperature offset does not seem to be constant in time. Rather than trying to correct the temperatures from this NGVM SN 012, we will consider them as questionable.

Temperature differences between the 30-m NGVM and the temperatures from adjacent SeaCATs at 25 and 35-m during WHOTS-1 are shown in Figure 5-15. For comparison, the differences between the SeaCATs temperatures are also shown. These plots indicate that there was no obvious offset in the NGVM temperatures, as the temperature differences from the adjacent SeaCATs during periods when a well-mixed layer was present fluctuate around zero (e.g. during days 350 to 400).

Temperature differences between the 125-m ADCP and the temperatures from adjacent MicroCATs at 120 and 135-m during WHOTS-1 are shown in Figure 5-16. For comparison, the differences between the MicroCATs temperatures are also shown. It is difficult to assess the quality of the ADCP temperature from these comparisons, as these sensors were located at the top of the thermocline, where we expect to find large temperature differences between adjacent sensors. However, an indication of the quality of the ADCP temperatures is given in the upper panel plot, which shows temperatures fluctuating closely around zero during short periods (e.g. days 450-470 and 500-520), when apparently the mixed layer deepened close to these levels (see bottom panel in Figure 5-16).

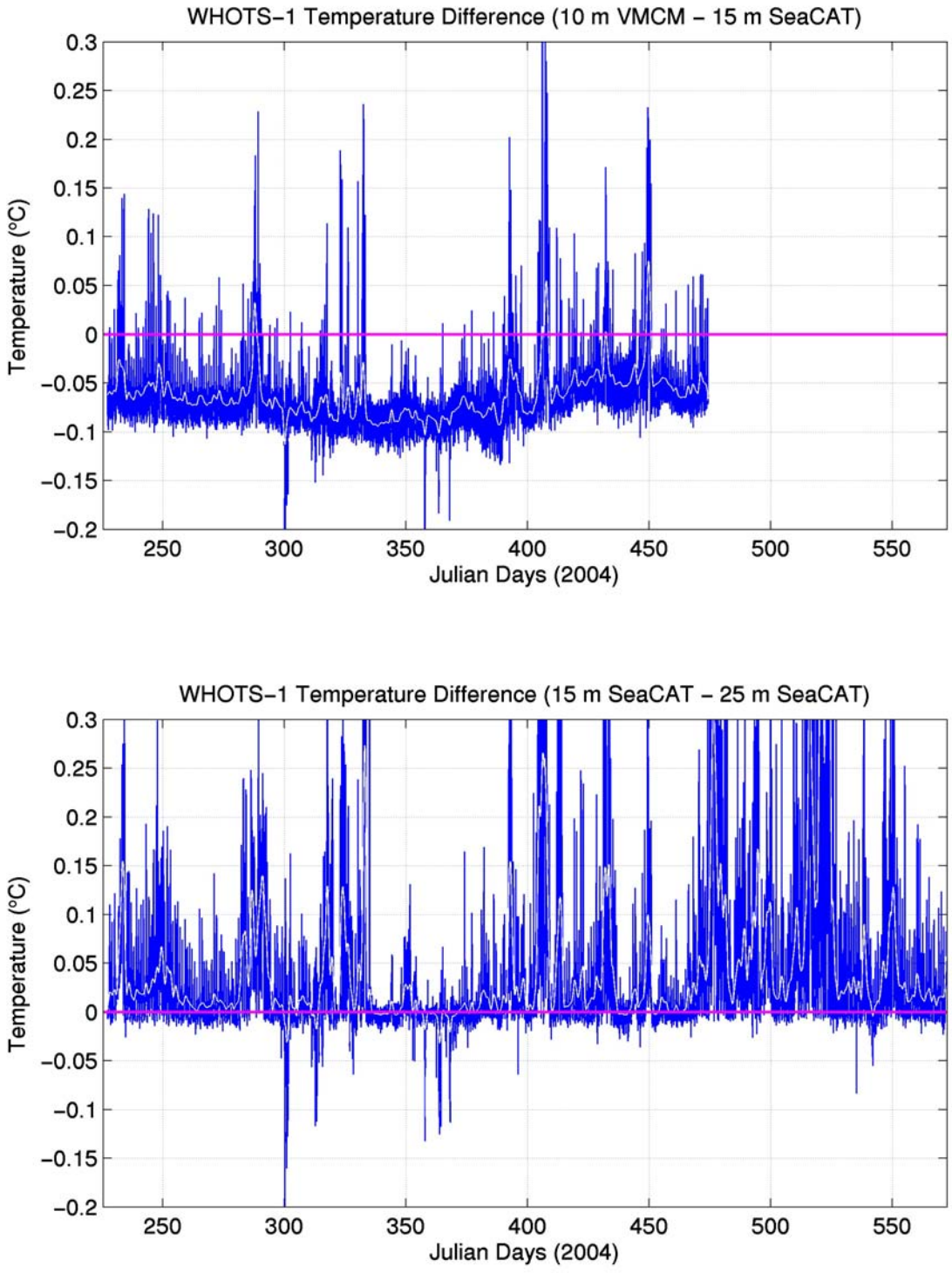

Figure 5-14. Temperature difference between the 10-m NGVM and the 15-m SeaCAT during the WHOTS-1 deployment (upper panel). Temperature difference between the 15-m SeaCAT and the 25-m SeaCAT during the WHOTS-1 deployment (lower panel). The white line is a 24-hour running mean of the differences.

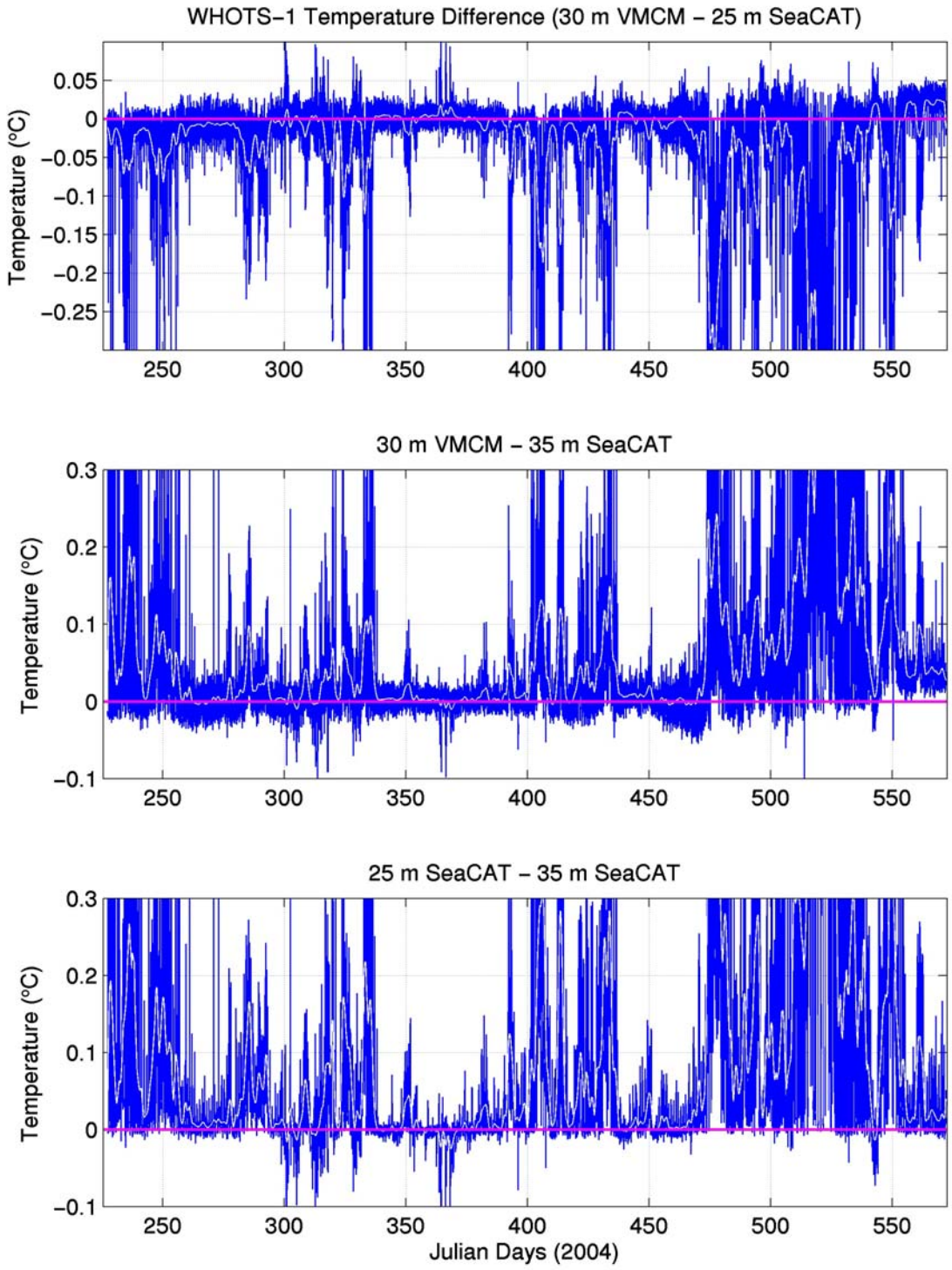

Figure 5-15. Temperature difference between the 30-m NGVM and the 25-m SeaCAT during the WHOTS-1 deployment (upper panel); between the 30-m NGVM and the 35-m SeaCAT (middle panel); and between the 25-m and the 35-m SeaCATs (lower panel). The white line is a 24-hour running mean of the differences.

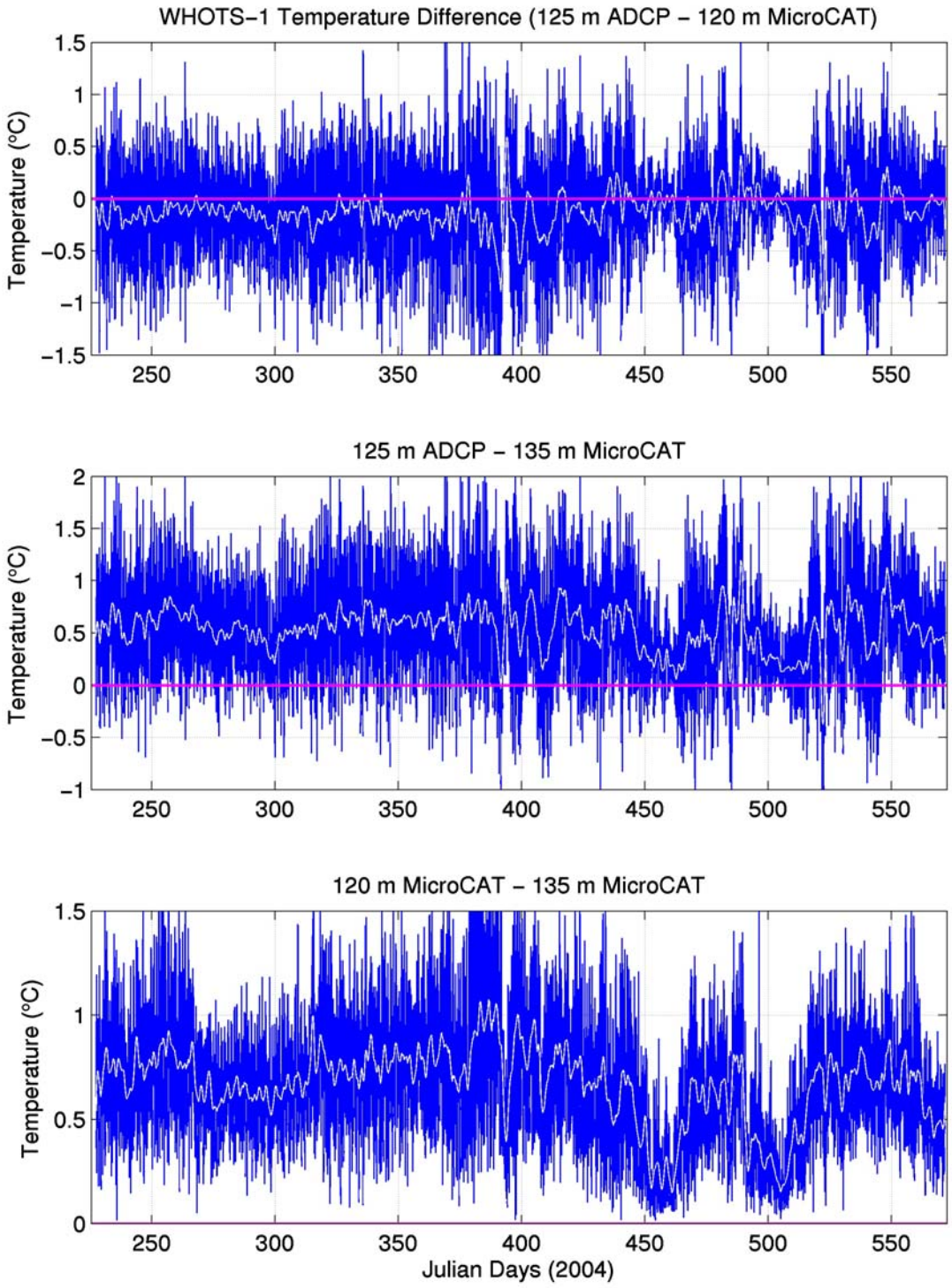

Figure 5-16. Temperature difference between the 125-m ADCP and the 120-m MicroCAT during the WHOTS-1 deployment (upper panel); between the 125-m ADCP and the 135-m MicroCAT (middle panel); and between the 120-m and the 135-m MicroCATs (lower panel). The white line is a 24-hour running mean of the differences.

WHOTS-2 NGVM and ADCP Temperature sensors stability

The upper panel of Figure 5-17 shows the difference between the 10-m NGVM and the 15-m MicroCAT temperatures during WHOTS-2. Also shown for comparison in the lower panel of the figure are the differences between MicroCAT temperatures at 15 and 25 m. The upper plot indicates that the NGVM temperature sensor functioned correctly for the duration of the record, as no noticeable offset was present, and the temperature fluctuations seem to be around zero, as in the differences between the 15 and 25-m MicroCATs.

Temperature differences between the 30-m NGVM and the temperatures from adjacent MicroCATs at 25 and 35-m during WHOTS-2 are shown in Figure 5-18. For comparison, the differences between the MicroCATs temperatures are also shown. These plots indicate that there was a small offset of about 0.01 °C in the NGVM with respect to the adjacent MicroCATs (see top and middle plots). This is particularly obvious during the long period when a relatively well-mixed layer was present during days 650 trough 780. During this period the MicroCATs temperature differences between 25 and 35 m (Figure 5-18 bottom panel) show a running mean of temperature differences fluctuating around the zero line, while the running mean of the differences between the MicroCATs and the NGVM show a 0.01 °C offset.

Temperature differences between the 125-m ADCP and the temperatures from adjacent MicroCATs at 120 and 135-m during WHOTS-2 are shown in Figure 5-19. For comparison, the differences between the MicroCATs temperatures are also shown. It is difficult to assess the quality of the ADCP temperature from these comparisons, as these sensors were located at the top of the thermocline, where we expect to find large temperature differences between adjacent sensors. However, an indication of the quality of the ADCP temperatures is given in the upper panel plot, which shows temperatures fluctuating closely around zero during short periods (e.g. days 800 to 840), when apparently the mixed layer deepened close to these levels (see bottom panel in Figure 5-19).

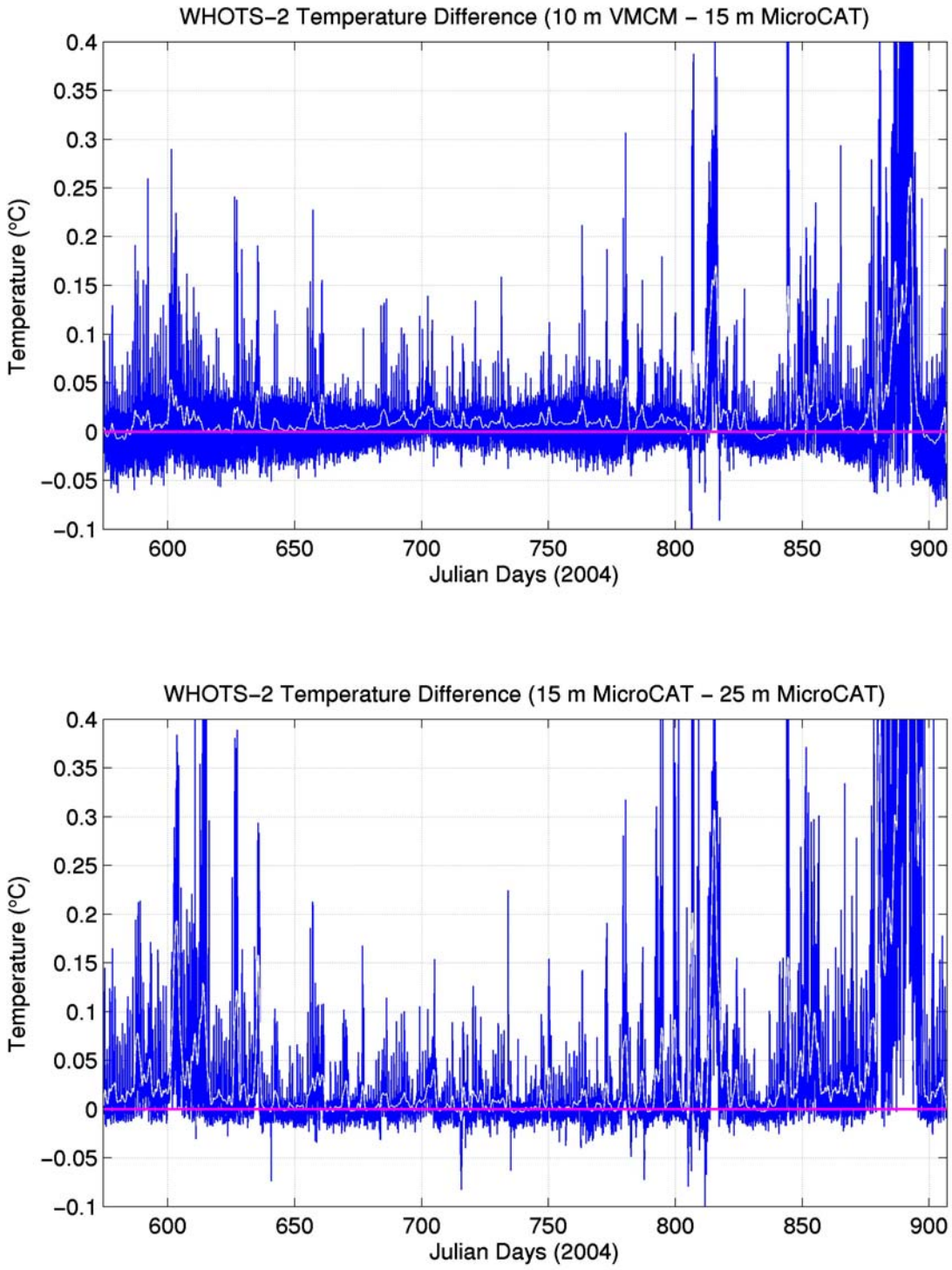

Figure 5-17. Temperature difference between the 10-m NGVM and the 15-m MicroCAT during the WHOTS-2 deployment (upper panel). Temperature difference between the 15-m MicroCAT and the 25-m MicroCAT during the WHOTS-2 deployment (lower panel). The white line is a 24-hour running mean of the differences.

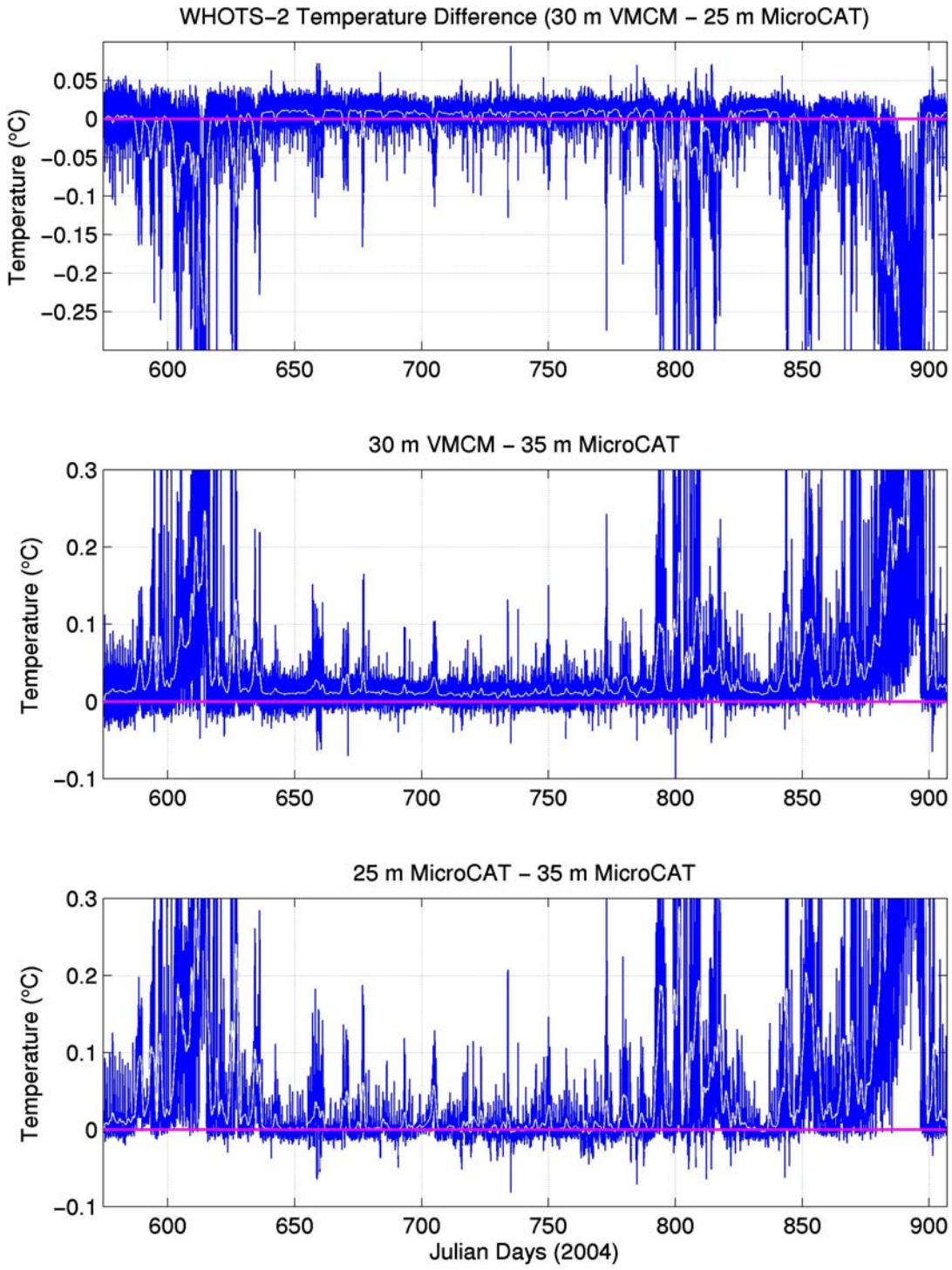

Figure 5-18. Temperature difference between the 30-m NGVM and the 25-m MicroCAT during the WHOTS-2 deployment (upper panel); between the 30-m NGVM and the 35-m MicroCAT (middle panel); and between the 25-m and the 35-m MicroCATs (lower panel). The white line is a 24-hour running mean of the differences.

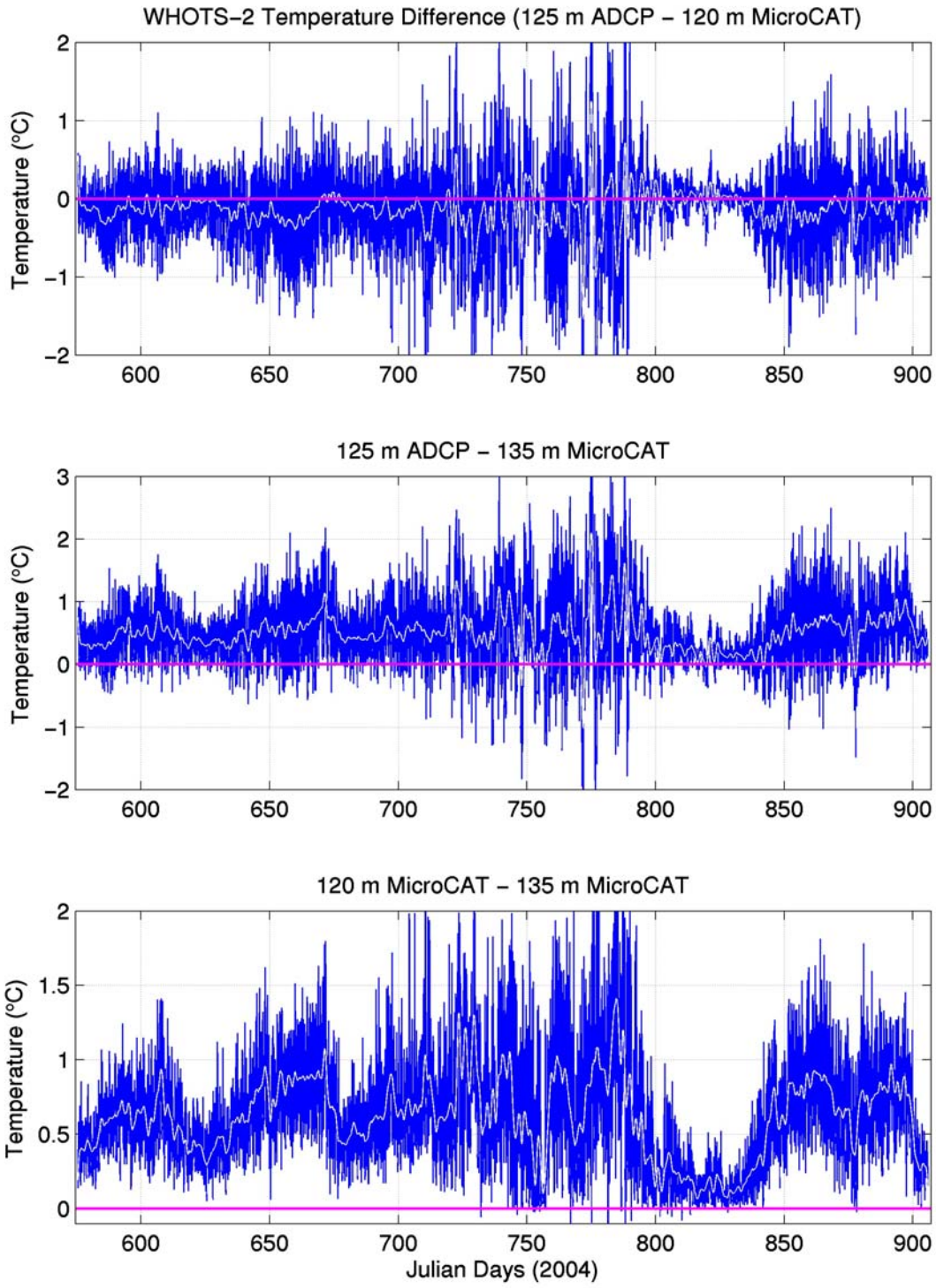

Figure 5-19. Temperature difference between the 125-m ADCP and the 120-m MicroCAT during the WHOTS-2 deployment (upper panel); between the 125-m ADCP and the 135-m MicroCAT (middle panel); and between the 120-m and the 135-m MicroCATs (lower panel). The white line is a 24-hour running mean of the differences.

4. Conductivity Calibration

The results of the Sea-Bird post-recovery conductivity calibrations indicated that some of the SeaCAT and MicroCAT sensors experienced relatively large offsets from their pre-deployment calibration. These were qualitatively confirmed by comparing the mooring data against CTD data from casts conducted near the mooring during HOT cruises, and also from the cross-calibration casts between the CTD and MicroCATs conducted after recovery. The causes of the conductivity offsets are not clear, and there may have been multiple causes. For some instruments the offset was positive, caused perhaps by biofouling of the conductivity cell while for others the offset was negative, caused possibly by scouring of the inside of the conductivity cell. A visual inspection of the instruments after recovery did not show any obvious signs of biofouling, however, the post-WHOTS-2 sensor inspection at Sea-Bird showed some scouring inside the conductivity cell for some of the MicroCATs (SN 2451, 2965, 3382, 3618, 3619, 3621, 3668, 3669, and 3670). It is unknown what could have caused this scouring. One possibility is that the continuous up and down motion of the instruments in a field with an abundance of diatoms eroded the inside of the cells over time.

Another characteristic of the offsets in the conductivity sensors is that their developments were not always linear in time. This is clearly illustrated by the results from two MicroCATs that logged data at the same depth during WHOTS-1. Figure 5-20 shows the temperature and conductivity differences between MicroCATs #3601 and #3602 that were located beneath the buoy (about 1 m below the surface). The temperature sensors do not show any significant drift for the duration of the deployment, however the conductivity differences show significant variability. A sudden offset between the sensors near Julian day 370 goes back to near-zero around day 395. A close inspection of the individual records indicates that the offset was due to sensor #3601, probably caused by a blocking or biofouling of the conductivity cell that was suddenly unblocked, perhaps by wave action. A gradual decrease in the conductivity differences followed this event, until day 520, when a steep decrease started, reaching a minimum of about -17 x 10^{-3} S/m (equivalent to -0.125 in salinity).

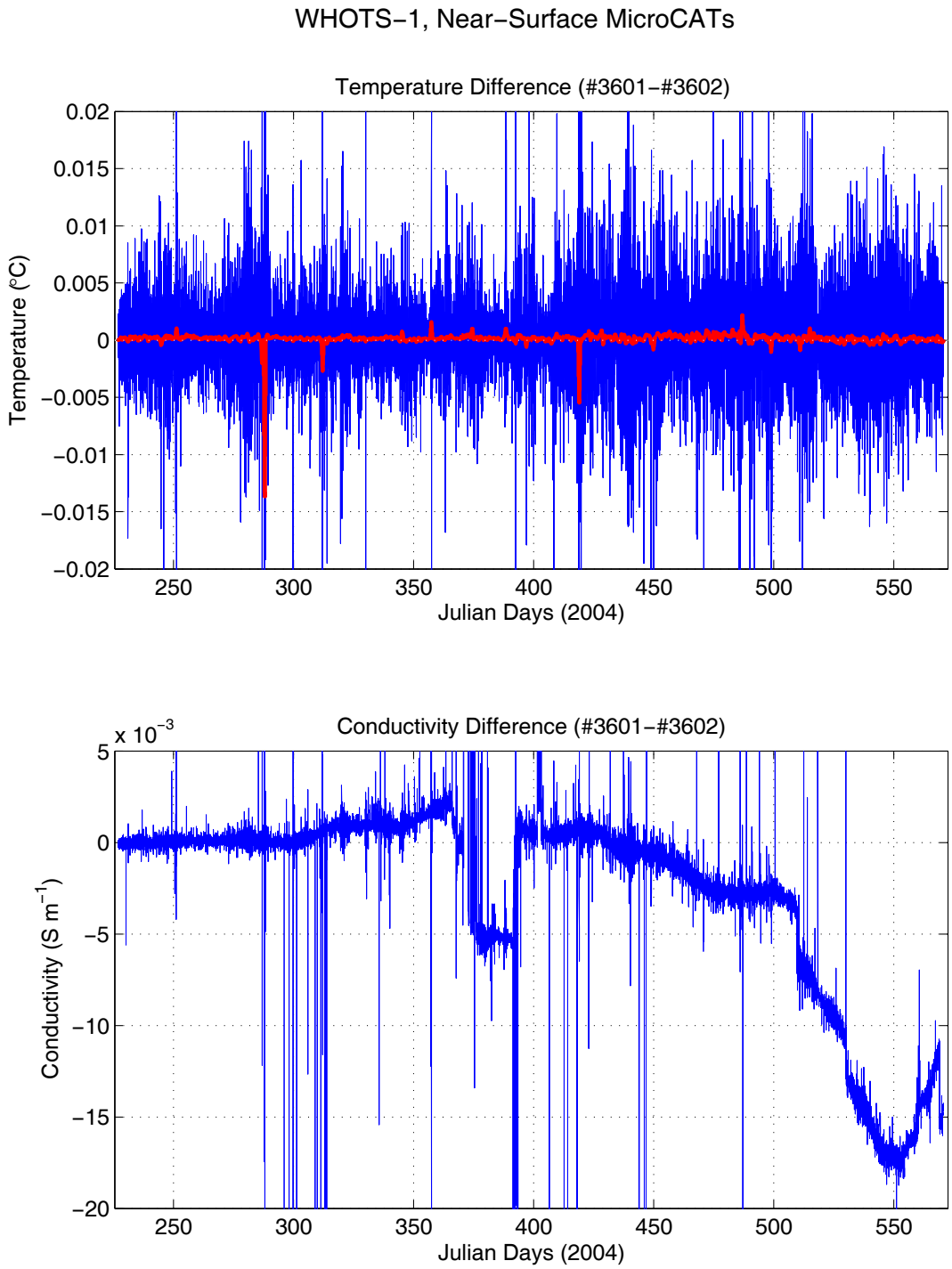

Figure 5-20 Temperature difference (top panel) and conductivity difference (lower panel) between MicroCATs #3601 and #3602 during WHOTS-1. The red line in the top panel is a 12-hr running mean.

Conductivity data from CTD profiles made between 200 and 1000 m away from the mooring during HOT cruises were available to obtain a correction for the conductivities from MicroCAT's #3601 and #3602. The conductivity differences between CTD data at 1 m and the MicroCAT data logged at the time of the casts are plotted in Figure 5-21. This figure shows differences of up to 20 x 10^{-3} Sm^{-1} by the end of the record for sensor #3601, similar to those observed in the differences between the two MicroCATs (Figure 5-20). This indicates that the sensor that caused the offset in that figure was #3601. Sensor #3602 also drifted during the deployment, but at a slower rate. The MicroCAT conductivities were corrected by matching them to the CTD conductivities in a stepwise manner, following the apparent behavior indicated by the MicroCATs conductivity differences.

The above comparison between conductivity sensors shows that the sensor's drift is not always linear, and its behavior can be highly variable. CTD calibration casts from HOT cruises are necessary to correct for this variability, however their usefulness is limited because of the frequency of the HOT cruises. For instance, no HOT cruise data were available between days 350 and 400 when sensor #3601 had a sudden offset. Also, there were no reliable CTD data to indicate exactly when sensor #3602 started its steep drift, which according to the MicroCAT comparison was around day 520 (Figure 5-20).

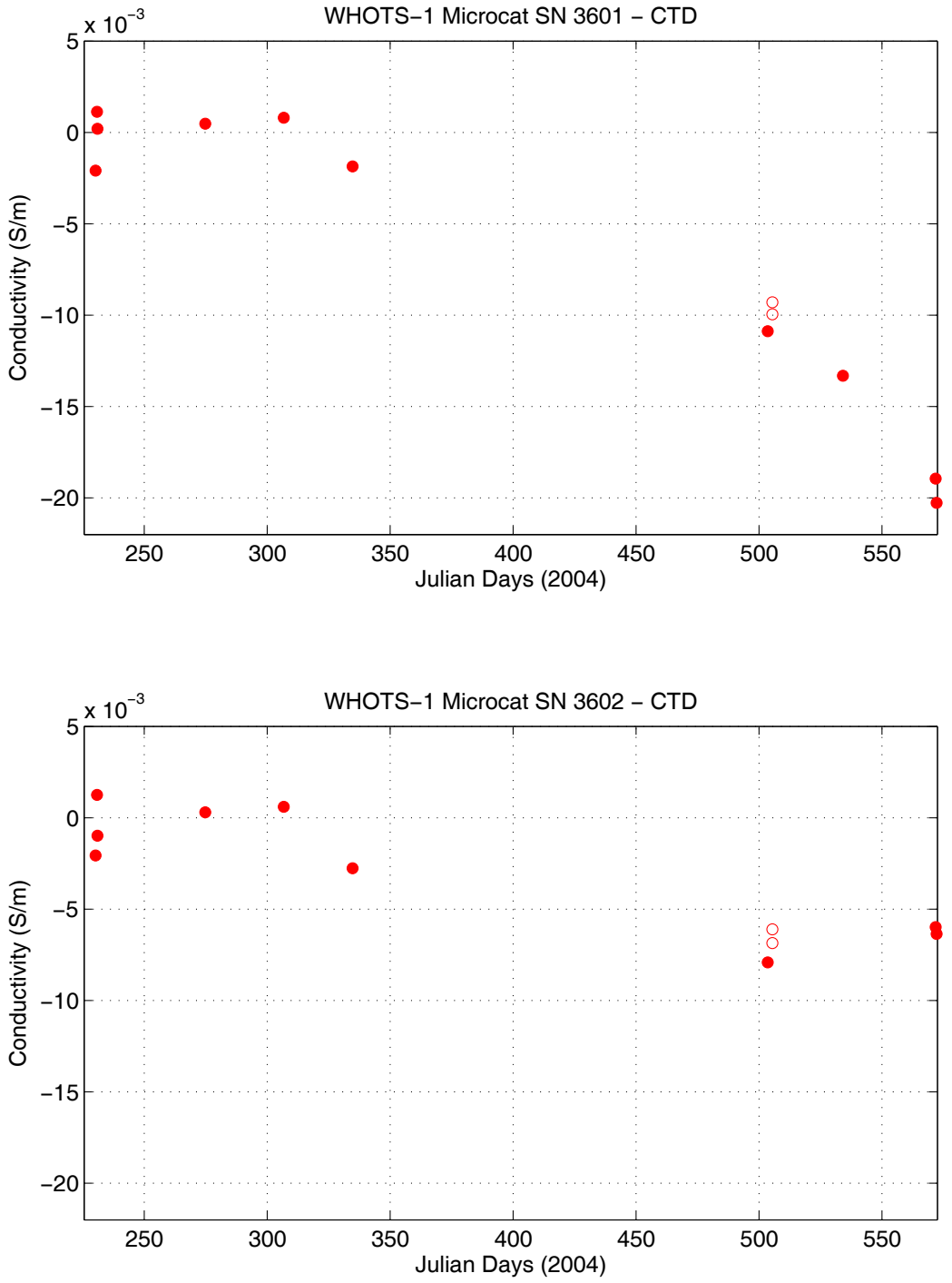

Figure 5-21 Conductivity differences between MicroCATs (#3601 and #3602) and CTD casts obtained during HOT cruises. Filled circles are from casts conducted between 200 and 1000 m away from the mooring. Open circles are from casts conducted within 5 km off the mooring.

Corrections of the conductivity data for the other SeaCATs and MicroCATs in the moorings were conducted by comparing them against CTD data from casts near the mooring, and from the cross-calibration casts between the CTD and MicroCATs. Casts conducted between 200 and 1000 m from the mooring were given extra weight in the correction, as compared to those conducted between 1 and 5 km away. Casts more than 5 km away from the mooring were not used. A quadratic fit to the CTD-MicroCAT/SeaCAT differences against time was applied for the majority of the sensors, and the corresponding correction was applied (see Figure 5-23). Some of the sensors had large offsets and/or obvious non-linear variability (as in sensor #3601 above). For these sensors, a stepwise correction was applied using the differences between consecutive sensors to determine when this particular sensor started to drift, and matching the data to the available CTD cast data. For periods when the stratification was weak, the conductivity difference between some of the neighboring sensors was near zero because they were only between 5 and 20 m apart. These periods were used as a reference to determine instances of sudden drift.

As an example, Figure 5-22 (upper panel) shows the salinity differences between instruments at 35 and 40 m with uncorrected conductivities during the WHOTS-1 deployment. These differences indicate that one of the instruments started to drift before day 500. The comparisons with the CTD data shown in Figure 5-22 (middle panel) indicate that sensor SN 1087 did not deviate significantly from the CTD measurements. On the other hand sensor SN 3381 at 40 m drifted by about 0.25 Sm^{-1} by the end of the record, however the available CTD casts are not sufficient to indicate when the drift started. The combined information from these two figures (in addition to the conductivity differences between sensor 3381 and other neighboring sensors) was used to obtain a correction to the conductivities for sensor 3381, yielding the corrected salinity differences shown in Figure 5-22 (bottom panel).

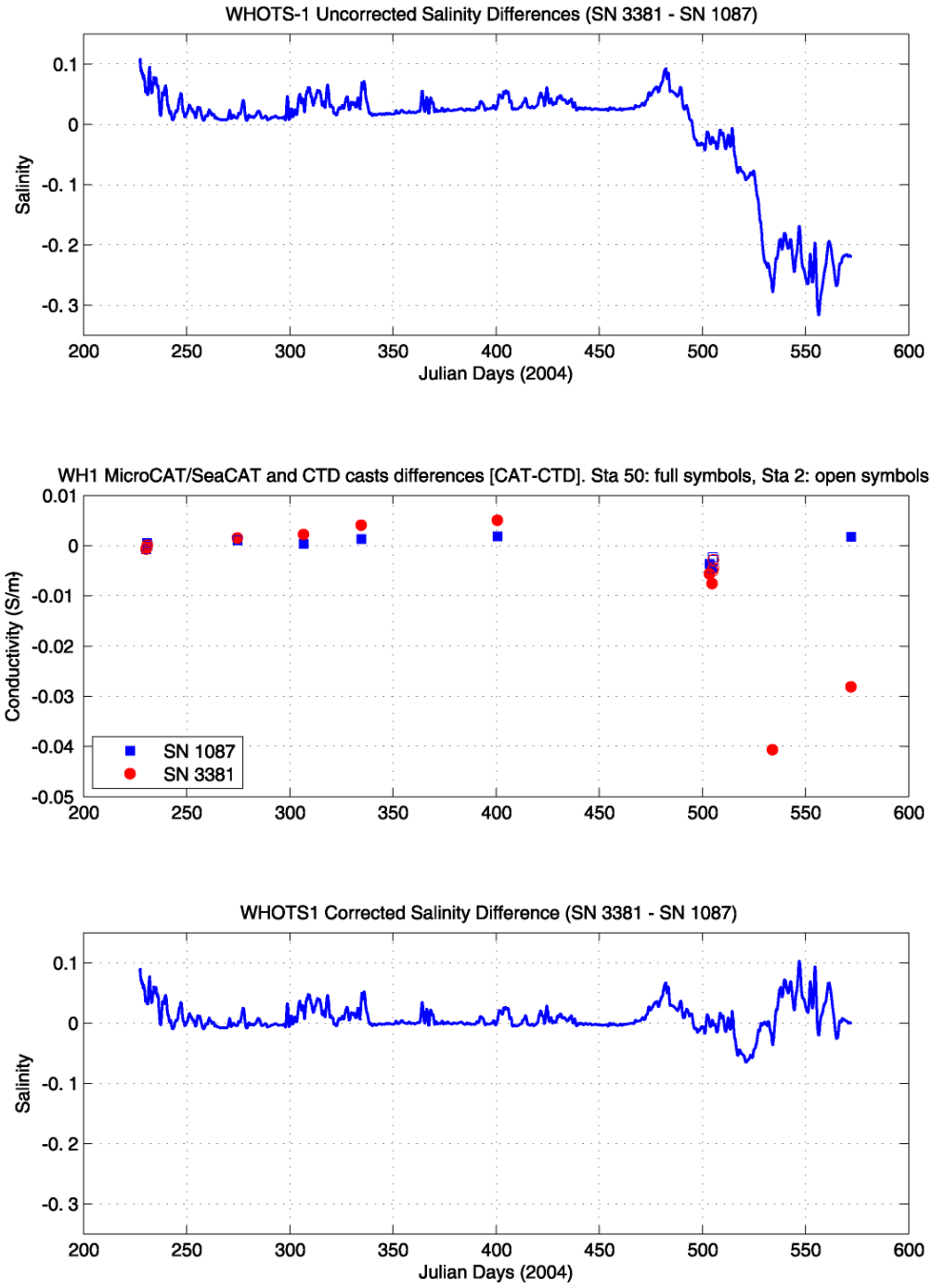

Figure 5-22 Uncorrected salinity differences between sensors SN 3381(40 m) and SN 1087(35 m) during WHOTS-1 (top panel). Conductivity differences between sensors SN 1087 and CTD casts (blue squares, middle panel), and between SN 3381 and CTD casts (red circles, middle panel). Corrected salinity differences between sensors SN 3381 and SN 1087 (bottom panel).

As a final quality control of our conductivity corrections, the buoyancy frequency between neighboring instruments was calculated. Incorrect conductivities yielded instabilities in the water column that were obviously not real, and one of the corresponding sensor's calibration had to be revised. The corrections applied to each of the conductivity sensors during WHOTS-1 and -2 can be seen in Figure 5-23 and Figure 5-24.

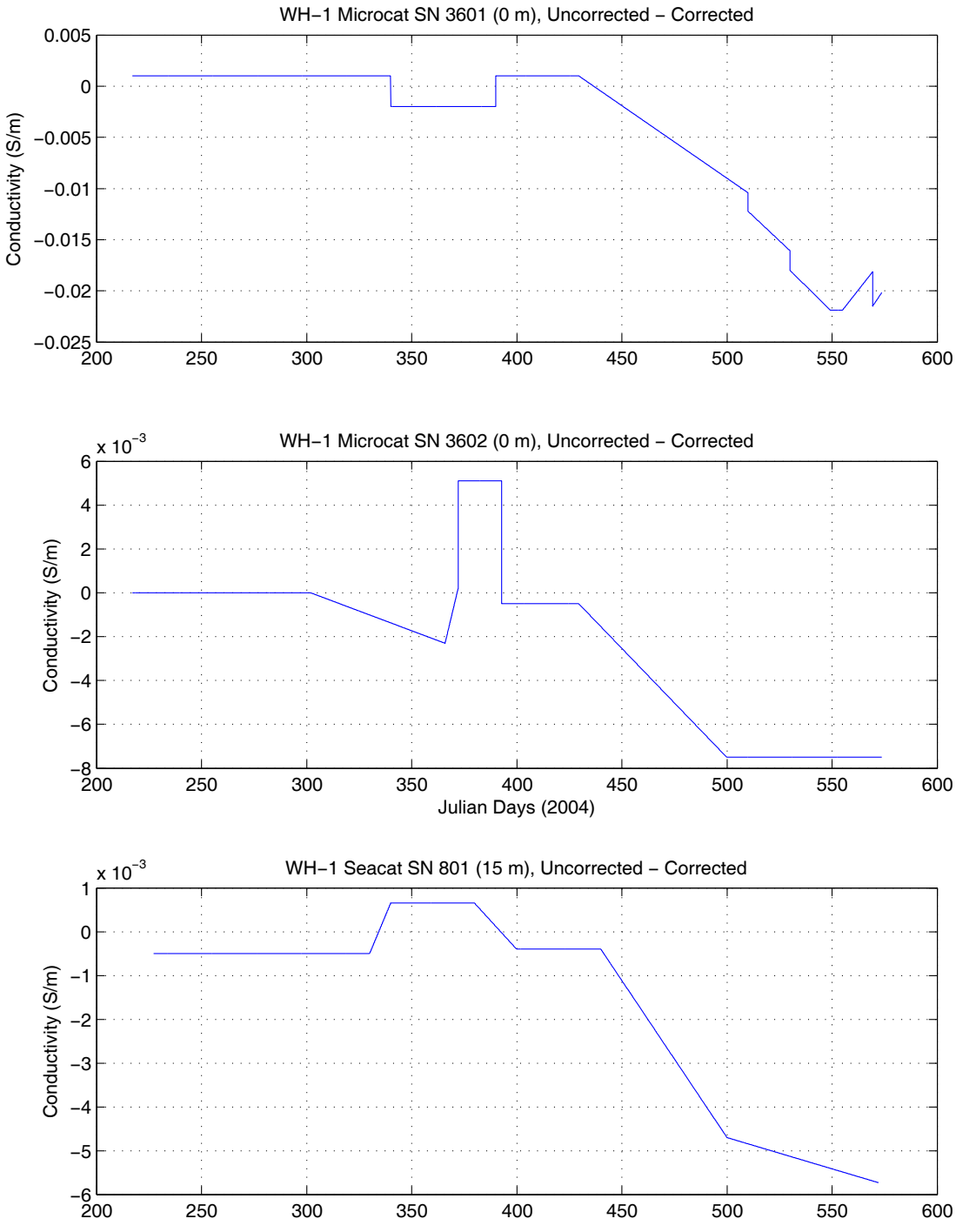

Figure 5-23 Conductivity sensor corrections for SeaCATs/MicroCATs during WHOTS-1

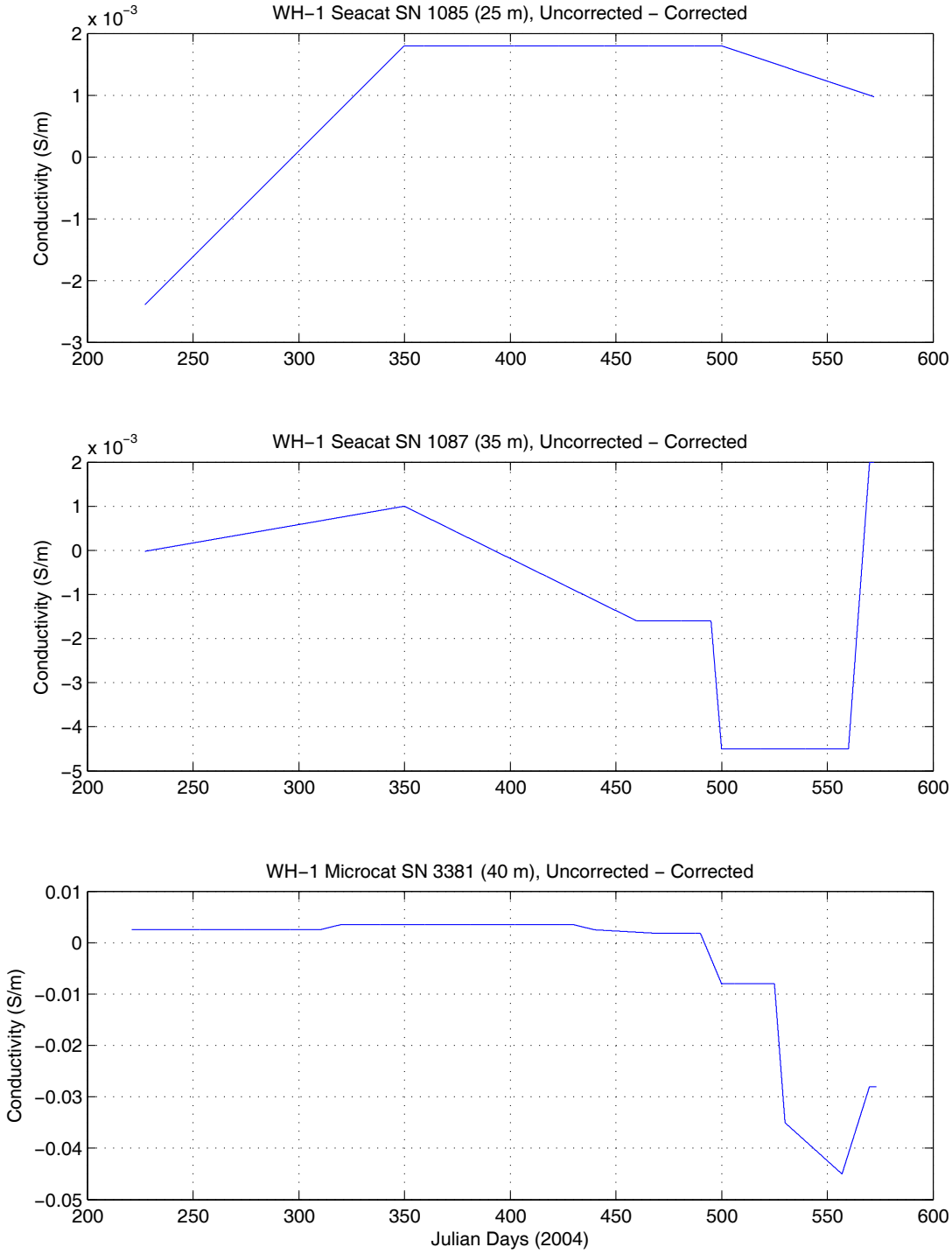

Figure 5.23 (Contd.)

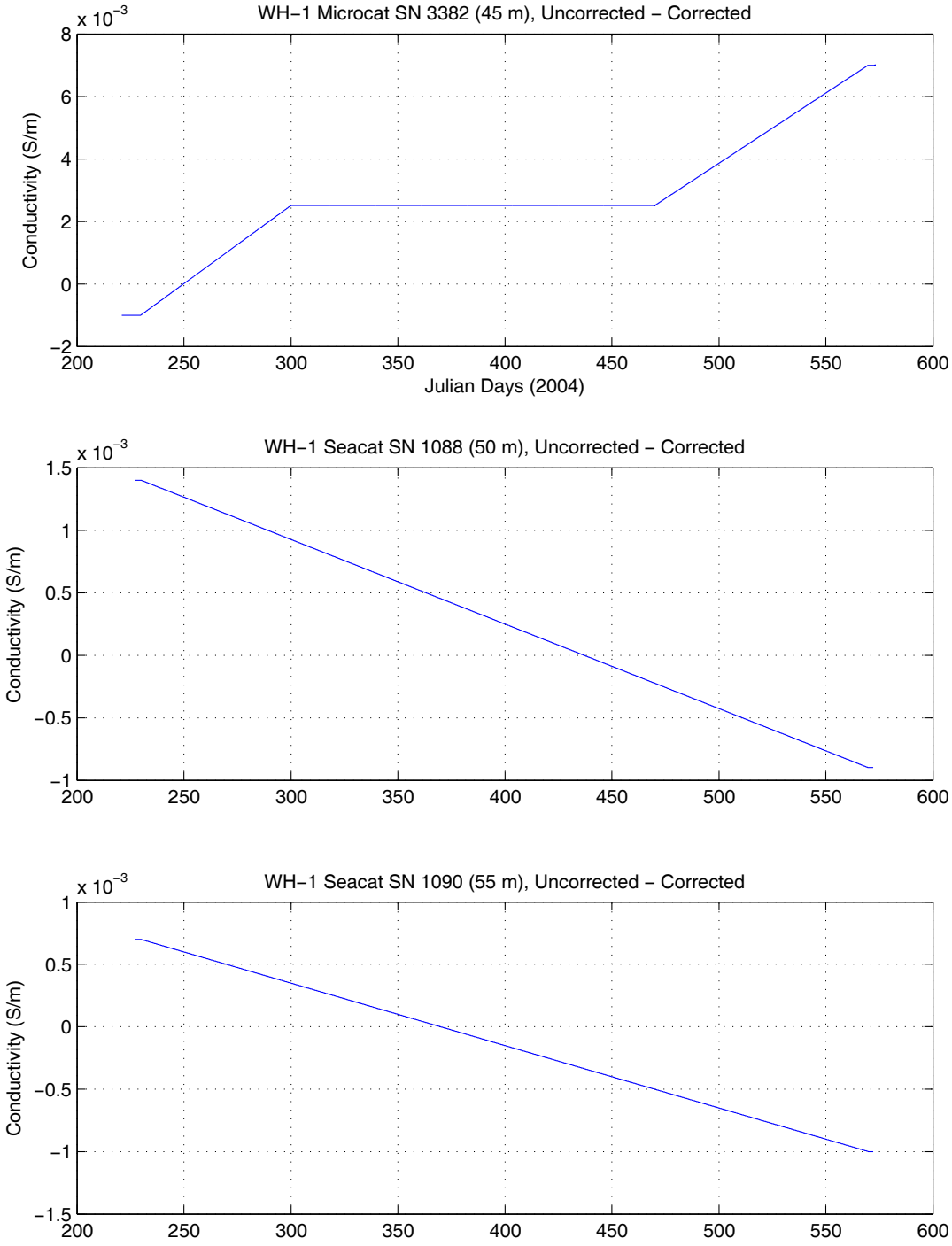

Figure 5.23 (Contd.)

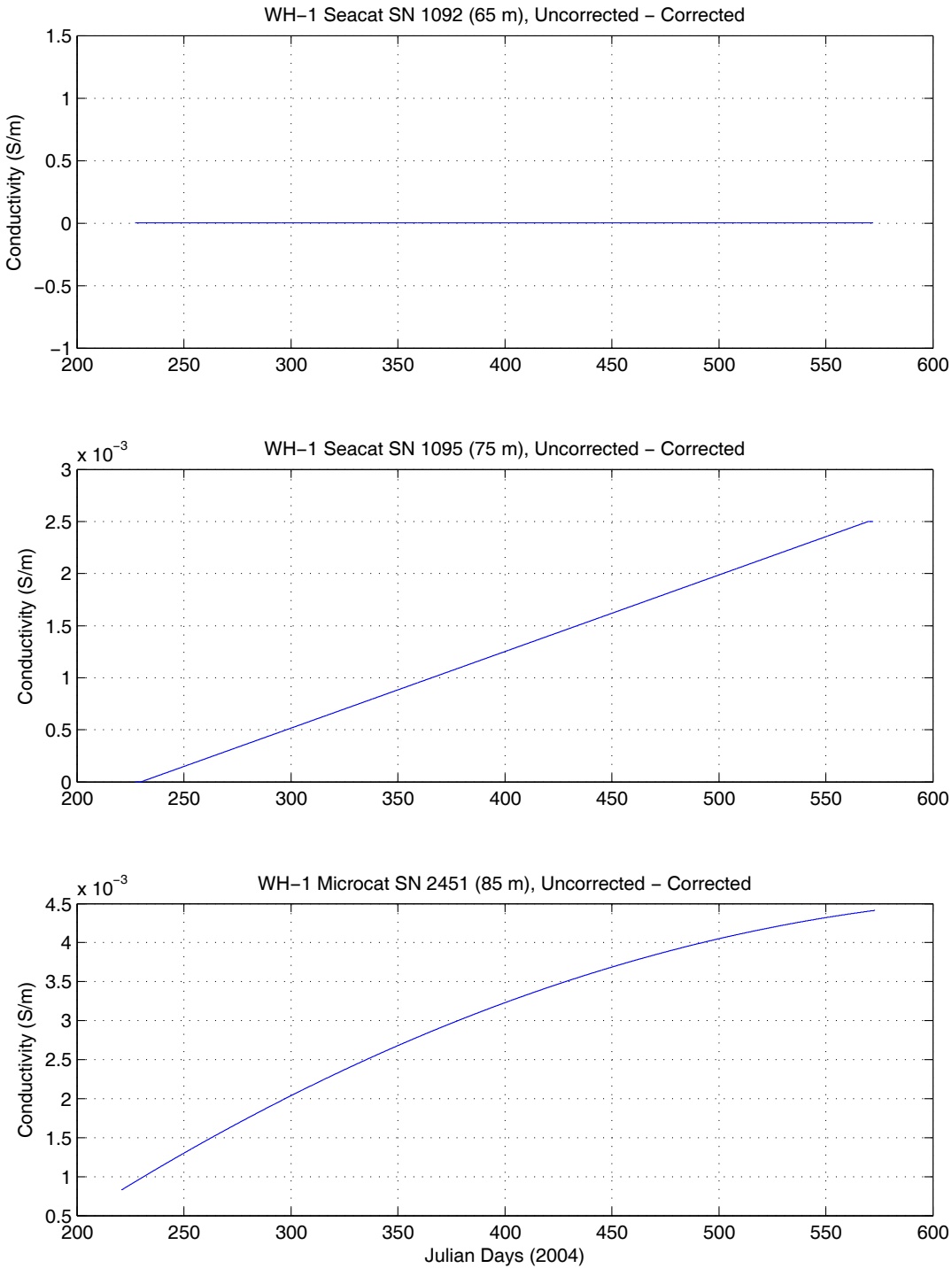

Figure 5.23 (Contd.)

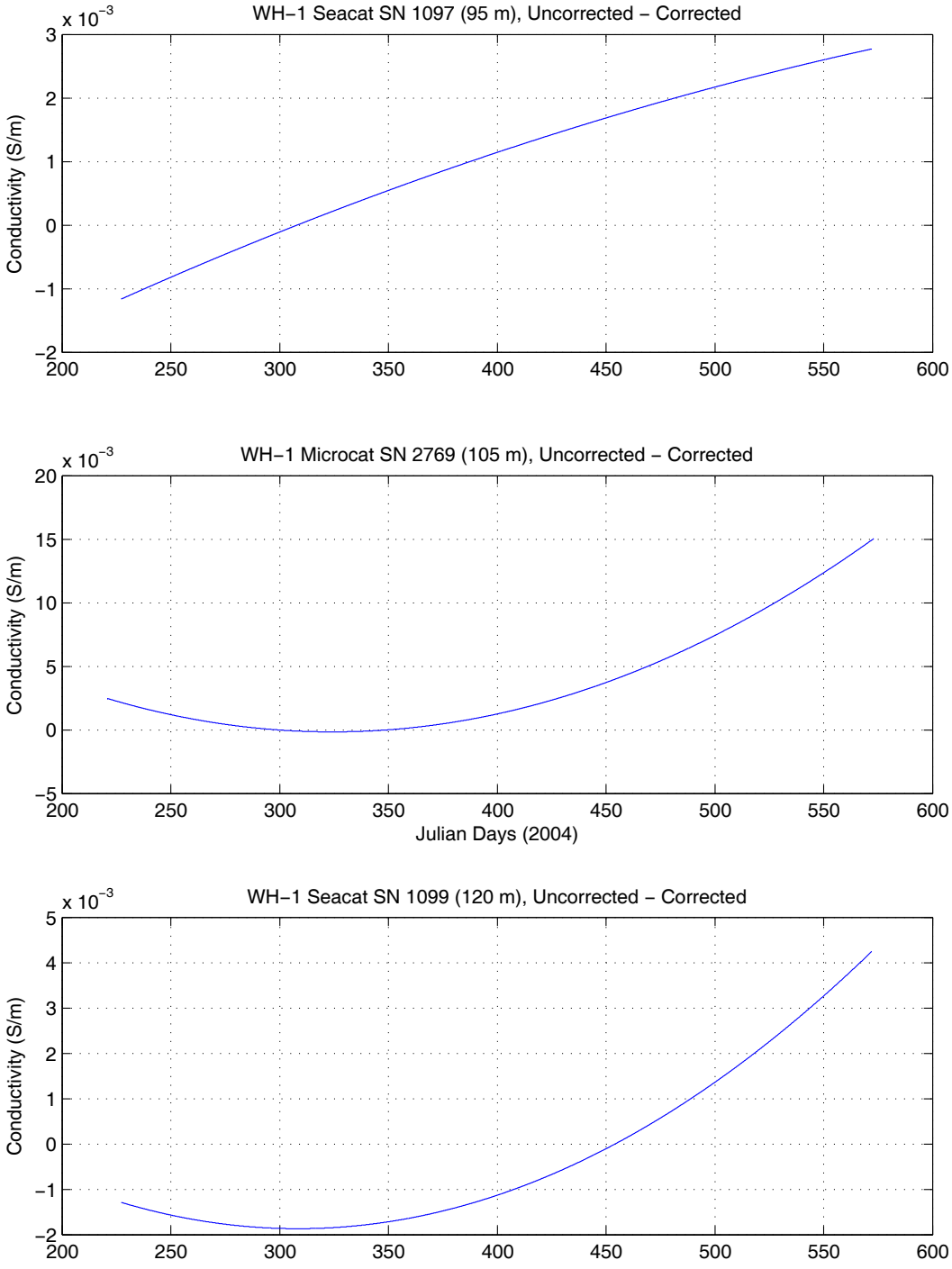

Figure 5.23 (Contd.)

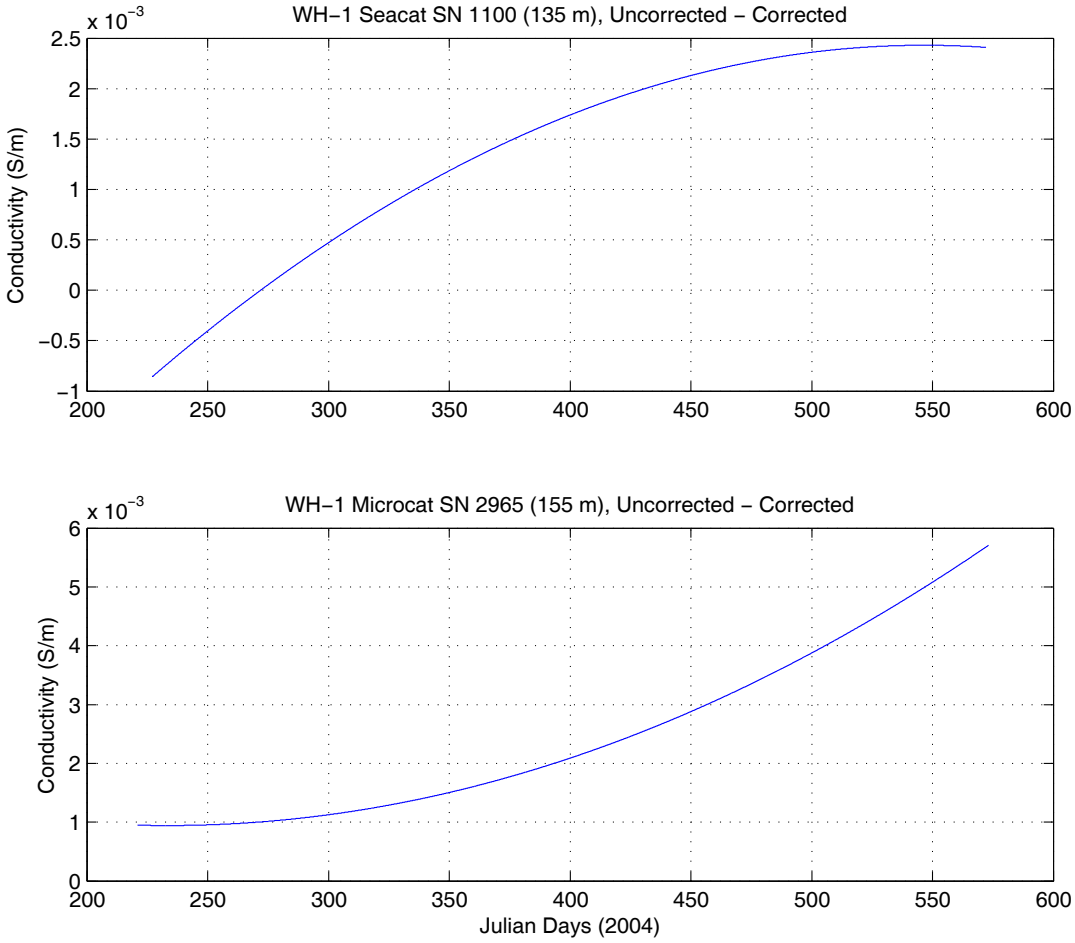

Figure 5.23 (Contd.)

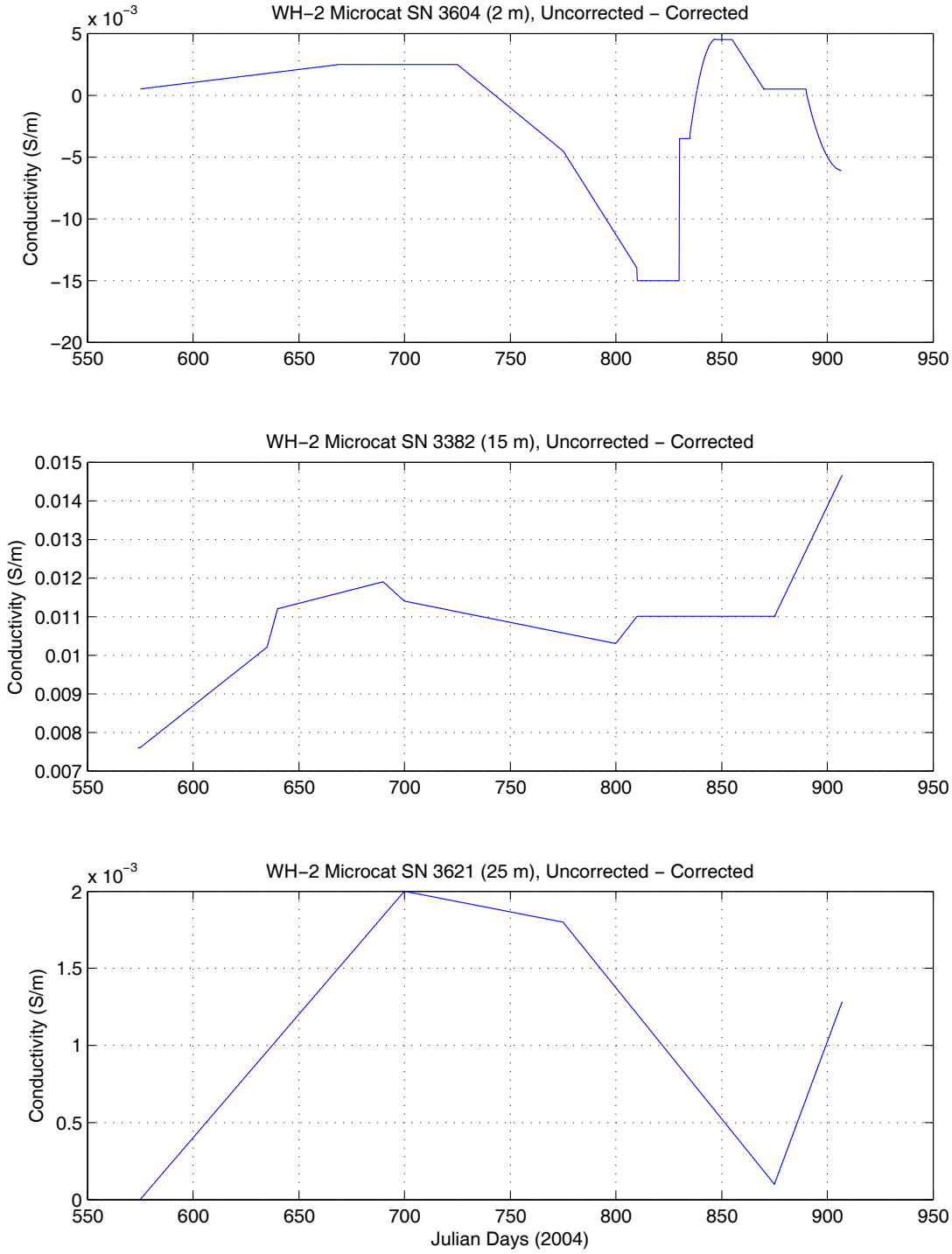

Figure 5-24 Conductivity sensor corrections for MicroCATs during WHOTS-2

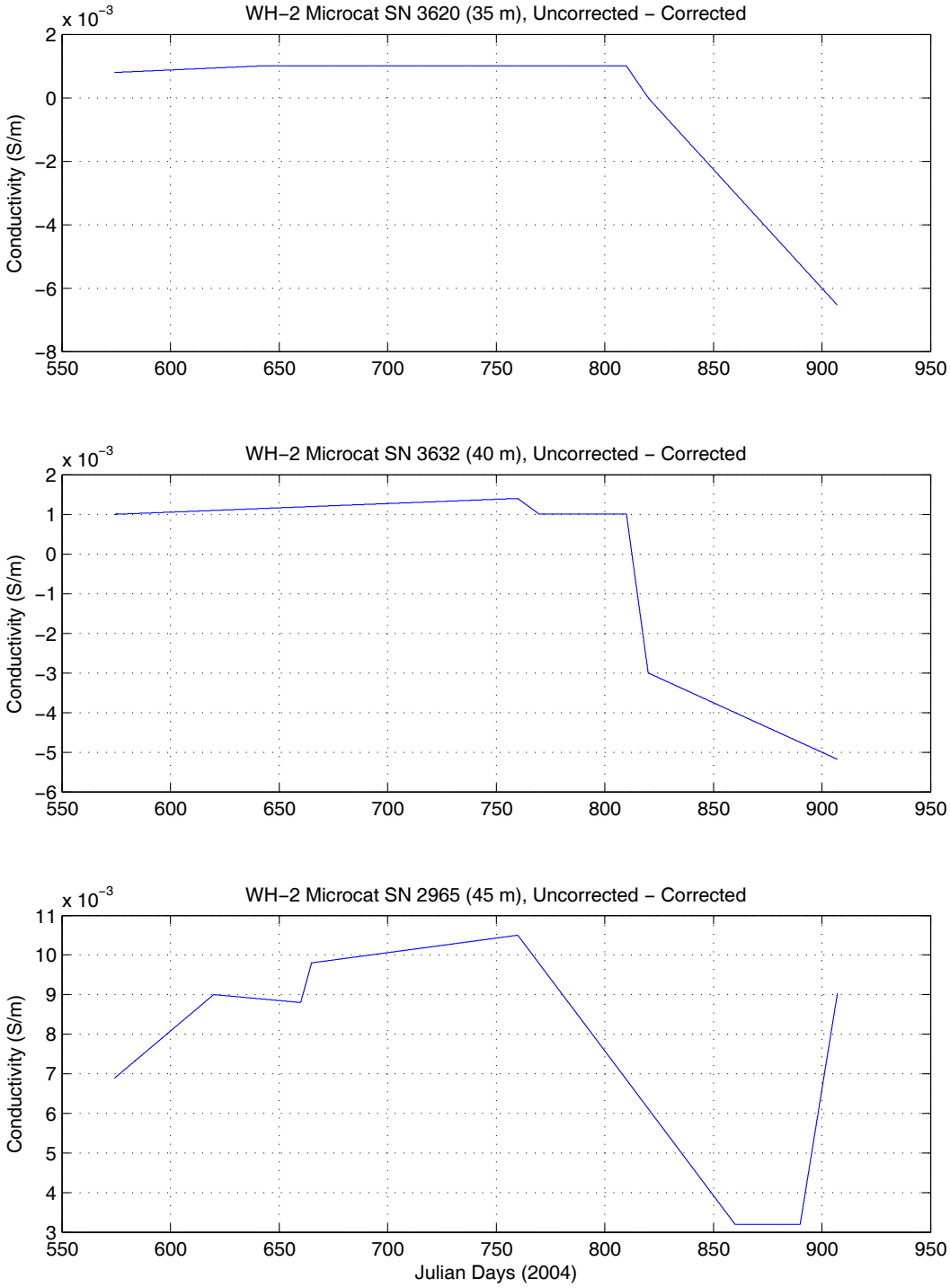

Figure 5.24 (Contd.)

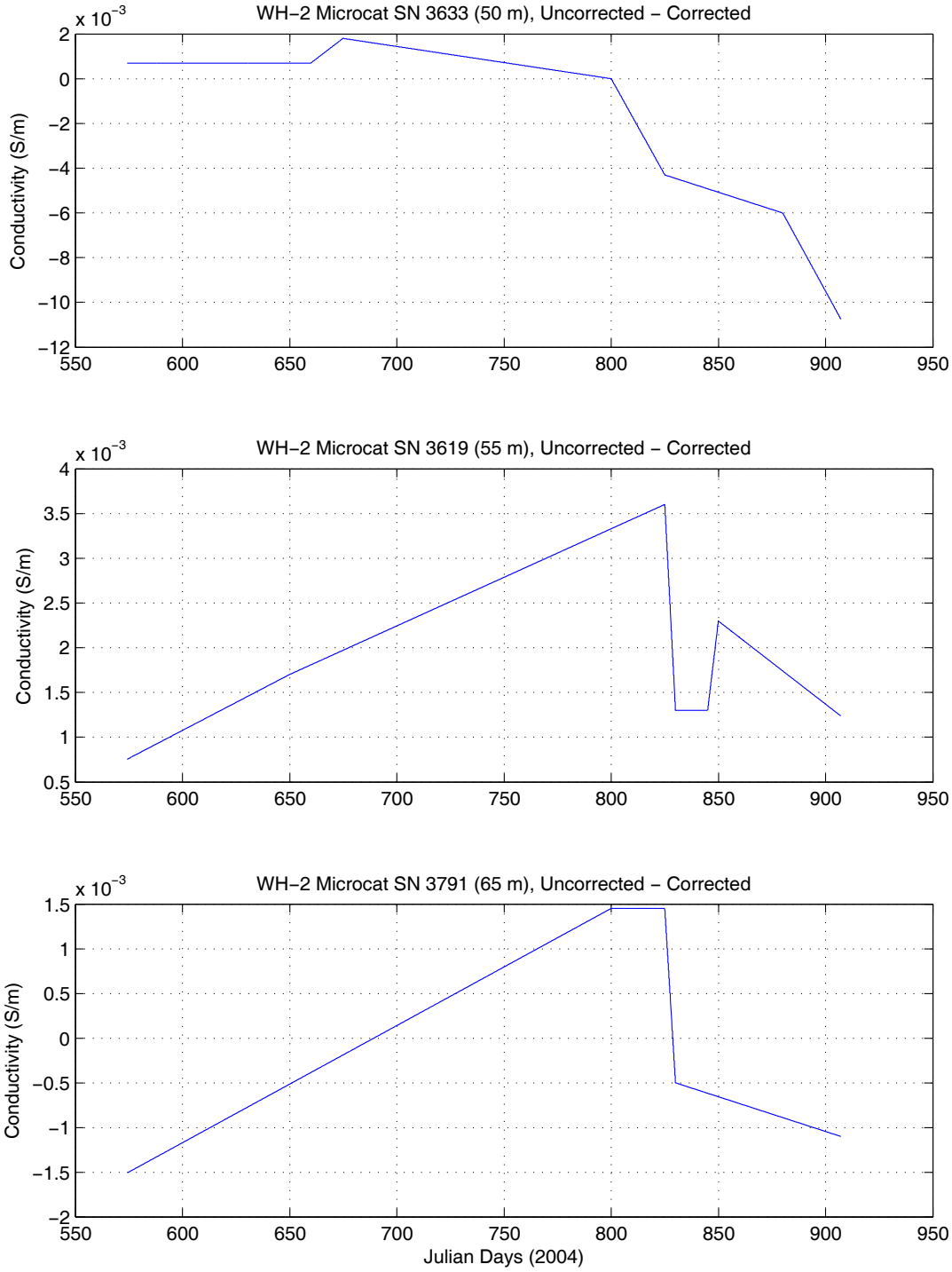

Figure 5.24 (Contd.)

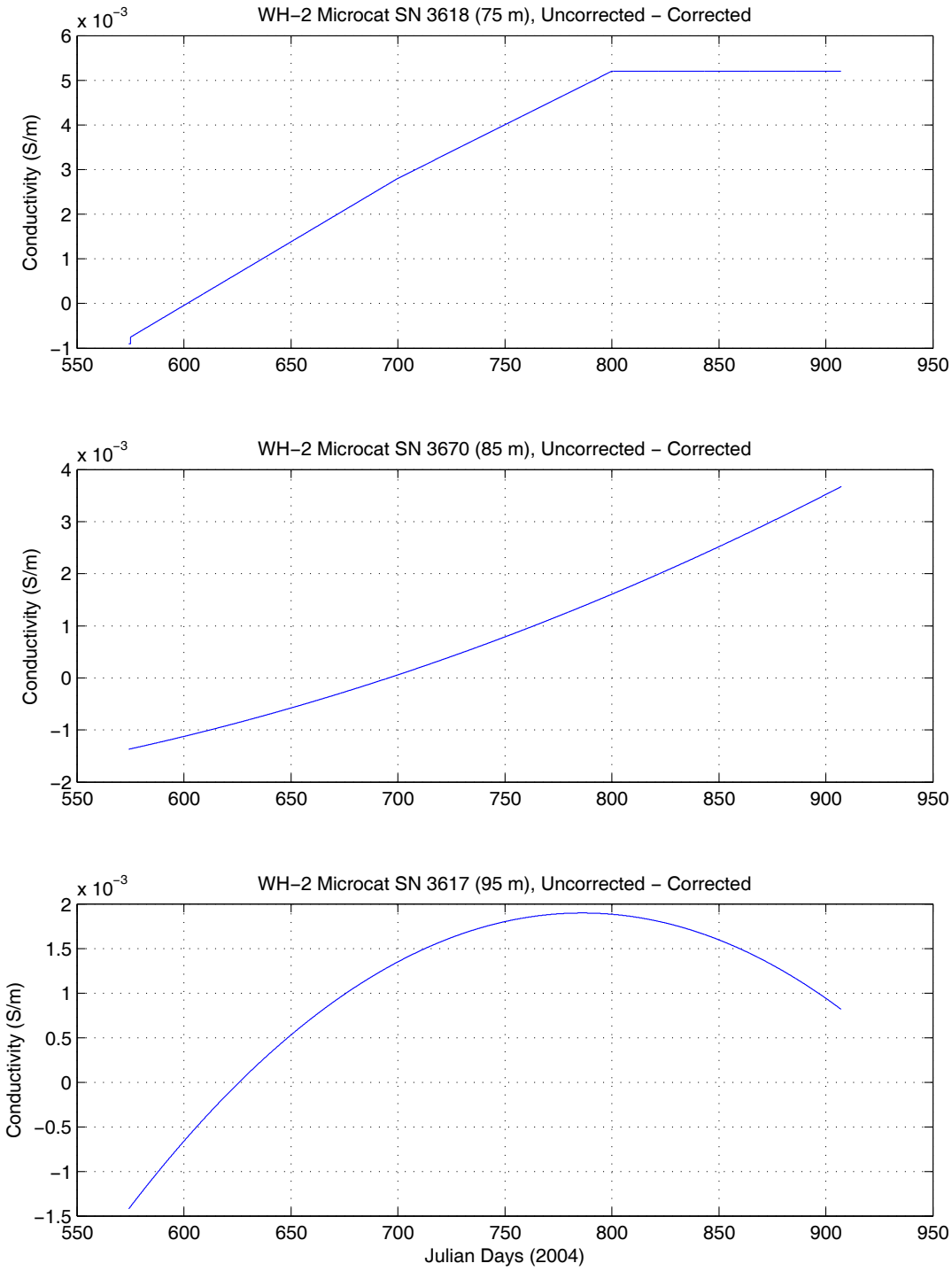

Figure 5.24 (Contd.)

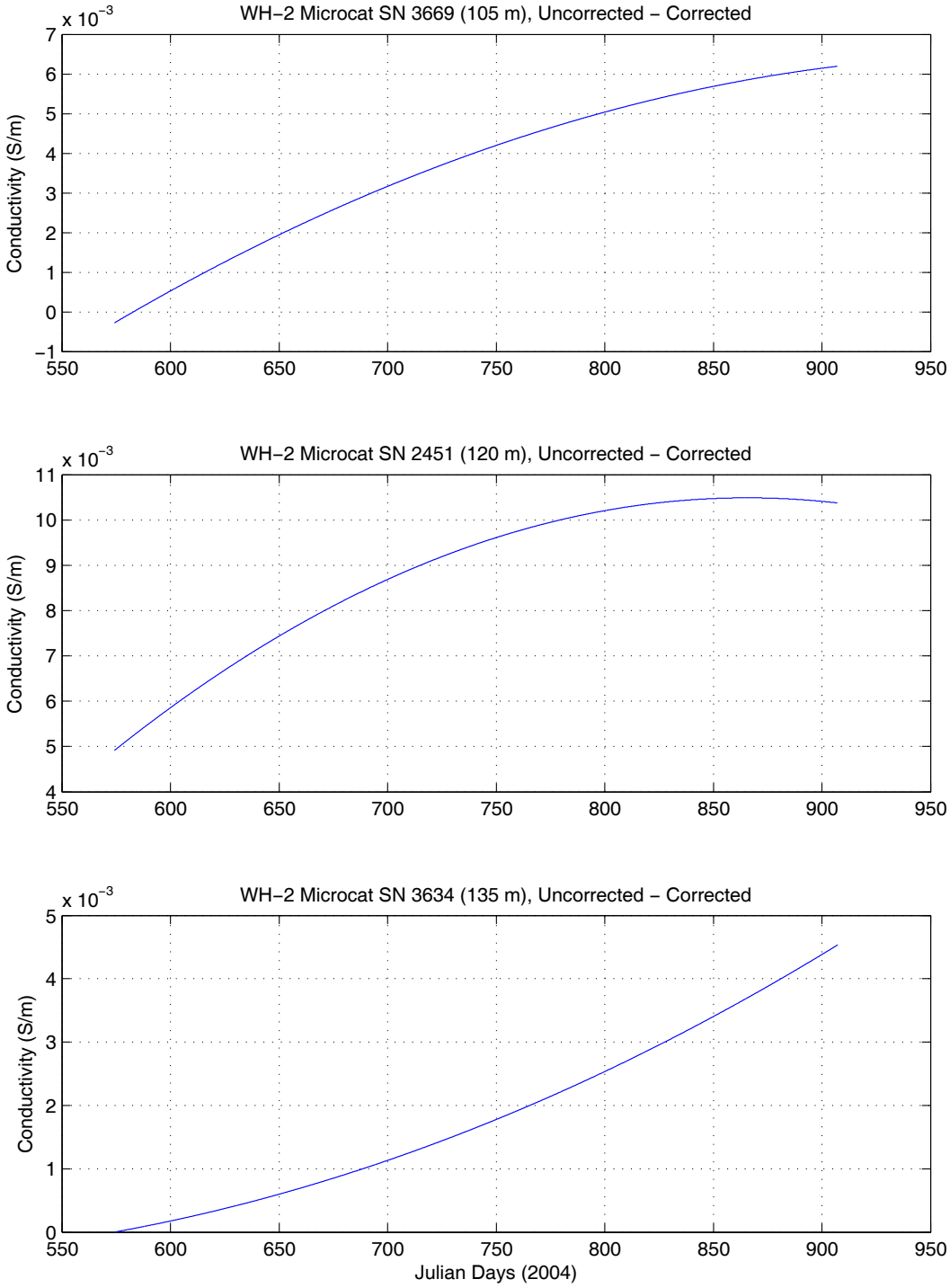

Figure 5.24 (Contd.)

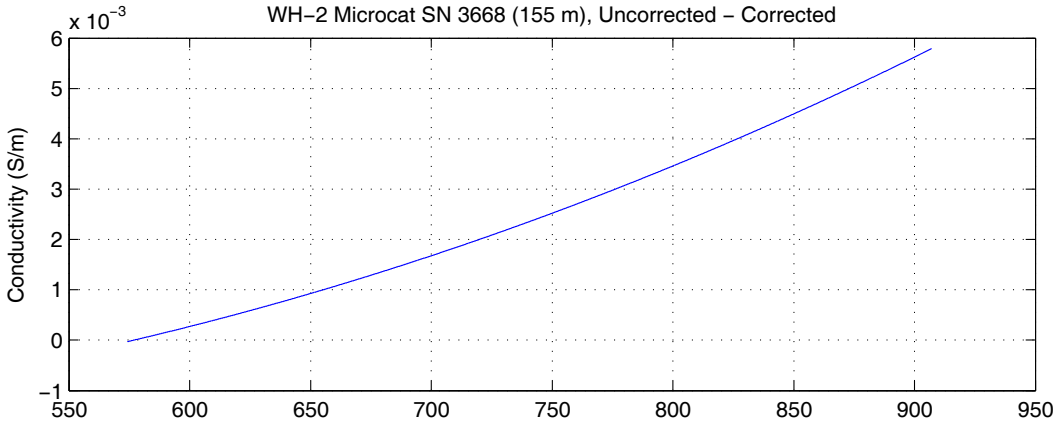

Figure 5.24 (Contd.)

B. Acoustic Doppler Current Profiler

A Teledyne/RD Instruments 307.2 kHz broadband Workhorse Sentinel ADCP was deployed in the upward looking configuration at 125 m depth on the WHOTS-1 and -2 moorings. The instrument was installed in an aluminum frame along with an external battery module to provide sufficient power for the intended period of deployment. The four ADCP beams were angled at 20° from the vertical line of the instrument. The ADCP was set to profile across 30 range cells of 4 m with the first bin centered 6.2 m from the transducer. The maximum range of the instrument was just short of 125 m. The specifications of the instrument are shown in Table 5.3.

Table 5.3 Specifications of the ADCP used for WHOTS –1 and –2 moorings.

Instrument	Description
ADCP	RDI Workhorse Sentinel, 300KHz Model: WHS300-I-UG86 Serial Number: 4891
Battery module	2 external battery packs Type:#757K6023-00

1. Compass Calibration

WHOTS-1

Prior to the WHOTS-1 deployment a field calibration of the internal ADCP compass was performed at Snug Harbor in Honolulu on 7 August 2004. The instrument was mounted in the deployment cage along with the external battery module and was located away from potential sources of magnetic field disturbances. Using the built-in calibration procedure, the instrument was tilted in one direction between 10 and 20 degrees and then rotated through 360 degrees at less than 5 ° /sec. The ADCP was then tilted in a different direction and a second rotation made. Based on the results from the first two rotations, calibration parameters are temporarily loaded and the instrument, tilted in a third direction is rotated once more to check the calibration. Results from the pre-deployment field calibration are shown in Table 5.4.

Table 5.4 Results from the WHOTS-1 pre-deployment ADCP (SN4891) compass field calibration procedure.

	Single Cycle Error (°)	Double Cycle Error (°)	Largest Double + Single Cycle Error (°)	RMS of 3rd Order and Higher + Random Error (°)	**Over all Error** (°)	Pitch Mean and Standard Deviation (°)	Roll Mean and Standard Deviation (°)
Before Calibration	3.02	0.76	3.78	0.22	**3.10**	12.89 ±0.52	0.19 ±0.31
	2.63	0.61	3.24	0.23	**2.74**	-1.43 ±0.50	-10.35 ±0.44
After Calibration	0.16	0.20	0.36	0.21	**0.32**	1.33 ±0.61	8.58 ±0.40

WHOTS-2

The field calibration of the ADCP compass prior to the WHOTS-2 deployment was carried out on board the *R/V Melville* during the mooring turnaround period on 26th July, 2005. The ADCP was hung from the rear A-frame allowing the necessary tilts and rotations to be made. These conditions are certainly not ideal for a calibration due to the ship motion and magnetic fields, but without returning to port this was the only available option. The ADCP was made to undergo the same procedures as described above and the overall error was found to be less than 5° (The exact error was not recorded) so the calibration matrix remained unchanged.

After the WHOTS-2 mooring was recovered, the performance of the ADCP compass was tested at Snug Harbor in the same location as the WHOTS-1 pre-deployment field calibration. The ADCP was mounted in a wooden frame attached to a turntable which was aligned with magnetic north using a surveyor's compass (see Figure 5-25). The turntable allowed the instrument to be rotated through 8 prescribed angles in 45° increments. The ADCP heading for each angle was recorded with the compass error being the difference between the two. The ADCP was rotated in both clockwise and anti-clockwise directions. Results from the test are plotted in Figure 5-26.

The built in calibration procedure was executed twice in the horizontal plane to confirm the results of the compass spins and these results are shown in Table 5.5. Differences between the clockwise and anti-clockwise rotation were < 0.1° and the RMS error observed was 3.3°. Typically the accuracy of the compass used in the workhorse ADCP is ±2°. No compass corrections were made.

Table 5.5 Results from the WHOTS-2 post-deployment ADCP (SN4891) compass field calibration procedure.

	Single Cycle Error (°)	Double Cycle Error (°)	Largest Double + Single Cycle Error (°)	RMS of 3rd Order and Higher + Random Error (°)	**Over all Error** (°)	Pitch Mean and Standard Deviation (°)	Roll Mean and Standard Deviation (°)
After Calibration	1.93	0.25	2.18	0.15	**1.92**	0.75 ±0.86	-0.04 ±0.55
	1.97	0.29	2.27	0.11	**1.96**	1.15 ±0.48	-0.50 ±0.50

Figure 5-25 Turntable used to test the performance of the internal compass of the ADCP SN4891 with external battery module installed.

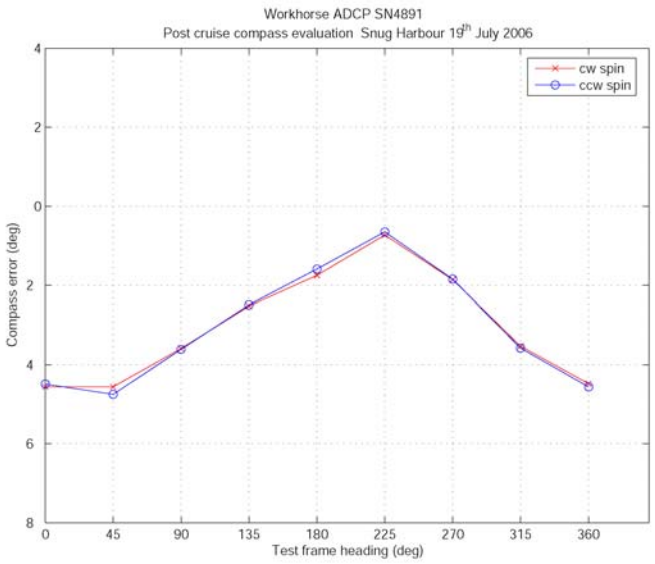

Figure 5-26 Results of the post cruise compass calibration conducted 19th July, 2006 on ADCP SN4891at Snug Harbor.

2. ADCP Configuration

Individual configurations for the WHOTS-1 and WHOTS-2 deployments are detailed in Appendices 1 and 2. The salient differences for each of the deployments are summarized below.

WHOTS-1

The ADCP was configured in a burst sampling mode consisting of 40 pings per ensemble in order to resolve low-frequency wave orbital motions. The interval between each ping was 4 seconds so the ensemble length was 160 seconds. The interval between ensembles was 10 minutes. Data were recorded in earth coordinates with a heading bias of 10.25° E used. False targets, usually fish, were screened by setting the threshold maximum to 70 counts. Velocity data were rejected if the difference in echo intensity among the four beams exceeded this threshold.

WHOTS-2

Due to a miscommunication during the WHOTS-2 cruise, the ADCP was not configured as it was during the previous deployment, i.e. in a burst sampling mode. The configuration still consisted of 40 pings per ensemble of 10 minutes interval but the ping interval was set to 15 seconds. Data were also recorded in earth coordinates but a heading bias was not set at the ADCP configuration level. The heading bias was applied instead during data processing. The false target threshold used was the default of 50 counts.

3. ADCP data processing procedures

Binary files output from the ADCP were read and converted to MATLAB™ binary files using scripts developed by Eric Firing's ADCP lab (http://current.soest.hawaii.edu). The beginning of the raw data files were truncated to a time after the mooring anchor was released in order to allow time for the anchor to reach the seabed and for the mooring motions that follow the impact of the anchor on the sea floor to dissipate. The pitch, roll, and ADCP temperature were examined in order to pick reasonable times that ensured good data quality but without unnecessarily discarding too much data (see Figure 5-27and Figure 5-28 for an example). Truncation at the end of the data files were chosen to be the ensemble prior to the time that the acoustic release signal was sent to avoid contamination due to the ascent of the instrument. The times of the first ensemble from the raw data, deployment and recovery time, along with the times of the truncated records of both deployments are shown in Table 5.6.

Table 5.6 ADCP record times (UTC) during WHOTS-1 and WHOTS-2 deployments.

	WHOTS-1	WHOTS-2
Raw file beginning and end times	10-Aug-2004 00:00 26-Jul-2005 02:10	27-Jul-2005 03:50 26-Jun-2006 03:00
Deployment and recovery times	12-Aug-2004 20:41 in water 13-Aug-2004 02:40 anchor over 25-Jul-2005 17:15 release triggered 25-Jul-2005 22:59 on deck	27-Jul-2005 19:37 in water 28-Jul-2005 01:43 anchor over 24-Jun-2006 18:30 release triggered 24-Jun-2006 20:56 on deck
Processed data beginning and end times	14-Aug-2004 00:00 25-Jul-2005 17:10	28-Jul-2005 09:40 24-Jun-2006 18:20

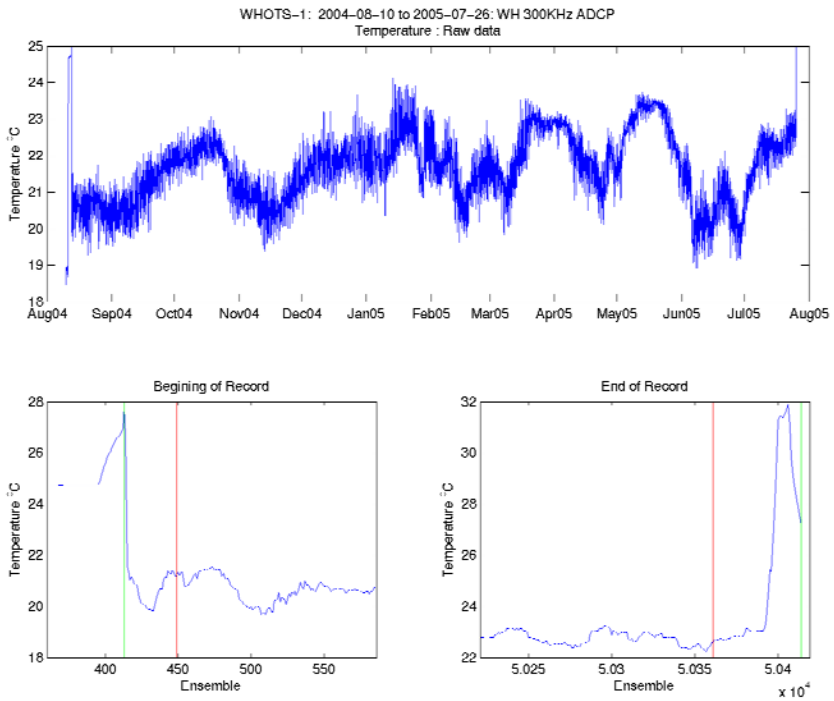

Figure 5-27 Temperature record from the ADCP during WHOTS-1 mooring (top panel). The bottom panel shows the beginning and end of the record with the green vertical line representing the in-water time during deployment and out-of-water time for recovery. The red line represents the anchor release and acoustic release trigger for deployment and recovery respectively.

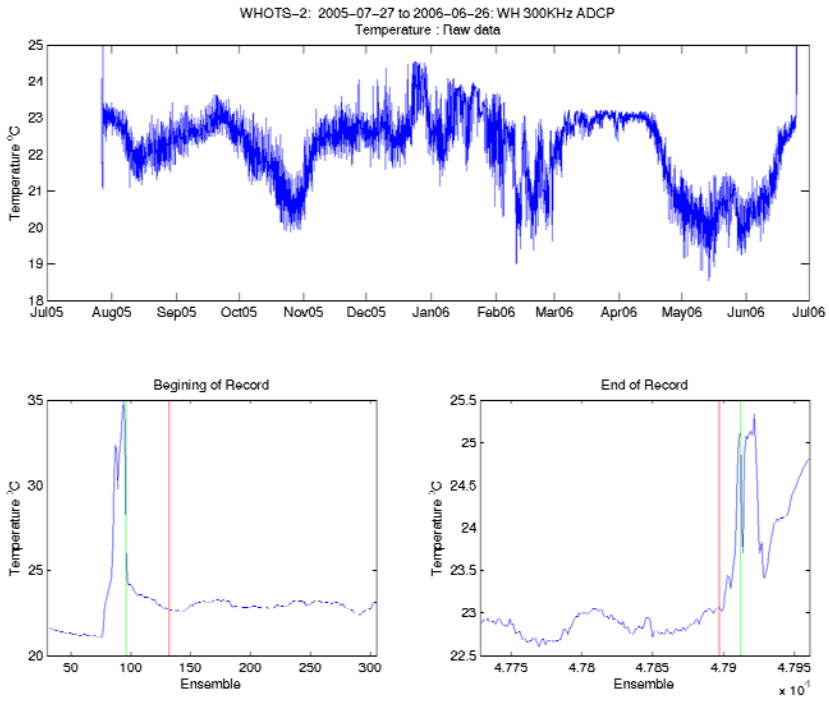

Figure 5-28 Same as in Figure 5.12, but for WHOTS-2.

Clock drift

Upon recovery the ADCP clock was compared with the ship's time server and the difference between the two recorded. It was found that for WHOTS-1 and WHOTS-2 deployments, the clock on the ADCP was fast by 8 minutes 43 seconds, and 8 minutes 30 seconds respectively. The fact that the two deployments experienced similar clock drifts leads to the assumption that the drift was linear with time and was not an abrupt change. The drift could then be corrected for. However the drift represents just one ensemble out of a total of nearly 50000 and so it was not corrected for.

Heading Bias

As mentioned in the ADCP configuration section, the data were recorded in earth coordinates. A heading bias, the angle between magnetic north and true north, could be included in the setup so that the output data were in true earth coordinates. Magnetic variation was obtained from the National Geophysical Data Center 'Geomag' calculator. (http://www.ngdc.noaa.gov/seg/geomag). For a year long deployment a constant value is

acceptable because the change in declination is small, approximately -0.02° year^{-1} at the WHOTS location. A heading bias of 10.25° was entered in the setup of the WHOTS-1 deployment. During the WHOTS-2 deployment the heading bias was not entered in the setup and the component velocities had to be rotated in the data processing stage with a bias of 10.2° being used.

Speed of sound

Due to the constant of proportionality between the Doppler shift and water speed, the speed of sound need only be measured at the transducer head (Firing, 1991). The sound speed used by the ADCP is calculated using a constant value of salinity (35) and temperature recorded by the transducer temperature sensor of the ADCP. Using CTD profiles conducted close to the mooring during the regular HOT cruises, (HOT-162 to HOT-182), and from the WHOTS deployment/recovery cruises the mean salinity at 125 dbar was 35.2. Mean CTD temperature was 22.2 °C and the mean ADCP temperature was 21.9 °C (Figure 5-29). The associated mean sound velocity difference is 0.6 m s^{-1} which represents a change of 0.04% so no correction was made.

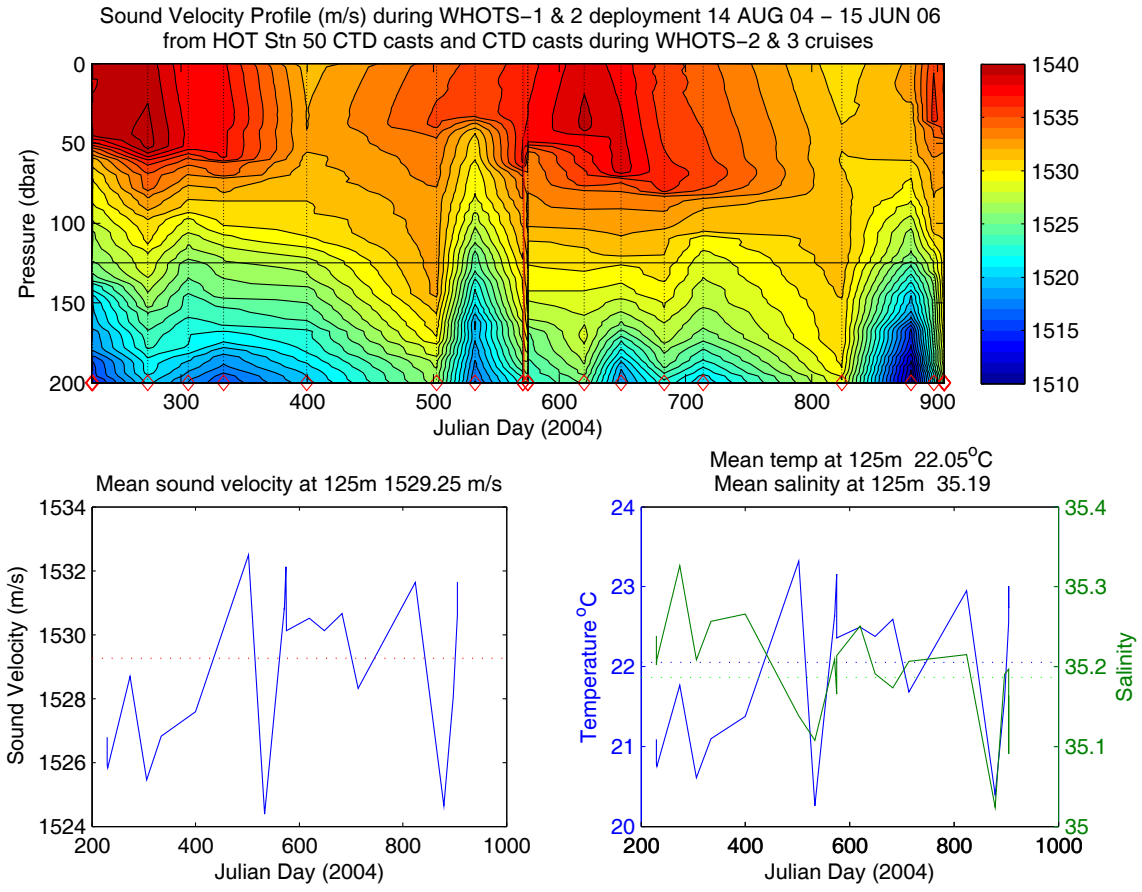

Figure 5-29 Sound Velocity profile (top panel) during the deployment of the WHOTS-1 and WHOTS-2 mooring from 2 dbar CTD data taken during regular HOT cruises and CTD profiles taken during the WHOTS-2 and WHOTS-3

recovery/deployment cruises (individual casts marked with a red diamond). The lower left panel shows the sound velocity at 125 m for the time series with the mean sound velocity indicated with the red line. The lower right panel shows the temperature and salinity at 125 m for the time series with the mean temperature indicated with the blue line and mean salinity indicated with the green line.

Quality Control

Quality control of the data involved the thorough examination of the velocity, attitude and diagnostic fields to determine the basis of the flagging scheme. Data were flagged in the order described below.

The first bin (closest to the transducer) is sometimes corrupted due to what is known as ringing. A period of time is needed for the sound energy produced during a transmit pulse at the transducer to dissipate before the ADCP is able to receive the returned echoes, This gap is known as the blanking interval and if it is too short, signal returns can be contaminated from the lingering noise from the transducer. The default value for the blanking interval, expressed as a distance of 1.76 m was used during the WHOTS-1 and WHOTS-2 deployments. Bins 1, 2 & 3 were examined and it was found that bin 1 was not coherent with bins 2 or 3 and showed more variability (see Figure 5-30). Furthermore, examination of the shear between these bins led to the conclusion that bin 1 was corrupted. Subsequently the whole of bin 1 was flagged and removed from the data set. It is recommended that the blanking interval be increased for future deployments.

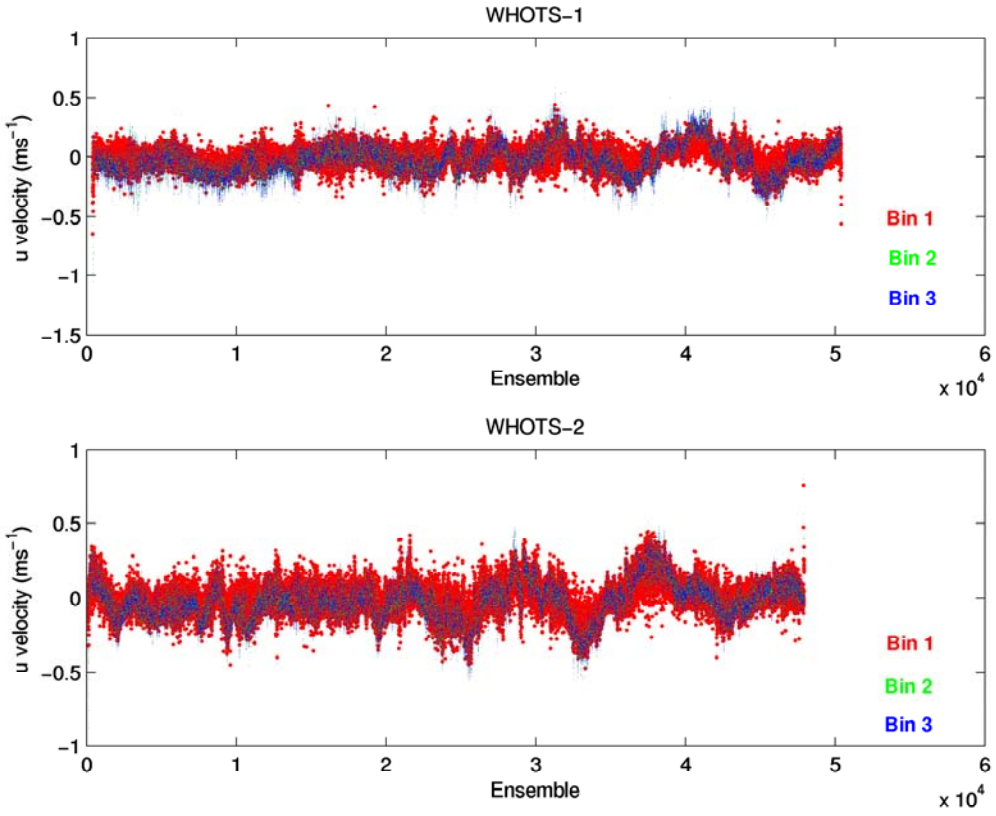

Figure 5-30 Eastward velocity component for WHOTS-1 (Upper panel) and WHOTS-2 (lower panel) showing the incoherence between depth bin 1 (red), and depth bins 2 (green) and 3 (blue) due to ringing.

For an upward looking ADCP within range of the sea surface with a beam angle of 20°, the upper 6% of the depth range is contaminated with sidelobe interference (RDI, 1996). This is a result of stronger signal reflection from the sea surface (than from scatterers) overwhelming the sidelobe suppression of the transducer. Data are flagged empirically using echo intensity (a measure of the strength of the return signal) from each beam to determine when the signal is contaminated with reflection from the sea surface. In practice, the majority of the data within the upper 4 bins (~14% of the vertical range) were flagged.

The use of four beams to resolve currents into their component velocities provides us with a second estimate of the vertical velocity. The difference between these two vertical velocities is defined as the error velocity and is useful for/in assessing data quality. Error velocities with an absolute magnitude greater than 0.15 m s^{-1} were flagged and removed.

An indication of data quality for each ensemble is given by the "percent good" data fields. The use of the percent good fields is determined by the coordinate transformation mode used during the data collection. With profiles transformed into earth coordinates (as is the case for WHOTS-1 and WHOTS-2 deployments) the percent good fields show the percentage of data that was made using 4 and 3 beam solutions in each depth cell within an ensemble, and the percentage that was rejected as a result of failing one of the criteria set during the instrument setup. Data

were flagged when data in each depth cell within an ensemble made from 3 or 4 beam solutions was 20% or less.

Data were rejected using correlation magnitude, which is the pulse-to-pulse correlation in a ping for each depth cell. If any one beam had a correlation magnitude of 20 counts or less that data point was flagged.

Originally, it was thought that the maximum vertical velocities experienced at the WHOTS site would be due to displacements as a result of the M2 tide. The maximum displacement would be 23 m which would give rise to vertical velocity of 0.03 cm s^{-1}. However based on histograms of raw data and partially cleaned data from the ADCP, this estimate seems of an order of magnitude too small (see Figure 5-31 and Figure 5-32). At present we are unsure as to the cause of these higher than anticipated velocities but based on the histograms of the partially cleaned observed data, depth cells with an absolute value of vertical velocity greater than 0.3 m s^{-1} were flagged.

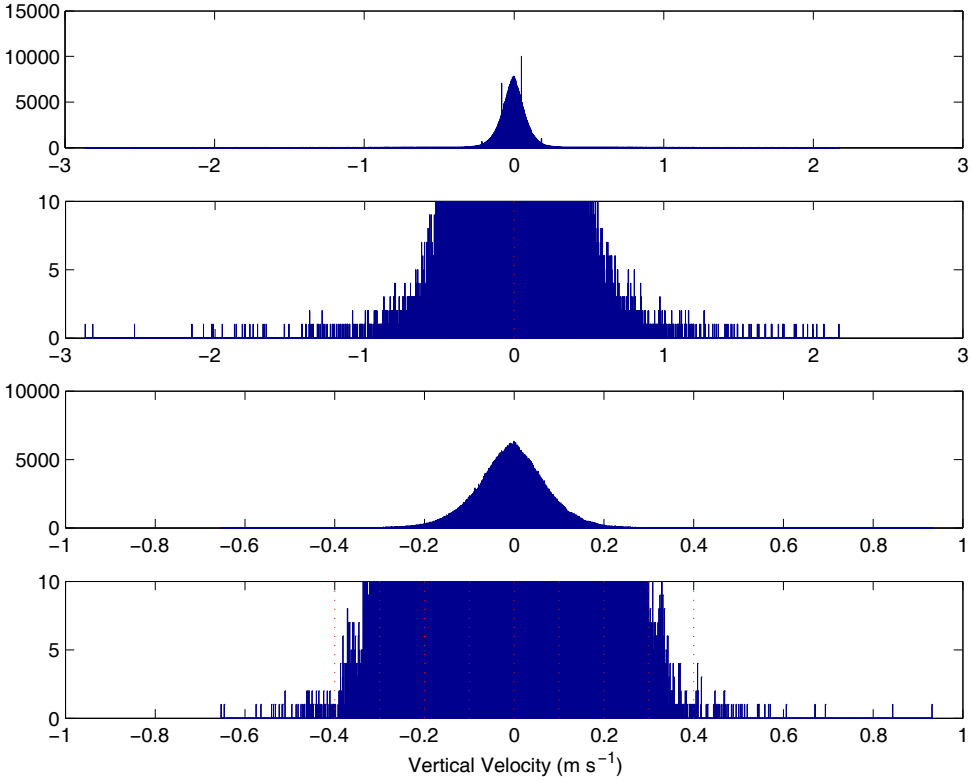

Figure 5-31 Histogram of vertical velocity for WHOTS-1 for raw data (top panel) and enlarged for clarity (upper middle panel), and for partial quality controlled data (lower middle panel) and enlarged for clarity (lower panel).

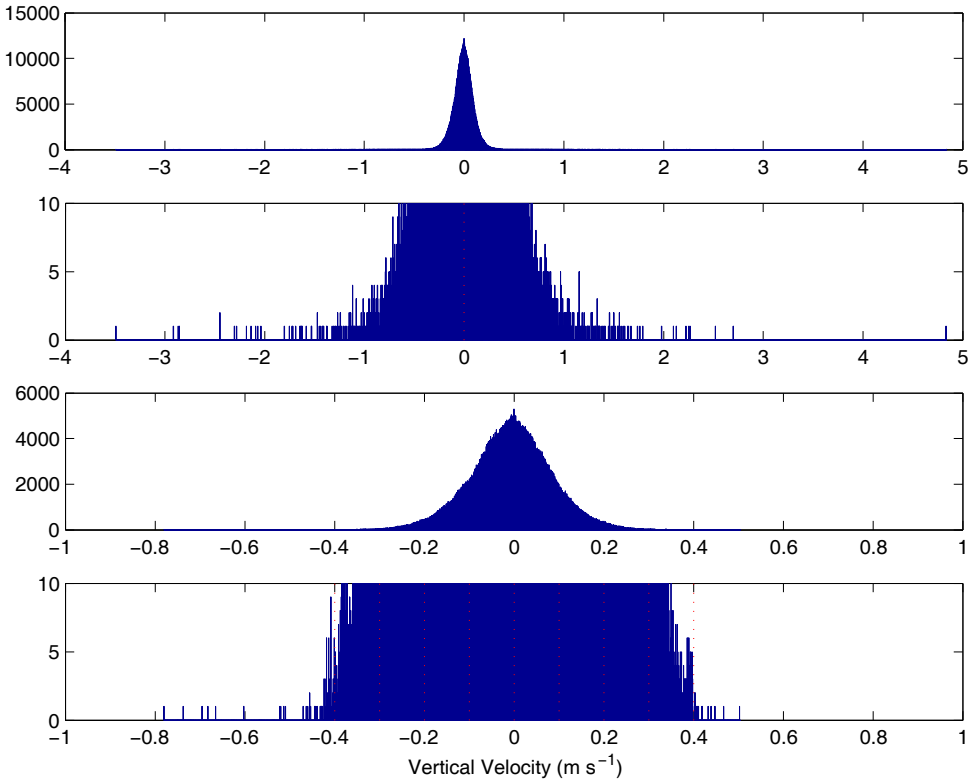

Figure 5-32 Same as Figure 5-31 but for WHOTS-2

Examination of east and north velocity components and of velocity magnitude during quality control revealed spikes that were vertically coherent to some degree throughout the profile (see Figure 5-33). There appeared to be no correlation between these data spikes and the diagnostic data output from the ADCP in particular pitch and roll data. At present the spike source is unknown but it is believed not to be real as the spikes generally stand out against a background of velocity data that are in good agreement.

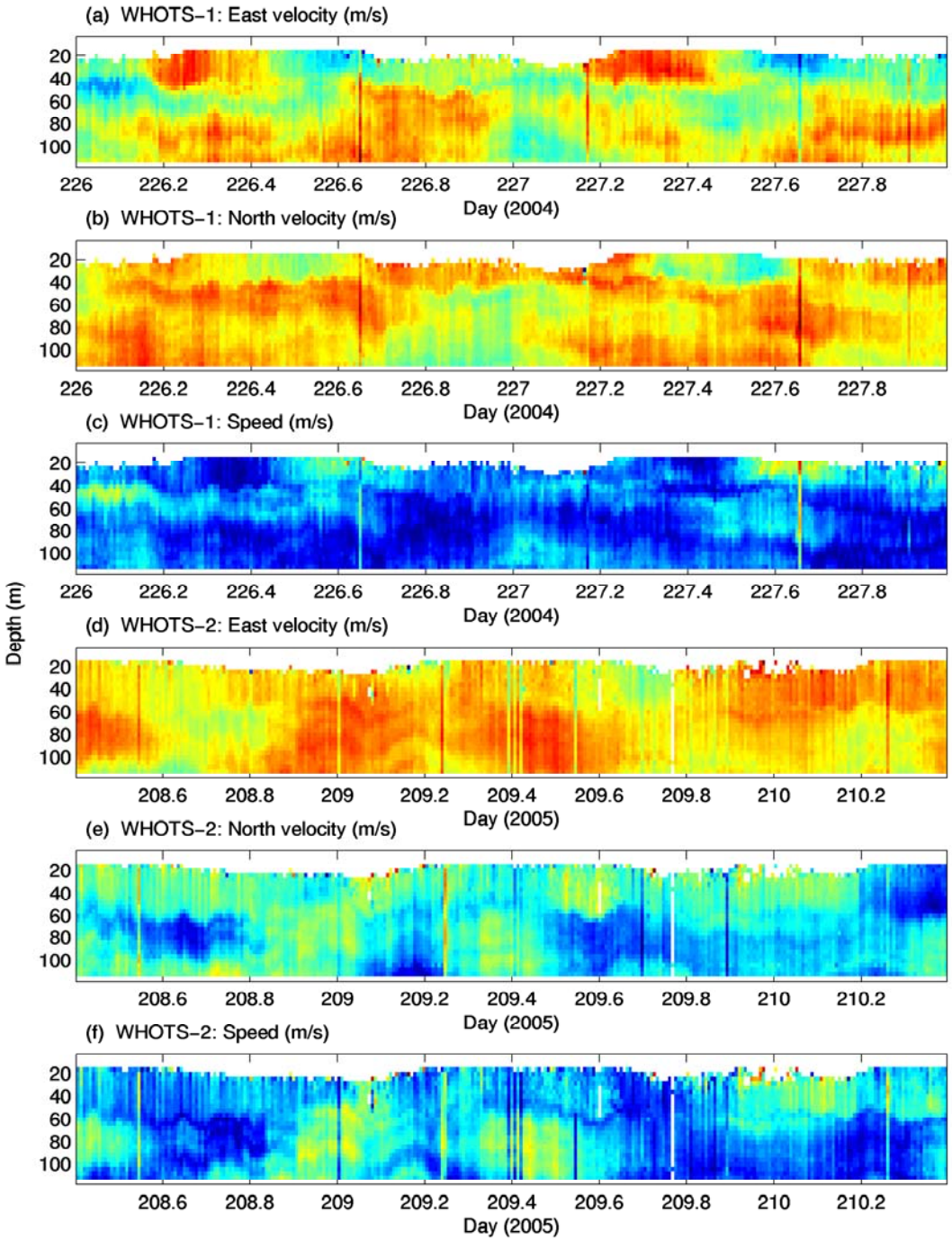

Figure 5-33 A 2 day subset of east (a & d) and north (b & e) velocity components and velocity magnitude (c & f) for WHOTS-1 and WHOTS-2 deployments respectively showing vertically coherent spikes.

A median filter was used in the removal of data spikes from data that had passed through the flagging process documented above. A vertical mean of both the east and west velocity components was taken across depth cells 2 to 20, as data across this range are generally considered to be of high quality and somewhat unaffected by the lack of scatterers and other factors that are responsible for the degradation of data quality in depth cells closer to the surface. After examining a number of different schemes, a 7-point median filter was applied to this vertical mean and points that were greater than a threshold value of 0.1 m s^{-1} were flagged.

Various possible causes for the existence of these vertically coherent spikes were tested, but unfortunately all of them were discharged. They were the following

- Mooring motion contamination

In order to determine if the mooring motion was causing the anomalous spikes, we estimated the mooring motion using the buoy's GPS positions available during the WHOTS-1 deployment. Although only one month of GPS data were available (see Section 5.D), the information was sufficient to conclude that the mooring motion was not the primary cause of the spikes. Figure 5-34 includes a 5-day section of the GPS calculated buoy's speed (bottom panel), together with plots of the ADCP zonal (upper two panels), and meridional current speeds (third and fourth panel). The vertically coherent ADCP spikes can be distinguished as stripes in the contour plots, and are more obvious in the vertically averaged speed plots (blue spikes). The times when these spikes occurred is indicated in the buoy GPS speed plot as vertical green lines. It is obvious that these times do not correspond with instances of particularly high buoy speeds. Only in two instances (near days 236 and 237.5) it appears that the spikes occurred during a high buoy's speeds, but a close analysis of the whole buoy speed record indicate no correlation between the appearance of the spikes and the buoy's speed.

In order to determine if the tilting of the mooring was related to the spikes occurrence, we compared the scatter plot of the ADCP pitch and roll using all the ADCP data, with another that included only the data with spikes. Figure 5-35 shows this comparison for the two deployments. In both plots the cloud of data with spikes (red circles) follows the same behavior than the rest of the data (blue circles), indicating that there was no particular relation between the spikes and the tilting of the ADCP.

- Wave orbital motion

In order to test the possibility that waves contributed to the appearance of the ADCP spikes, the wave data from the Datawell directional buoy located approximately 5 miles offshore of Waimea Bay on the north of O'ahu was used. No relation was found between the significant wave height and the occurrence of ADCP spikes.

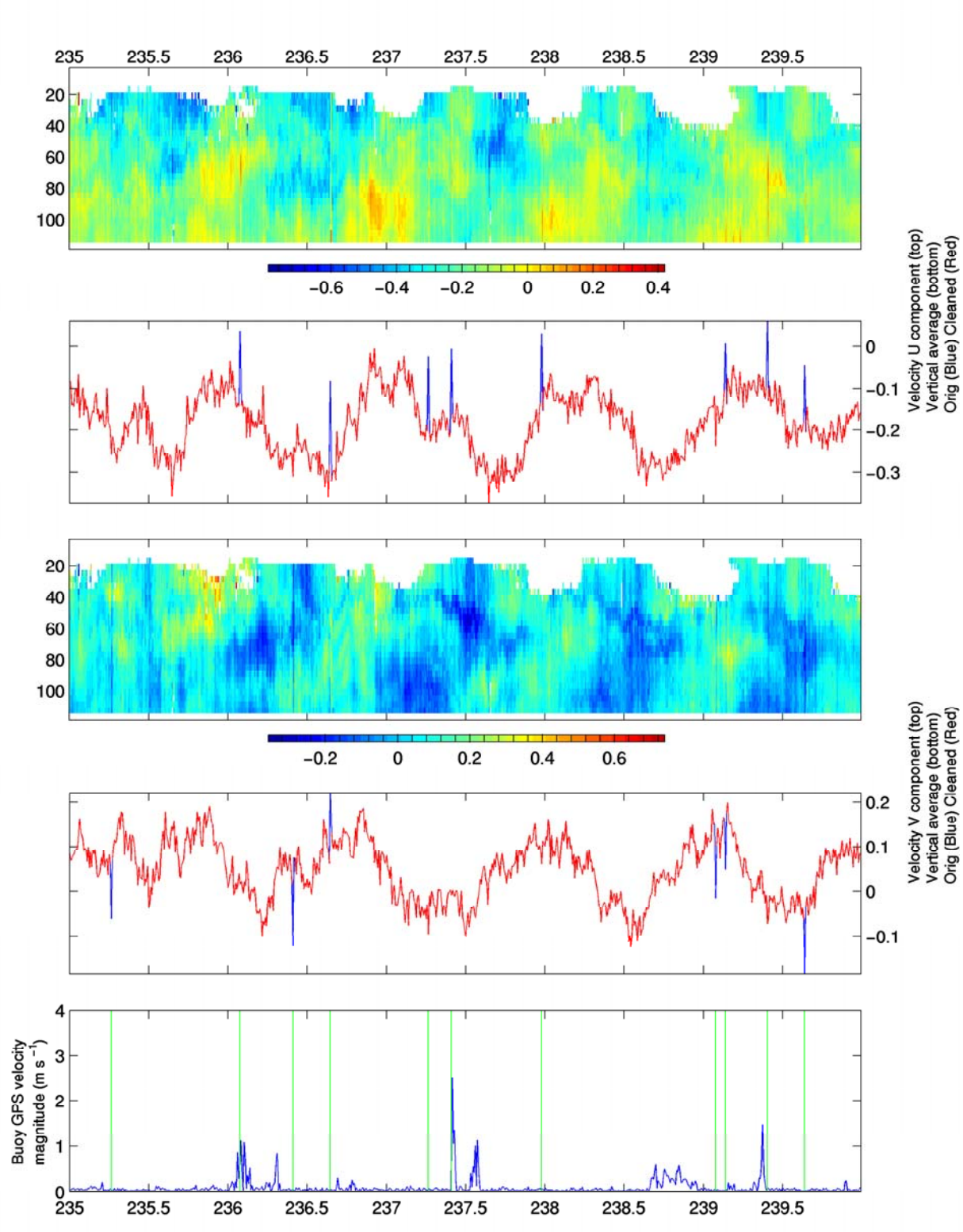

Figure 5-34. Contours of zonal (first panel), and meridional (third panel) ADCP speed in depth and time during five days of the WHOTS-1 mooring deployment. Vertical averaged zonal (second panel), and meridional (fourth panel) speeds (red line), the blue line shows the spikes in the data. Buoy speeds calculated with GPS data (bottom panel) during the same time period as the ADCP. The vertical lines indicate the times of the spikes in the ADCP data.

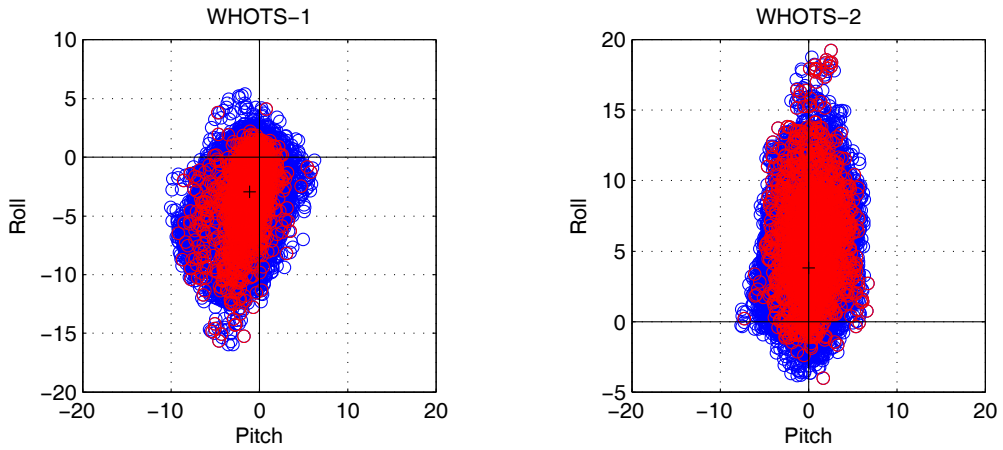

Figure 5-35. Scatter plots of ADCP pitch and roll during WHOTS-1 (left plot), and WHOTS-2 (right plot) deployments (blue circles). The red circles correspond to data with spikes in ADCP speed.

We also verified that the occurrence of the spikes was not related to the ADCP zonal, meridional or vertical speeds, or to the ADCP diagnostics data of amplitude and correlation. In addition, we verified that there was no particular pattern in the sign of the spikes; i.e. the distribution of positive spikes was the same as the distribution of negative spikes for both deployments. Other sources of contamination that could have caused the spikes are noise from ships or whales.

C. Next Generation Vector Measuring Current Meter (NGVM)

NGVM data from the WHOTS-1 deployment were processed by the WHOI/UOP group. A copy of the processing report is in Appendix 3 in Section 8.C, and it can also be found together with the data at the following FTP site: ftp://ftp.whoi.edu/pub/users/lhutto/WHOTS1. NGVM data from the WHOTS-2 deployment were processed at UH. The records were truncated to 2 hours after deployment allowing time for mooring motions associated with the sinking anchor to die out. A magnetic variation of 10.2° was applied to the velocity components. NGVM record times are shown in Table 5.7.

Table 5.7 Record times (UTC) for the NGVMs at 10 m and 30 m during the WHOTS-1 and WHOTS-2 deployments

	WHOTS-1		WHOTS-2	
	NGVM012	NGVM019	NGVM066	NGVM068
Raw file beginning and end times	05-Aug-2004 20:29 18-Apr-2005 05:15	05-Aug-2004 20:29 25-Jul-2005 17:15	16-Jul-2005 02:14 28-Jun-2006 20:49	16-Jul-2005 02:14 28-Jun-2006 20:36
Deployment and recovery times	13-Aug-2004 02:40 25-Jul-2005 17:15	13-Aug-2004 02:40 25-Jul-2005 17:15	28-Jul-2005 01:42 24-Jun-2006 18:30	28-Jul-2005 01:42 24-Jun-2006 18:30

Processed file beginning and end times	13-Aug-2004 03:40 25-Jul-2005 17:15	13-Aug-2004 03:40 25-Jul-2005 17:15	28-Jul-2005 03:42 24-Jun-2006 18:30	28-Jul-2005 03:42 24-Jun-2006 18:30

Velocity data from the NGVM at 30 m was compared with the ADCP data from the equivalent depth cell (bin 23) for the WHOTS-1 and WHOTS-2 deployments. A running mean filter of length 1 day was applied to both the NGVM and ADCP horizontal velocity data and the differences computed (Figure 5-36 and Figure 5-37). The mean difference was 0.0014 ±0.048 m s^{-1} for the eastward component and 0.0004 ±0.055 m s^{-1} for the northward component. ADCP data were too sparse to make a comparison with the NGVM situated at 10 m.

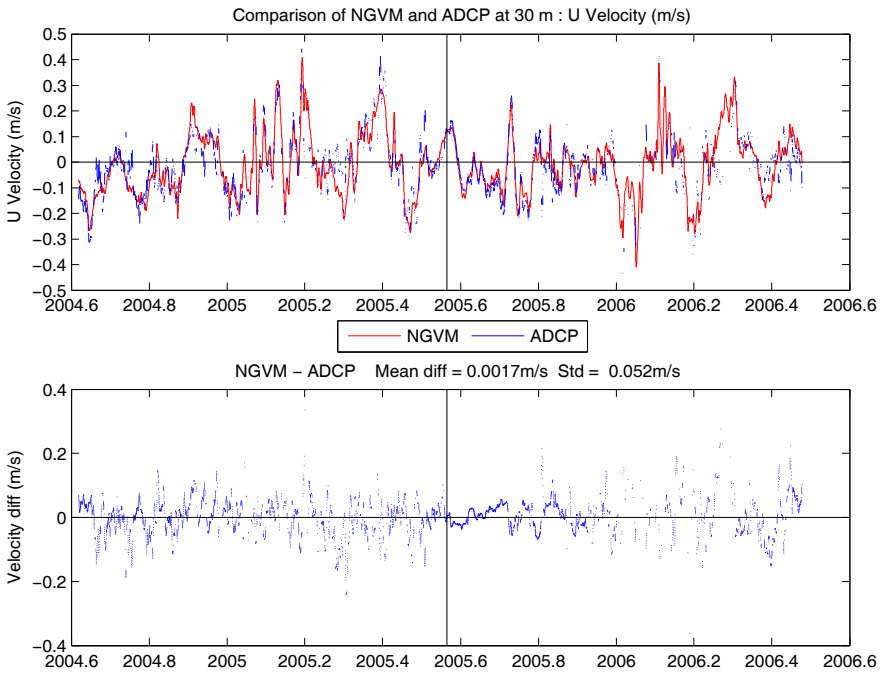

Figure 5-36 East velocity data (m s^{-1}) observed with the NGVM at 30 m (red) plotted with ADCP data (blue) from the equivalent depth cell (top panel). The differences between the NGVM and the ADCP are plotted in the lower panel.

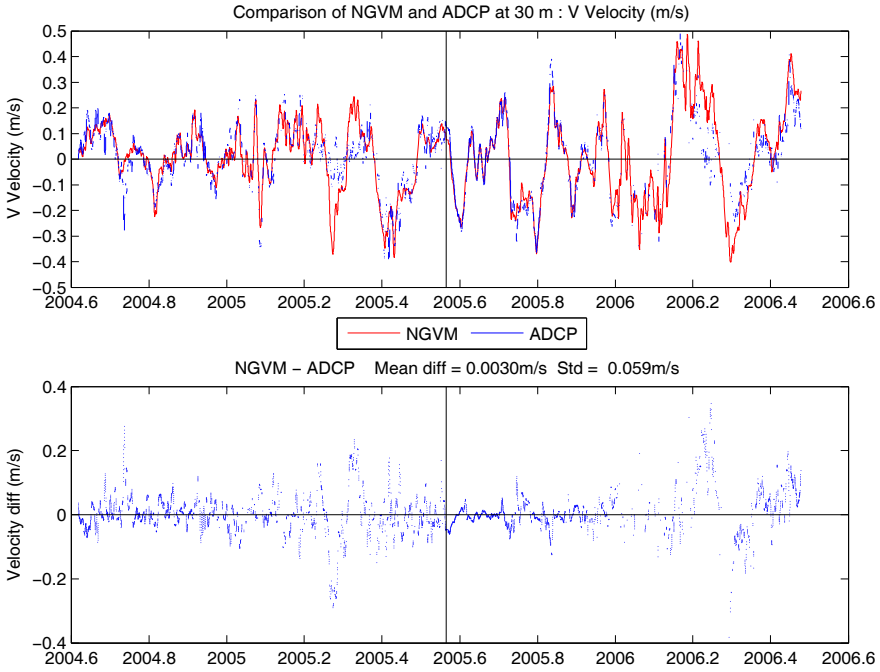

Figure 5-37 North velocity data (m s^{-1}) observed with the NGVM at 30 m (red) plotted with ADCP data (blue) from the equivalent depth cell (top panel). The differences between the NGVM and the ADCP are plotted in the lower panel.

Velocity differences between the NGVM and the ADCP were compared with wave data from the Datawell directional buoy located approximately 5 miles offshore of Waimea Bay on the north of O'ahu, (see Appendix 4 in Section 8.D for buoy details). As mentioned in Section 5.B.2, a burst sampling scheme was utilized for the WHOTS-1 deployment in order to resolve orbital motions due to large swell. However, the subsequent deployment, WHOTS-2, did not utilize a burst sampling scheme and any influence due to swell might be reflected in a larger disparity with the NGVM data. Velocity differences greater than 0.1 m s^{-1} were identified (Figure 5-38 and Figure 5-39 marked in red below), but do not seem to correlate with episodes of large swell for either deployment. We conclude that orbital wave motions from large swell do not adversely affect the velocity data and that there appears to be no bias from the different sampling schemes used for the two deployments.

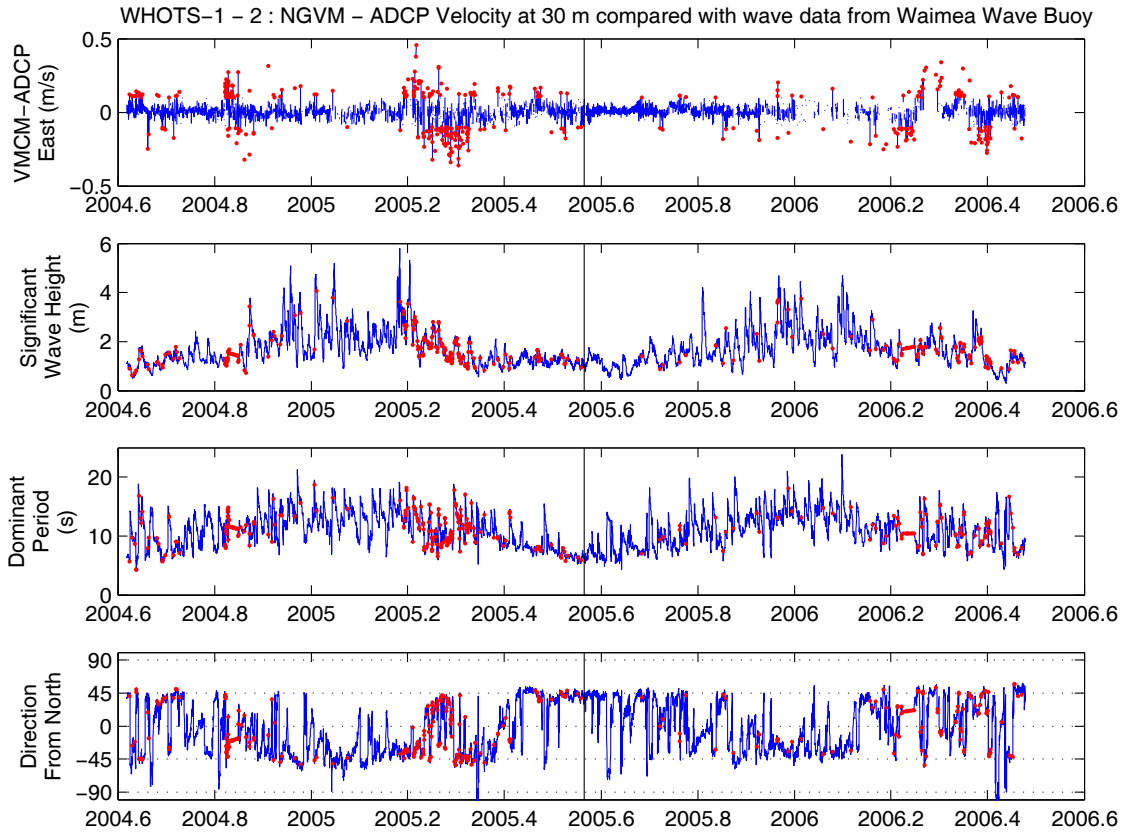

Figure 5-38 Differences in east velocity component (m s^{-1}) between the 30 m NGVM and the moored ADCP for the same depth (upper panel). Significant wave height (m), dominant period (s) and direction from due north recorded by the Datawell buoy offshore of Waimea Bay (lower 3 panels respectively).

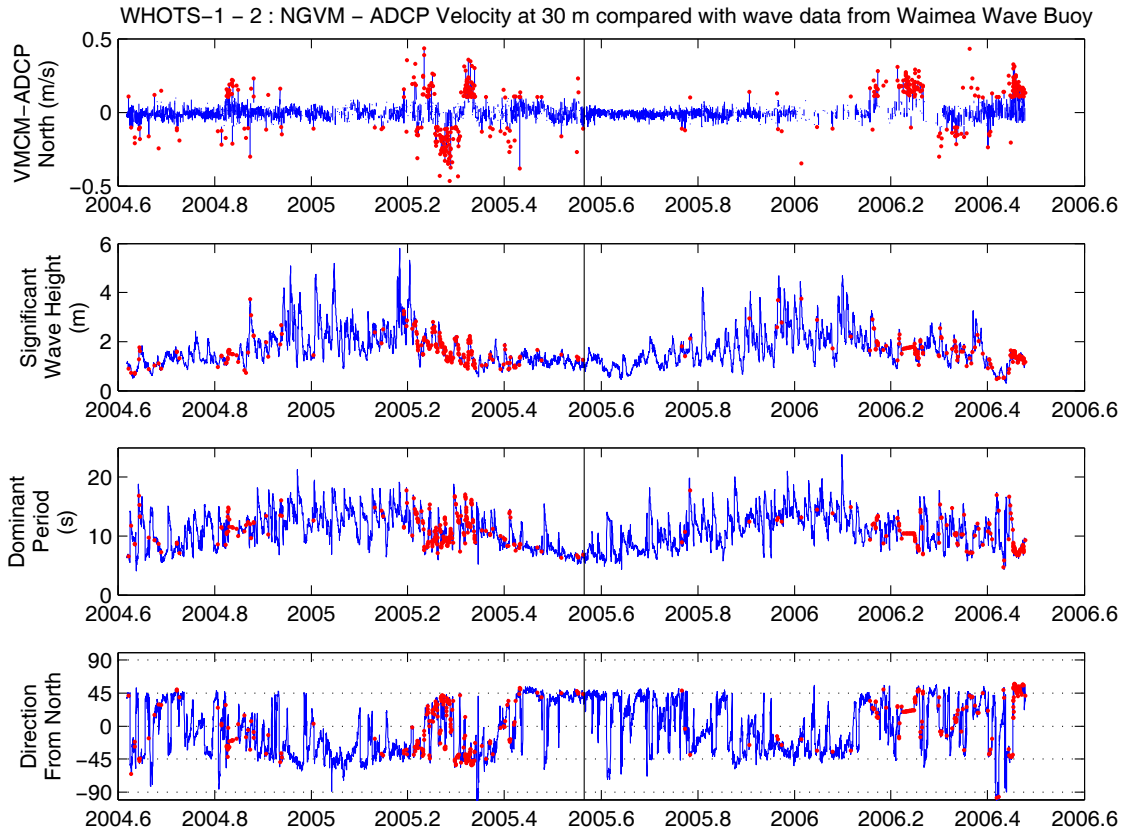

Figure 5-39 Differences in north velocity component (m s^{-1}) between the 30 m NGVM and the moored ADCP for the same depth (upper panel). Significant wave height (m), dominant period (s) and direction from due north recorded by the Datawell buoy offshore of Waimea Bay (lower 3 panels respectively).

D. Global Positioning System Receiver and ARGOS Positions

Seimac Global Positioning System receivers SN 69024 and SN 73930 were attached to the tower tops of the buoys during the WHOTS-1 and WHOTS-2 deployments respectively. Data return from the receivers were poor with approximately 31 days from WHOTS-1 and 2 ½ days from WHOTS-2 of usable data being recovered (Table 5.8). The reasons for the failure of the units are unclear.

Table 5.8 GPS record times (UTC) during WHOTS-1 and WHOTS-2 deployments.

	WHOTS-1	WHOTS-2
Raw file beginning and end times	04-Aug-2004 03:10 02-Jul-2005 22:23	16-Jul-2005 19:01 26-Jun-2006 00:34
Processed data beginning and end times	13-Aug-2004 05:16 13-Sep-2004 22:38	28-Jul-2005 01:42 26-Jul-2005 07:48

The nominal sampling interval was 10 minutes although there are some small gaps present in the records for both deployments. Records were truncated to approximately 1 hour after the anchor was released. Data were screened for points that were greater than 2.5 nautical miles from the surveyed anchor positions for each deployment which was considered to be the buoy watch circle radius. The velocity magnitude was calculated and positions that resulted in speeds greater than 1 m s^{-1} were removed. Data were interpolated onto a regular time interval in order to compute spectra.

ARGOS positions were available during the WHOTS-1 and –2 deployments and provided additional information on the buoy's motion. These positions were available at random times, with a mean interval between data of about 2 hr. For comparison, Figure 5-40 shows the ARGOS buoy's positions together with the GPS positions during the WHOTS-1 deployment. The standard deviation of the difference between these two records is about 600 m.

The ARGOS positions of the WHOTS-1 buoy for the duration of the deployment are in Figure 5-41, and shows the color-coded positions according to their data quality. The data quality is determined by its distance from the satellite track. Data of a better quality have a higher flag number: 3 is for a distance less than 150 m, 2 is for a distance between 150 and 350 m, and 1 is for a distance between 350 and 1000 m. For the duration of the deployment, the buoy had a mean position of about 3 km from the anchor, with a standard deviation of about 600 m. The buoy's location was mostly west of the anchor. A similar figure for the WHOTS-2 deployment (Figure 5-42) indicates that the buoy had a mean position of also about 3 km from the anchor, with a standard deviation of about 700 m. The buoy during this deployment was also located west of the anchor most of the time.

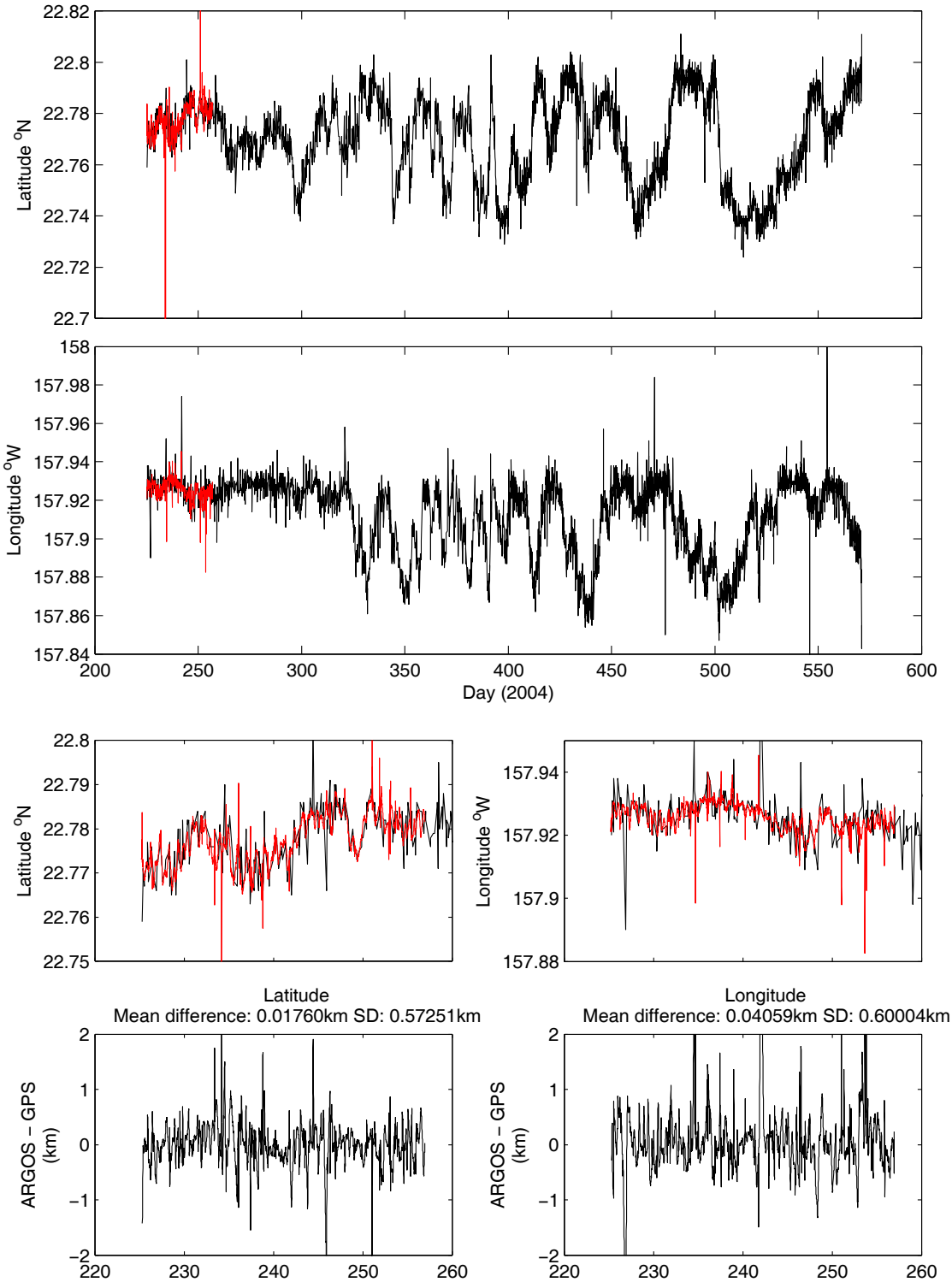

Figure 5-40. WHOTS-1 buoy position from ARGOS data (black line), and from GPS data (red line). The top and two middle panels show the latitude and longitude of the buoy. The bottom panel shows the difference between the GPS positions and the ARGOS positions interpolated to the GPS times.

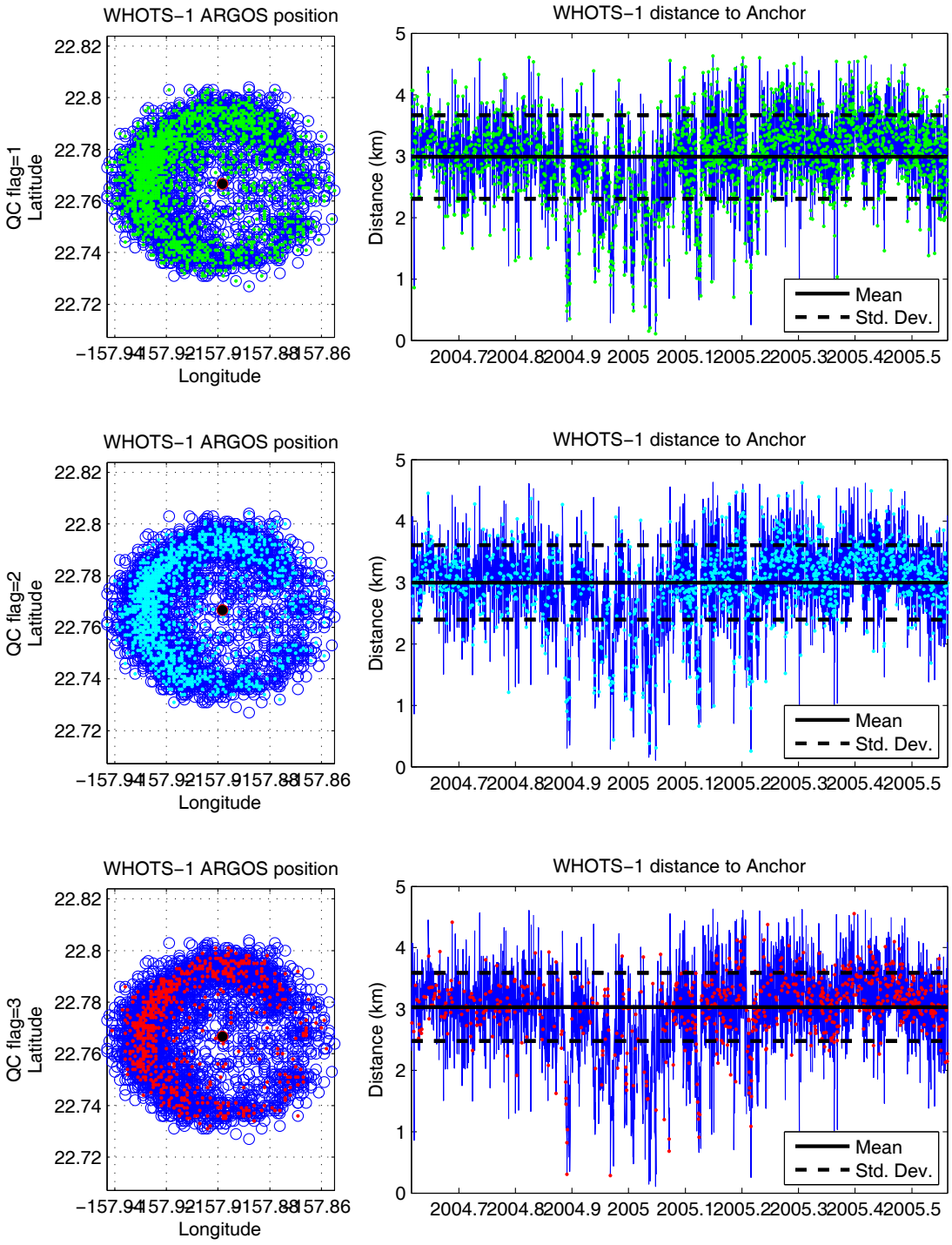

Figure 5-41. WHOTS-1 buoy ARGOS positions (circles, left panels), and distance from its anchor (blue line, right panels). The data are colored according to their quality control flag, 1: green, 2: light blue, 3: red. The black circle in the center of the left side panels is the location of the mooring's anchor. The black line in the right panel plots is the mean distance between the buoy and its anchor, and the dashed line is the mean plus minus one standard deviation.

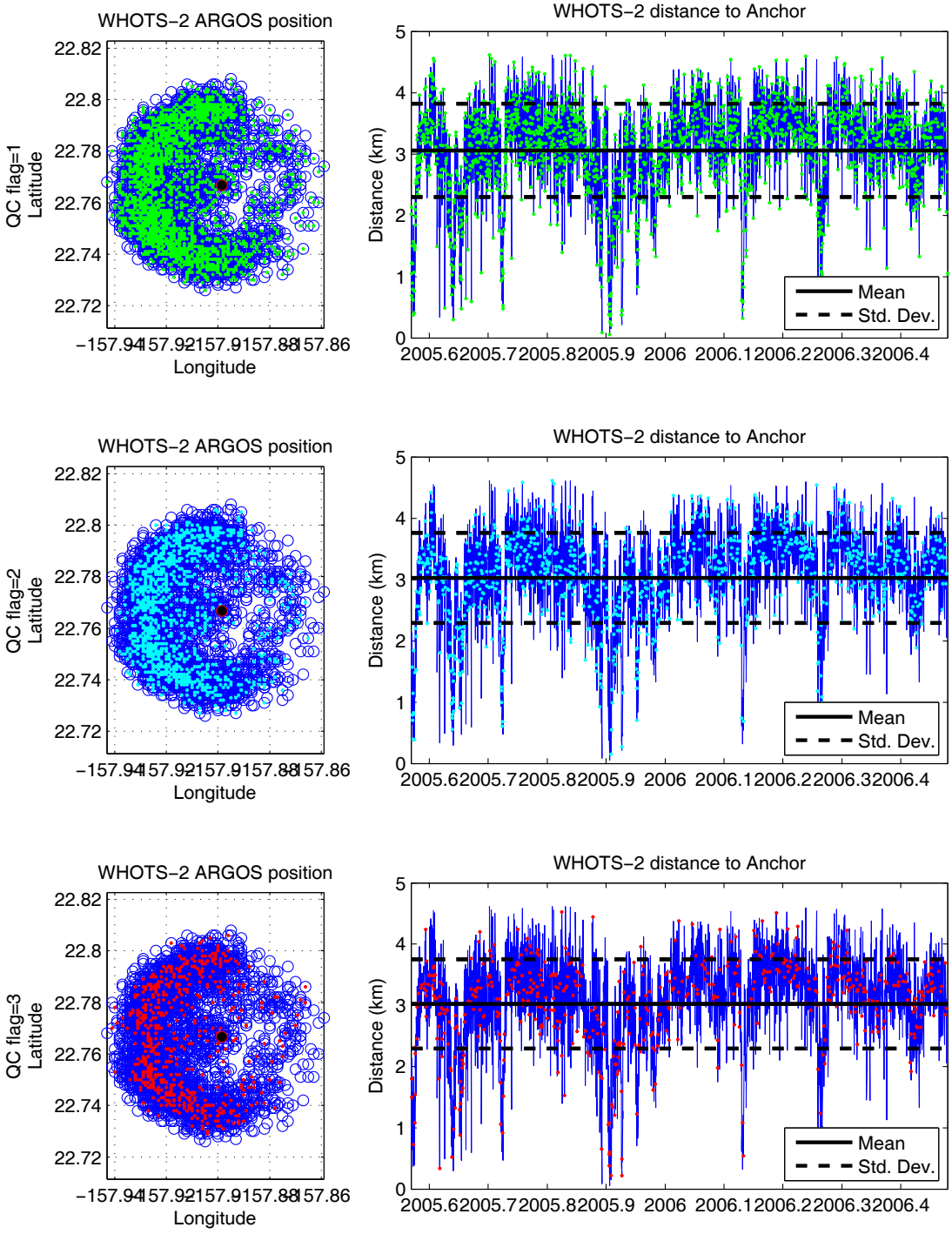

Figure 5-42. Same as in Figure 5-41, but for the WHOTS-2 buoy.

6. Results

A. CTD Profiling Data

Profiles of temperature, salinity and potential density (σ_θ) from the casts obtained during the WHOTS-2 (Figure 6-1), and -3 deployment cruises are presented in Figure 6-2 through Figure 6-18, together with the results of bottle determination of salinity, and of dissolved oxygen for WHOTS-2.

The hydrographic data collected during the WHOTS-2 cruise are presented in a series of contour plots along the two main cruise transects North-South, and Northwest-Southeast. Figure 6-1 shows the location of the casts. Color contoured plots of temperature, salinity, potential density (σ_θ), dissolved oxygen, and fluorescence are shown in Figure 6-19 through Figure 6-32.

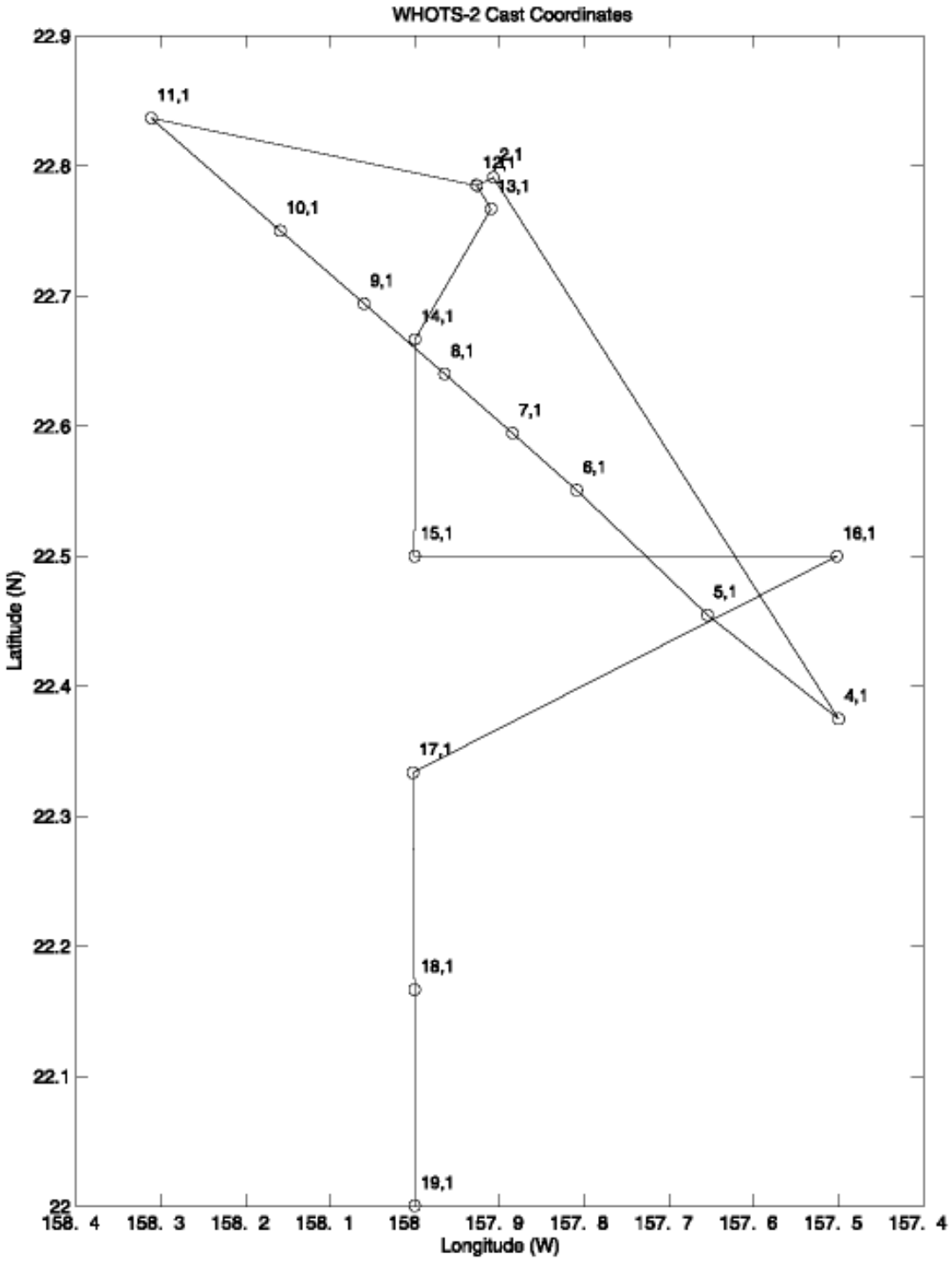

Figure 6-1. Location of stations/casts during WHOTS-2 cruise.

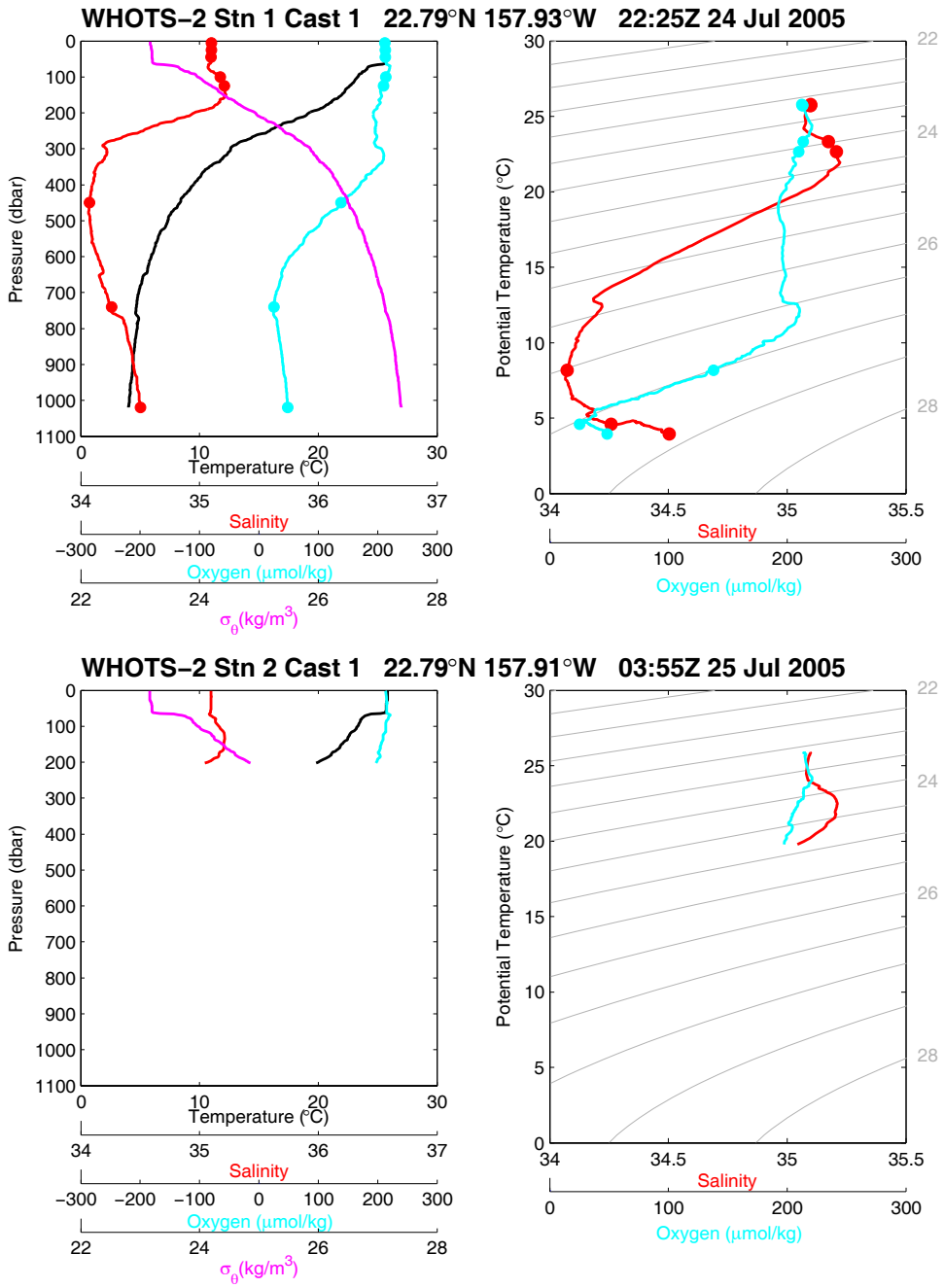

Figure 6-2. [Upper left panel] Profiles of CTD temperature, salinity, oxygen and potential density (σ_θ) as a function of pressure, including discrete bottle salinity and dissolved oxygen samples (when available) for station 2 cast 1 during WHOTS-2 cruise. [Upper right panel] Profiles of CTD salinity and oxygen as a function of potential temperature, including discrete bottle salinity and dissolved oxygen samples (when available) for station 2 cast 1 during WHOTS-2 cruise. [Lower left panel] Same as in the upper left panel, but for station 2 cast 2. [Lower right panel] Same as in the upper right panel, but for station 2 cast 2.

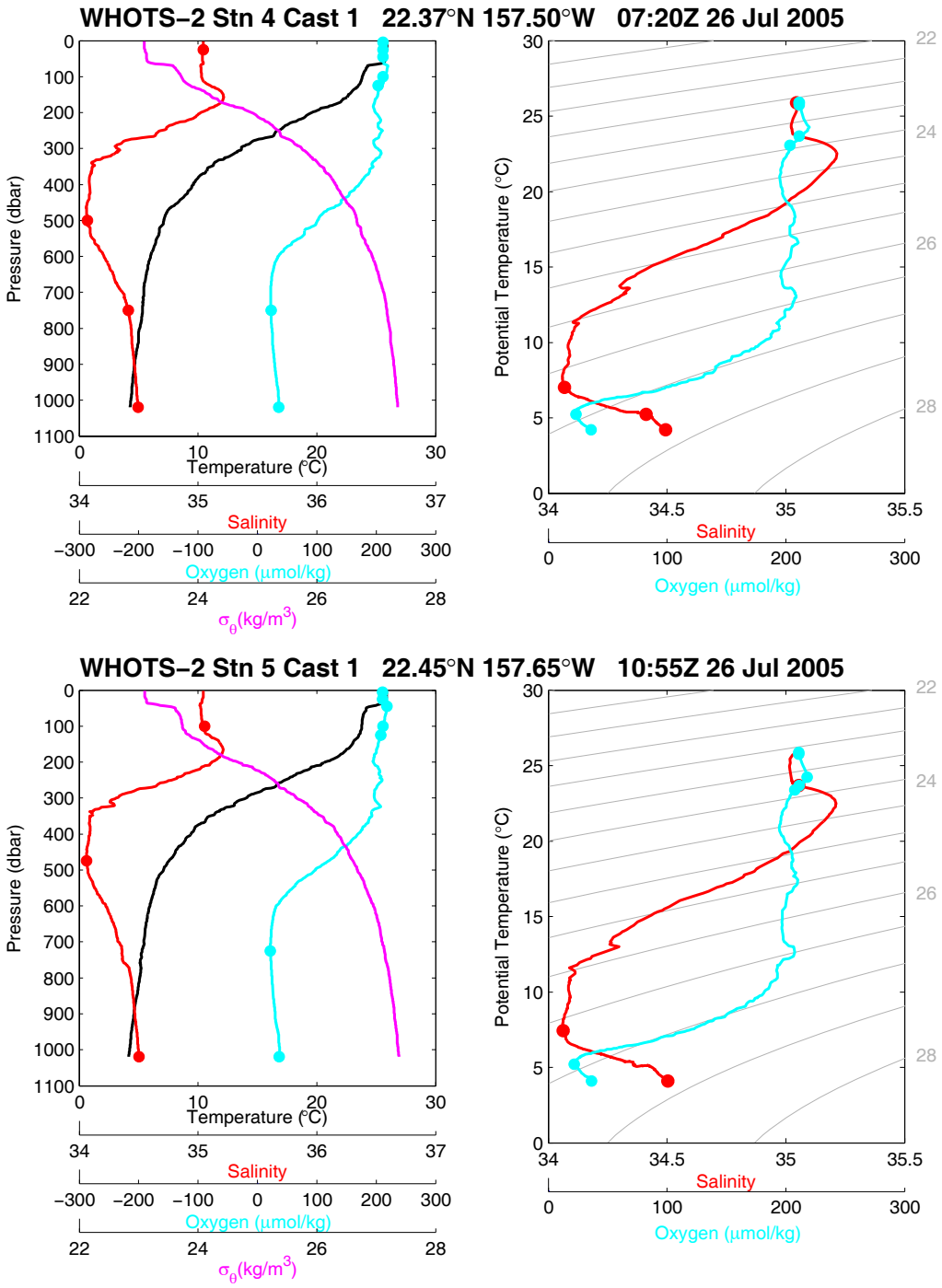

Figure 6-3. [Upper panels] Same as in Figure 6-2, but for station 4, cast 1. [Lower panels] Same as in Figure 6-2, but for station 5, cast 1.

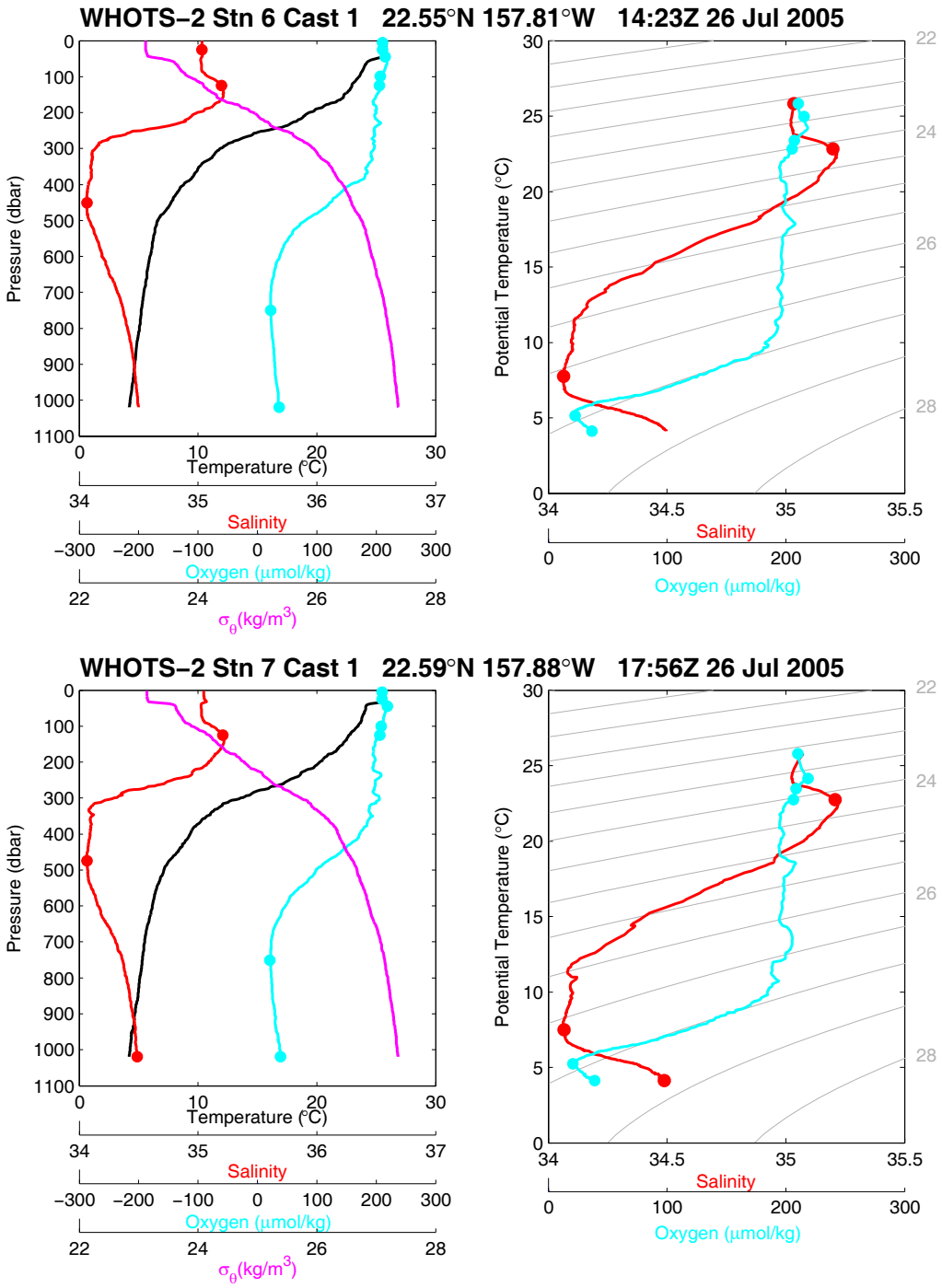

Figure 6-4. [Upper panels] Same as in Figure 6-2, but for station 6, cast 1. [Lower panels] Same as in Figure 6-2, but for station 7, cast 1.

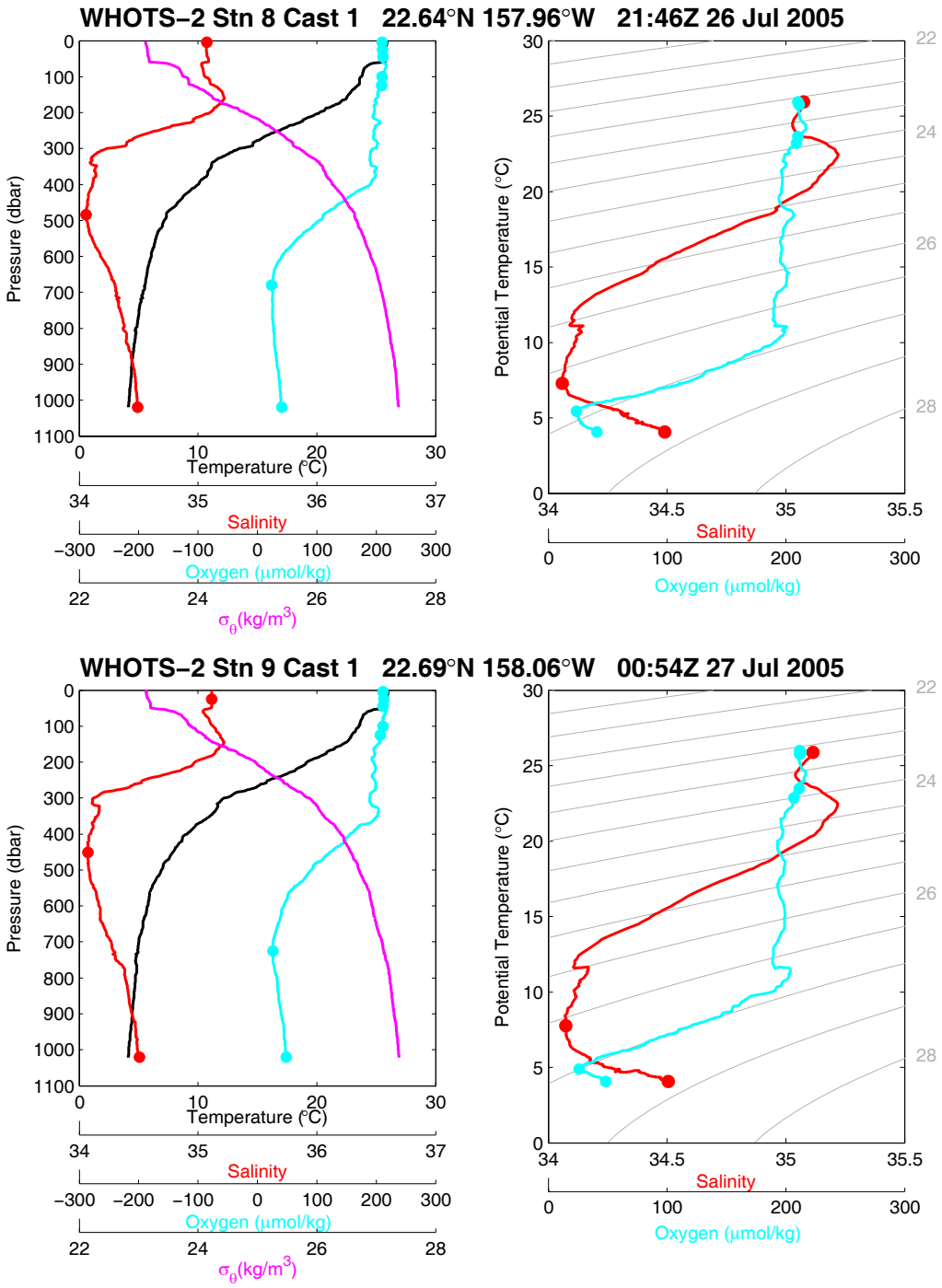

Figure 6-5. [Upper panels] Same as in Figure 6-2, but for station 8, cast 1. [Lower panels] Same as in Figure 6-2, but for station 9, cast 1.

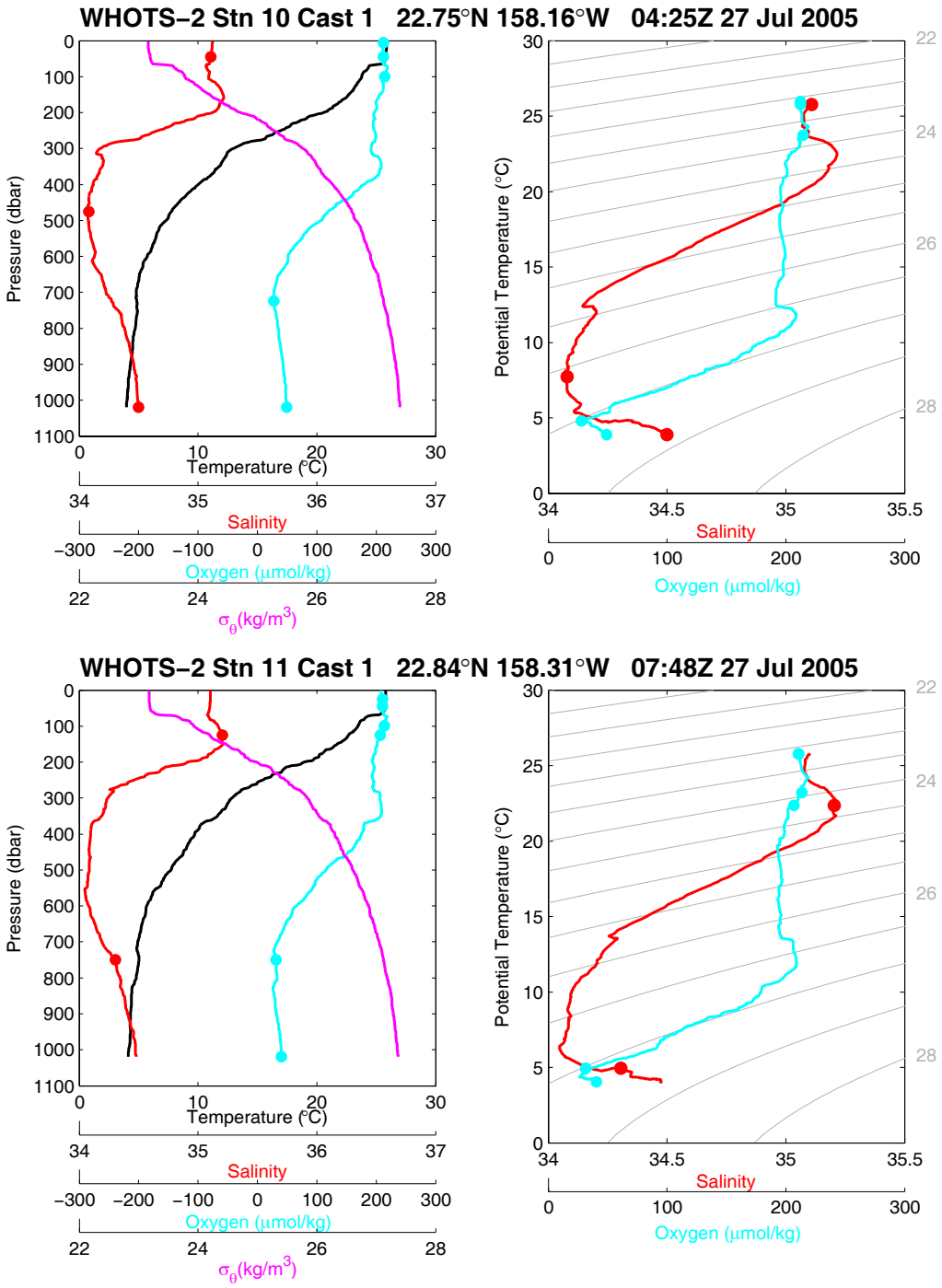

Figure 6-6. [Upper panels] Same as in Figure 6-2, but for station 10, cast 1. [Lower panels] Same as in Figure 6-2, but for station 11, cast 1.

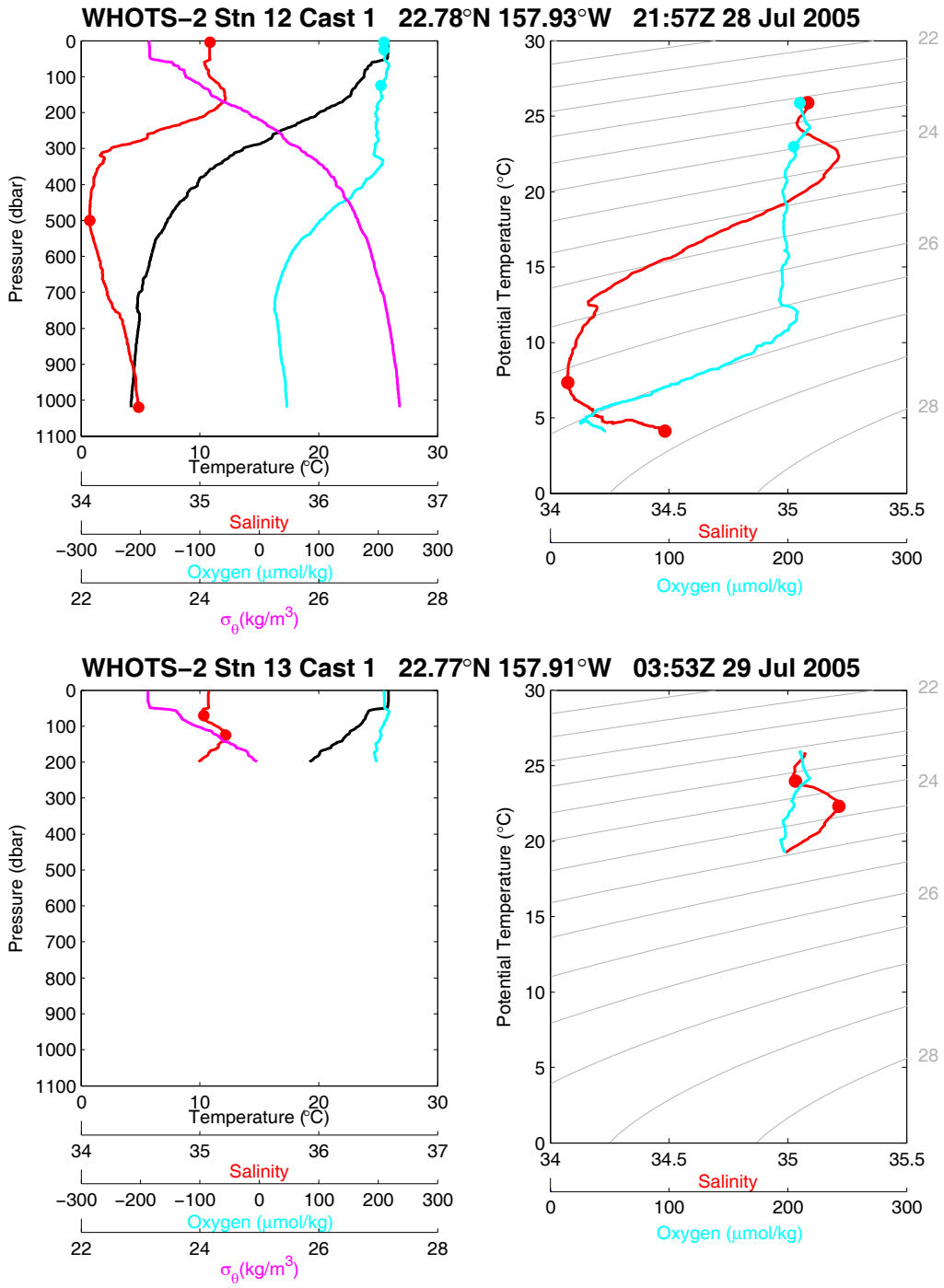

Figure 6-7. [Upper panels] Same as in Figure 6-2, but for station 12, cast 1. [Lower panels] Same as in Figure 6-2, but for station 13, cast 1.

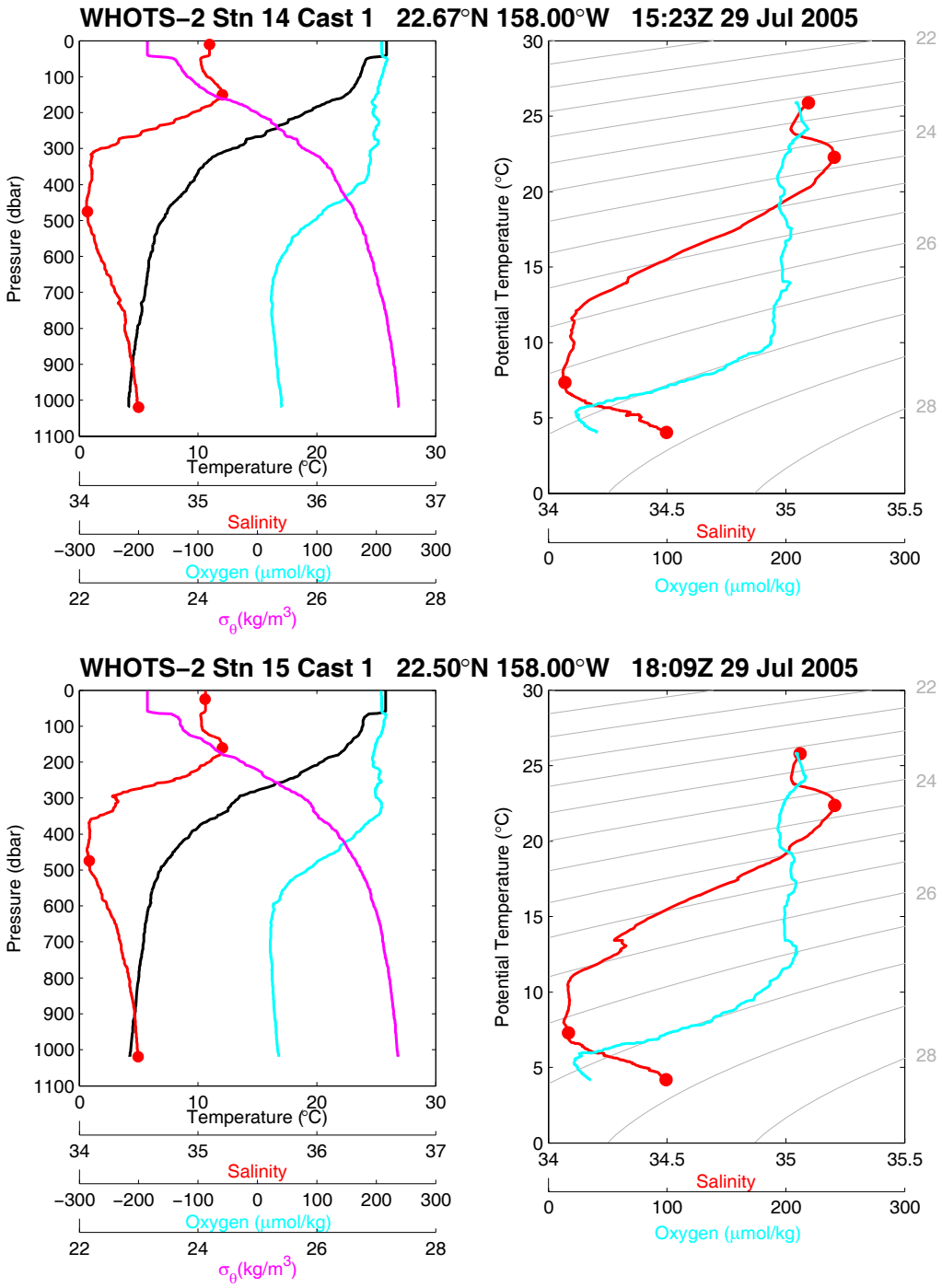

Figure 6-8. [Upper panels] Same as in Figure 6-2, but for station 14, cast 1. [Lower panels] Same as in Figure 6-2, but for station 15, cast 1.

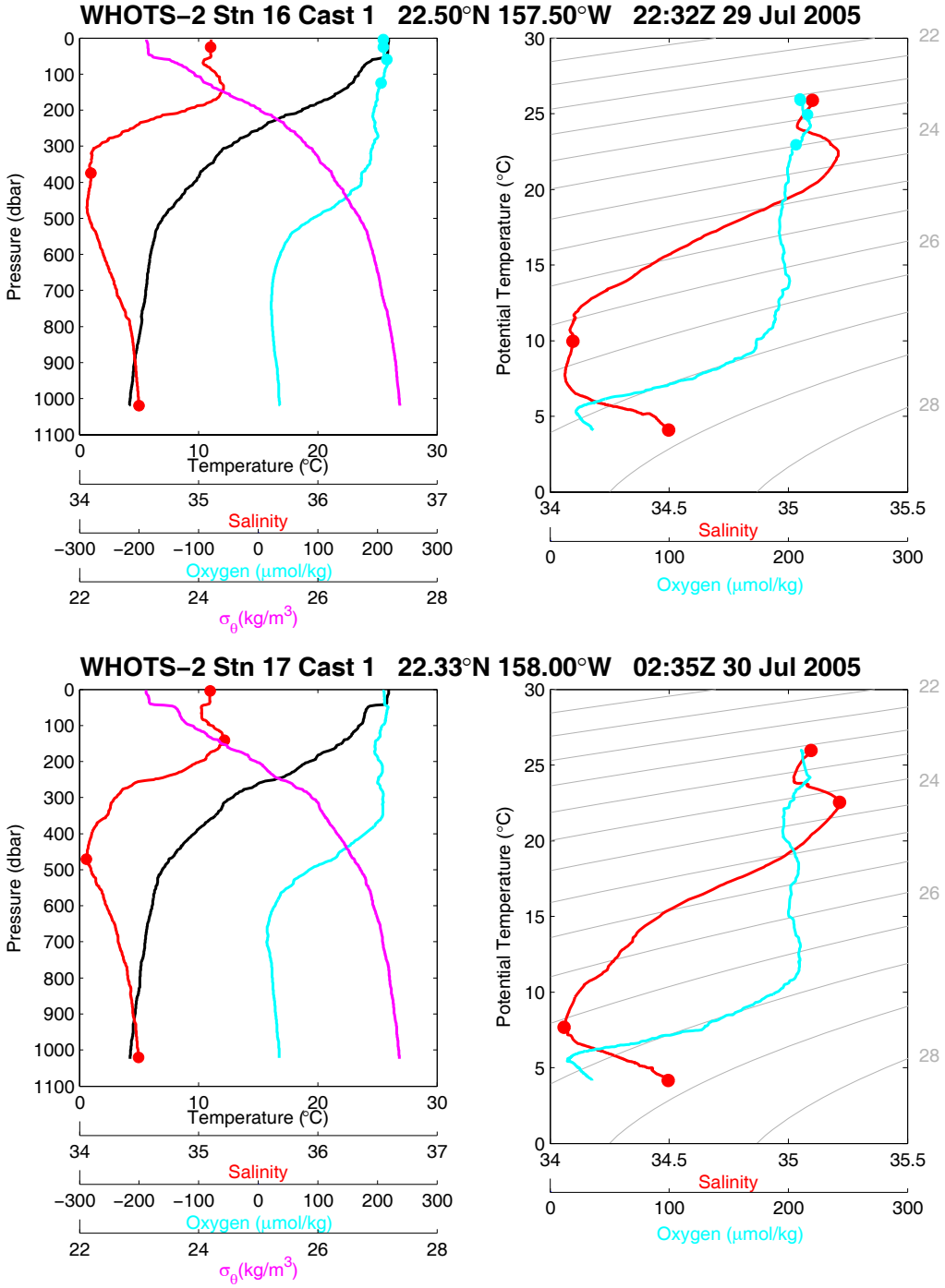

Figure 6-9. [Upper panels] Same as in Figure 6-2, but for station 16, cast 1. [Lower panels] Same as in Figure 6-2, but for station 17, cast 1.

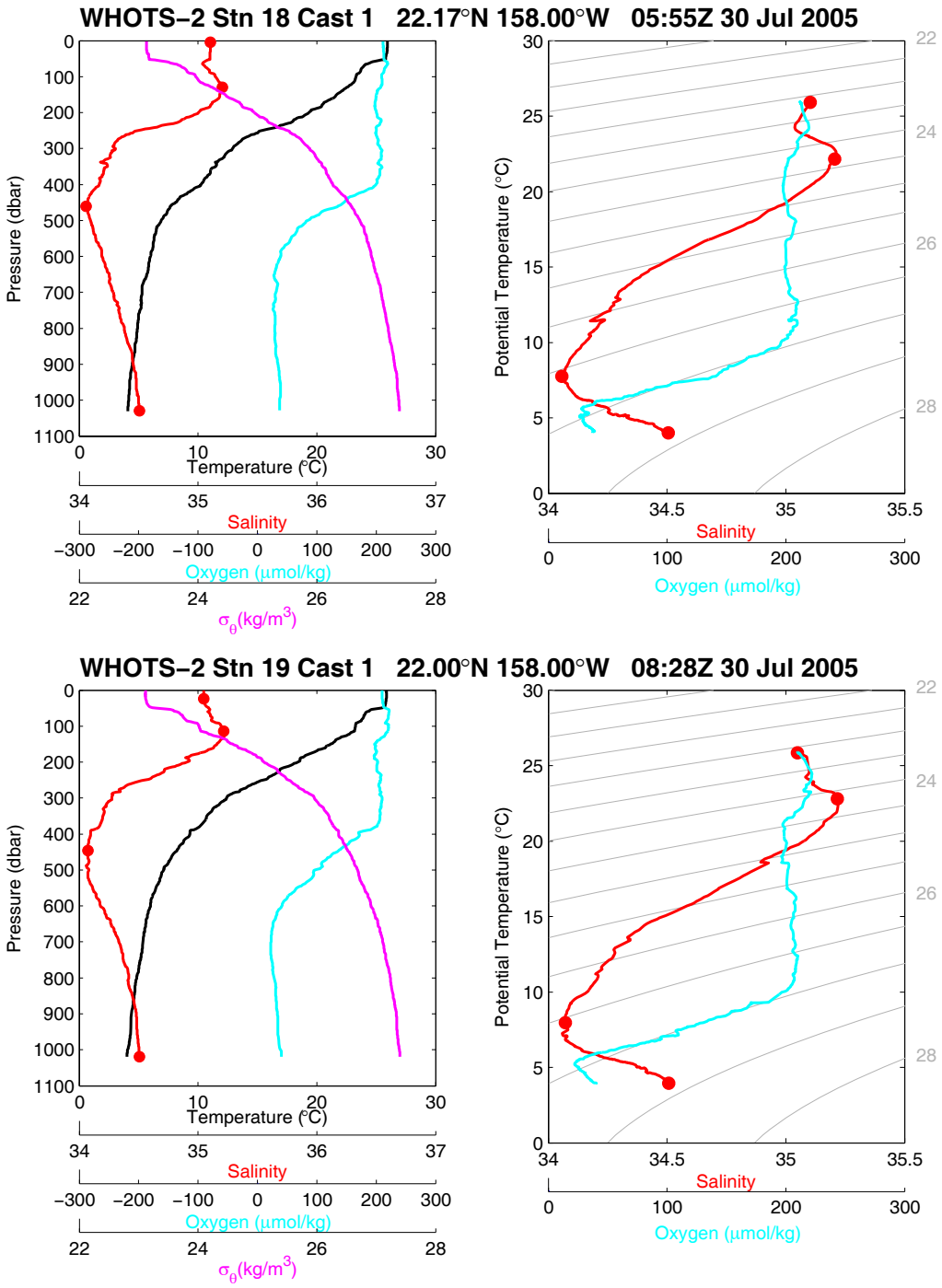

Figure 6-10. [Upper panels] Same as in Figure 6-2, but for station 18, cast 1. [Lower panels] Same as in Figure 6-2, but for station 19, cast 1.

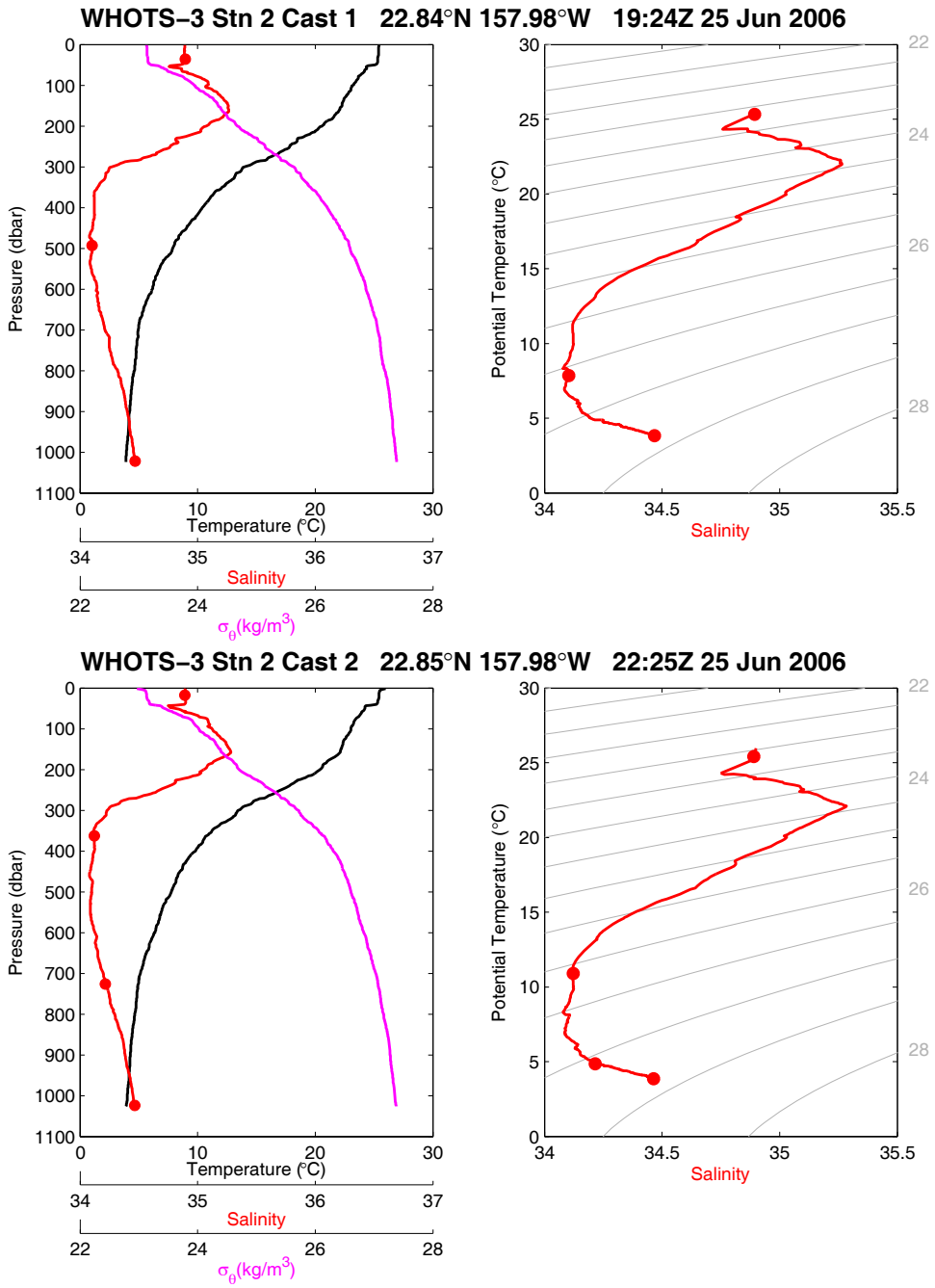

Figure 6-11. [Upper left panel] Profiles of CTD temperature, salinity, and potential density (σ_θ) as a function of pressure, including discrete bottle salinity samples for station 2 cast 1 during WHOTS-3 cruise. [Upper right panel] Profile of CTD salinity as a function of potential temperature, including discrete bottle salinity samples for station 2 cast 1 during WHOTS-3 cruise. [Lower left panel] Same as in the upper left panel, but for station 2 cast 2. [Lower right panel] Same as in the upper right panel, but for station 2 cast 2.

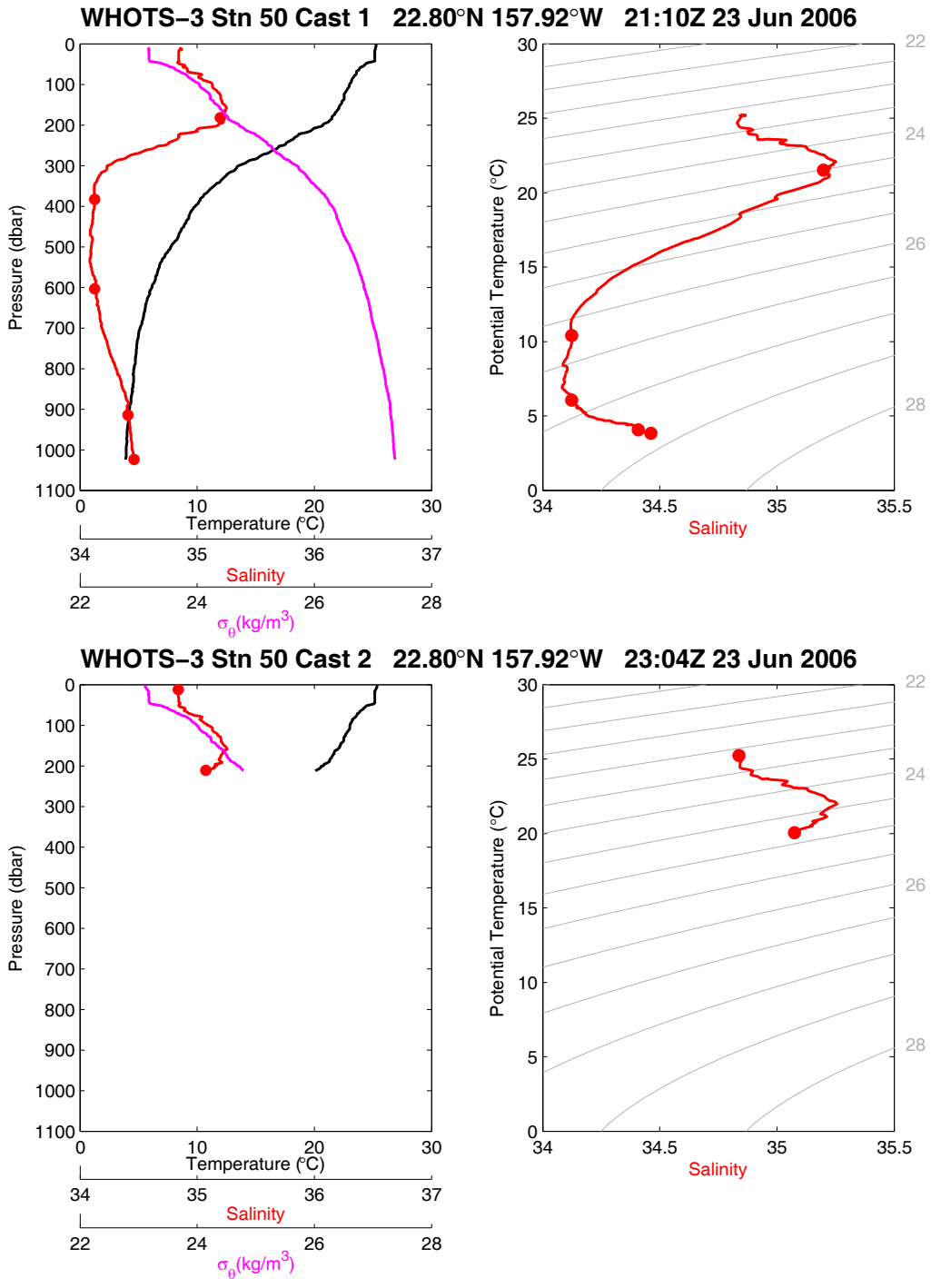

Figure 6-12. [Upper panels] Same as in Fig. 6.11, but for station 50, cast 1. [Lower panels] Same as in Fig. 6.11, but for station 50, cast 2.

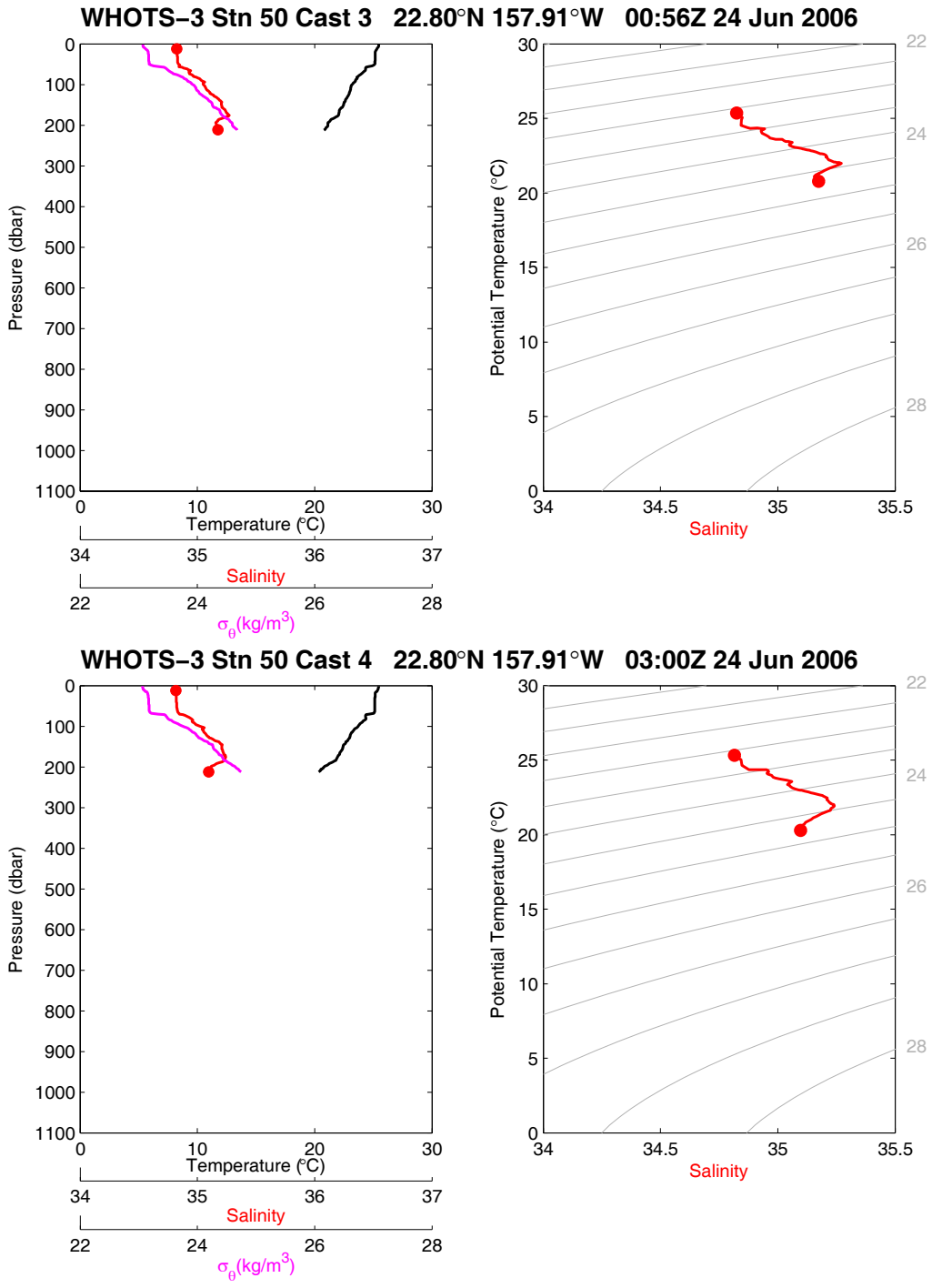

Figure 6-13. [Upper panels] Same as in Fig. 6.11, but for station 50, cast 3. [Lower panels] Same as in Fig. 6.11, but for station 50, cast 4.

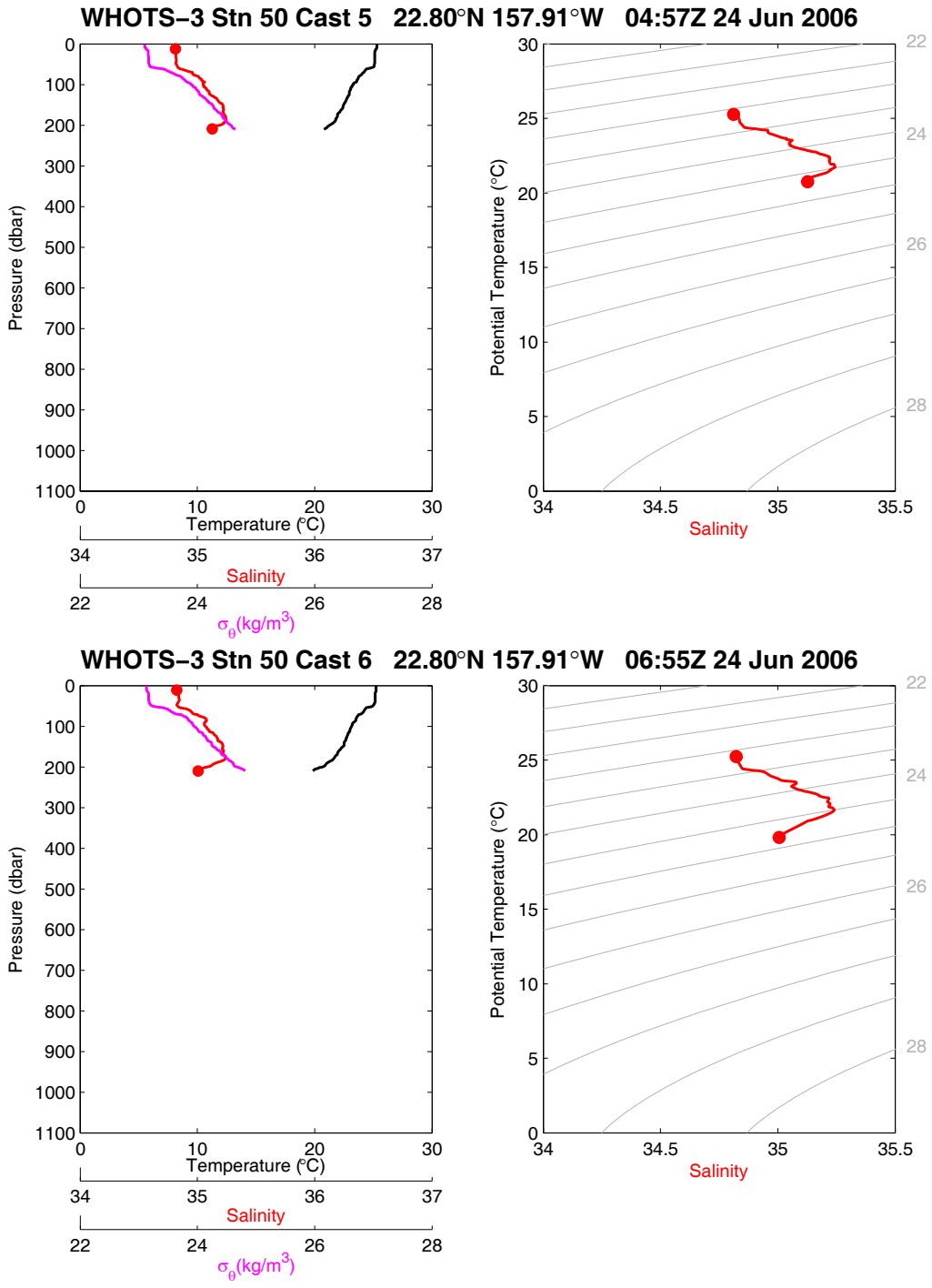

Figure 6-14. [Upper panels] Same as in Fig. 6.11, but for station 50, cast 5. [Lower panels] Same as in Fig. 6.11, but for station 50, cast 6.

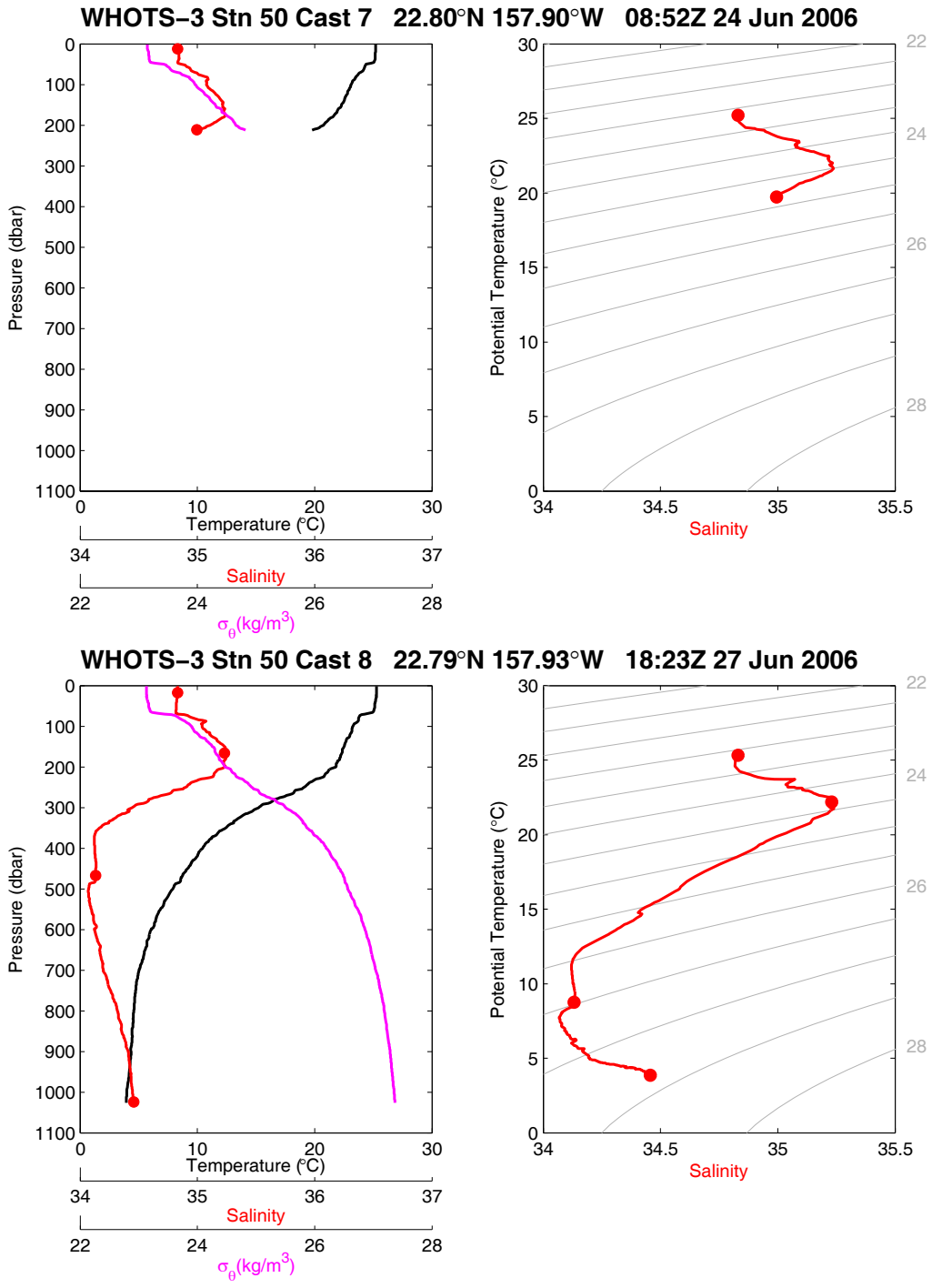

Figure 6-15. [Upper panels] Same as in Fig. 6.11, but for station 50, cast 7. [Lower panels] Same as in Fig. 6.11, but for station 50, cast 8.

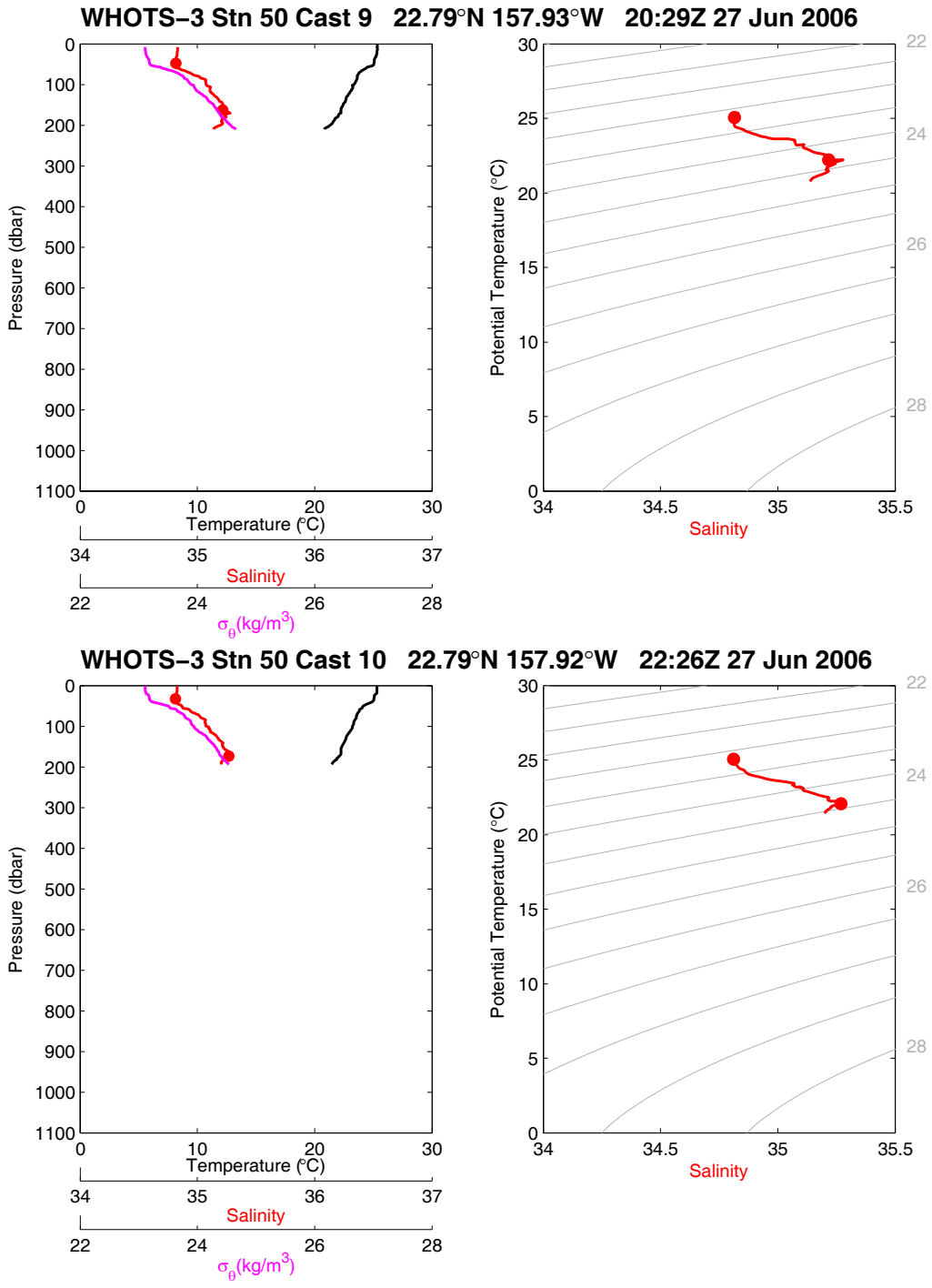

Figure 6-16. [Upper panels] Same as in Fig. 6.11, but for station 50, cast 9. [Lower panels] Same as in Fig. 6.11, but for station 50, cast 10.

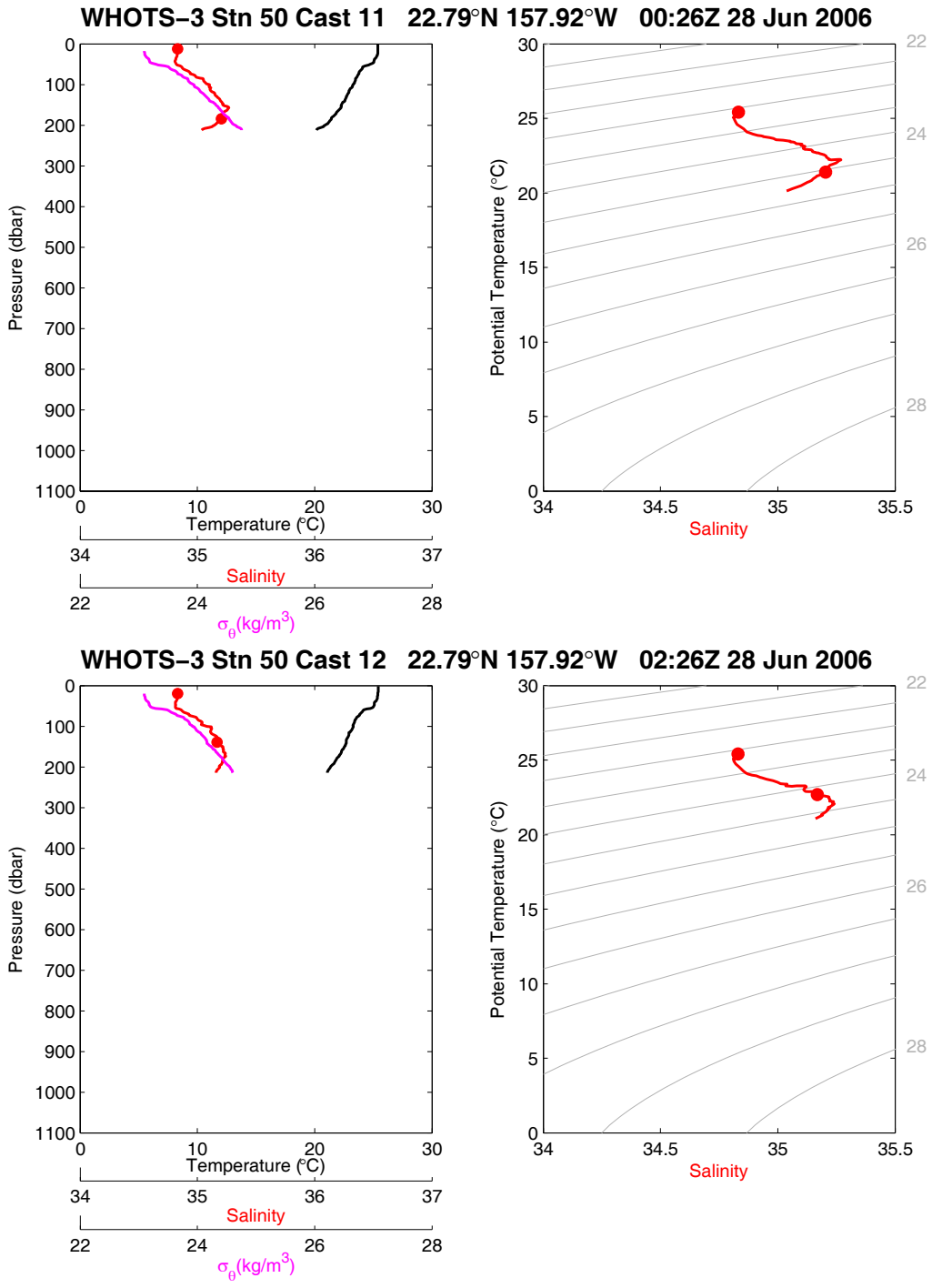

Figure 6-17. [Upper panels] Same as in Fig. 6.11, but for station 50, cast 11. [Lower panels] Same as in Fig. 6.11, but for station 50, cast 12.

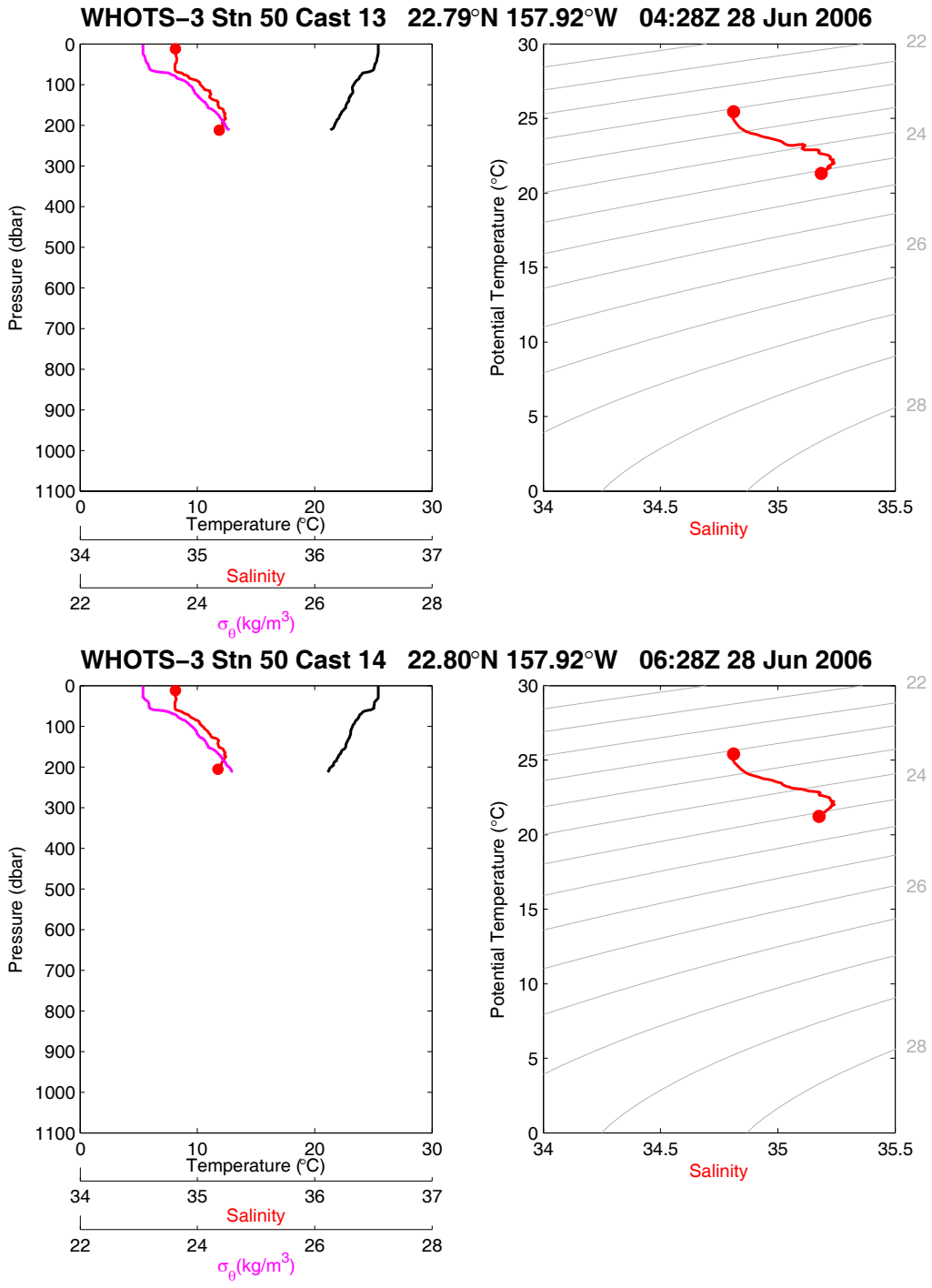

Figure 6-18. [Upper panels] Same as in Fig. 6.11, but for station 50, cast 13. [Lower panels] Same as in Fig. 6.11, but for station 50, cast 14.

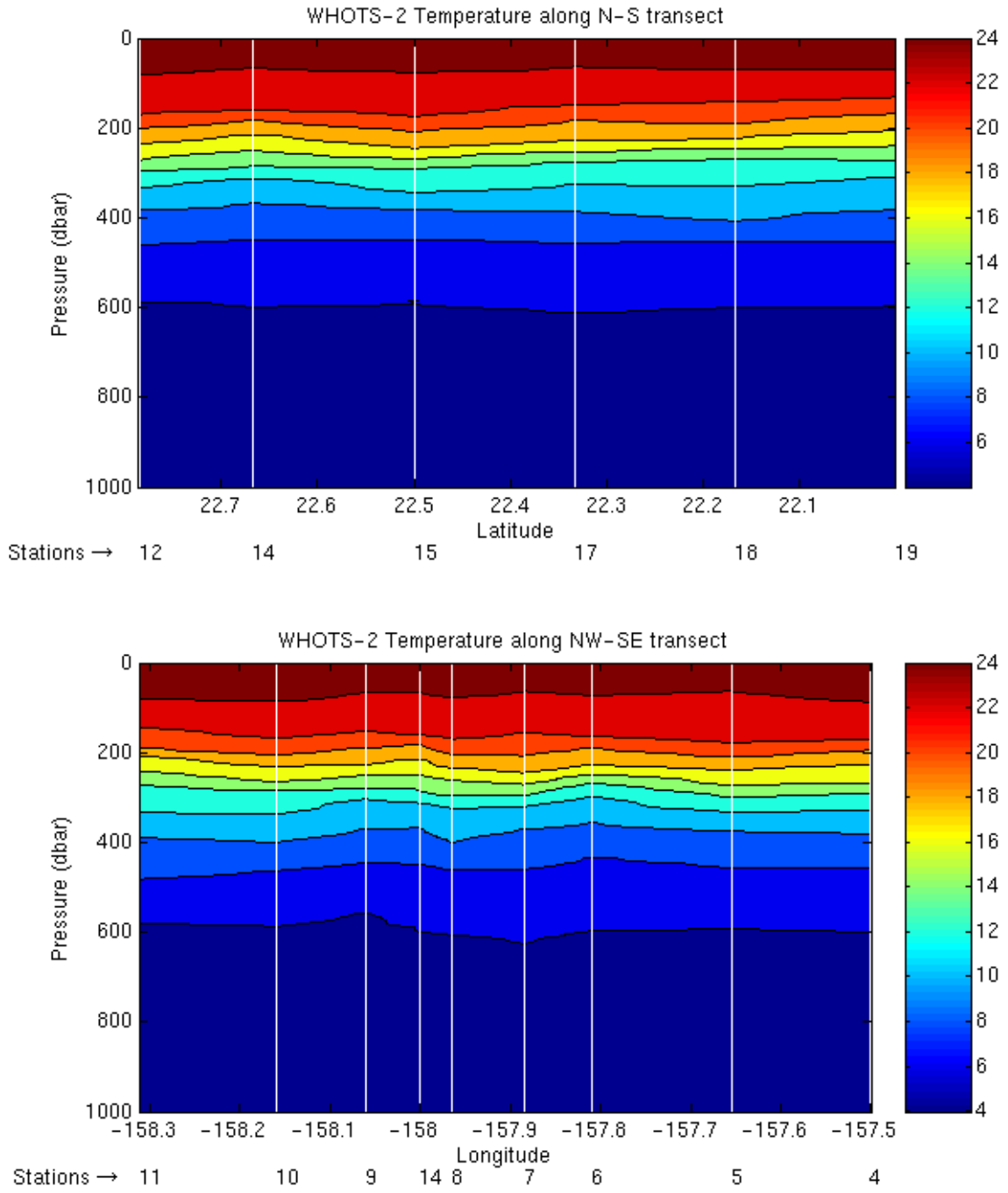

Figure 6-19 [Upper panel] Temperatures along the North-South transect as a function of pressure for the upper 1000-dbar during WHOTS-2 cruise. [Lower panel] Temperatures along the Northwest-Southeast transect. The vertical lines indicate the location of the CTD stations.

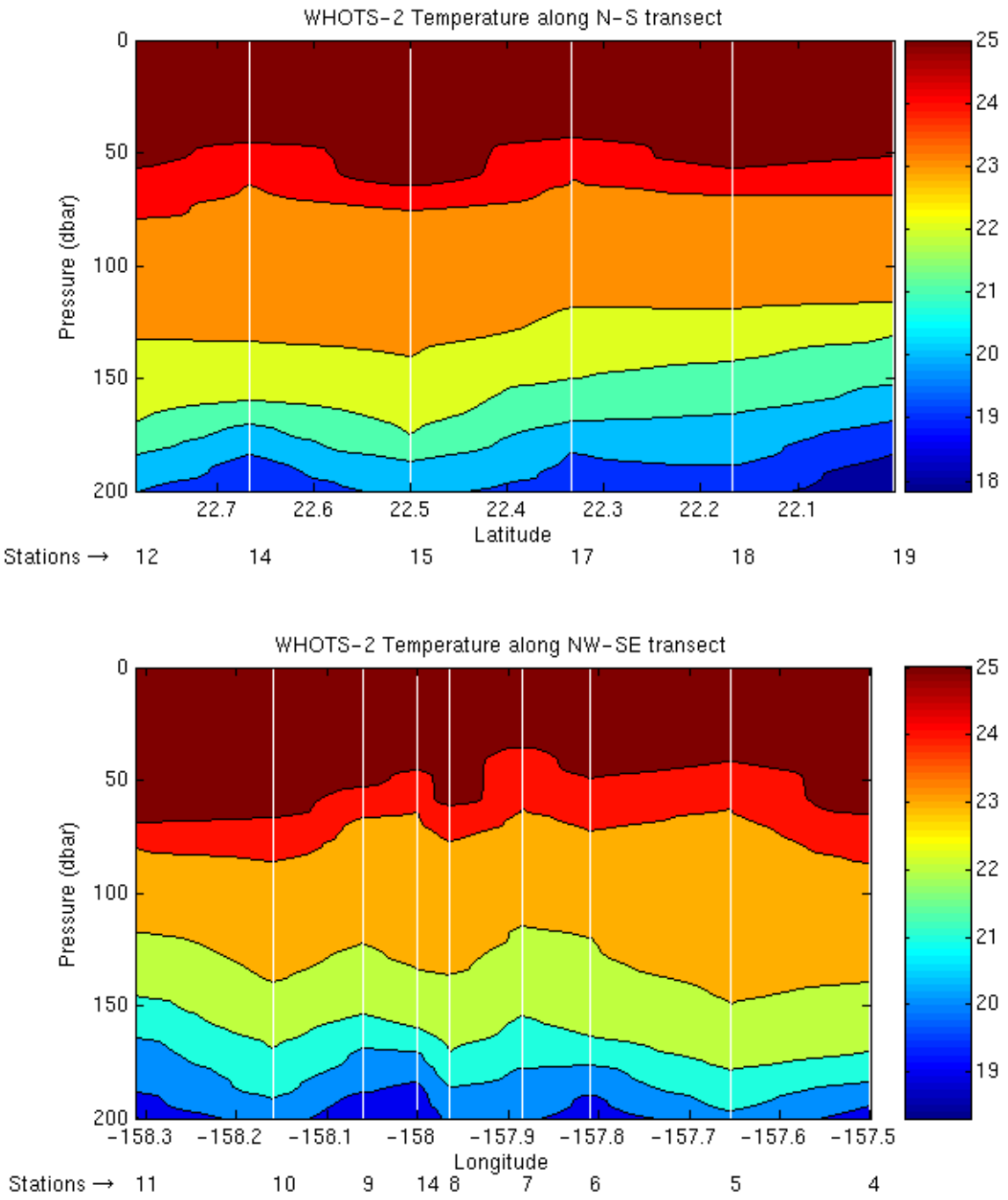

Figure 6-20 [Upper panel] Temperatures along the North-South transect as a function of pressure for the upper 200-dbar during WHOTS-2 cruise. [Lower panel] Temperatures along the Northwest-Southeast transect. The vertical lines indicate the location of the CTD stations.

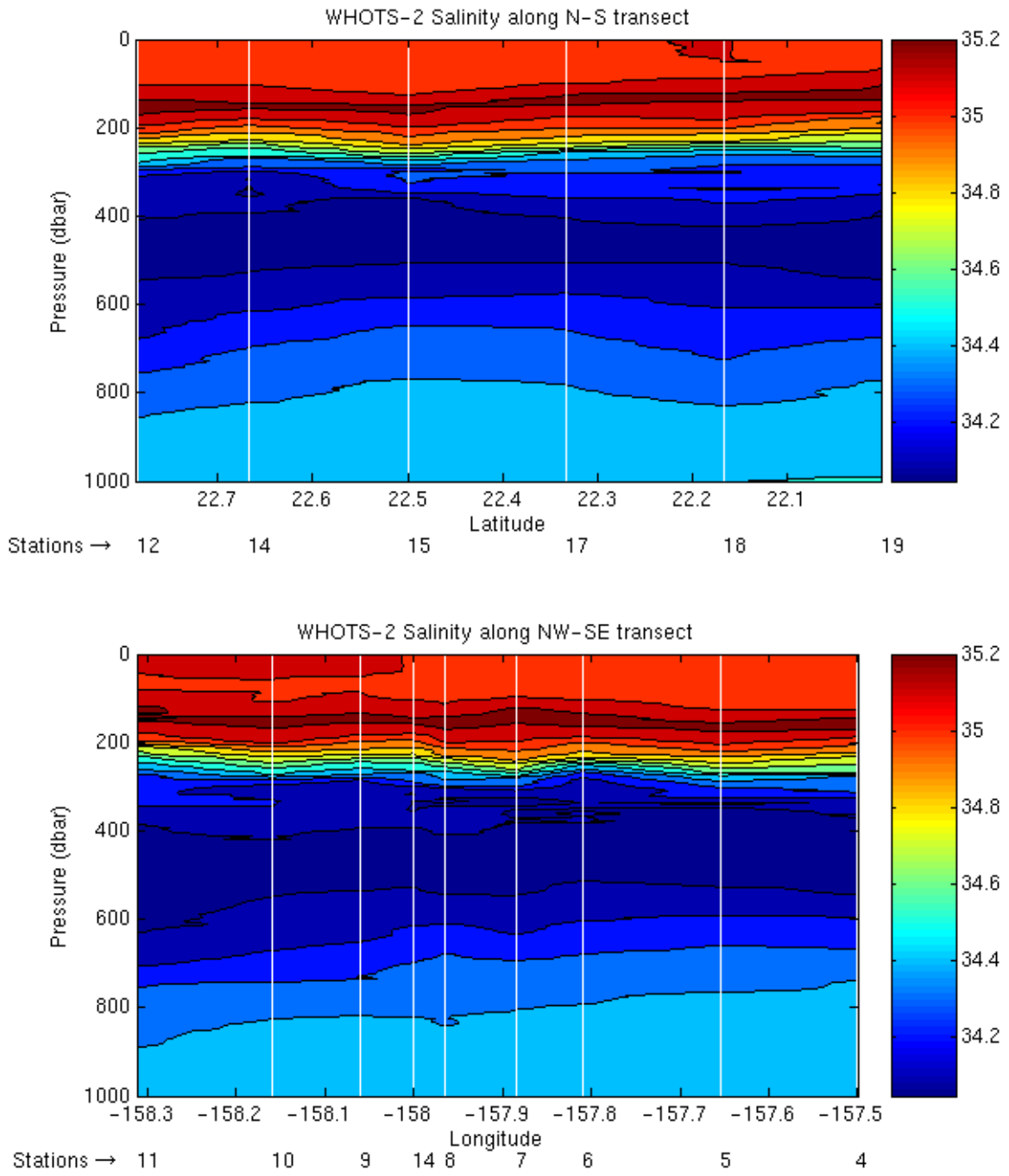

Figure 6-21 [Upper panel] Salinities along the North-South transect as a function of pressure for the upper 1000-dbar during WHOTS-2 cruise. [Lower panel] Salinities along the Northwest-Southeast transect. The vertical lines indicate the location of the CTD stations.

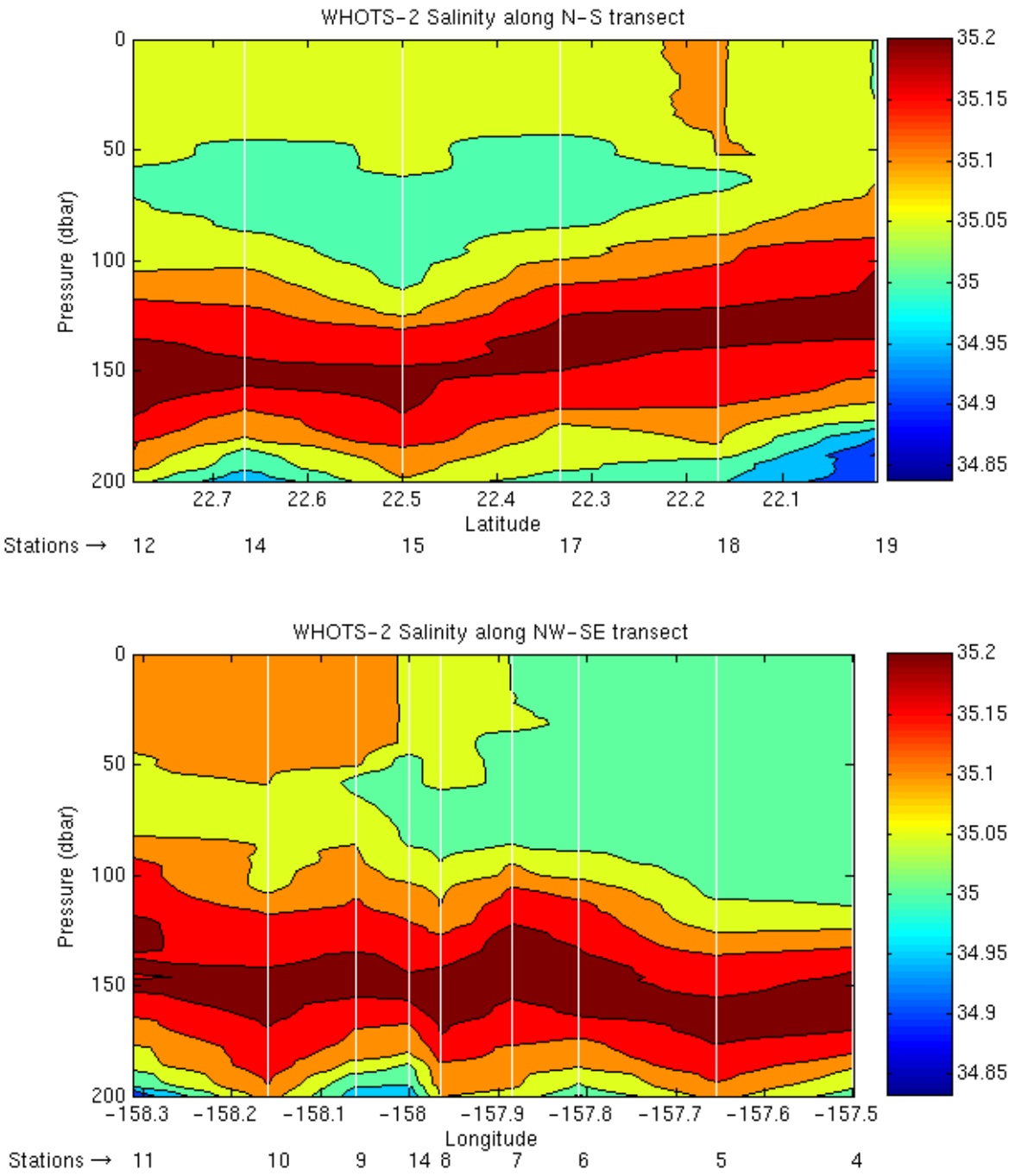

Figure 6-22 [Upper panel] Salinities along the North-South transect as a function of pressure for the upper 200-dbar during WHOTS-2 cruise. [Lower panel] Salinities along the Northwest-Southeast transect. The vertical lines indicate the location of the CTD stations.

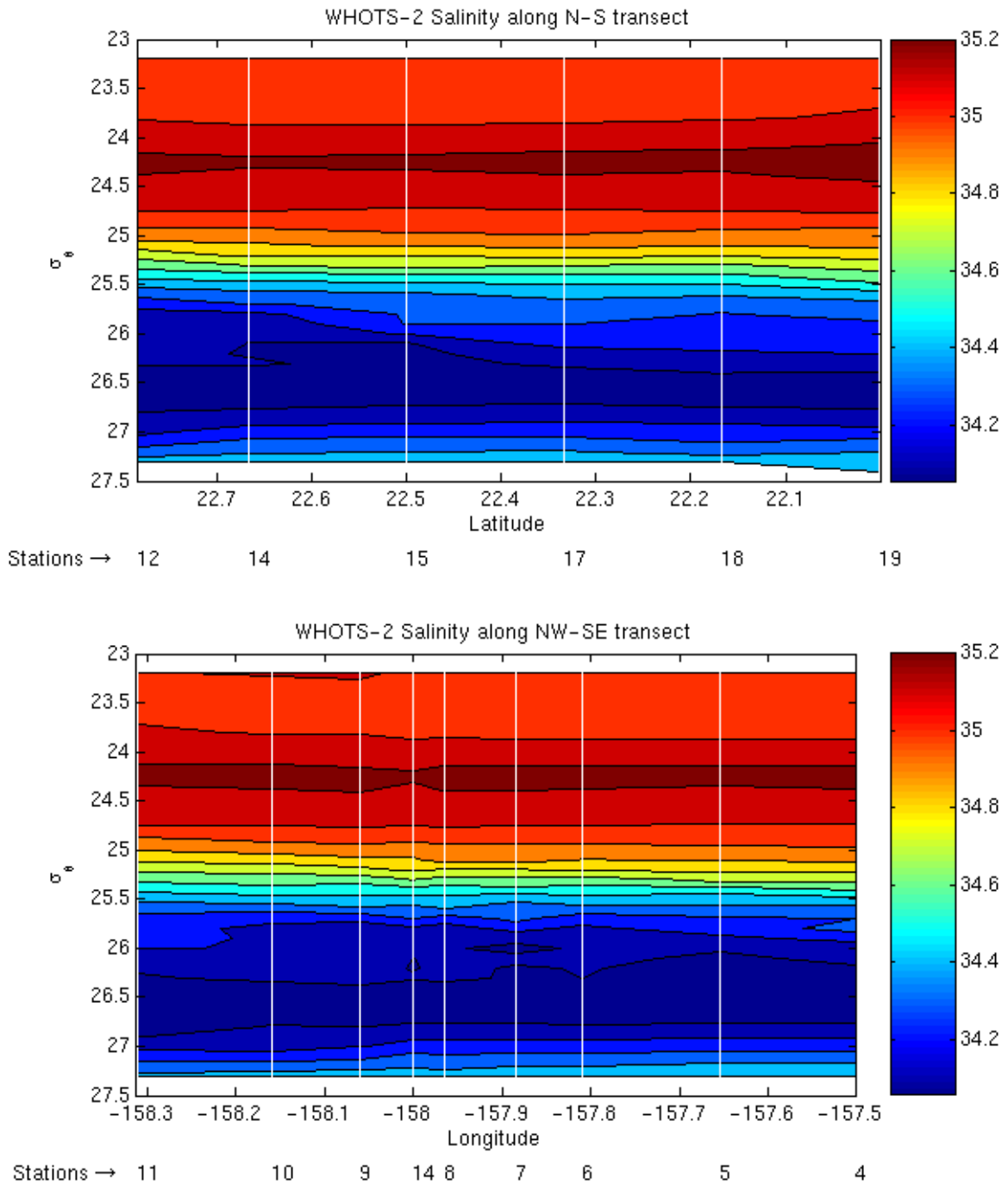

Figure 6-23 [Upper panel] Salinities along the North-South transect as a function of potential density (σ_θ) during WHOTS-2 cruise. [Lower panel] Salinities along the Northwest-Southeast transect. The vertical lines indicate the location of the CTD stations.

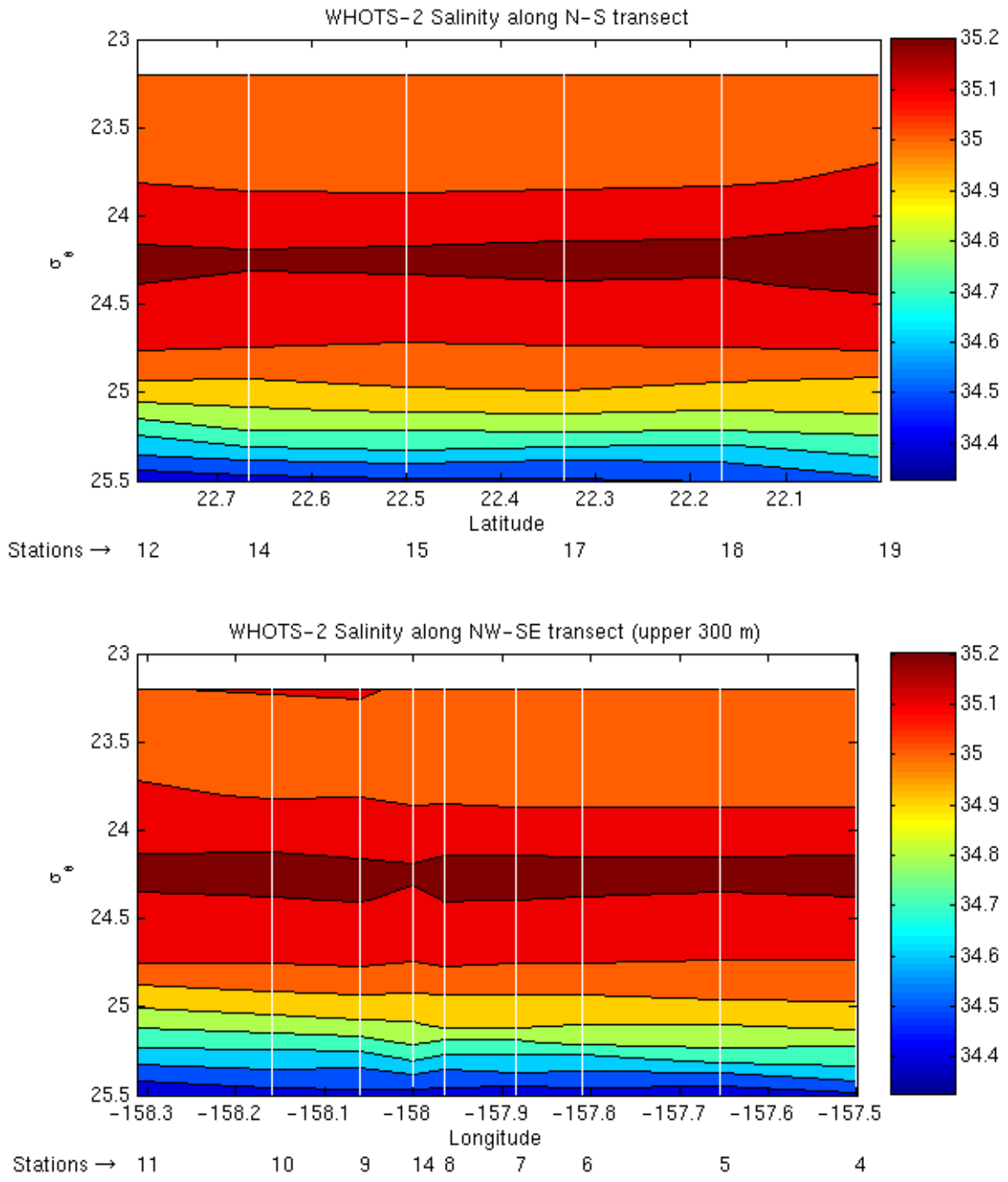

Figure 6-24[Upper panel] Salinities along the North-South transect as a function of potential density (σ_θ) in the upper 300 m during WHOTS-2 cruise. [Lower panel] Salinities along the Northwest-Southeast transect. The vertical lines indicate the location of the CTD stations.

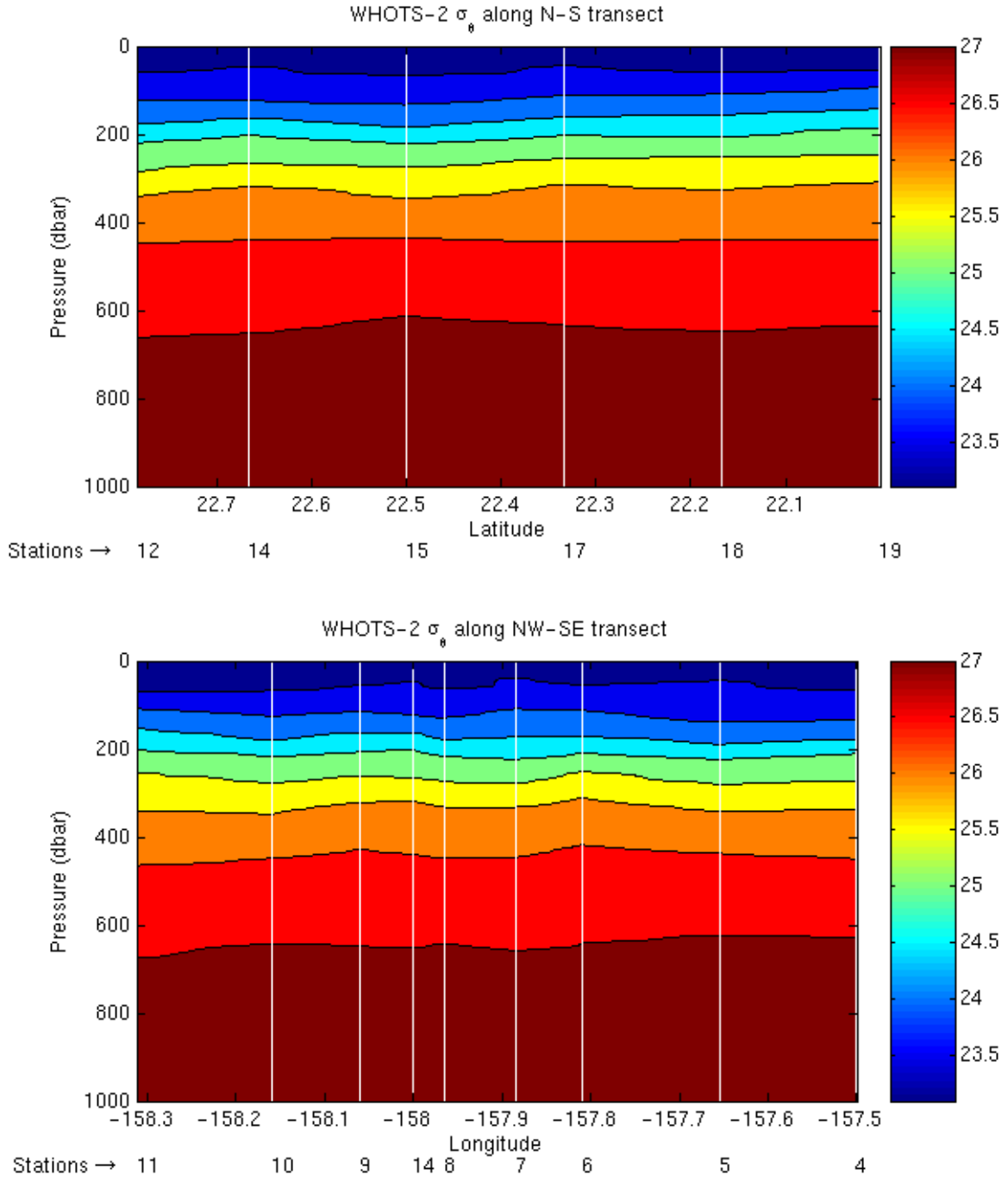

Figure 6-25 [Upper panel] Potential density (σ_θ) along the North-South transect as a function of pressure for the upper 1000-dbar during WHOTS-2 cruise. [Lower panel] Potential density (σ_θ) along the Northwest-Southeast transect. The vertical lines indicate the location of the CTD stations.

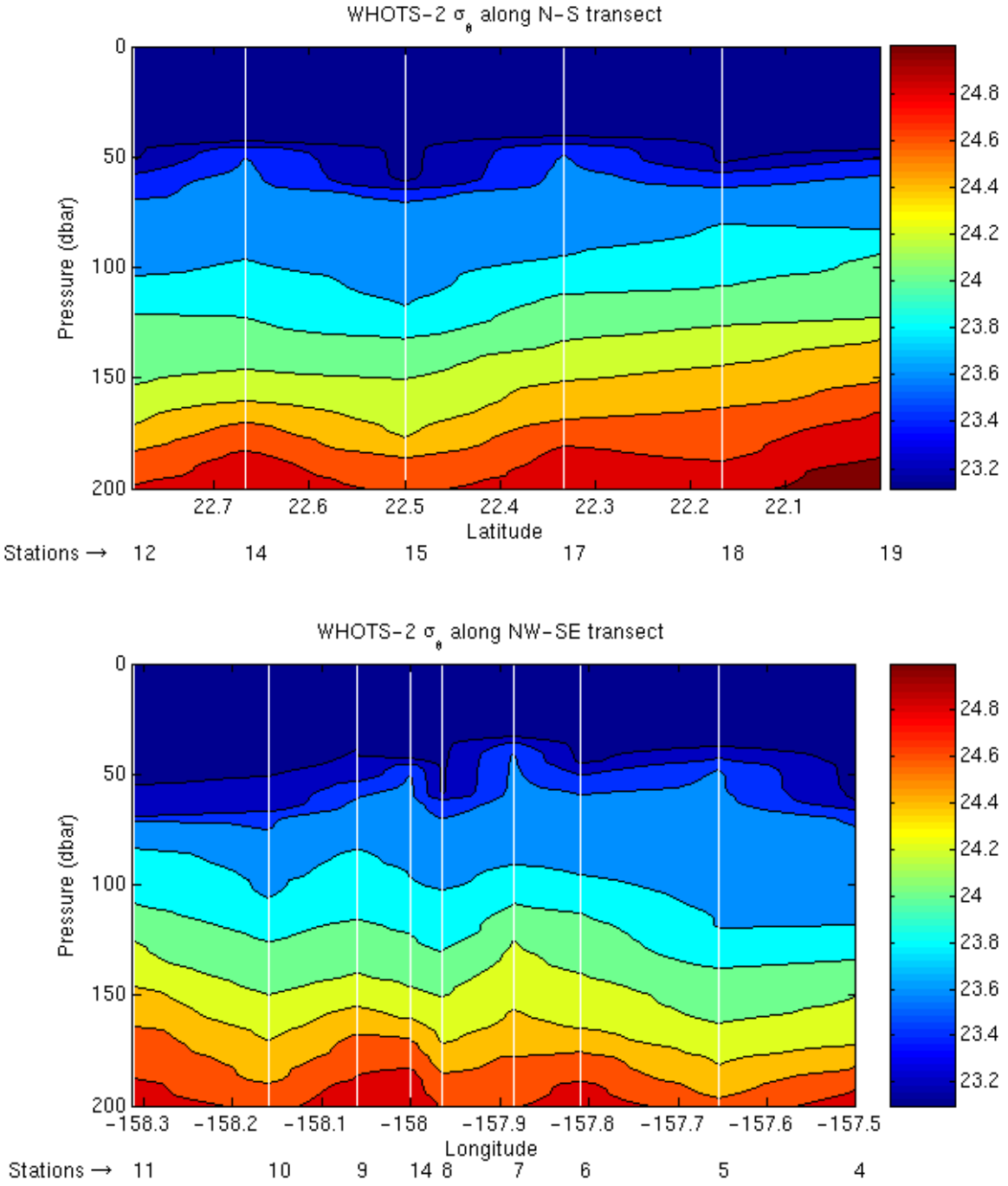

Figure 6-26 [Upper panel] Potential density (σ_θ) along the North-South transect as a function of pressure for the upper 200-dbar during WHOTS-2 cruise. [Lower panel] Potential density (σ_θ) along the Northwest-Southeast transect. The vertical lines indicate the location of the CTD stations.

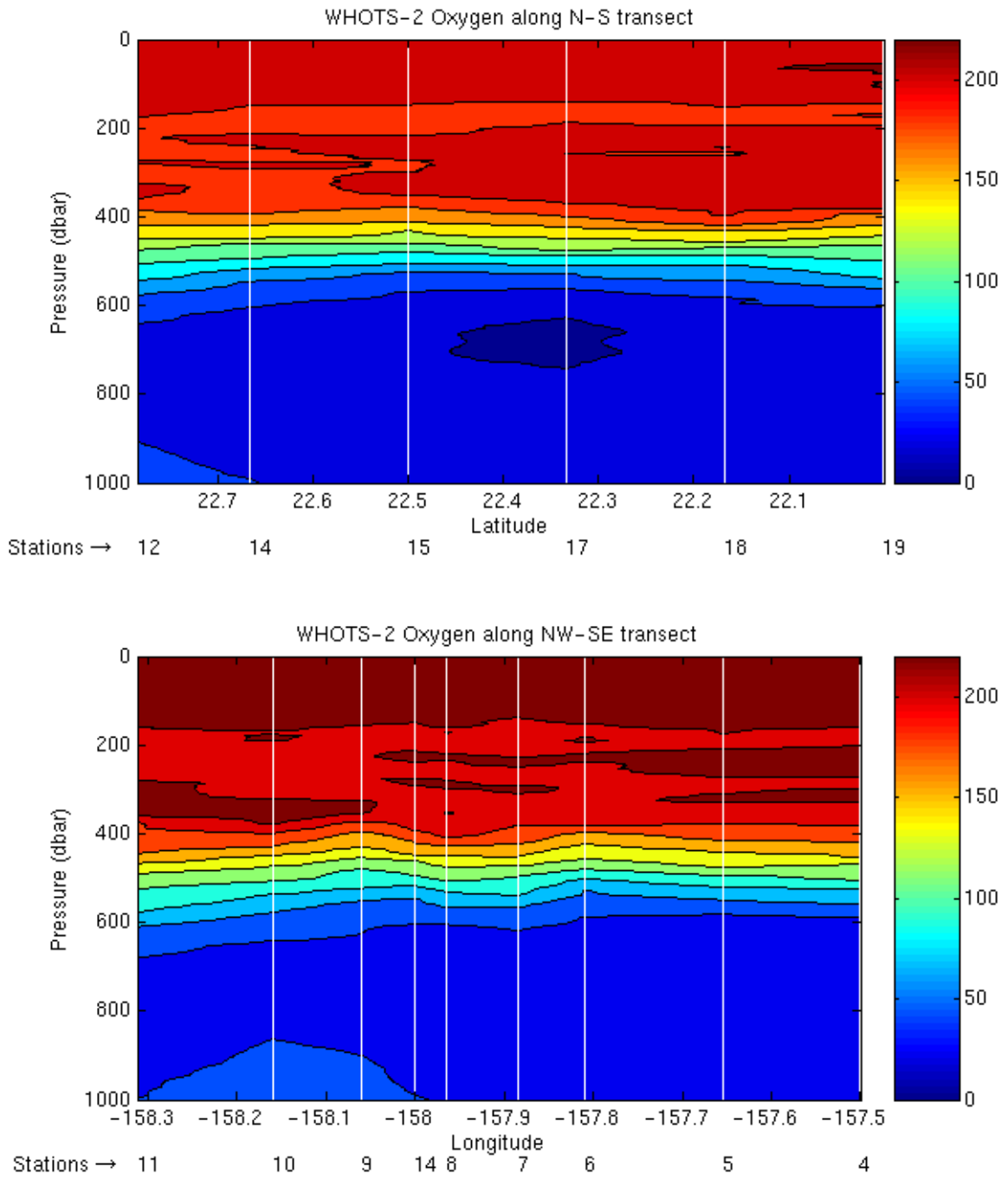

Figure 6-27 [Upper panel] Dissolved oxygen (µmol/kg) along the North-South transect as a function of pressure for the upper 1000-dbar during WHOTS-2 cruise. [Lower panel] Dissolved oxygen along the Northwest-Southeast transect. The vertical lines indicate the location of the CTD stations.

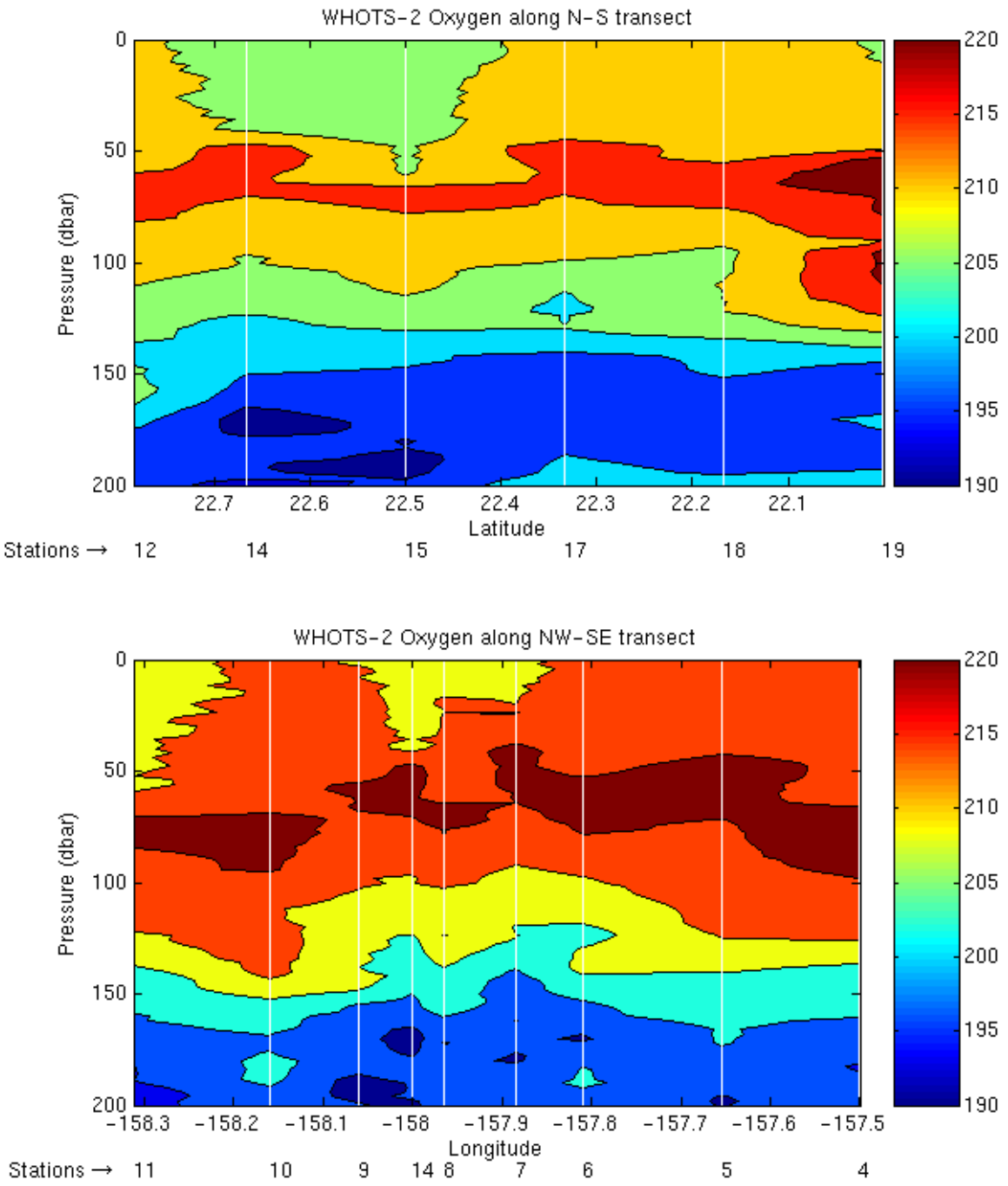

Figure 6-28 [Upper panel] Dissolved oxygen (µmol/kg) along the North-South transect as a function of pressure for the upper 200-dbar during WHOTS-2 cruise. [Lower panel] Dissolved oxygen along the Northwest-Southeast transect. The vertical lines indicate the location of the CTD stations.

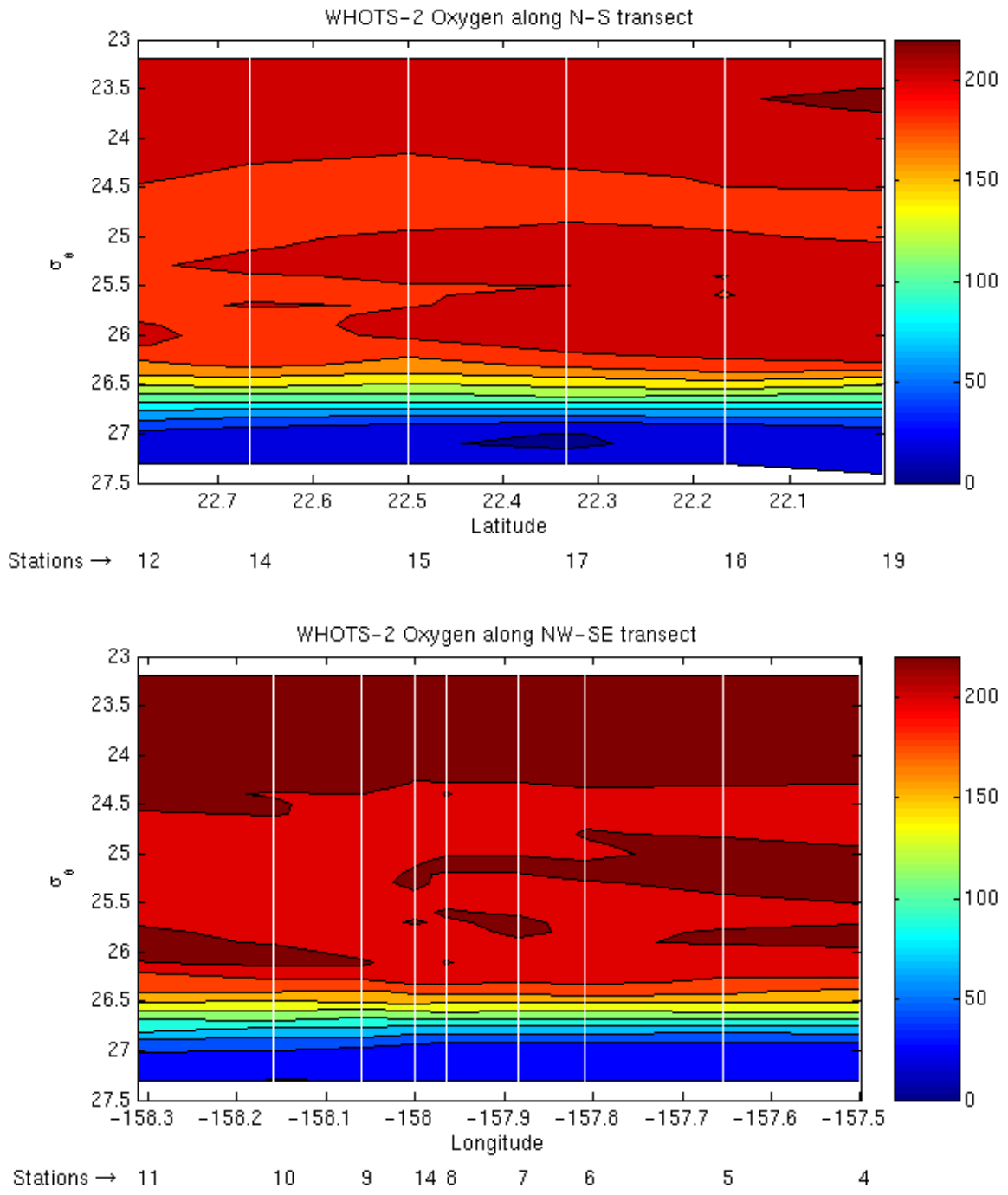

Figure 6-29 [Upper panel] Dissolved oxygen (µmol/kg) along the North-South transect as a function of potential density (σ_θ) during WHOTS-2 cruise. [Lower panel] Dissolved oxygen along the Northwest-Southeast transect. The vertical lines indicate the location of the CTD stations.

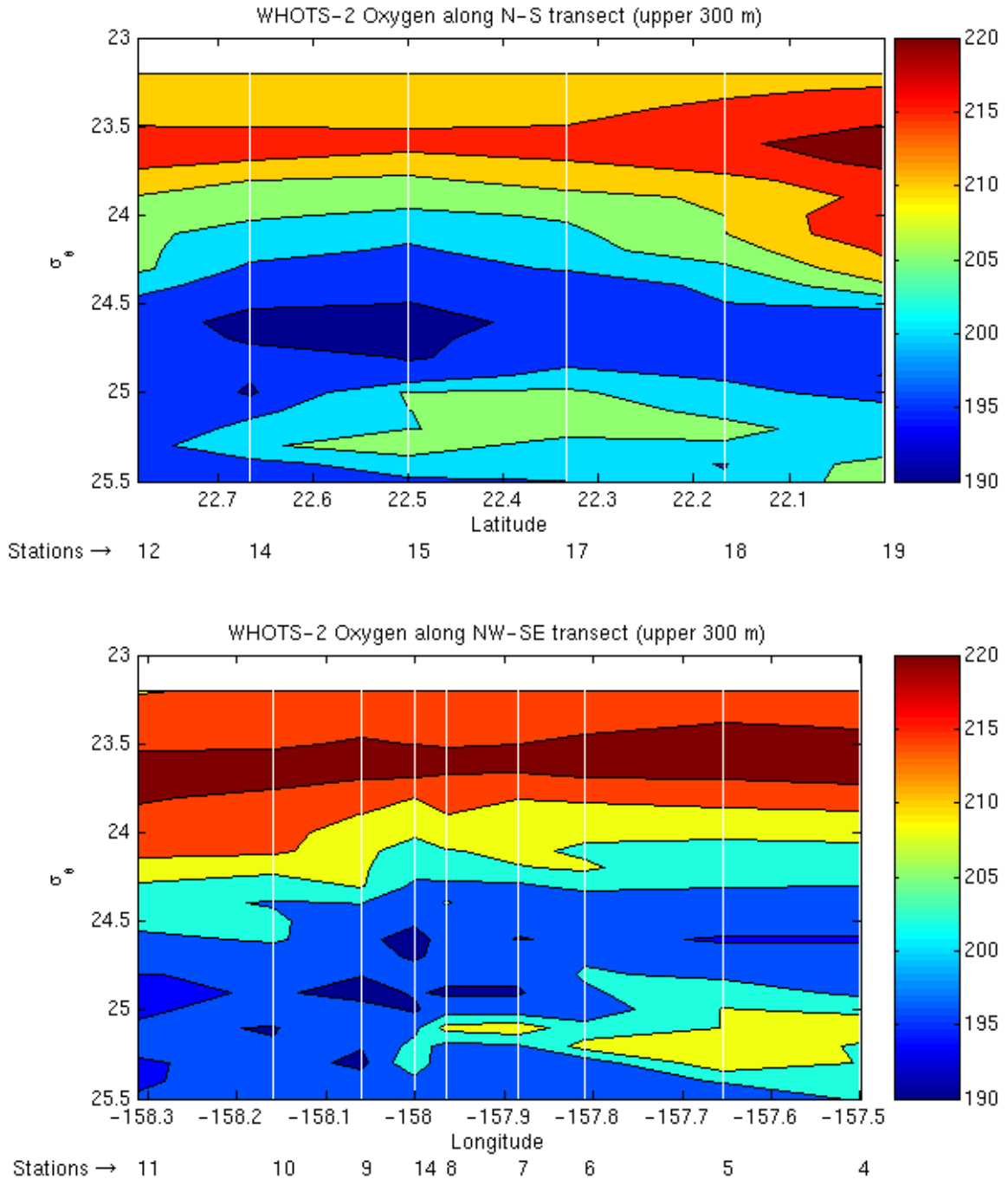

Figure 6-30 [Upper panel] Dissolved oxygen (µmol/kg) along the North-South transect as a function of potential density (σ_θ) in the upper 300 m during WHOTS-2 cruise. [Lower panel] Dissolved oxygen along the Northwest-Southeast transect. The vertical lines indicate the location of the CTD stations.

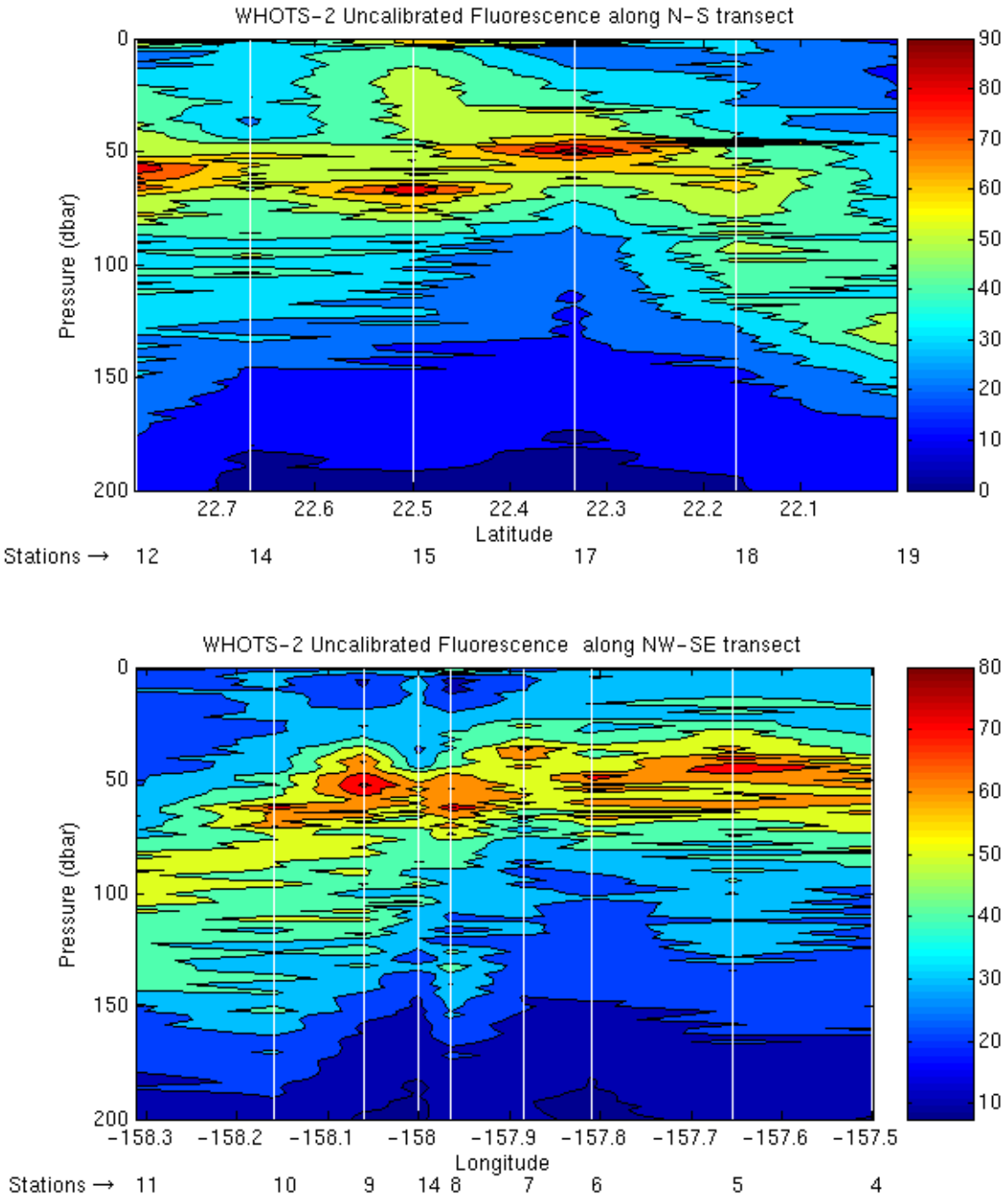

Figure 6-31 [Upper panel] Fluorescence (mV) along the North-South transect as a function of pressure in the upper 200-dbar during WHOTS-2 cruise. [Lower panel] Fluorescence along the Northwest-Southeast transect. The vertical lines indicate the location of the CTD stations.

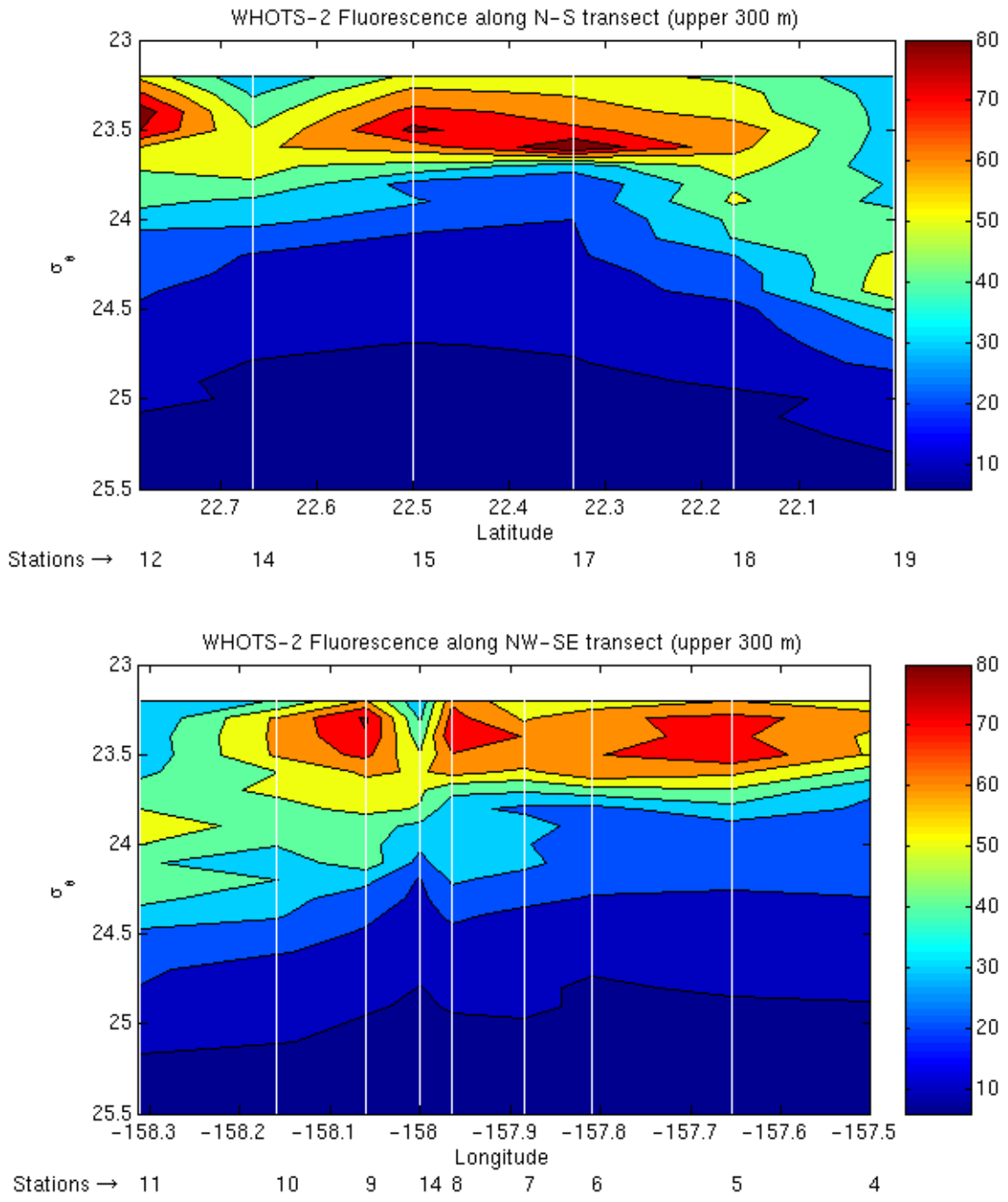

Figure 6-32 [Upper panel] Fluorescence (mV) along the North-South transect as a function of potential density (σ_θ) in the upper 300 m during WHOTS-2 cruise. [Lower panel] Fluorescence along the Northwest-Southeast transect. The vertical lines indicate the location of the CTD stations.

B. Thermosalinograph data

Underway measurements of near surface temperature and near surface salinity from thermosalinograph as well as navigation for the WHOTS-2 cruise are presented in Figure 6-33 and Figure 6-34. Similar plots for data collected during the WHOTS-3 cruise are in Figure 6-35 and Figure 6-36.

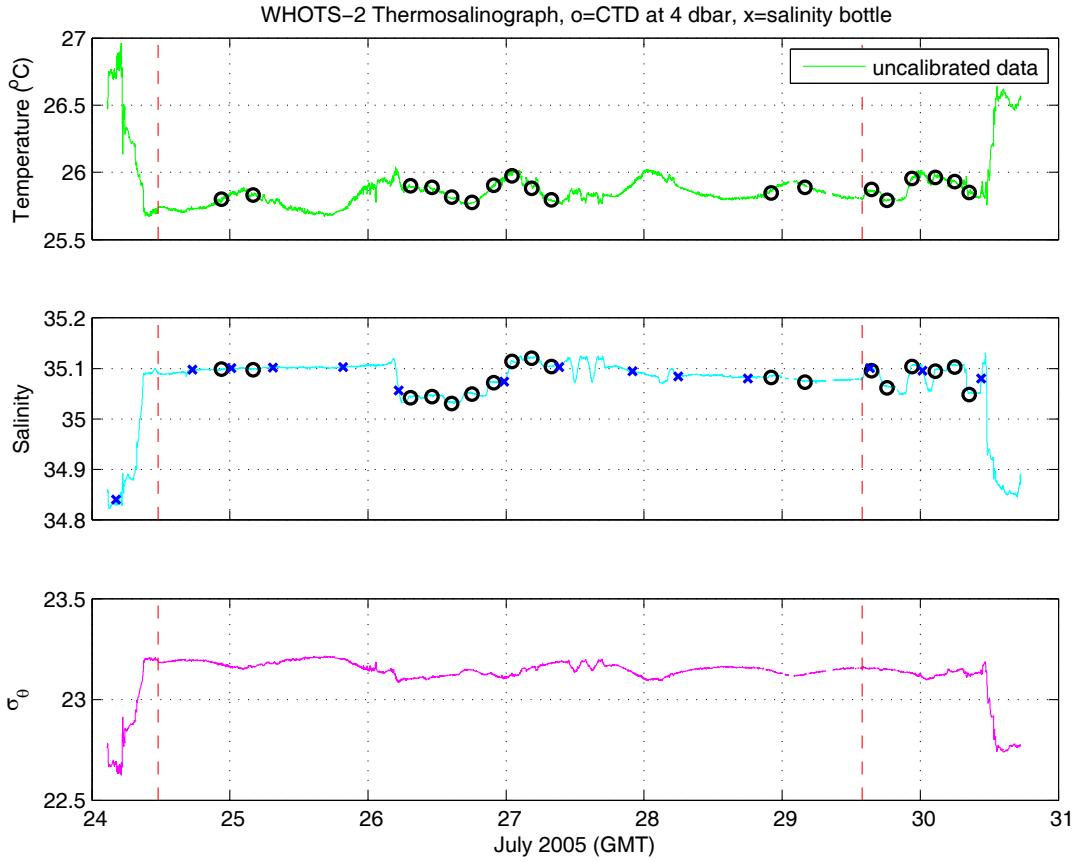

Figure 6-33 Final processed temperature (upper panel), salinity (middle panel) and potential density (σ_θ) (lower panel) data from the continuous underway system on board the RV Melville *during the WHOTS-2 cruise. Temperature and salinity taken from 4-dbar CTD data (circles) and salinity bottle sample data (crosses) are superimposed. The dashed vertical red line indicates the period while at Station ALOHA and the WHOTS site.*

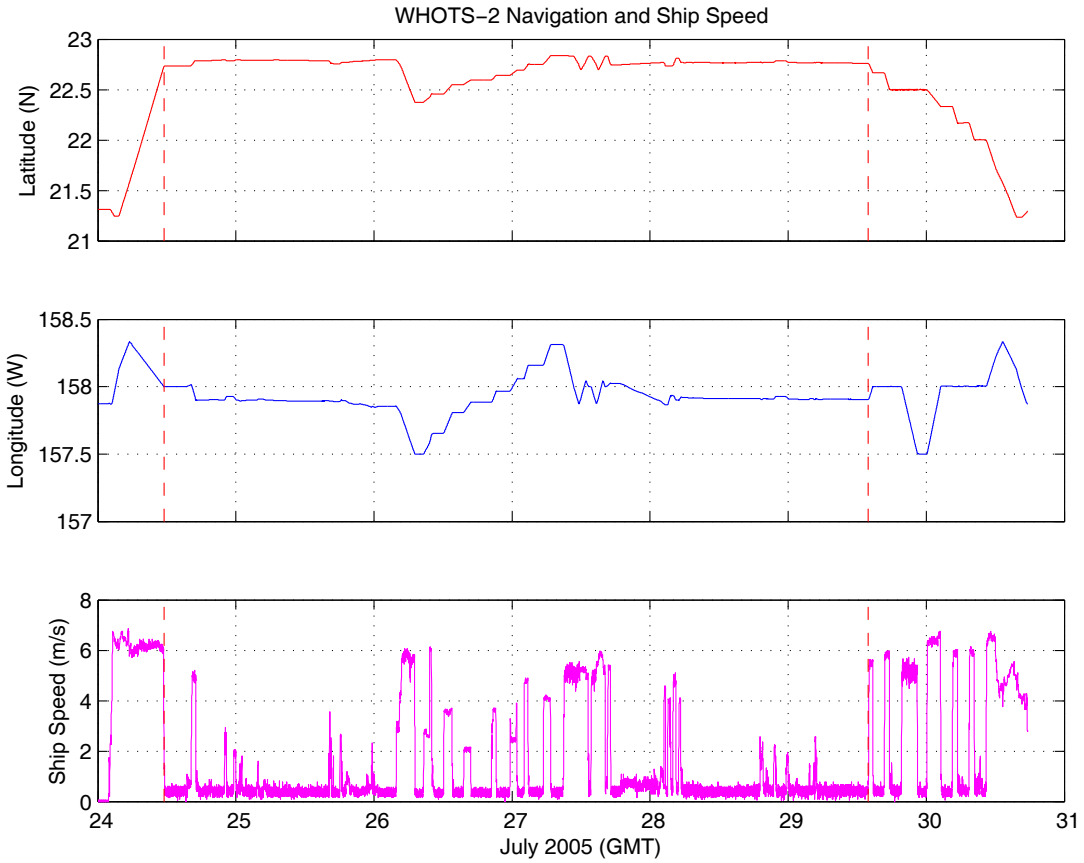

Figure 6-34 Timeseries of latitude (upper panel), longitude (middle panel), and ship's speed (lower panel) during the WHOTS-3 cruise.

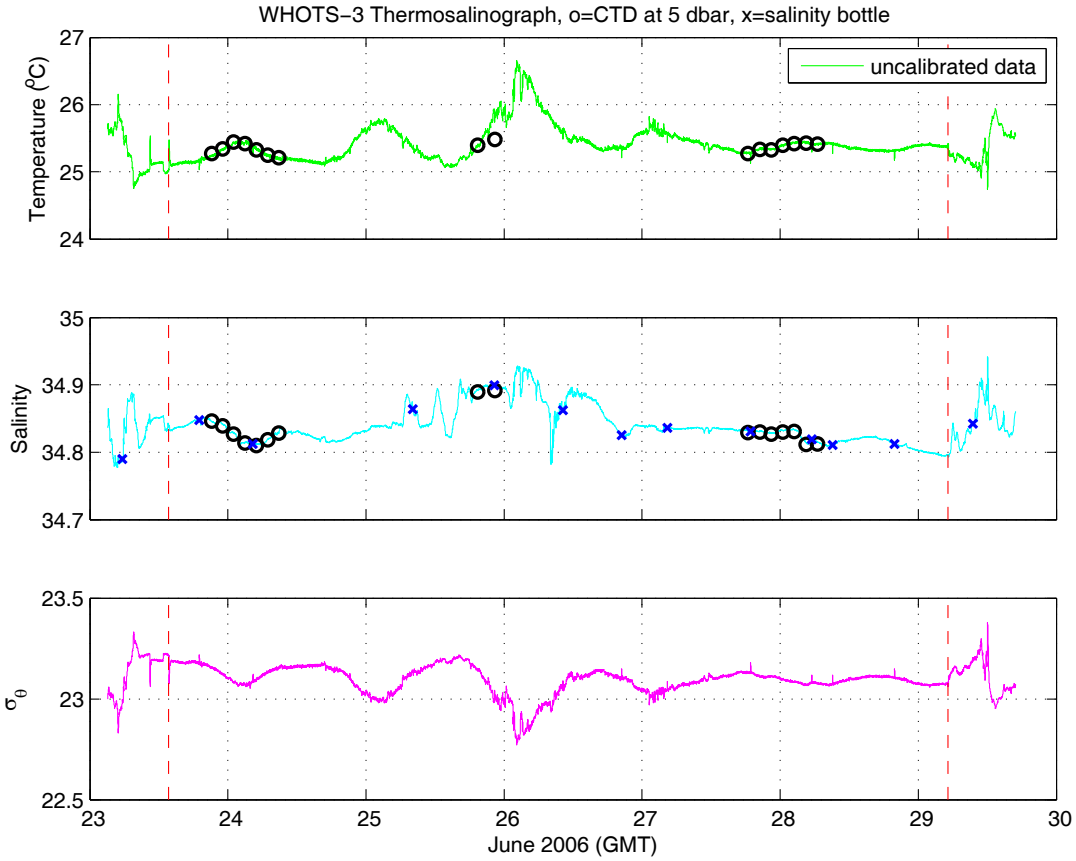

Figure 6-35 Final processed temperature (upper panel), salinity (middle panel) and potential density (σ_θ) (lower panel) data from the continuous underway system on board the RV Roger Revelle *during the WHOTS-3 cruise. Temperature and salinity taken from 6-dbar CTD data (circles) and salinity bottle sample data (crosses) are superimposed. The dashed vertical red line indicates the period of occupation of Station ALOHA and the WHOTS site.*

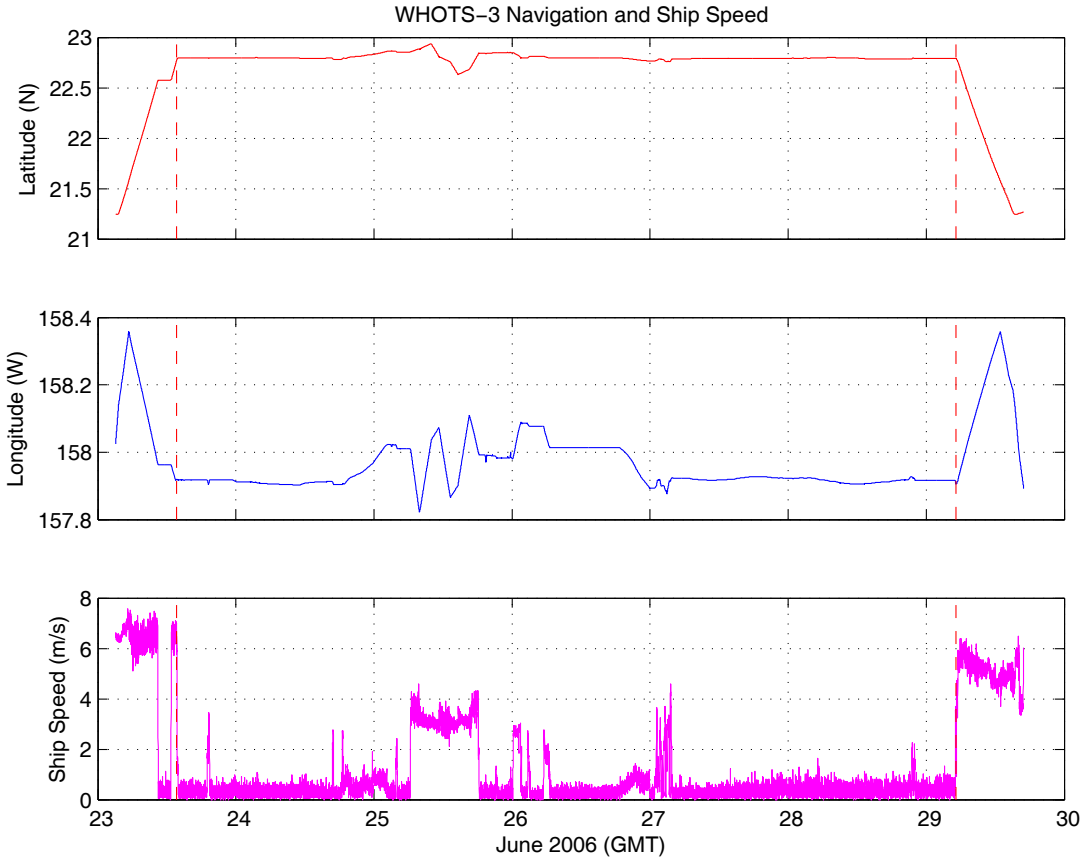

Figure 6-36 Timeseries of latitude (upper panel), longitude (middle panel), and ship's speed (lower panel) during the WHOTS-3 cruise.

C. SeaCAT/MicroCAT data

The temperature and salinity measured by the SeaCATs and MicroCATs during the mooring deployments are presented in Figure 6-37 to Figure 6-44 for each of the depths where the instruments were located. The potential density (σ_θ) is also plotted in Figure 6-45 to Figure 6-48.

Contoured plots of temperature and salinity as a function of depth are presented in Figure 6-49; and contoured plots of potential density (σ_θ) and buoyancy frequency as a function of depth are in Figure 6-50.

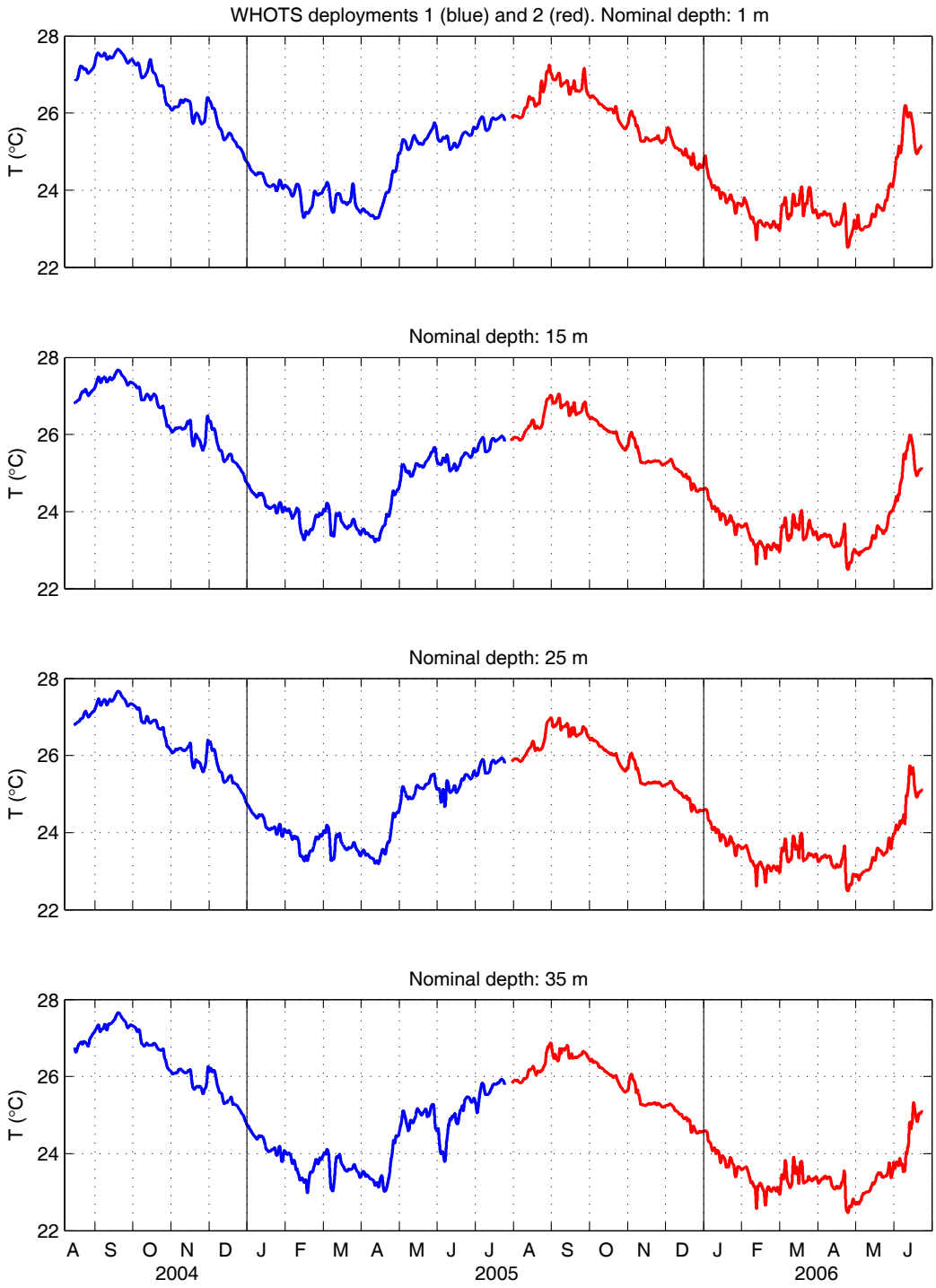

Figure 6-37 Temperatures from SeaCATs/ MicroCATs during WHOTS-1 (blue line), and WHOTS-2 (red line) deployments at 1, 15, 25, and 35 m.

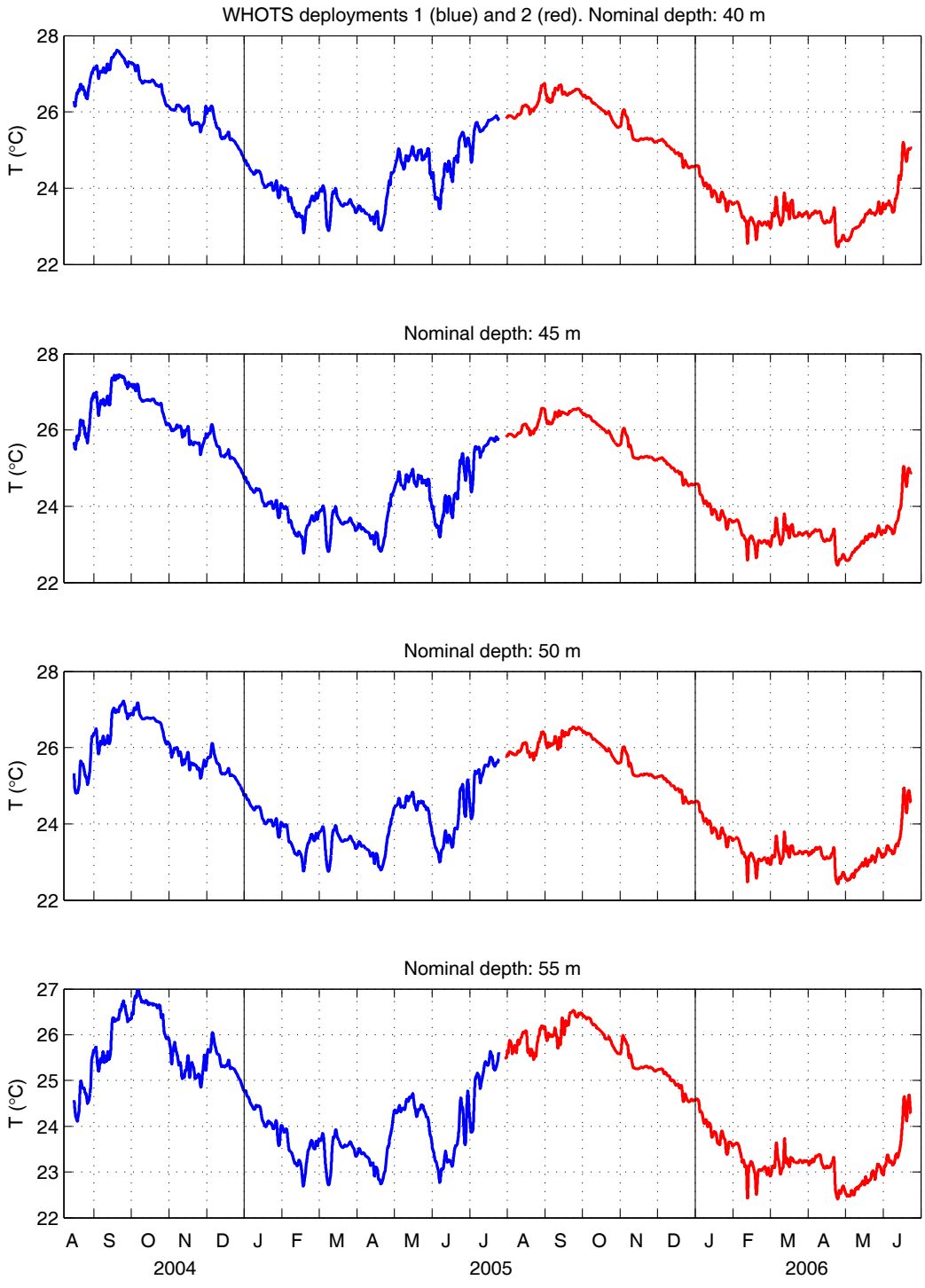

Figure 6-38 Same as in Figure 6-37, but at 40, 45, 50, and 55 m.

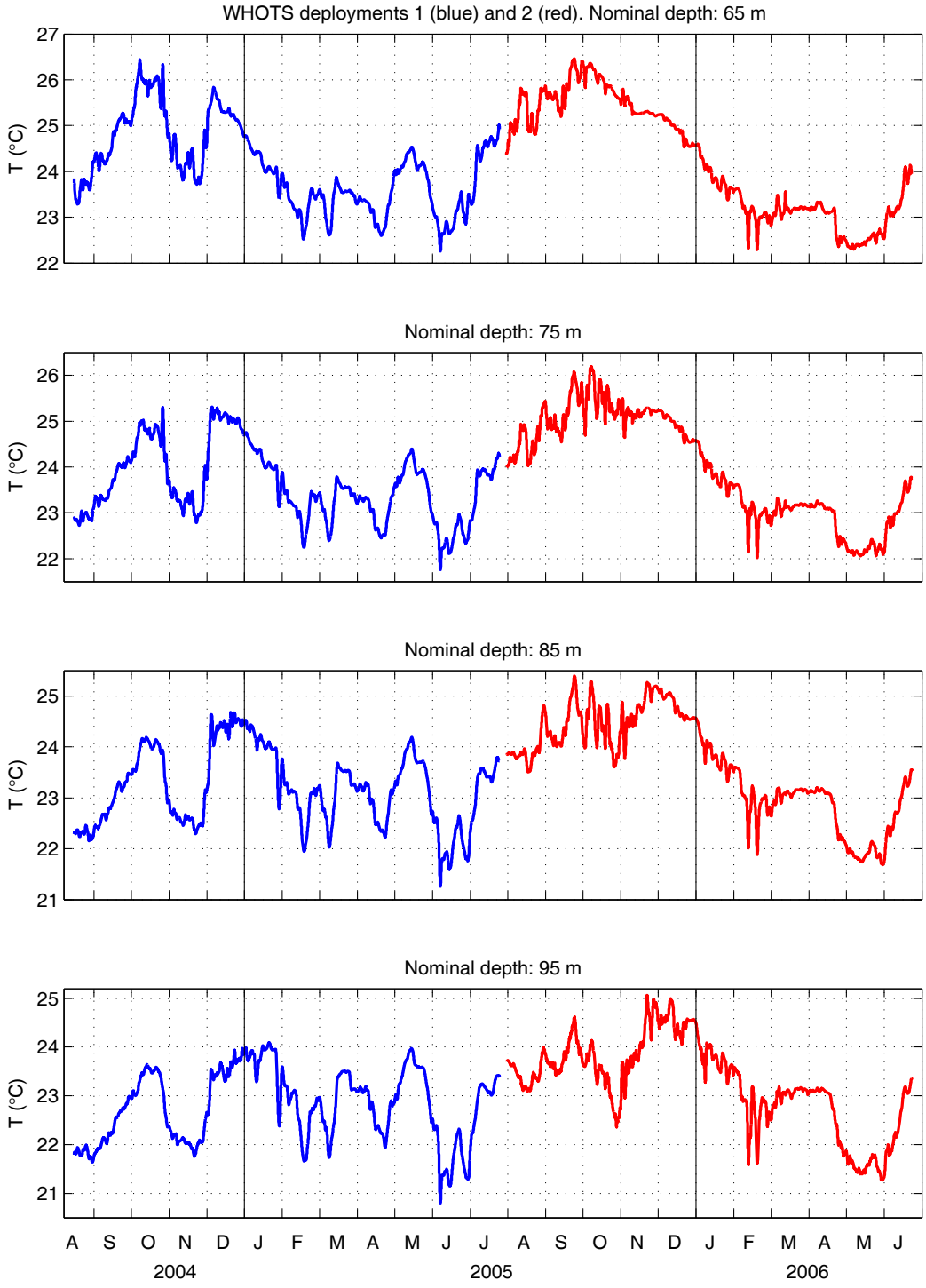

Figure 6-39 Same as in Figure 6-37, but at 65, 75, 85, and 95 m.

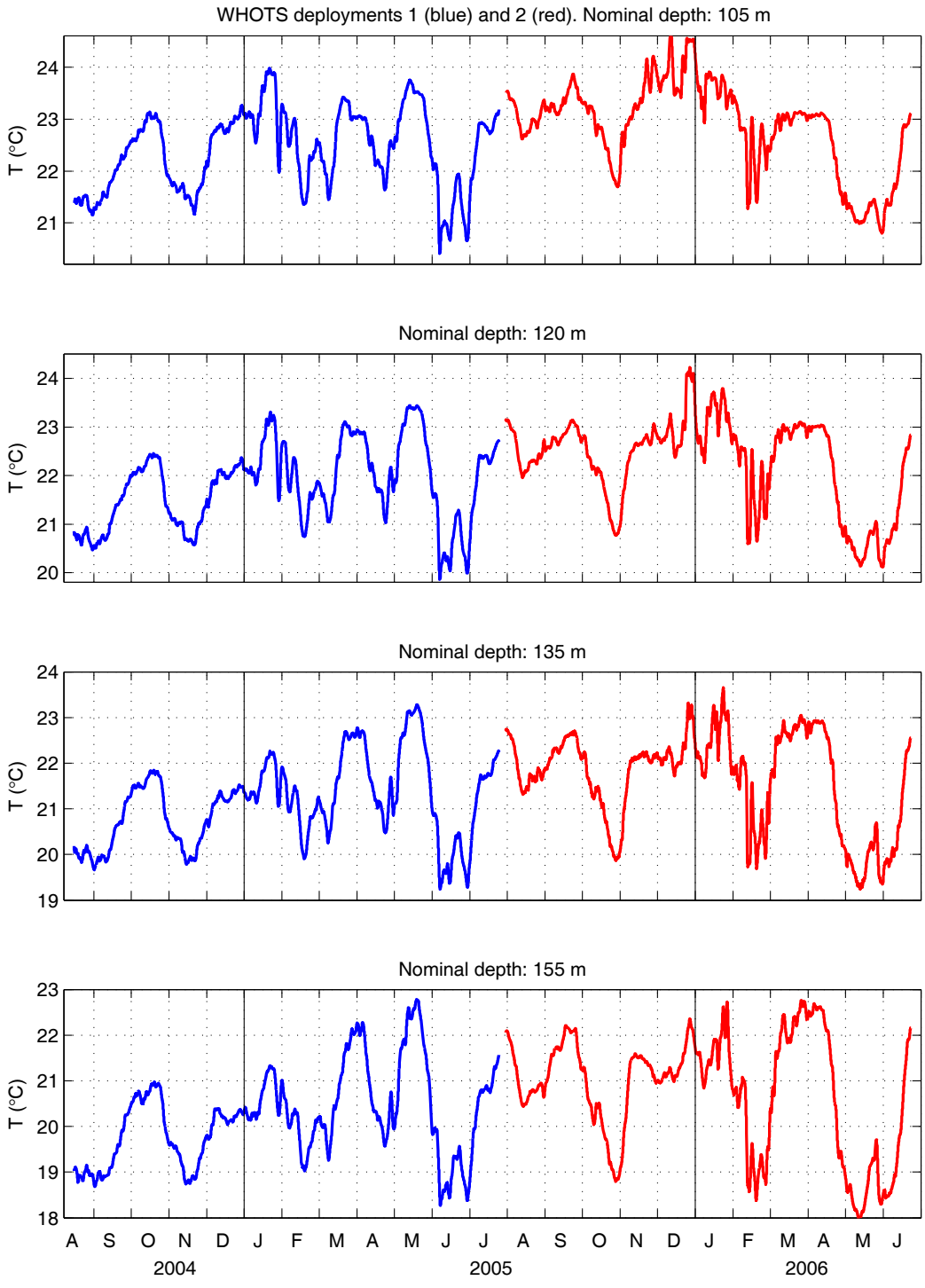

Figure 6-40 Same as in Figure 6-38, but at 105, 120, 135, and 155 m.

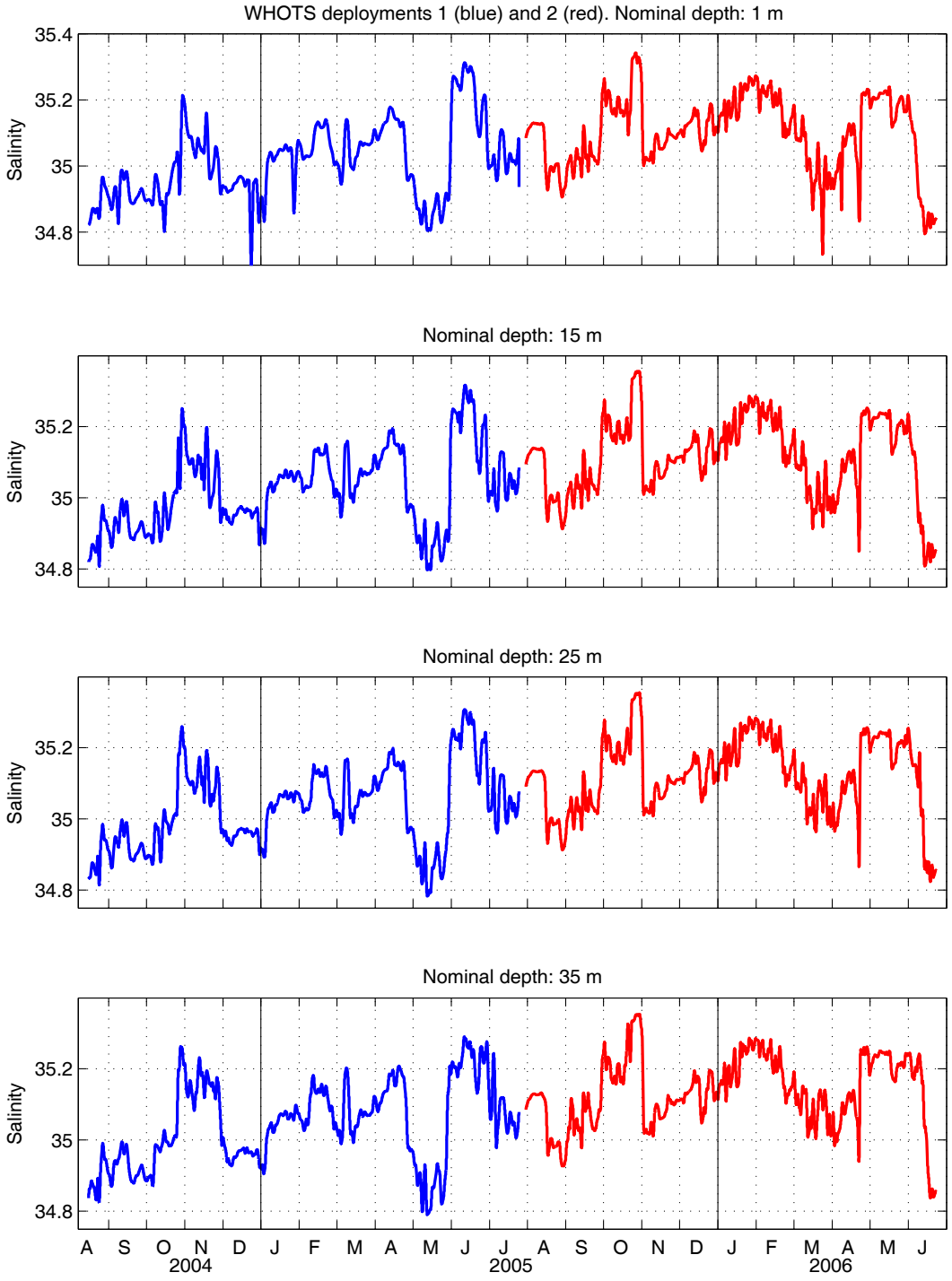

Figure 6-41 Salinities from SeaCATs/ MicroCATs during WHOTS-1 (blue line), and WHOTS-2 (red line) deployments at 1, 15, 25, and 35 m.

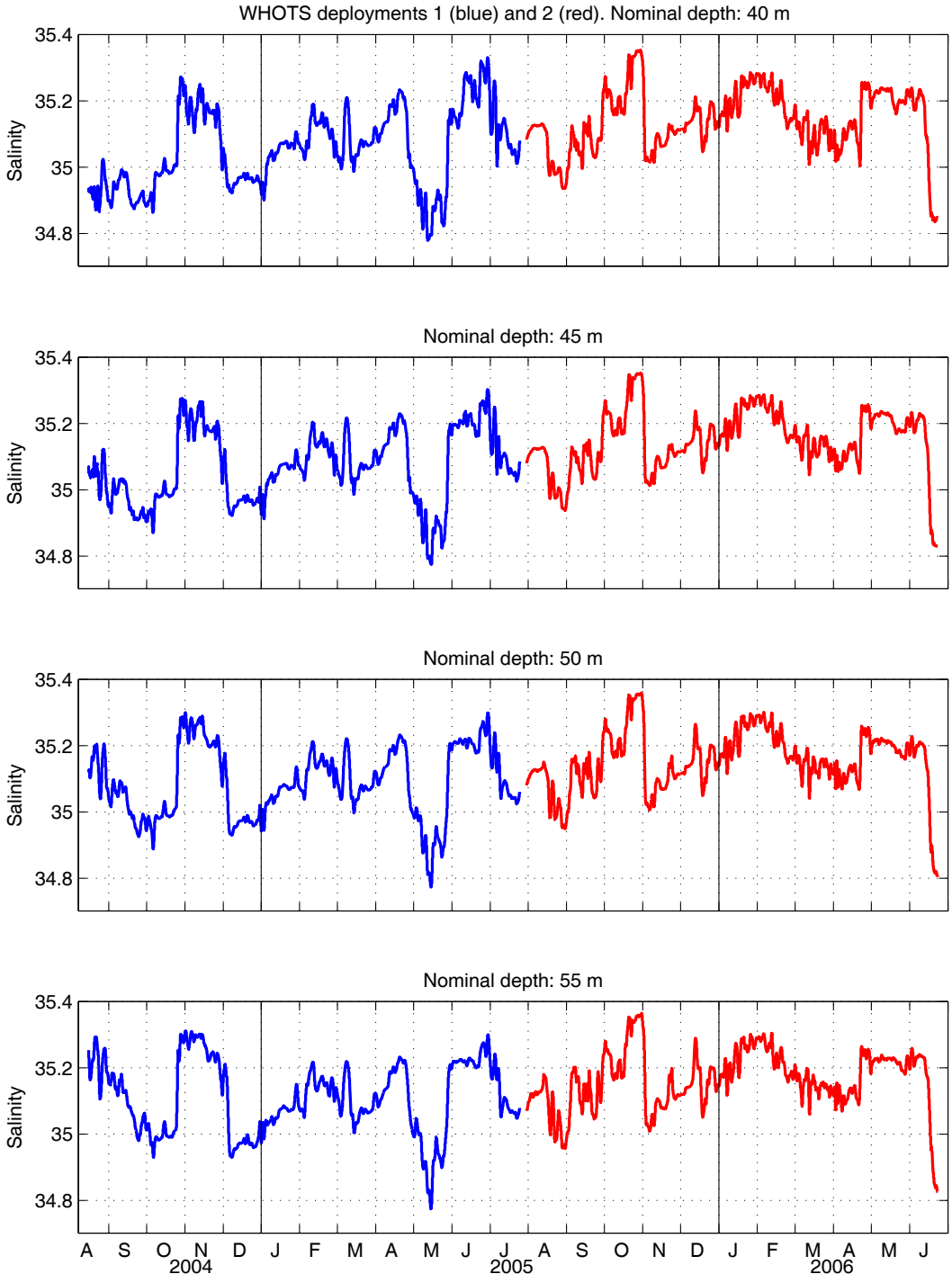

Figure 6-42 Same as in Figure 6-41, but at 40, 45, 50, and 55 m.

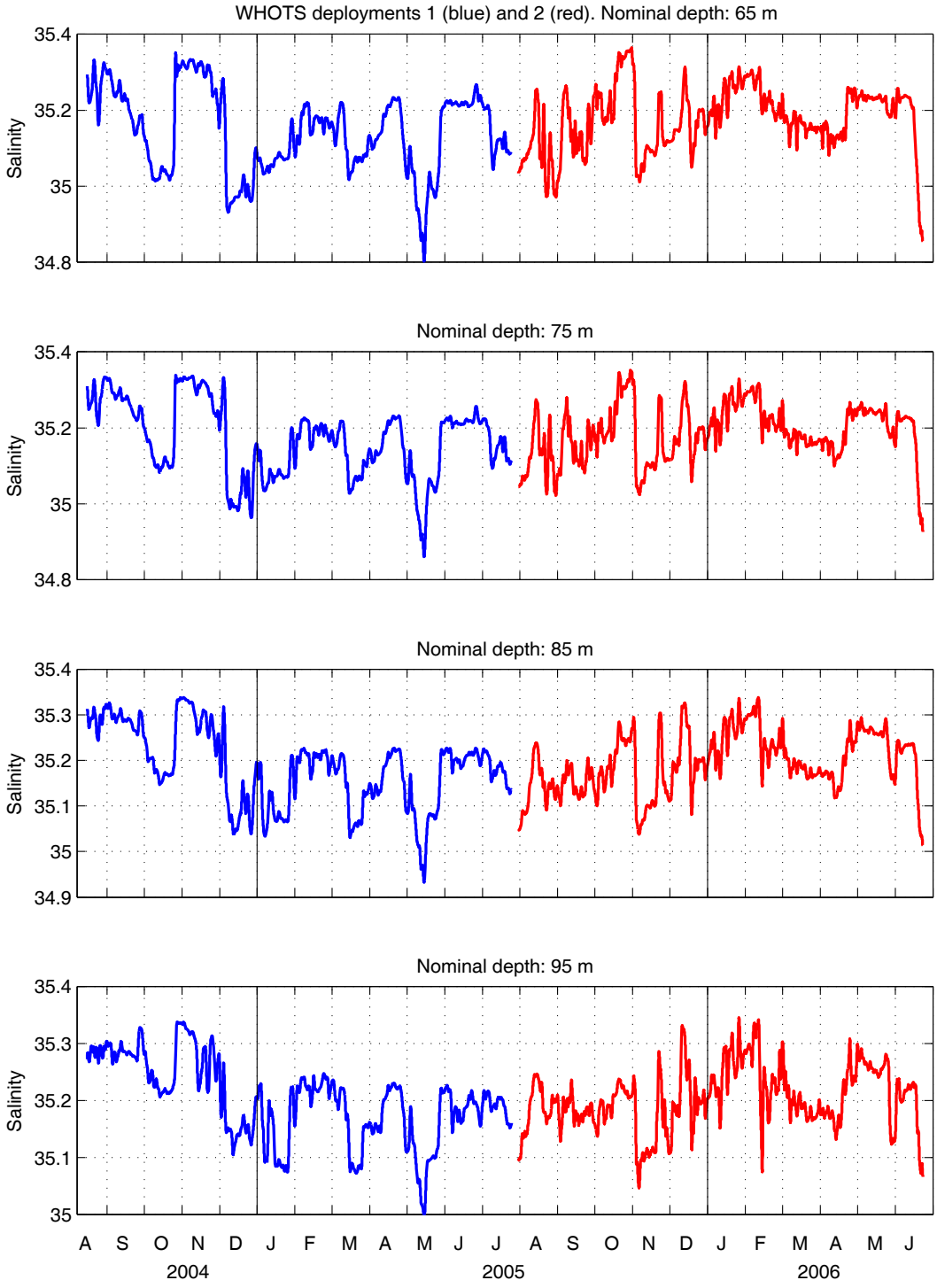

Figure 6-43 Same as in Figure 6-41, but at 65, 75, 85, and 95 m.

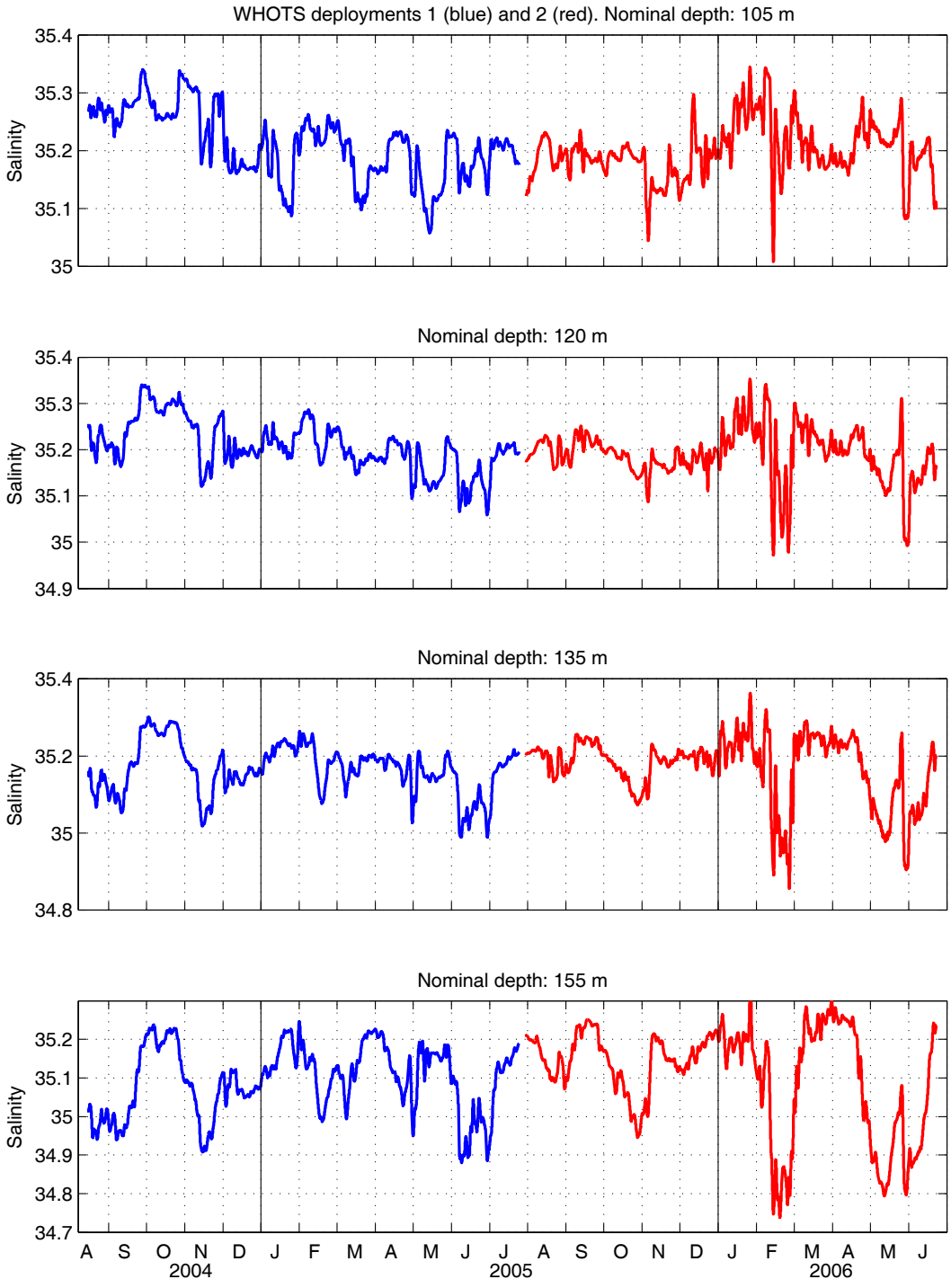

Figure 6-44 Same as in Figure 6-41, but at 105, 120, 135, and 155 m.

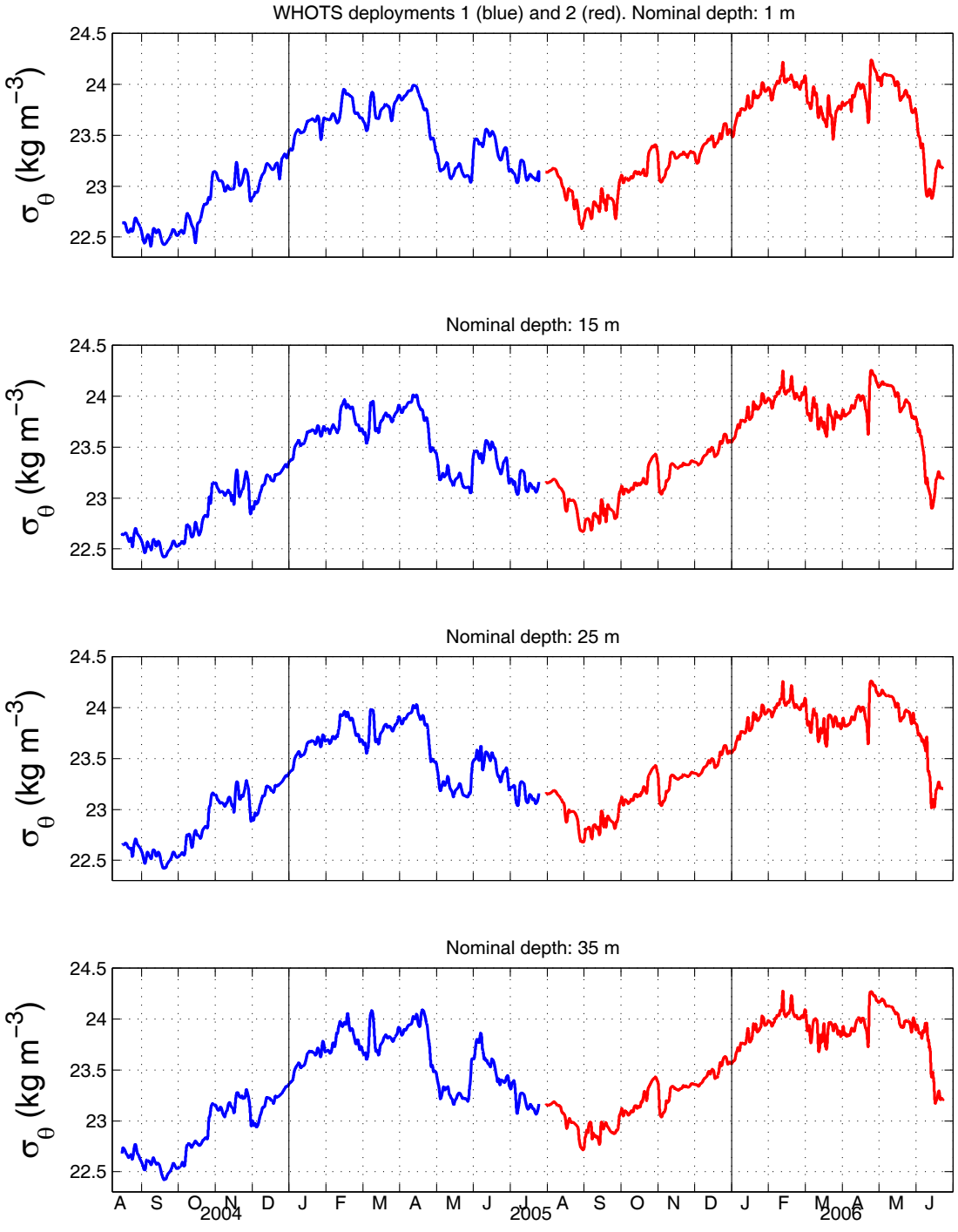

Figure 6-45 Potential density (σ_θ) from SeaCATs/ MicroCATs during WHOTS-1 (blue line), and WHOTS-2 (red line) deployments at 1, 15, 25, and 35 m.

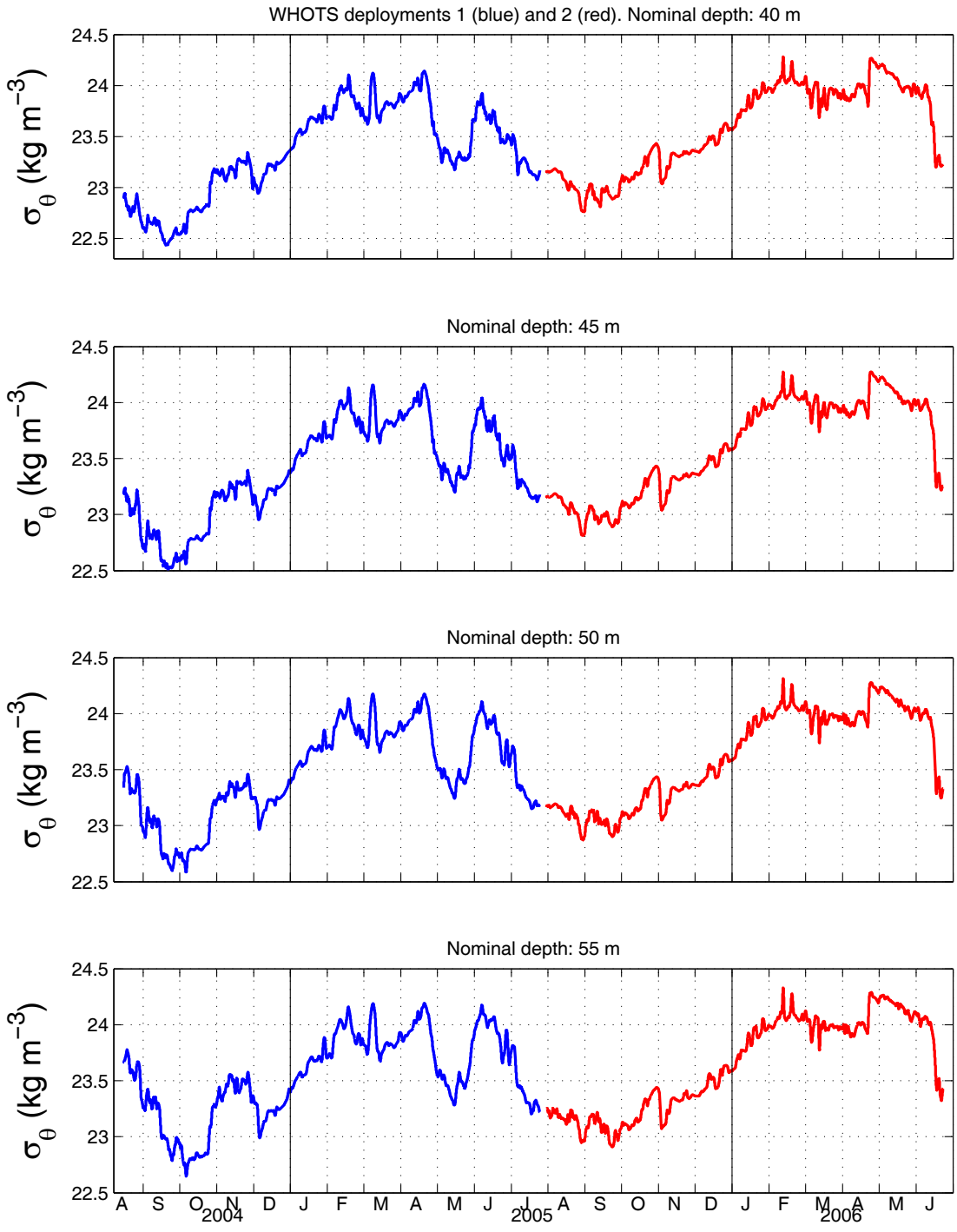

Figure 6-46 Same as in Figure 6-45, but at 40, 45, 50, and 55 m.

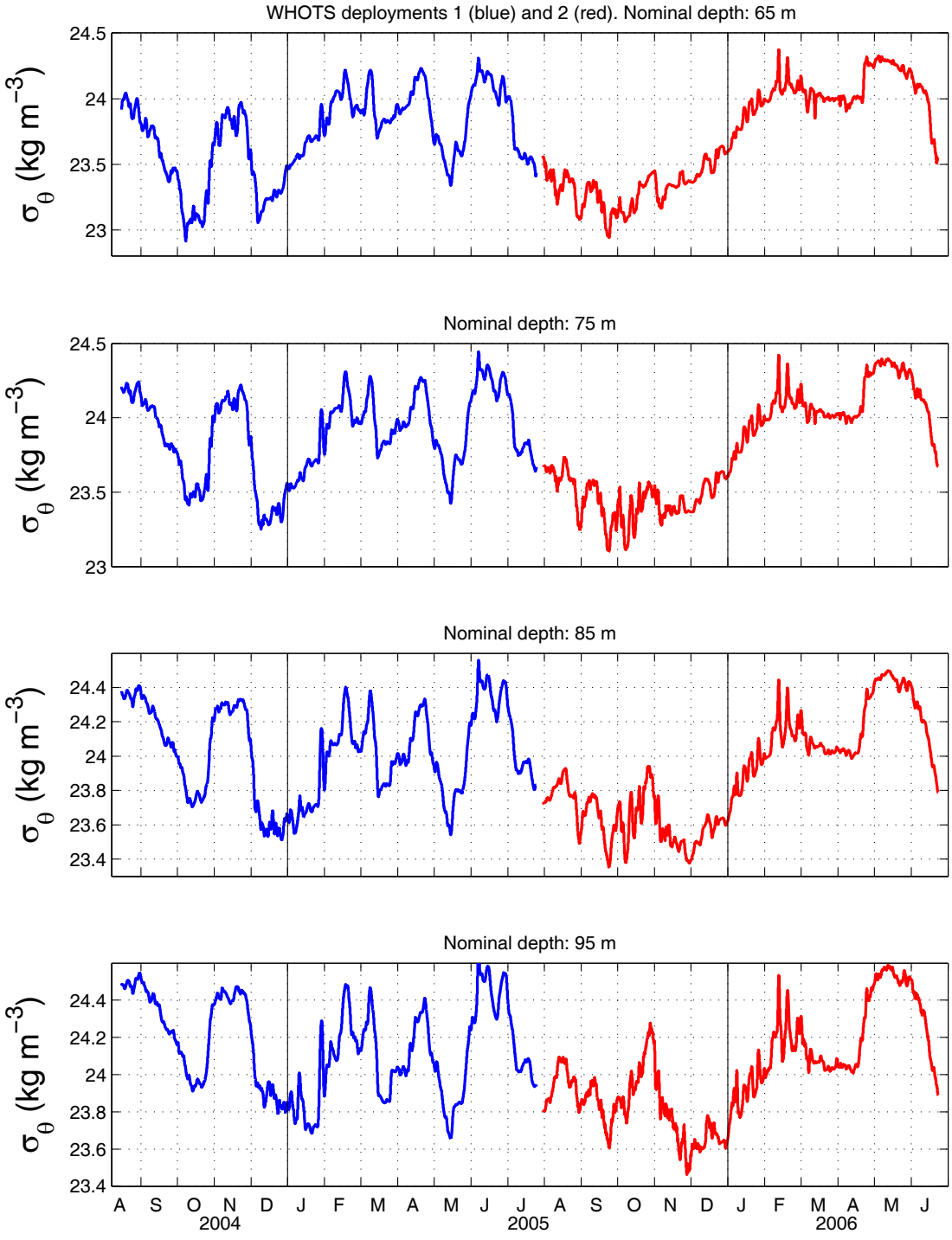

Figure 6-47 Same as in Figure 6-45, but at 65, 75, 85, and 95 m.

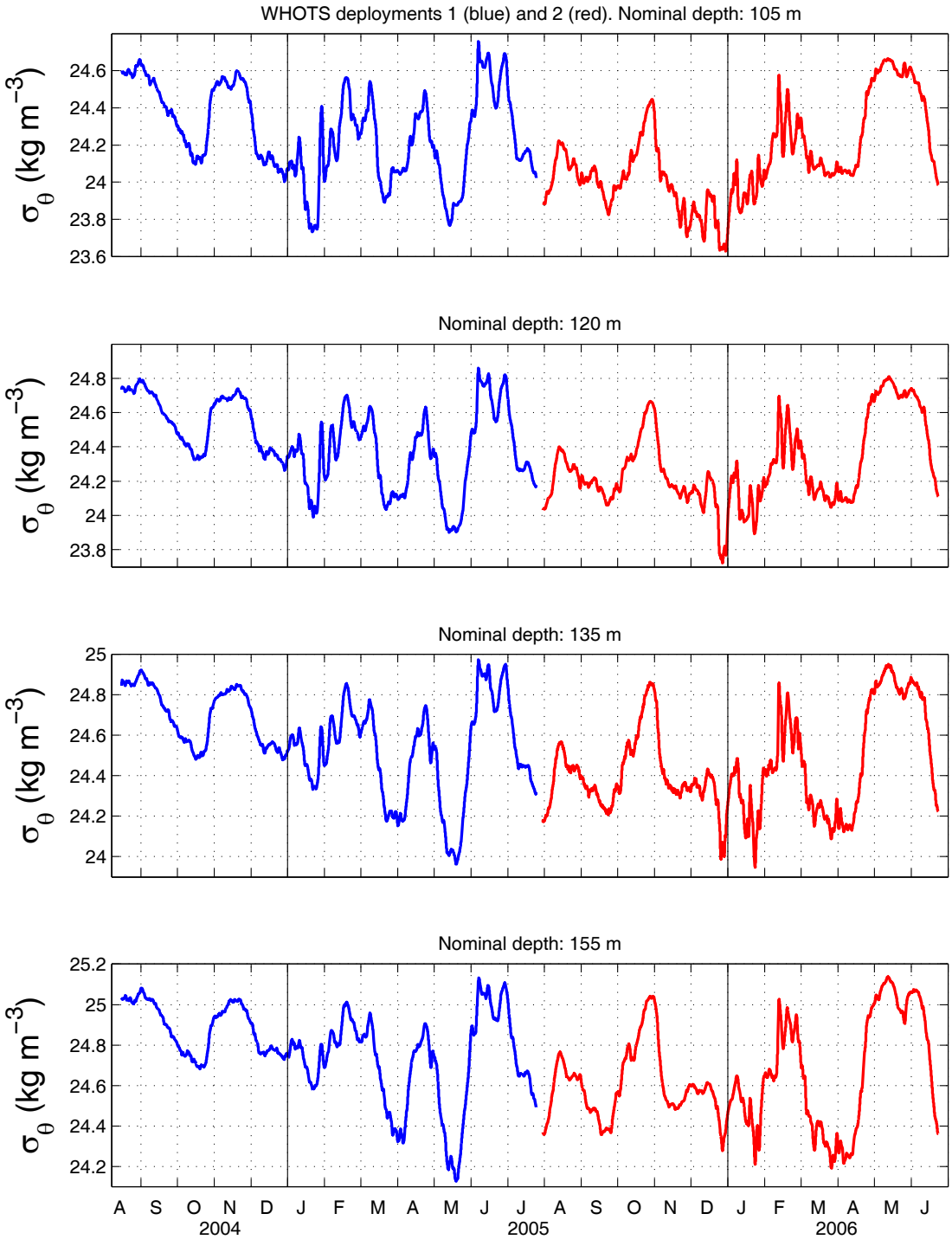

Figure 6-48 Same as in Figure 6-45, but at 105, 120, 135, and 155 m.

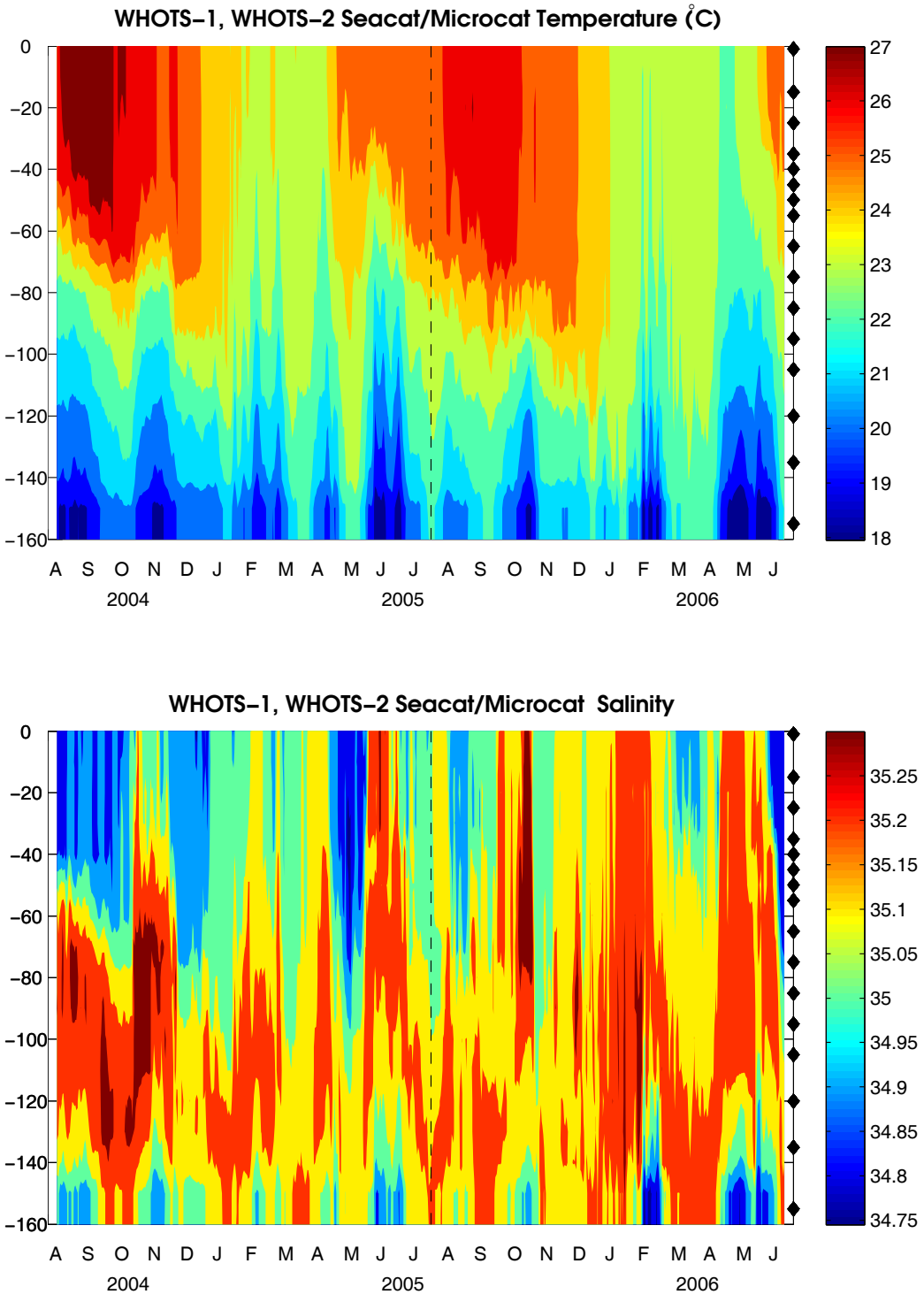

Figure 6-49 Contour plots of temperature (upper panel), and salinity (lower panel) versus depth from SeaCATs/ MicroCATs during WHOTS-1, and WHOTS-2 deployments. The vertical dashed line indicates the transition between WHOTS-1 and WHOTS-2. The diamonds along the right axis indicate the instruments depths.

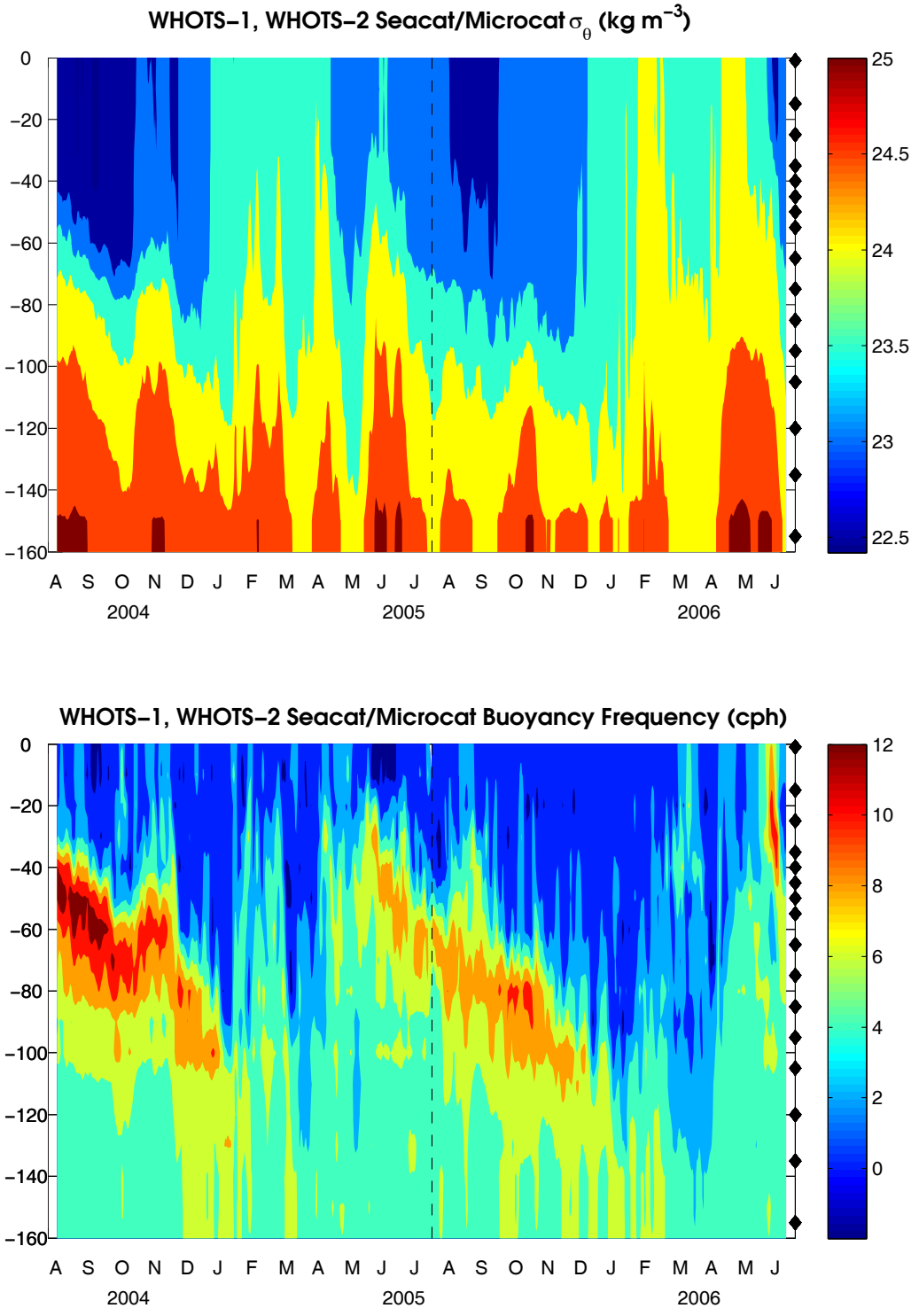

Figure 6-50 Contour plots of potential density (σ_θ, upper panel), and buoyancy frequency (lower panel) versus depth from SeaCATs/MicroCATs during WHOTS-1, and WHOTS-2 deployments. The vertical dashed line indicates the transition between WHOTS-1 and WHOTS-2. The diamonds along the right axis indicate the instruments depths.

D. Moored ADCP data

Contoured plots of smoothed horizontal and vertical velocity as a function of depth during the mooring deployments are presented in Figure 6-51 to Figure 6-53. A staggered timeseries of smoothed horizontal and vertical velocities are shown in Figure 6-54 to Figure 6-56.

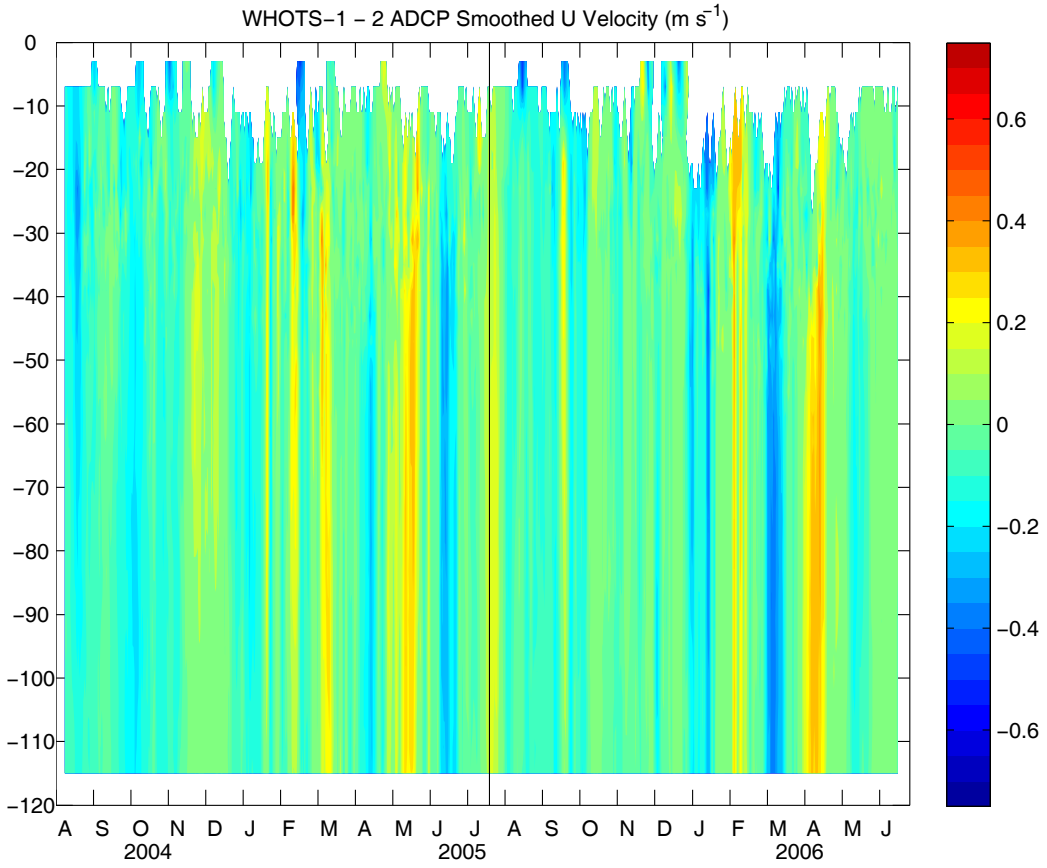

Figure 6-51 Contour plot of east velocity component (m s^{-1}) versus depth and time from the moored WH-300 ADCP from the WHOTS-1 and WHOTS-2 deployments (separated by the vertical black line).

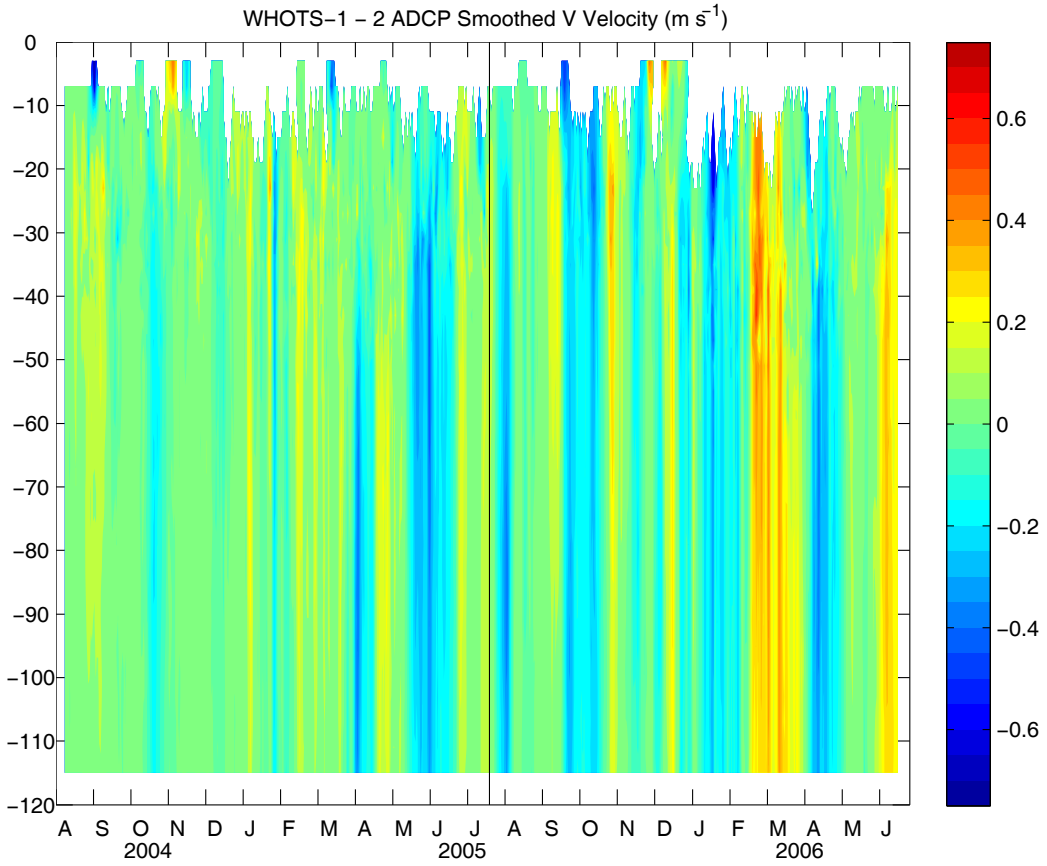

Figure 6-52 Contour plot of north velocity component (m s^{-1}) versus depth and time from the moored WH-300 ADCP from the WHOTS-1 and WHOTS-2 deployments (separated by the vertical black line).

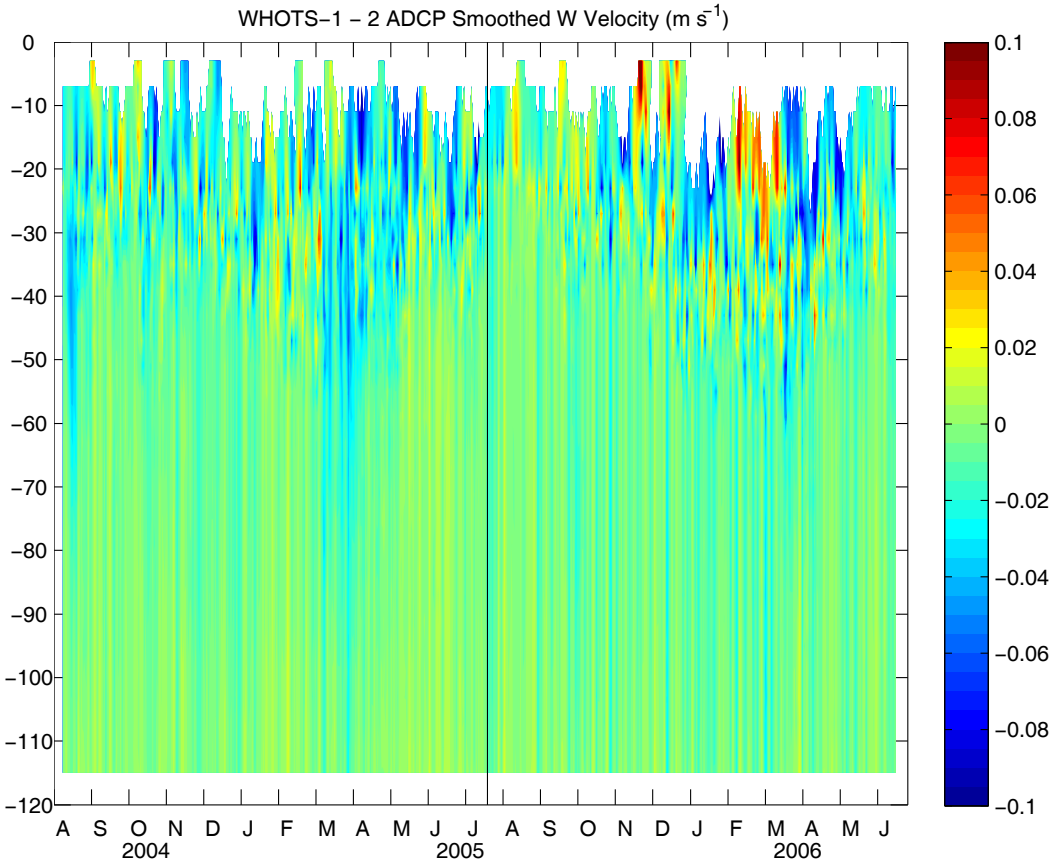

Figure 6-53 Contour plot of vertical velocity component (m s^{-1}) versus depth and time from the moored WH-300 ADCP from the WHOTS-1 and WHOTS-2 deployments (separated by the vertical black line).

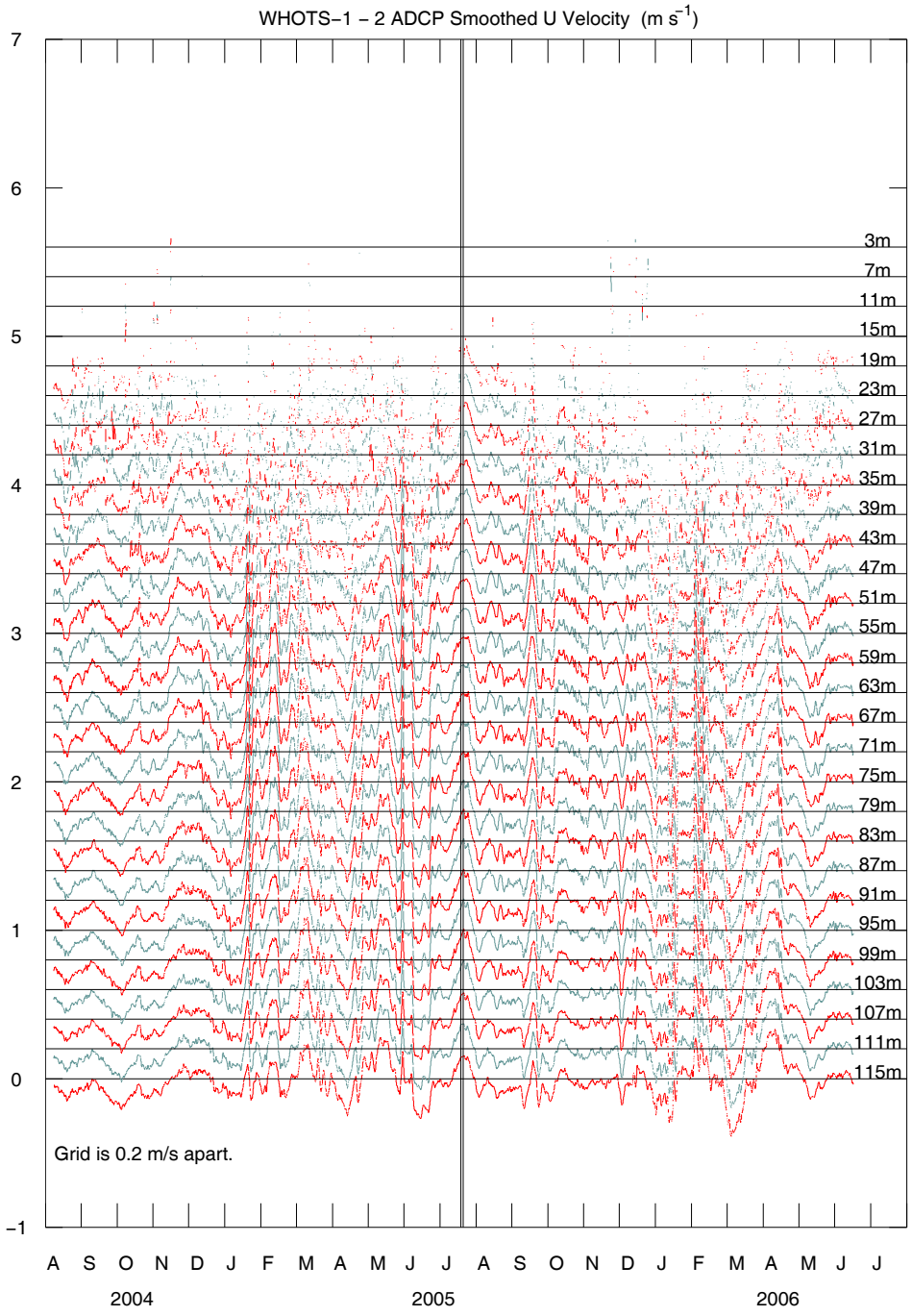

[P J2]

Figure 6-54 Staggered plot of east velocity component (m s^{-1}) versus time for each depth range for the WHOTS-1 and WHOTS-2 deployment. The spacing is 0.2 m s^{-1}. The two vertical black lines show the end of the first deployment and the start of the second.

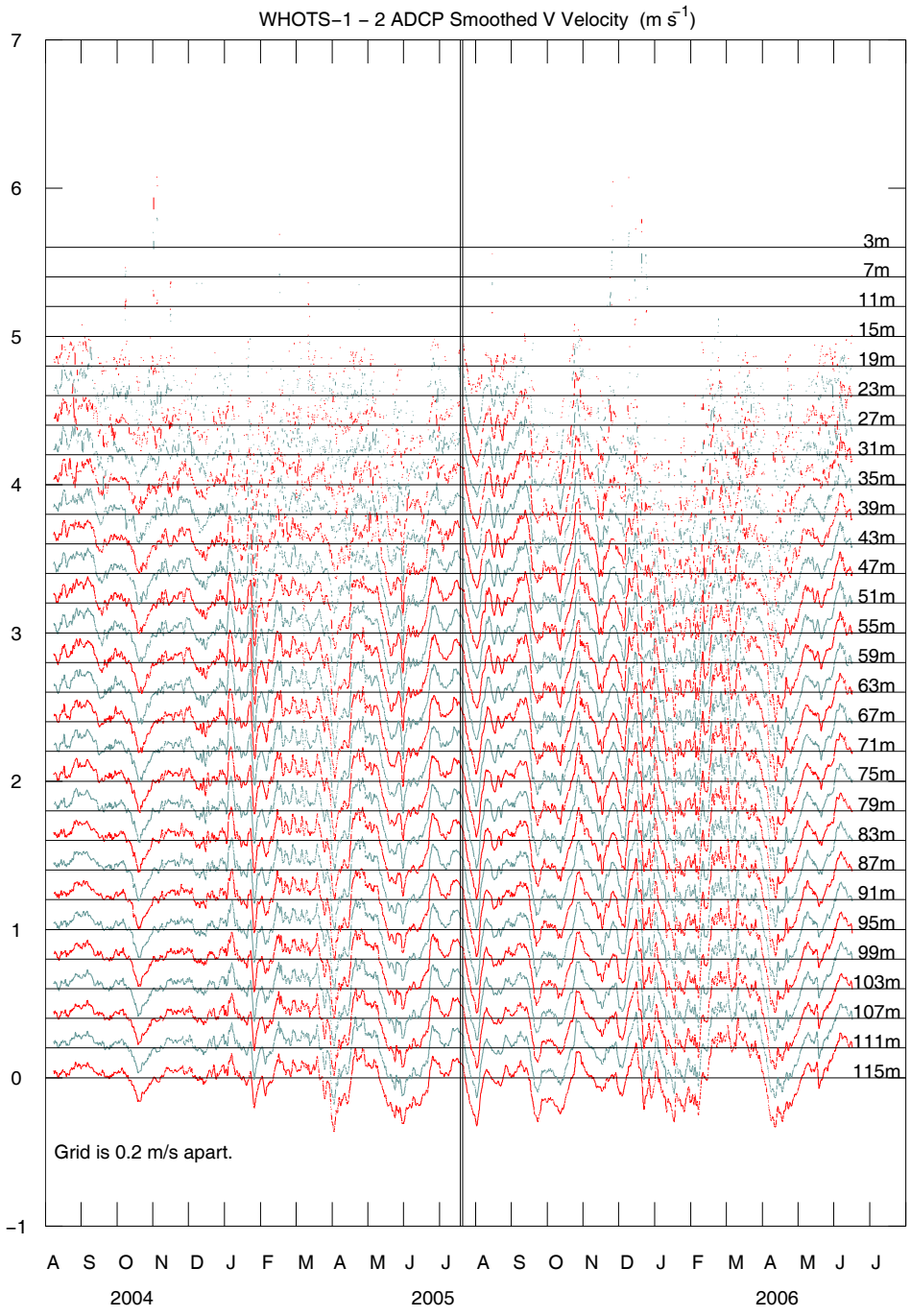

Figure 6-55 Staggered plot of north velocity component versus time for each depth range for the WHOTS-1 and WHOTS-2 deployment. The spacing is 0.2 m s^{-1}. The two vertical black lines show the end of the first deployment and the start of the second.

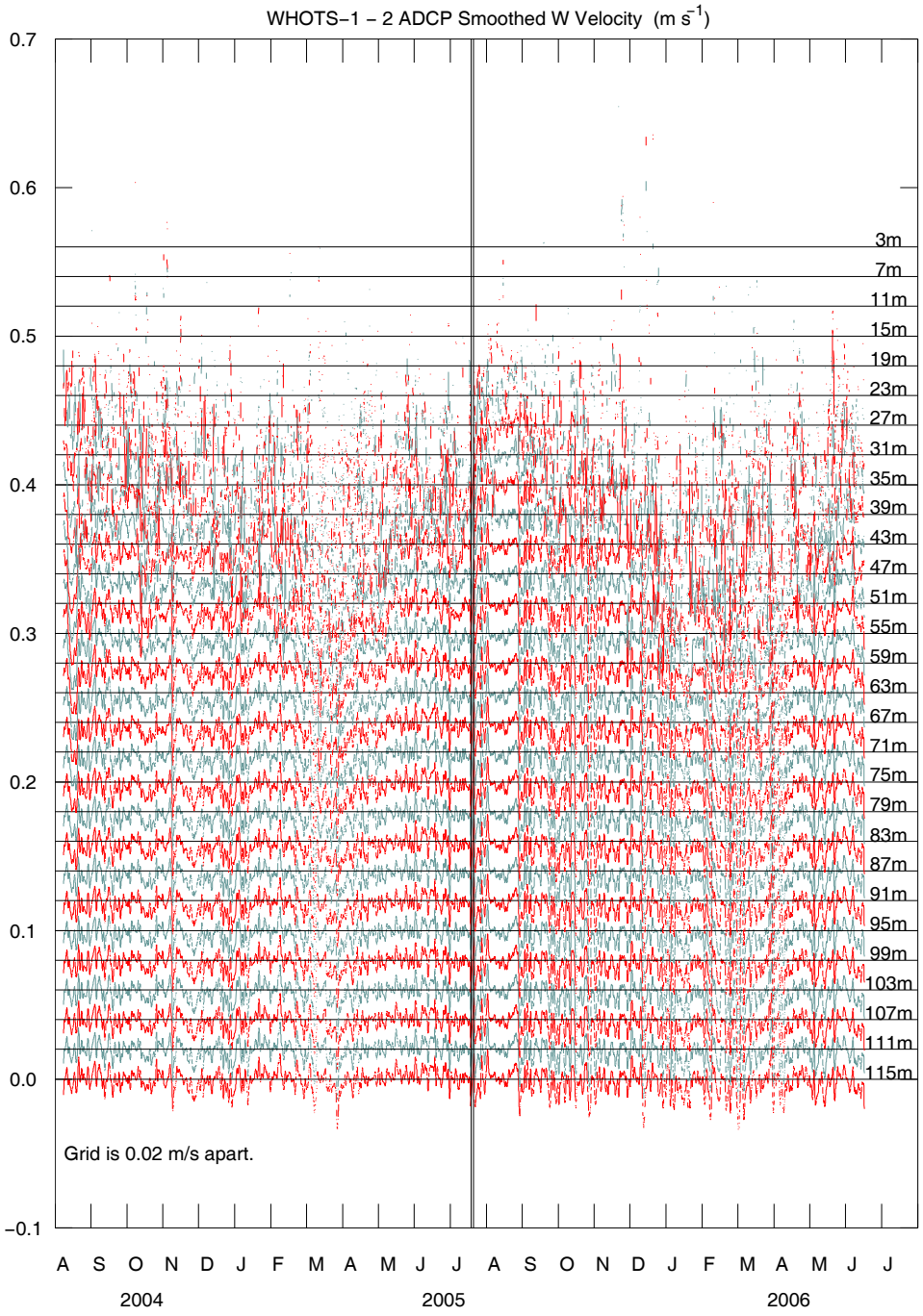

Figure 6-56 Staggered plot of vertical velocity component versus time for each depth range for the WHOTS-1 and WHOTS-2 deployment. The spacing is 0.02 m s^{-1}. The two vertical black lines show the end of the first deployment and the start of the second.

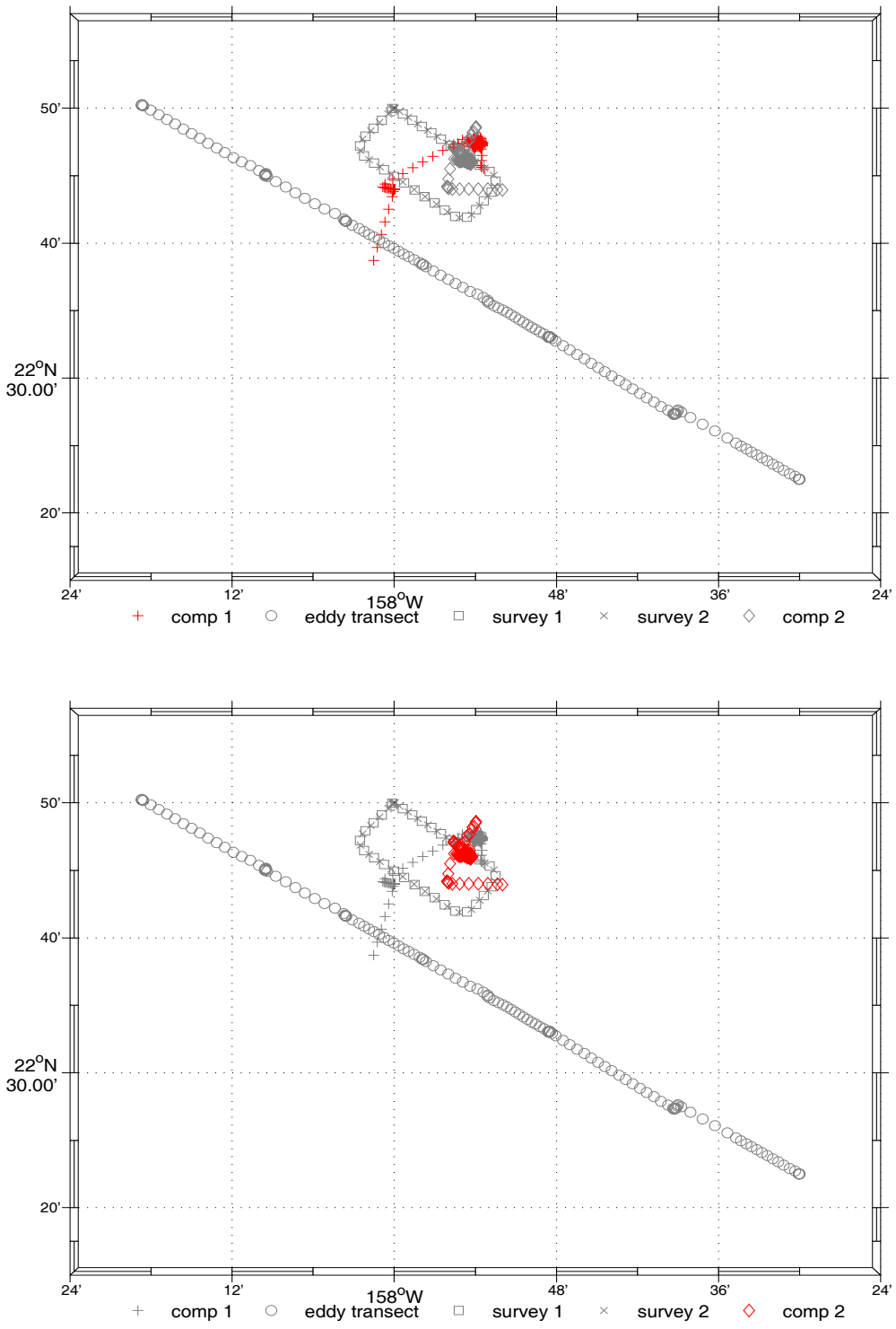

Figure 6-57 Location of the ship (highlighted in red) during the inter-comparison period with the WHOTS-1 mooring before recovery (upper panel) and the inter-comparison period with the WHOTS-2 mooring after deployment (lower panel), during the WHOTS-2 cruise.

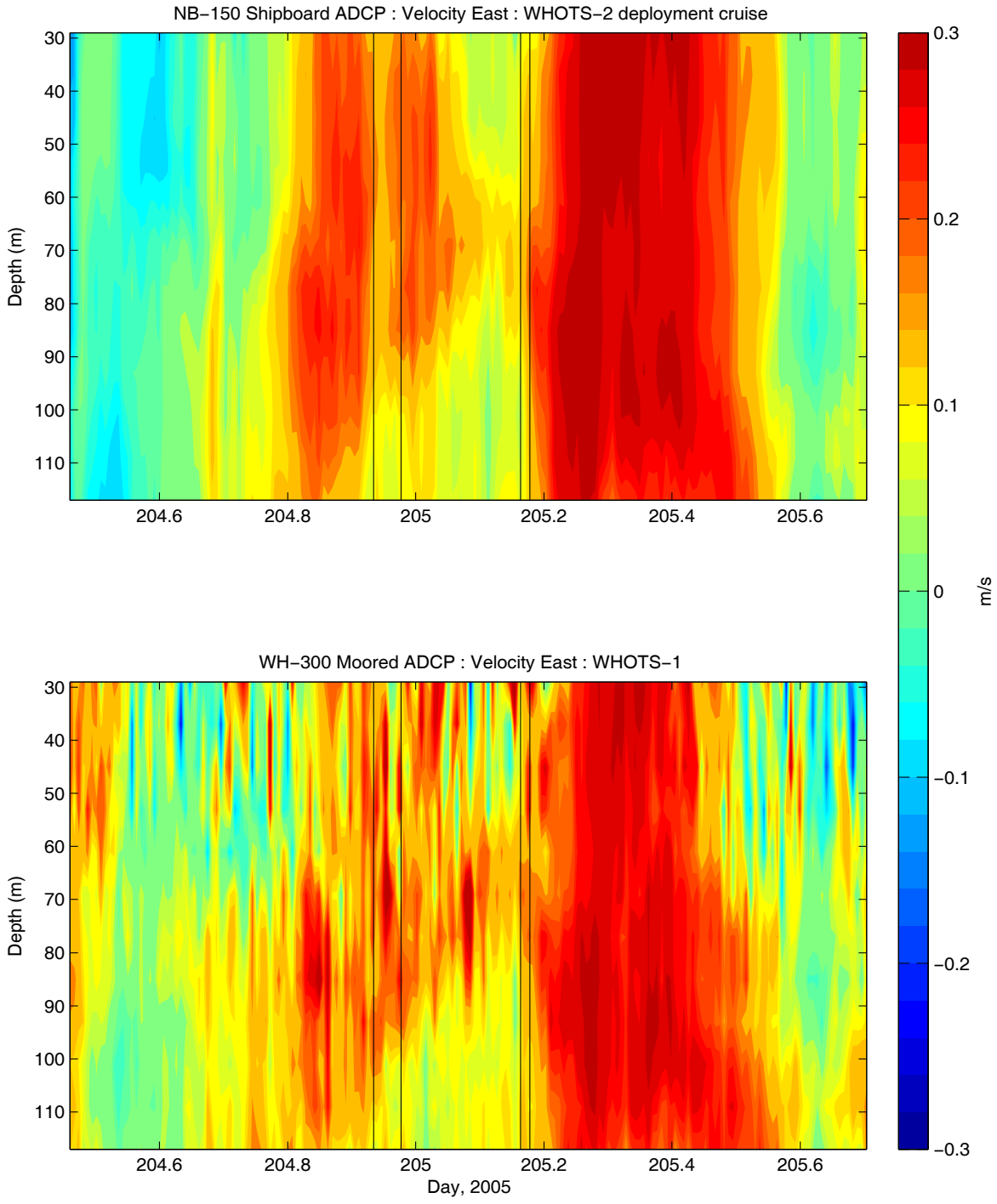

Figure 6-58 Contour of east velocity component (m s^{-1}) from the narrow band 150 KHz shipboard ADCP (upper panel) and the moored ADCP from the WHOTS-1 deployment as a function of time and depth, during the WHOTS-2 cruise. Times when the CTD rosette were in the water are identified between the two sets of black lines.

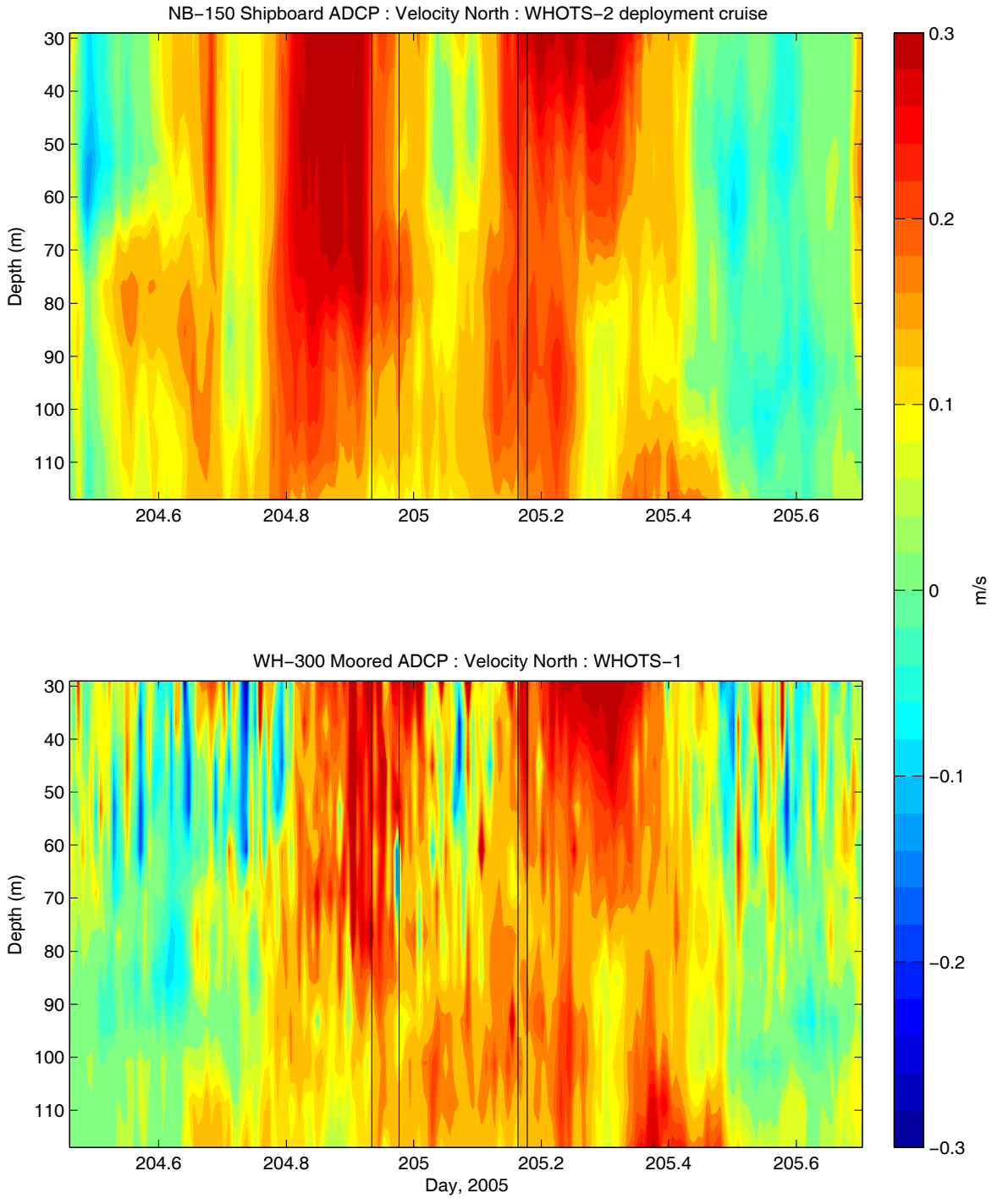

Figure 6-59 Contour of north velocity component (m s^{-1}) from the narrow band 150 KHz shipboard ADCP (upper panel) and the moored ADCP from the WHOTS-1 deployment, as a function of time and depth during the WHOTS-2 cruise. Times when the CTD rosette were in the water are identified between the two sets of black lines.

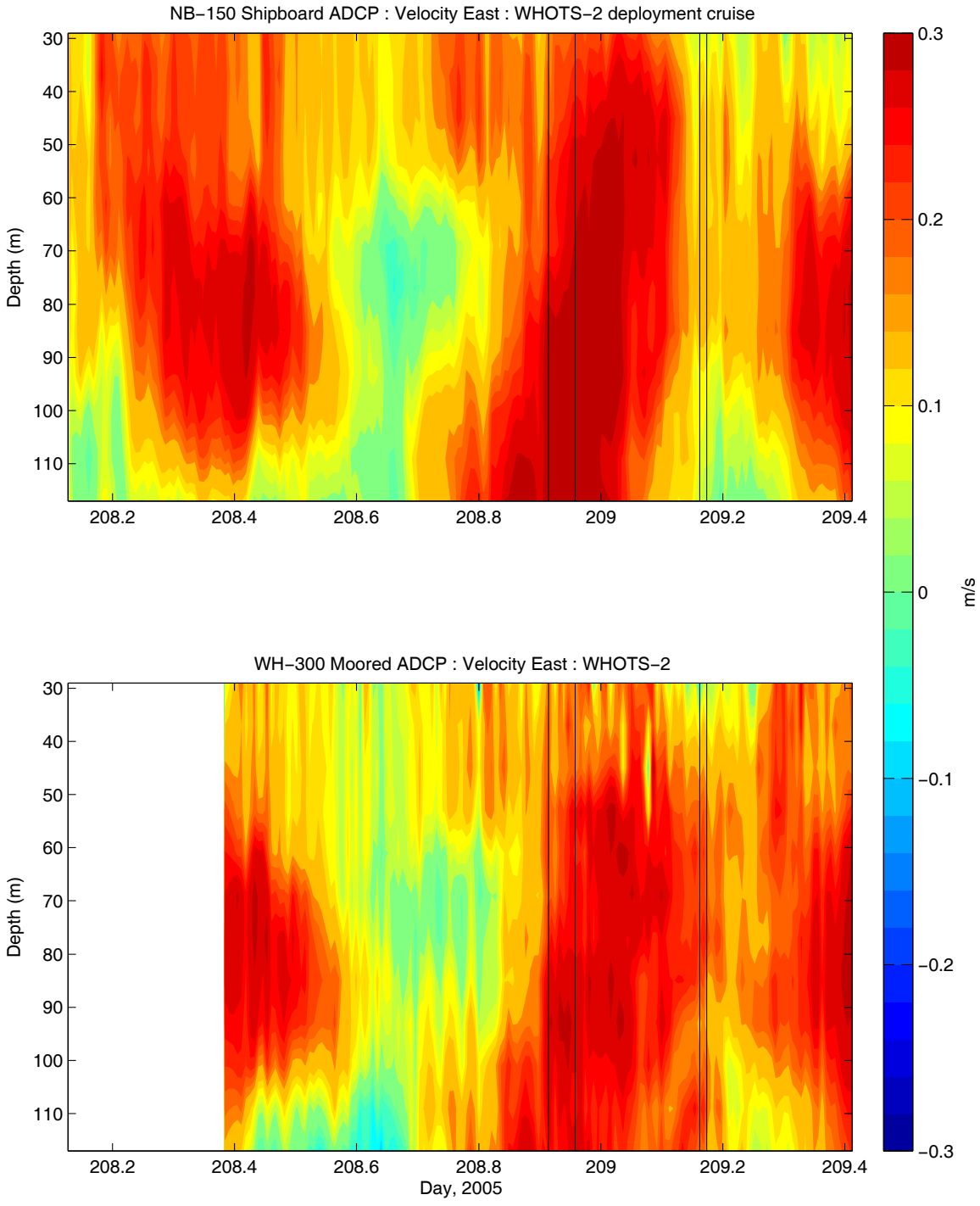

Figure 6-60 Contour of east velocity component (m s^{-1}) from the narrow band 150 KHz shipboard ADCP (upper panel) and the moored ADCP from the WHOTS-2 deployment as a function of time and depth, during the WHOTS-2 cruise. Times when the CTD rosette were in the water are identified between the two sets of black lines.

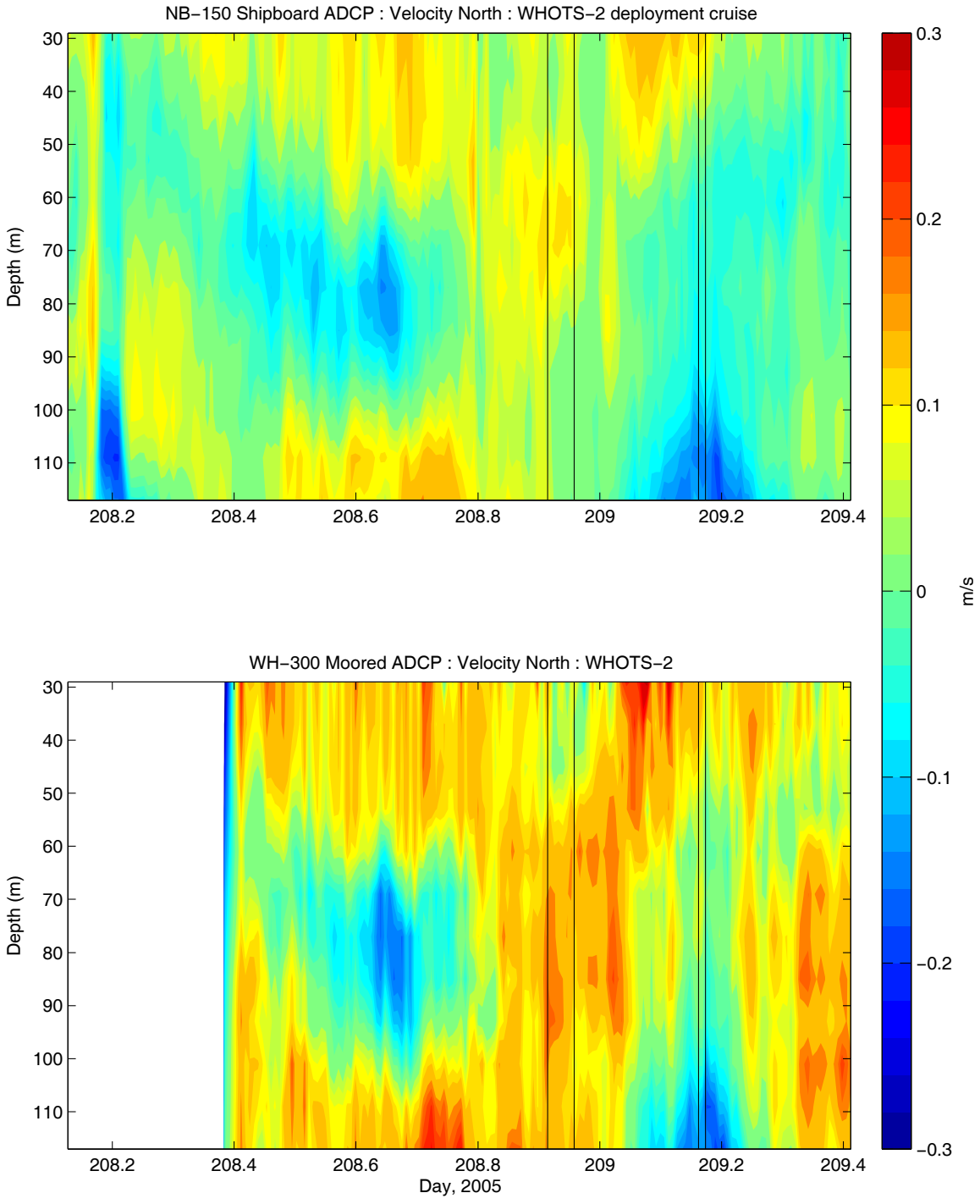

Figure 6-61 Contour of north velocity component (m s^{-1}) from the narrow band 150 KHz shipboard ADCP (upper panel) and the moored ADCP from the WHOTS-2 deployment, as a function of time and depth during the WHOTS-2 cruise. Times when the CTD rosette were in the water are identified between the two sets of black lines.

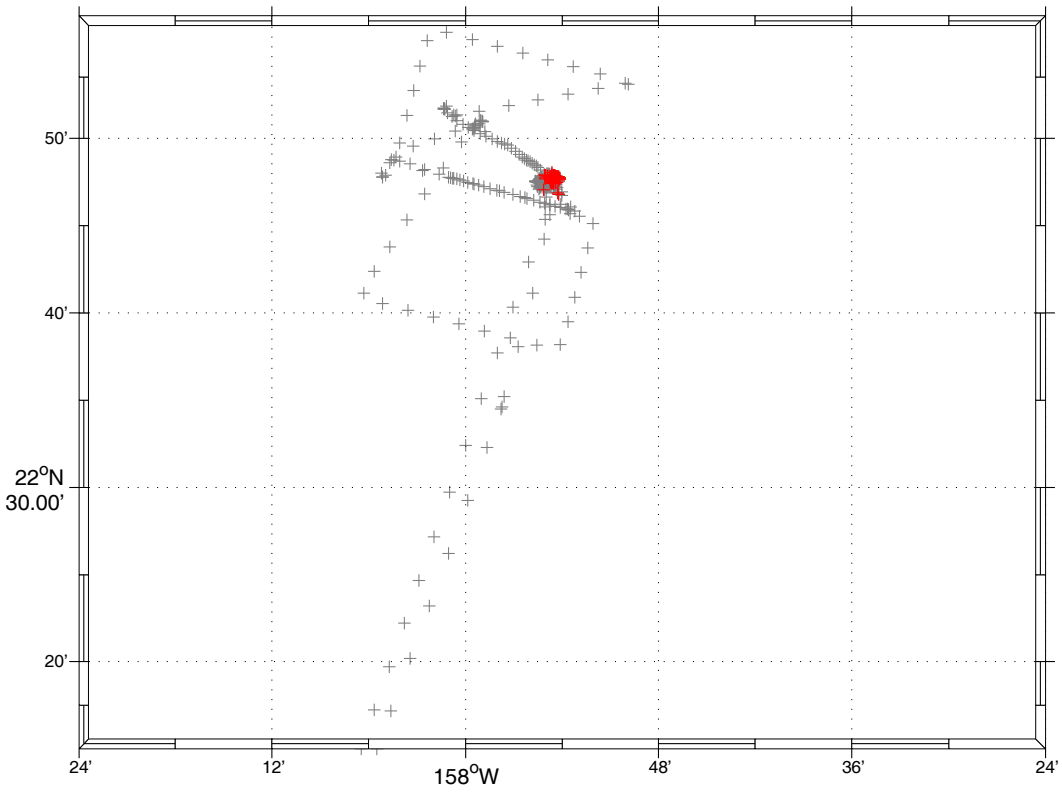

Figure 6-62 Location of the R/V Roger Revelle (highlighted in red) during the inter-comparison period with the WHOTS-2 mooring before recovery during the WHOTS-3 cruise.

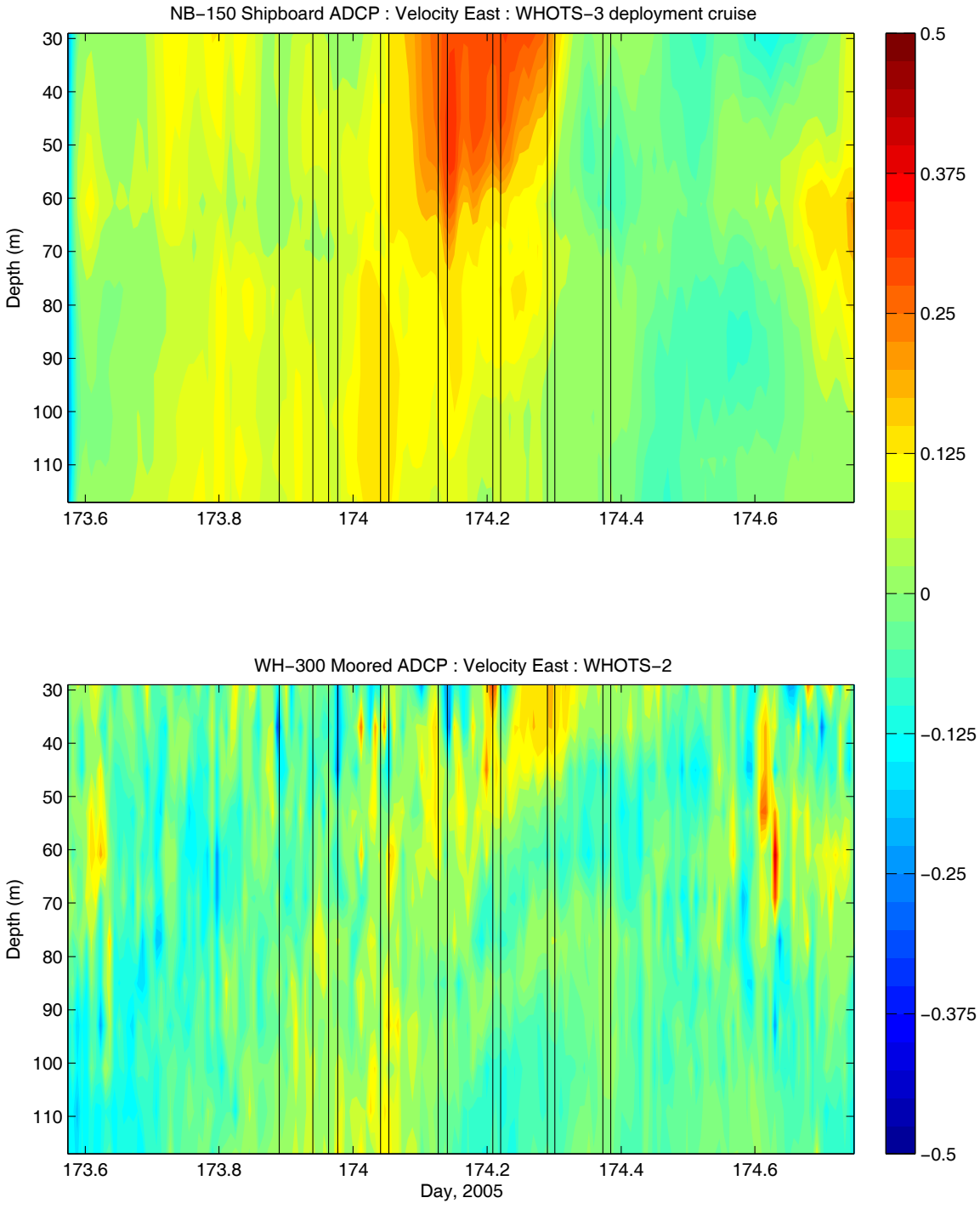

Figure 6-63 Contour of east velocity component (m s^{-1}) from the narrow band 150 KHz shipboard ADCP (upper panel) and the moored ADCP from the WHOTS-2 deployment, as a function of time and depth during the WHOTS-3 cruise. Times when the CTD rosette were in the water are identified between the two sets of black lines.

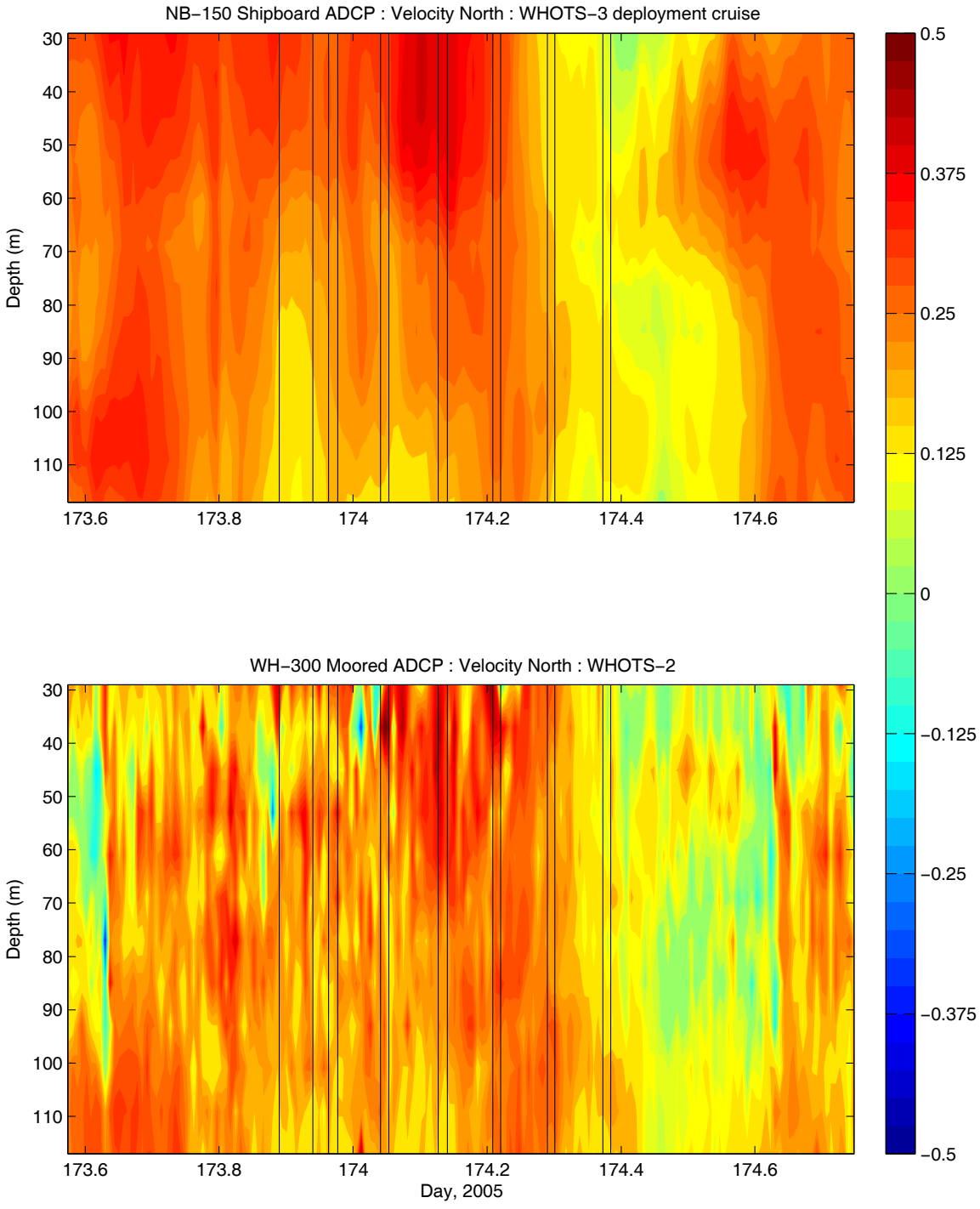

Figure 6-64 Contour of north velocity component (m s^{-1}) from the narrow band 150 KHz shipboard ADCP (upper panel) and the moored ADCP from the WHOTS-2 deployment, as a function of time and depth during the WHOTS-3 cruise. Times when the CTD rosette were in the water are identified between the two sets of black lines.

E. Shipboard ADCP

Contours of horizontal velocity measurements as a function of depth from the narrow band 150 KHz shipboard ADCP from the northwest transect plotted in time are presented in Figure 6-65 and Figure 6-66.

Comparisons between the moored ADCP and available shipboard ADCP obtained during regular HOT cruises are shown in Figure 6-70 to Figure 6-99. ARGOS data from the buoy was used to determine the distance of the buoy from the ship during the four-day cruise. The comparison was made over a six-hour period either side of the closest point of approach.

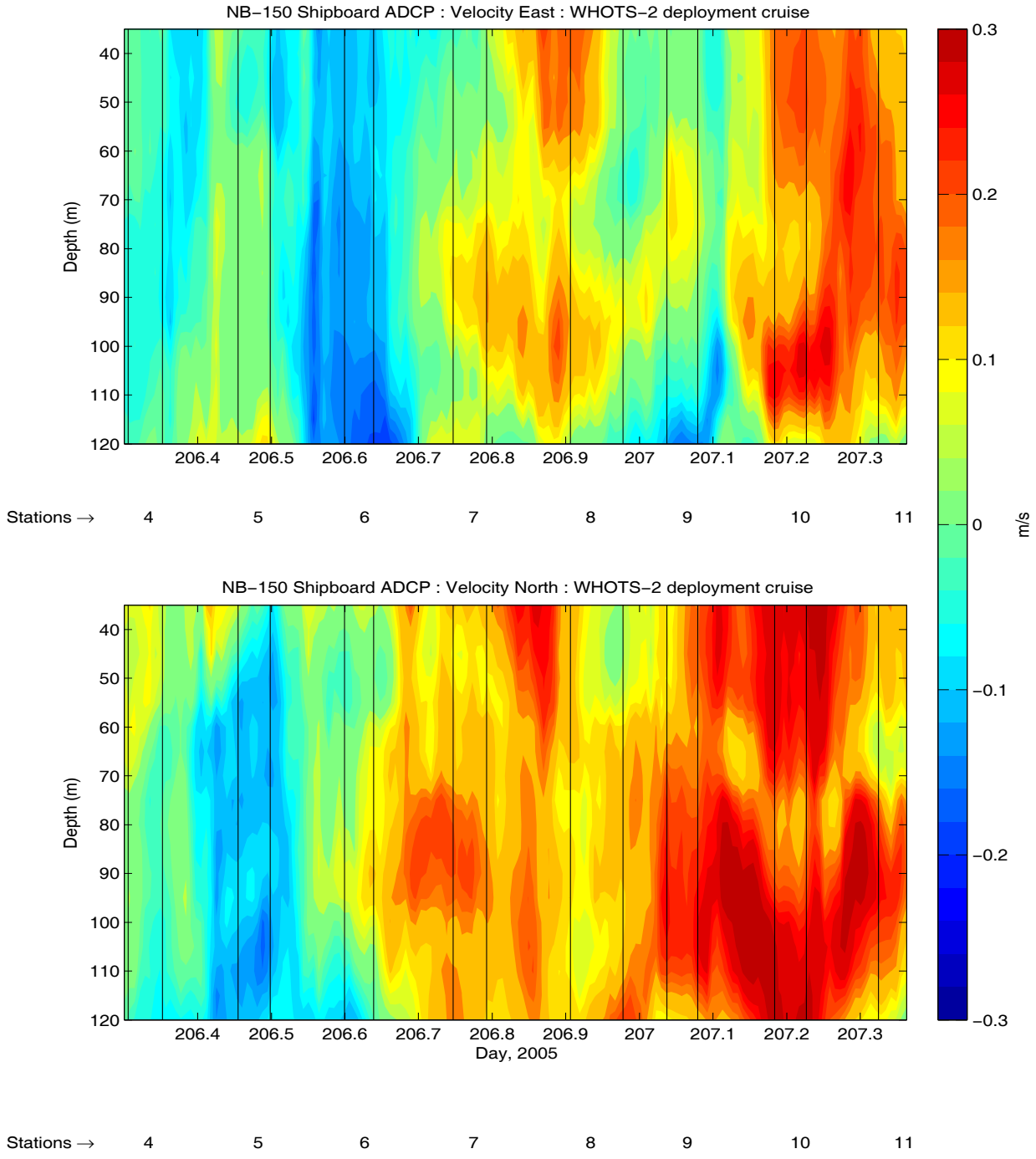

Figure 6-65 Contour plot of east velocity (m s^{-1}) component (upper panel) and north velocity (m s^{-1}) (lower panel) as a function of time and depth along the north-west transect occupying Stations 4 to 11 (see Figure 6-1) during the WHOTS-2 cruise.

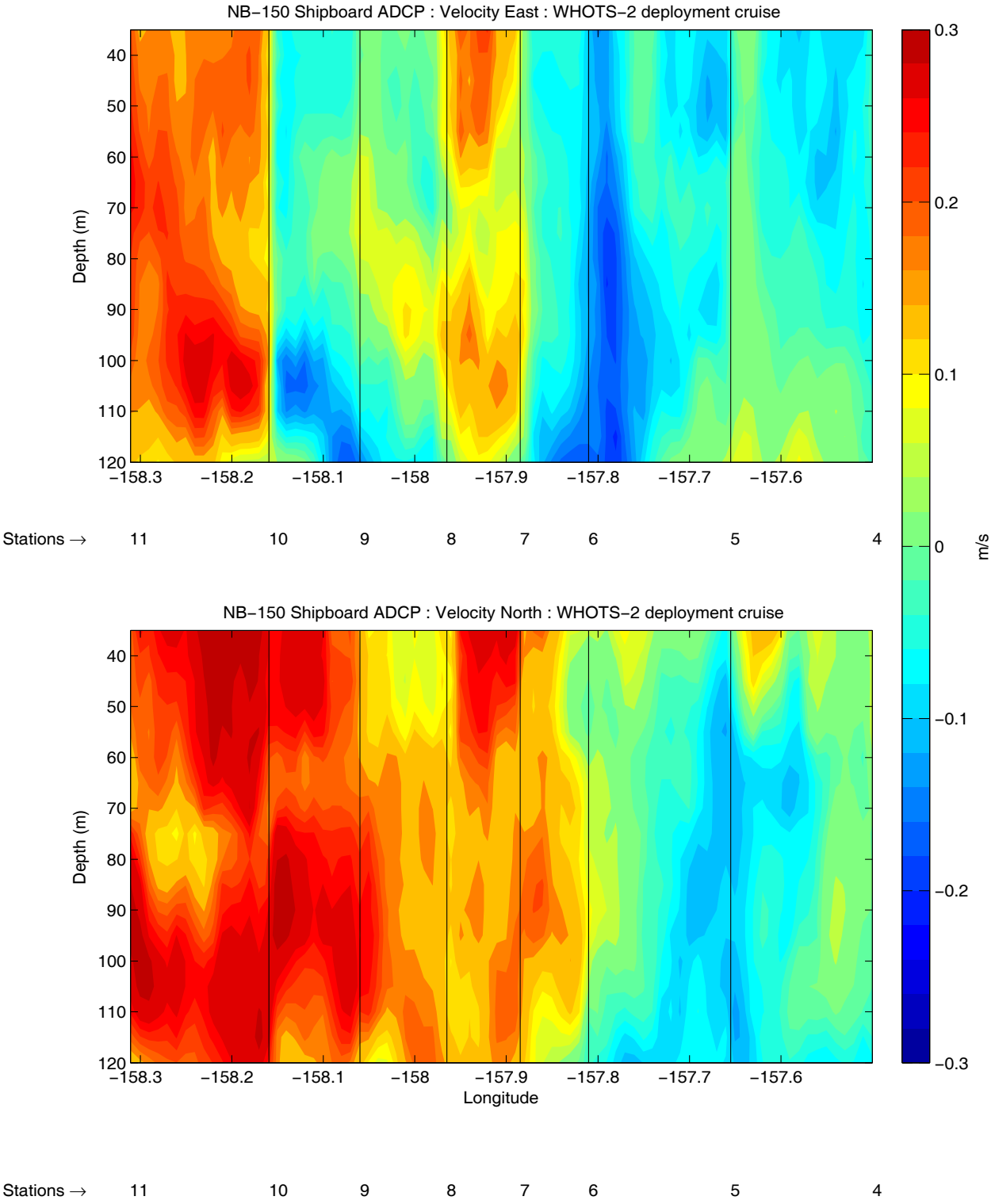

Figure 6-66 Contour plot of east velocity (m s^{-1}) component (upper panel) and north velocity m s^{-1}) (lower panel) as a function of time and depth along the north-west transect occupying Stations 4 to 11 (see Figure 6-1) during the WHOTS-2 cruise. The vertical lines indicate the location of the CTD stations.

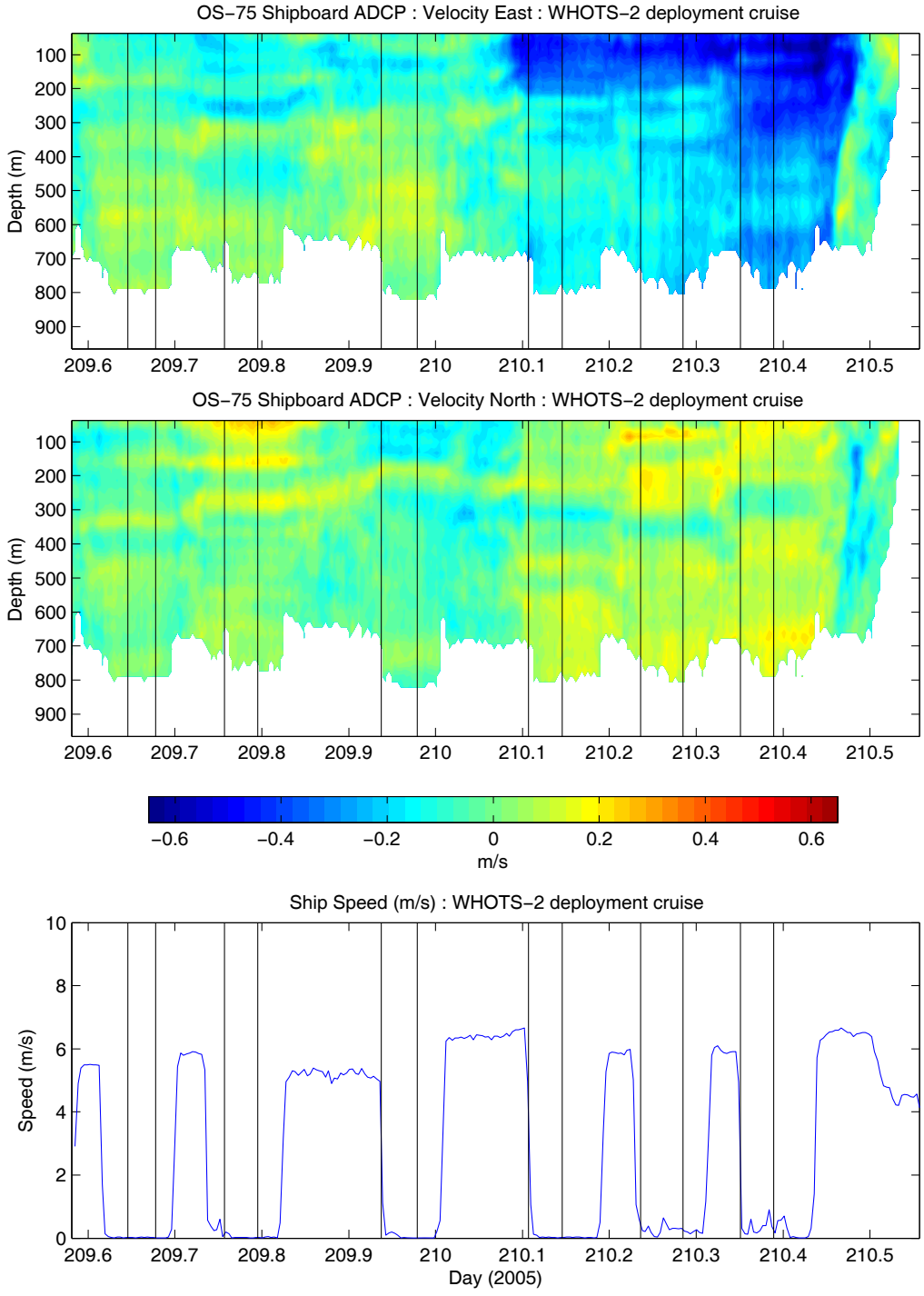

Figure 6-67 Contour plot of east velocity (m s^{-1}) component (upper panel) and north velocity m s^{-1}) (middle panel) as a function of time and depth along the north-south transect occupying Stations 14 to 19 (see Figure 6-1) during the WHOTS-2 cruise. The lower panel shows the ship speed in m s^{-1} during the transect. The pairs of vertical lines indicate the in-water and out of the water times of the CTD casts at each station.

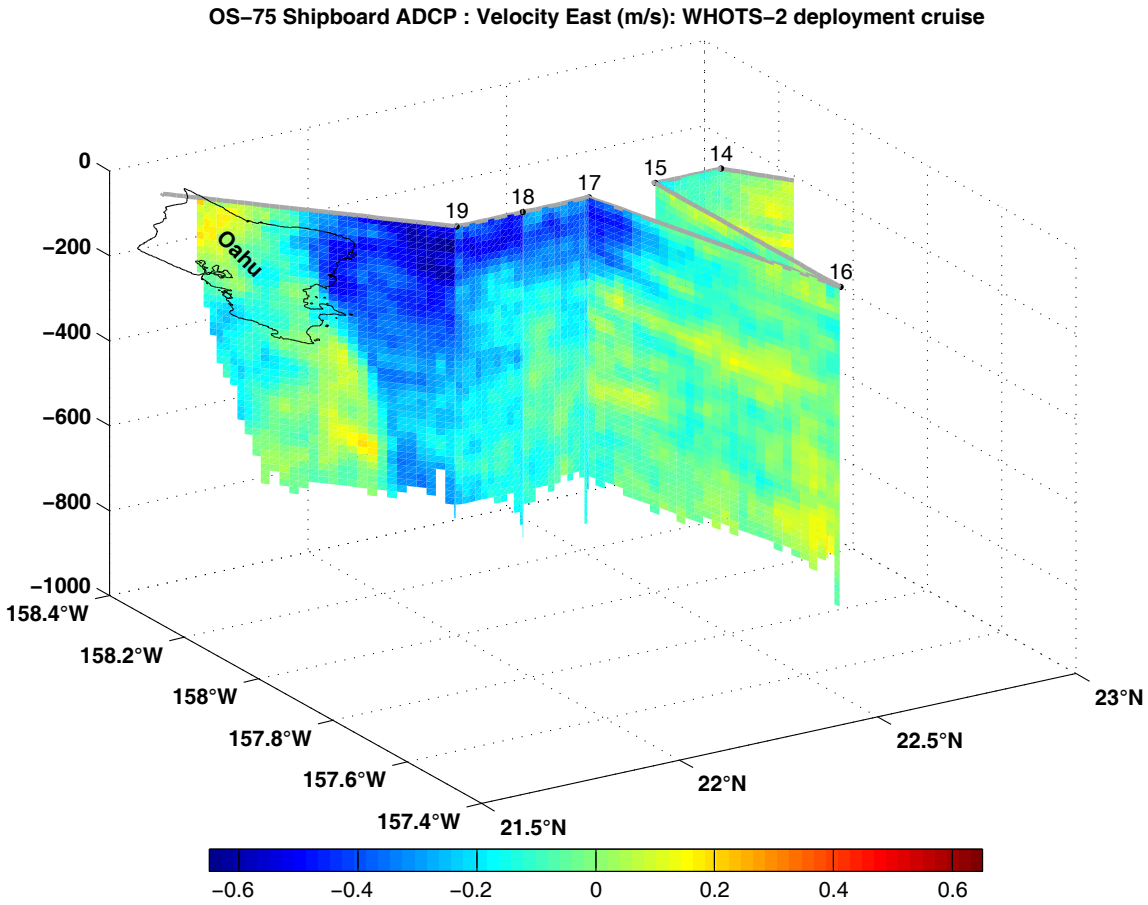

Figure 6-68 East velocity (m s^{-1}) component along the north-south transect occupying stations 14 to 19 (see Figure 6-1) during the WHOTS-2 cruise.

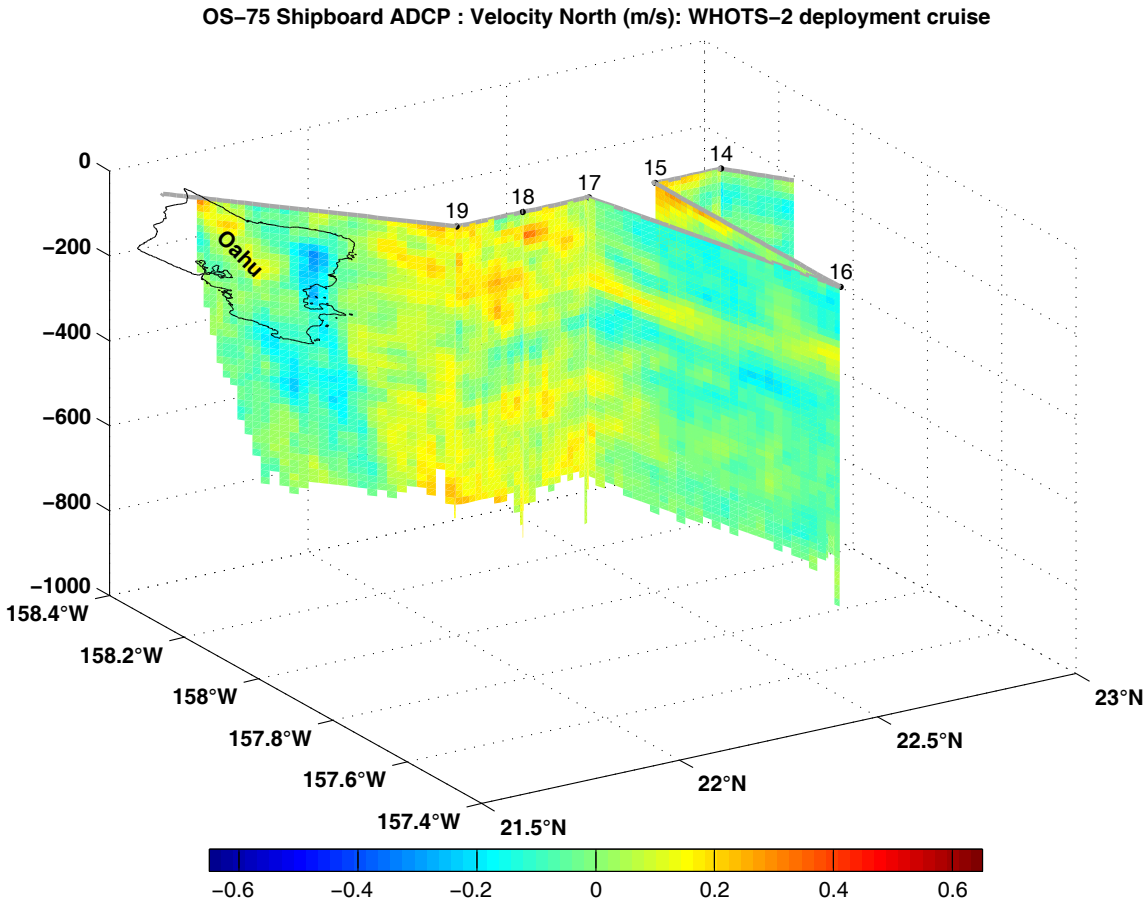

Figure 6-69 North velocity (m s^{-1}) component along the north-south transect occupying stations 14 to 19 (see Figure 6-1) during the WHOTS-2 cruise.

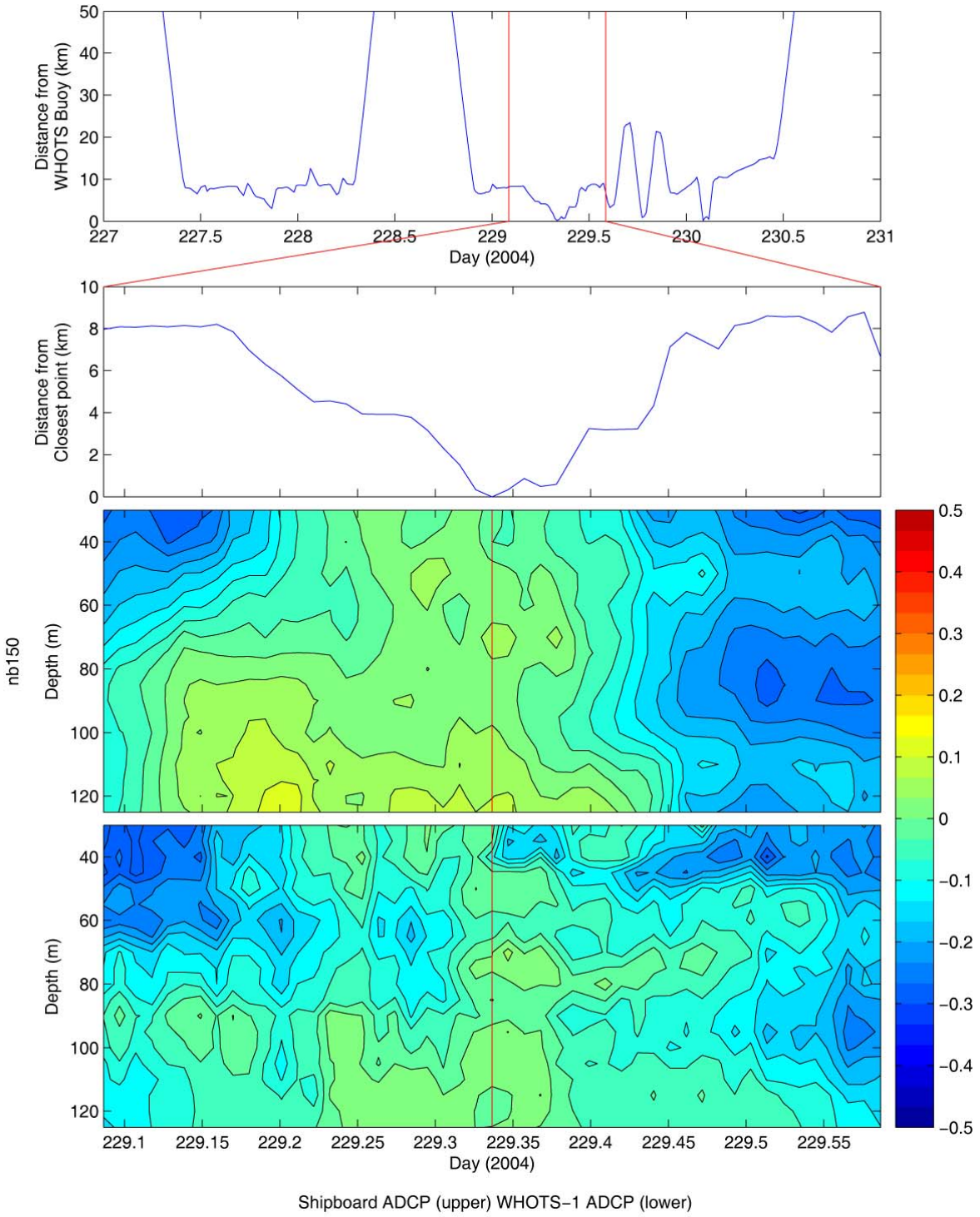

Figure 6-70 Distance of the ship from the WHOTS buoy using ARGOS position data for the duration of the cruise HOT-162 (top panel). [The red lines indicate a six-hour period either side of the closest point of approach.] Distance from the closest point of approach over the 12-hour period (second panel). East velocity component (m s^{-1}) from the narrow band 150 KHz shipboard ADCP (third panel) compared with east velocity component from the moored ADCP from the WHOTS-1 deployment for the same time (lower panel).

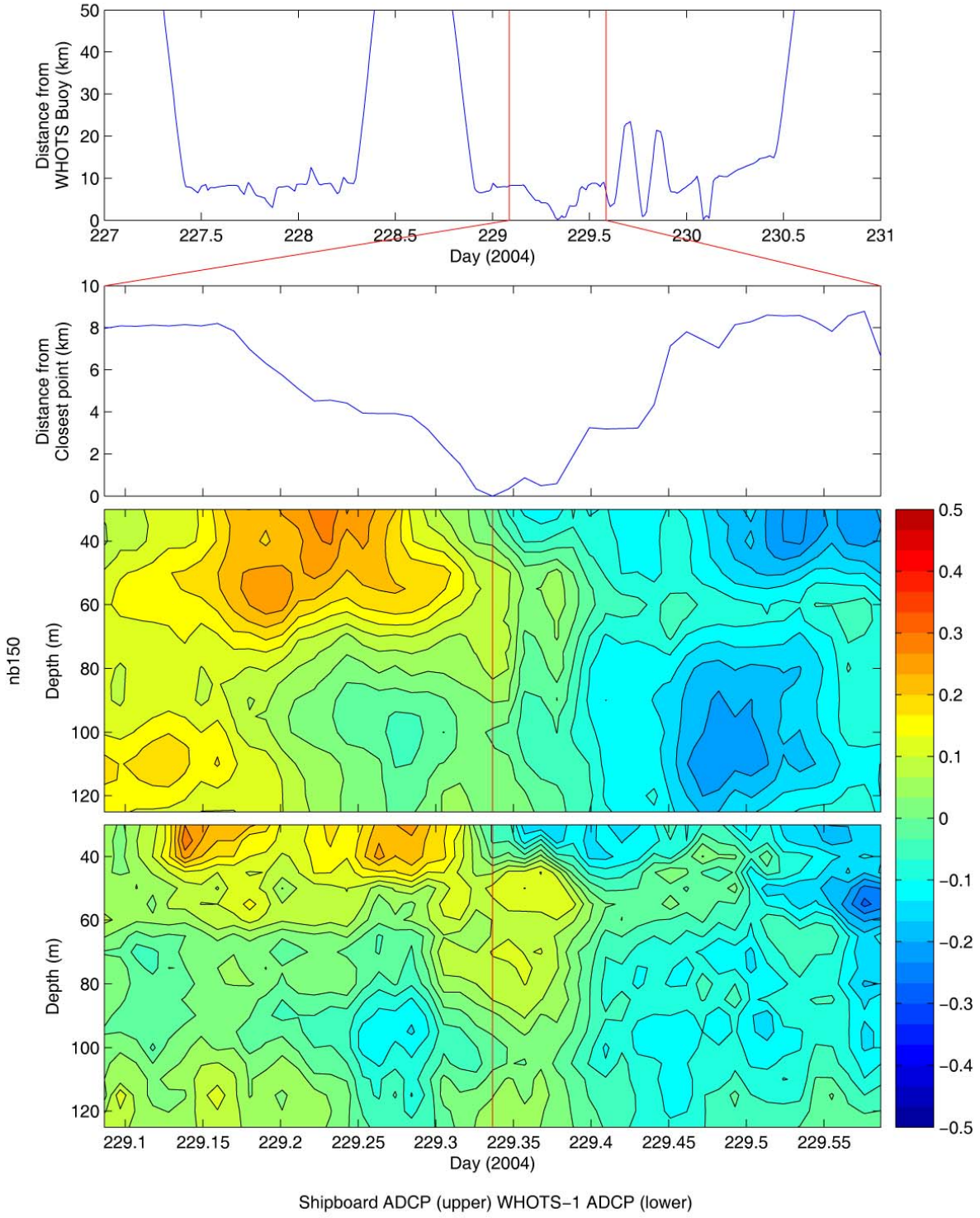

Figure 6-71 Distance of the ship from the WHOTS buoy using ARGOS position data for the duration of the cruise HOT-162 (top panel). [The red lines indicate a six-hour period either side of the closest point of approach.] Distance from the closest point of approach over the 12-hour period (second panel). North velocity component (m s^{-1}) from the narrow band 150 KHz shipboard ADCP (third panel) compared with north velocity component from the moored ADCP from the WHOTS-1 deployment for the same time (lower panel).

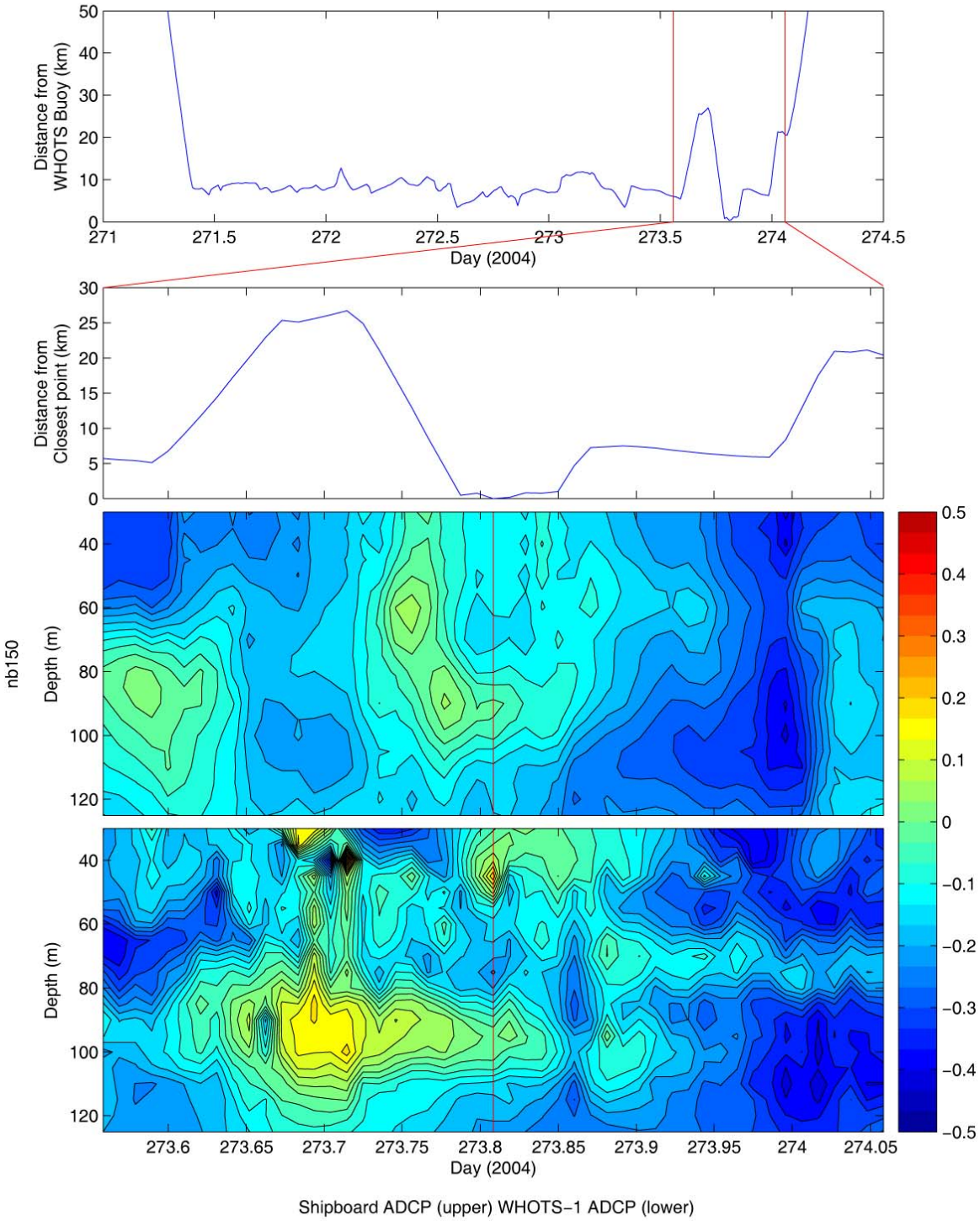

Figure 6-72 Distance of the ship from the WHOTS buoy using ARGOS position data for the duration of the cruise HOT-163 (top panel). [The red lines indicate a six-hour period either side of the closest point of approach.] Distance from the closest point of approach over the 12-hour period (second panel). East velocity component (m s^{-1}) from the narrow band 150 KHz shipboard ADCP (third panel) compared with east velocity component from the moored ADCP from the WHOTS-1 deployment for the same time (lower panel).

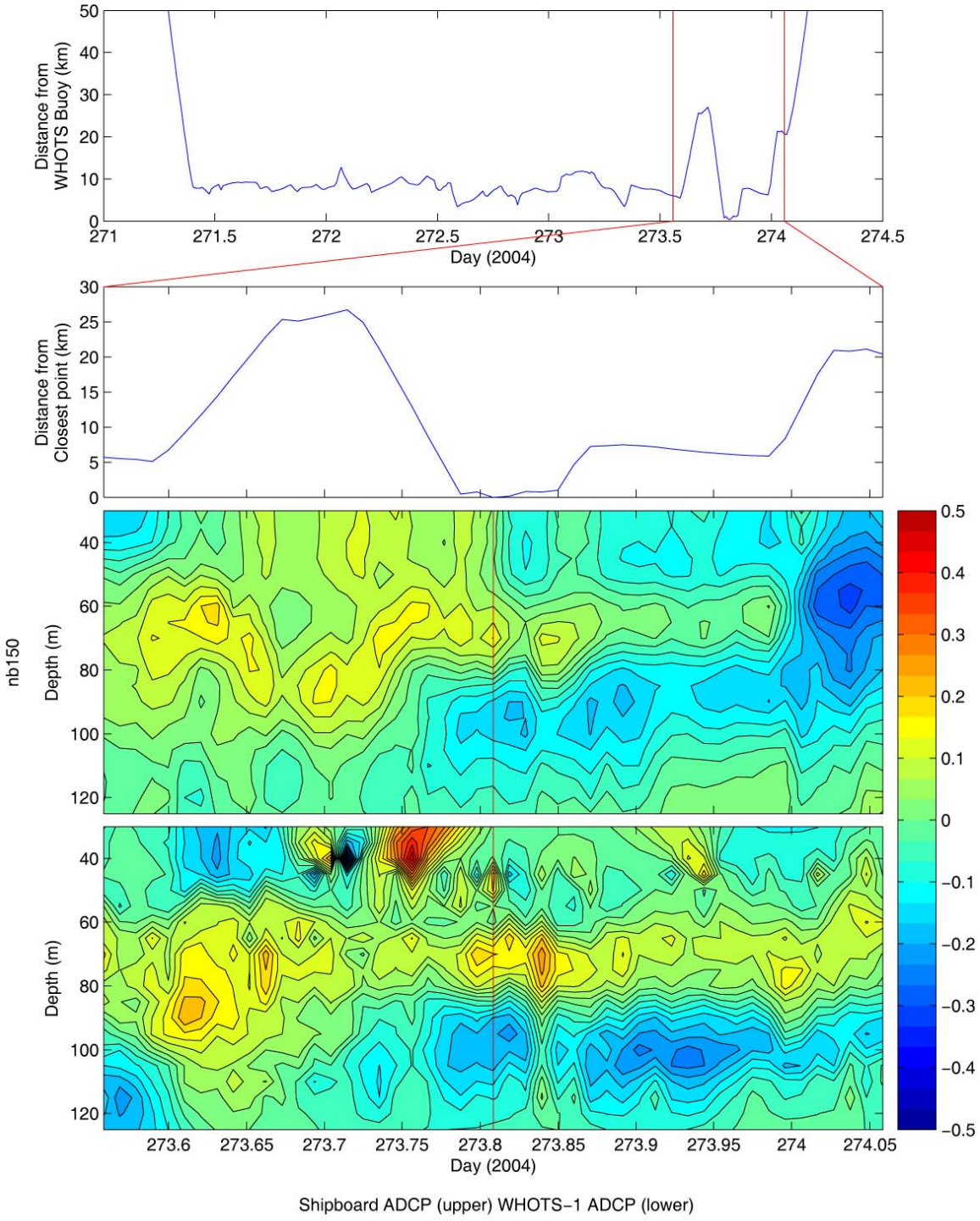

Figure 6-73 Distance of the ship from the WHOTS buoy using ARGOS position data for the duration of the cruise HOT-163 (top panel). [The red lines indicate a six-hour period either side of the closest point of approach.] Distance from the closest point of approach over the 12-hour period (second panel). North velocity component (m s^{-1}) from the narrow band 150 KHz shipboard ADCP (third panel) compared with north velocity component from the moored ADCP from the WHOTS-1 deployment for the same time (lower panel).

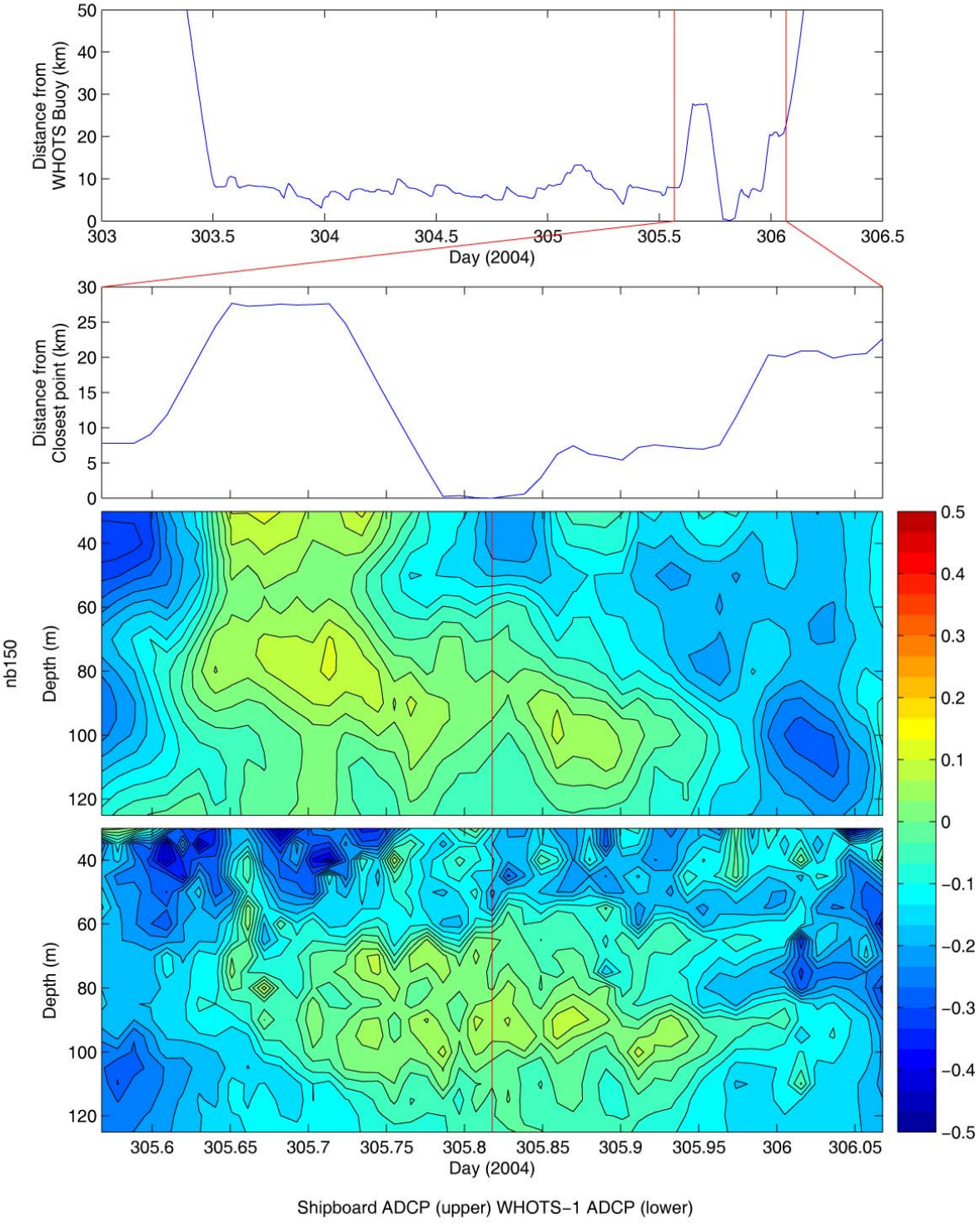

Figure 6-74 Distance of the ship from the WHOTS buoy using ARGOS position data for the duration of the cruise HOT-164 (top panel). [The red lines indicate a six-hour period either side of the closest point of approach.] Distance from the closest point of approach over the 12-hour period (second panel). East velocity component (m s^{-1}) from the narrow band 150 KHz shipboard ADCP (third panel) compared with east velocity component from the moored ADCP from the WHOTS-1 deployment for the same time (lower panel).

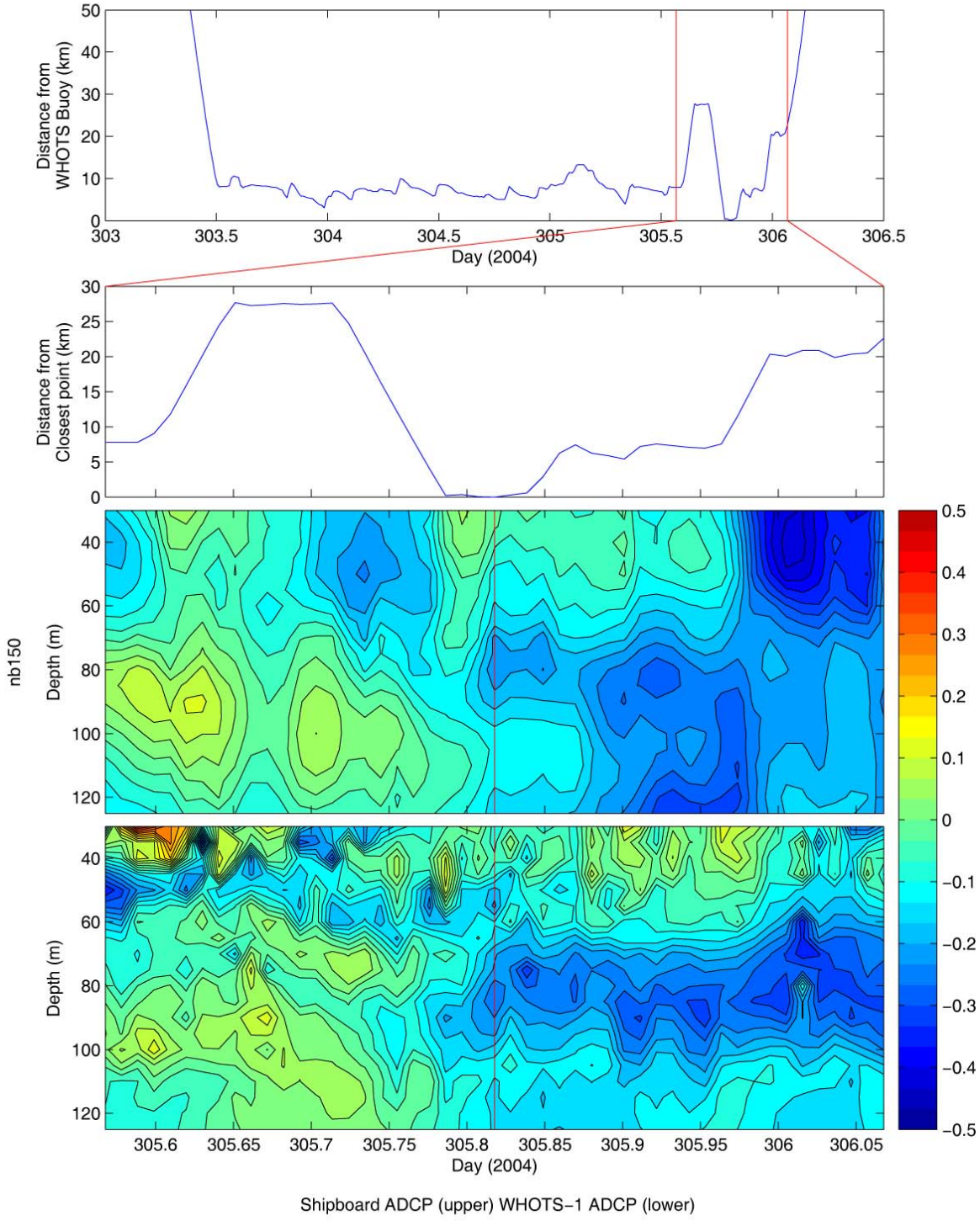

Figure 6-75 Distance of the ship from the WHOTS buoy using ARGOS position data for the duration of the cruise HOT-164 (top panel). [The red lines indicate a six-hour period either side of the closest point of approach.] Distance from the closest point of approach over the 12-hour period (second panel). North velocity component (m s^{-1}) from the narrow band 150 KHz shipboard ADCP (third panel) compared with north velocity component from the moored ADCP from the WHOTS-1 deployment for the same time (lower panel).

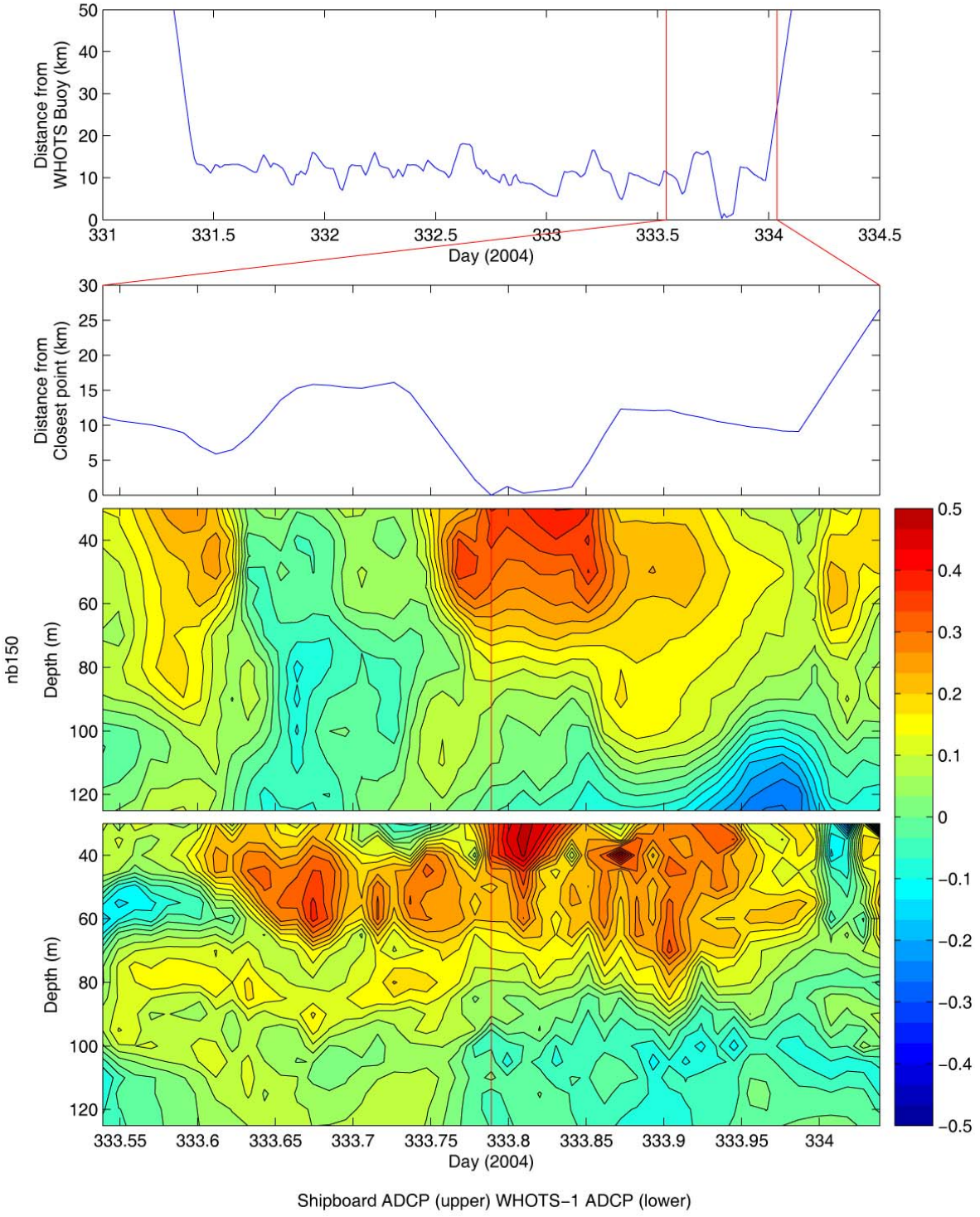

Figure 6-76 Distance of the ship from the WHOTS buoy using ARGOS position data for the duration of the cruise HOT-165 (top panel). [The red lines indicate a six-hour period either side of the closest point of approach.] Distance from the closest point of approach over the 12-hour period (second panel). East velocity component (m s^{-1}) from the narrow band 150 KHz shipboard ADCP (third panel) compared with east velocity component from the moored ADCP from the WHOTS-1 deployment for the same time (lower panel).

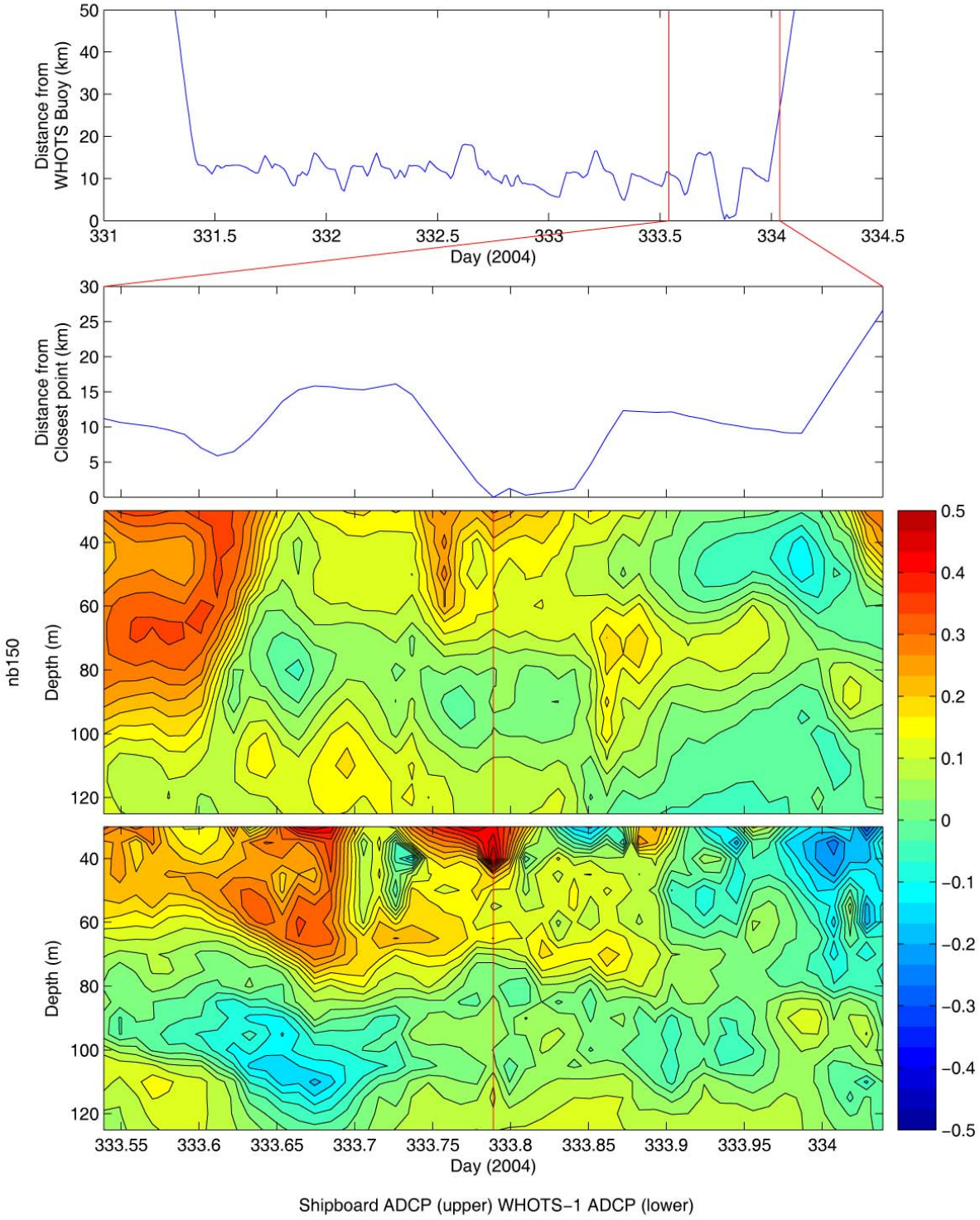

Figure 6-77 Distance of the ship from the WHOTS buoy using ARGOS position data for the duration of the cruise HOT-165 (top panel). [The red lines indicate a six-hour period either side of the closest point of approach.] Distance from the closest point of approach over the 12-hour period (second panel). North velocity component (m s^{-1}) from the narrow band 150 KHz shipboard ADCP (third panel) compared with north velocity component from the moored ADCP from the WHOTS-1 deployment for the same time (lower panel).

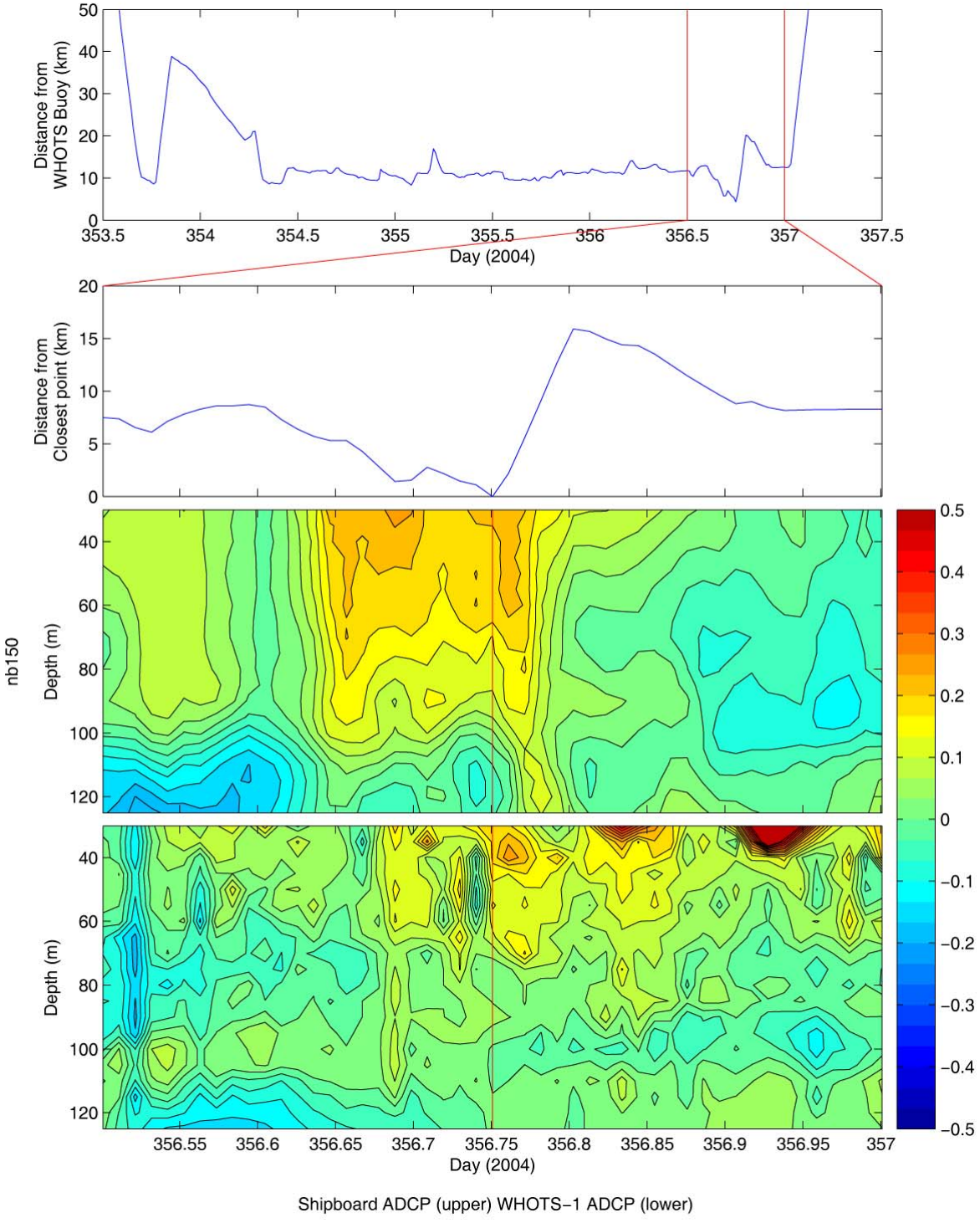

Figure 6-78 Distance of the ship from the WHOTS buoy using ARGOS position data for the duration of the cruise HOT-166 (top panel). [The red lines indicate a six-hour period either side of the closest point of approach.] Distance from the closest point of approach over the 12-hour period (second panel). East velocity component (m s^{-1}) from the narrow band 150 KHz shipboard ADCP (third panel) compared with east velocity component from the moored ADCP from the WHOTS-1 deployment for the same time (lower panel).

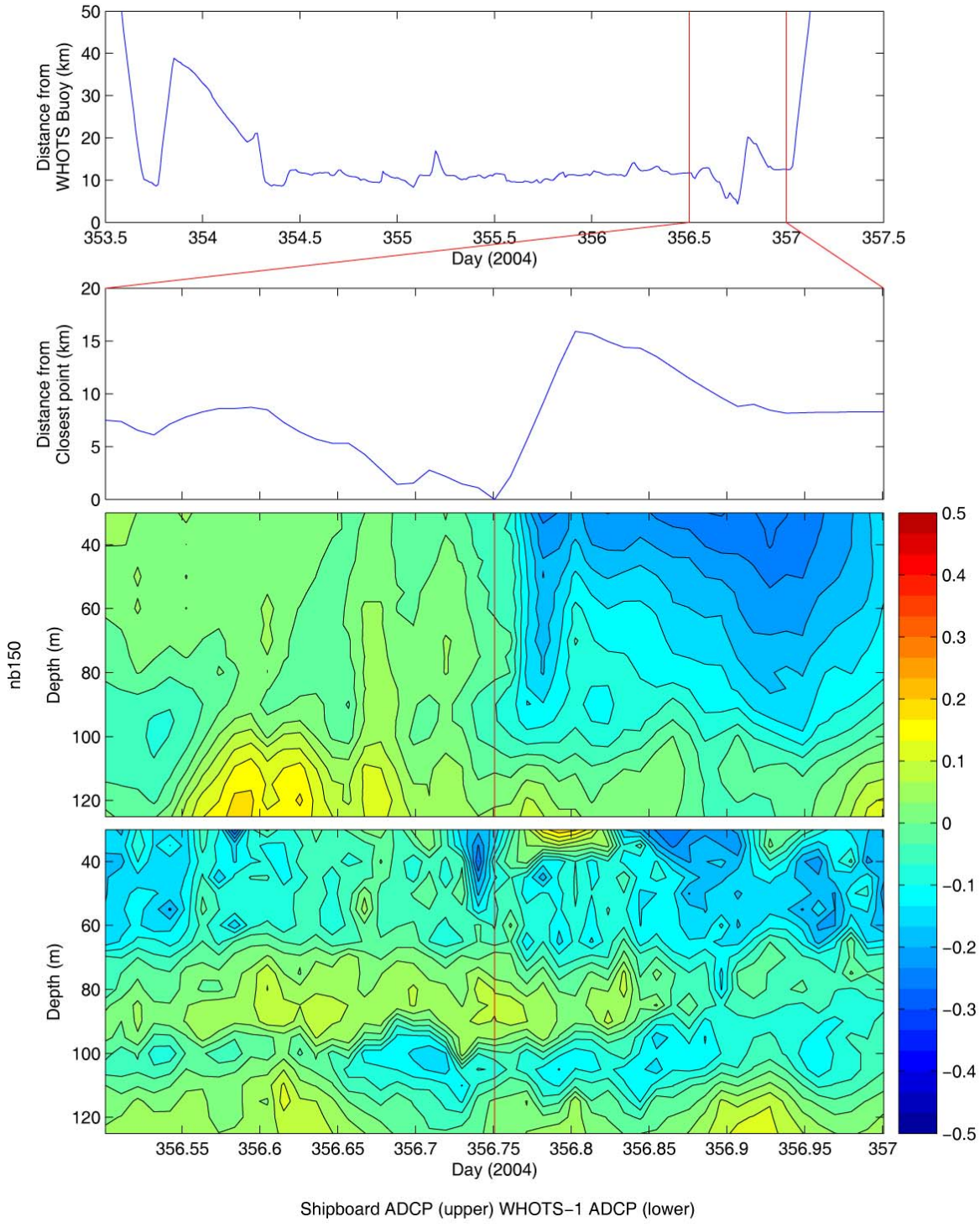

Figure 6-79 Distance of the ship from the WHOTS buoy using ARGOS position data for the duration of the cruise HOT-166 (top panel). [The red lines indicate a six-hour period either side of the closest point of approach.] Distance from the closest point of approach over the 12-hour period (second panel). North velocity component (m s^{-1}) from the narrow band 150 KHz shipboard ADCP (third panel) compared with north velocity component from the moored ADCP from the WHOTS-1 deployment for the same time (lower panel).

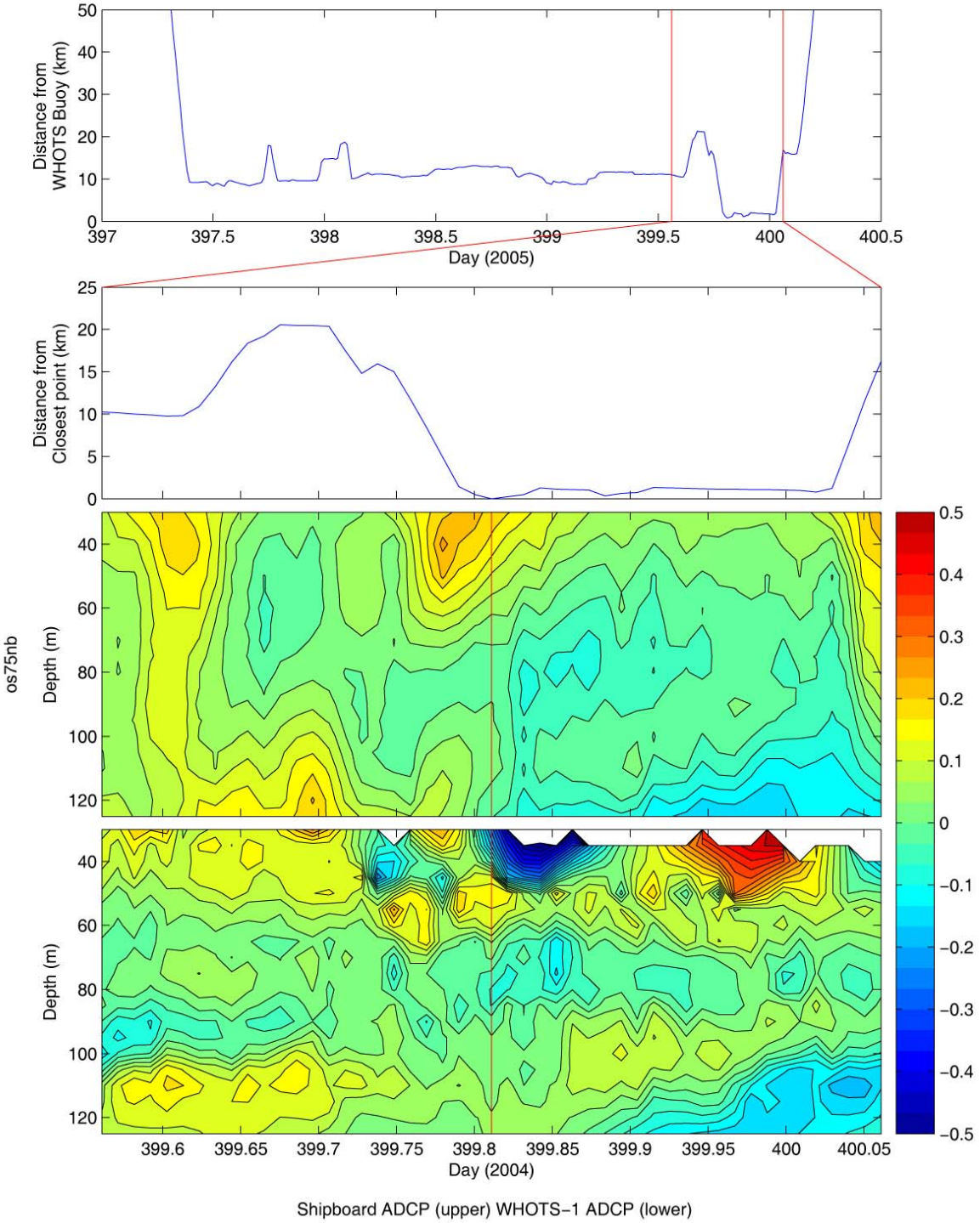

Figure 6-80 Distance of the ship from the WHOTS buoy using ARGOS position data for the duration of the cruise HOT-167 (top panel). [The red lines indicate a six-hour period either side of the closest point of approach.] Distance from the closest point of approach over the 12-hour period (second panel). East velocity component (m s^{-1}) from the Ocean surveyor narrow band 75 KHz shipboard ADCP (third panel) compared with east velocity component from the moored ADCP from the WHOTS-1 deployment for the same time (lower panel).

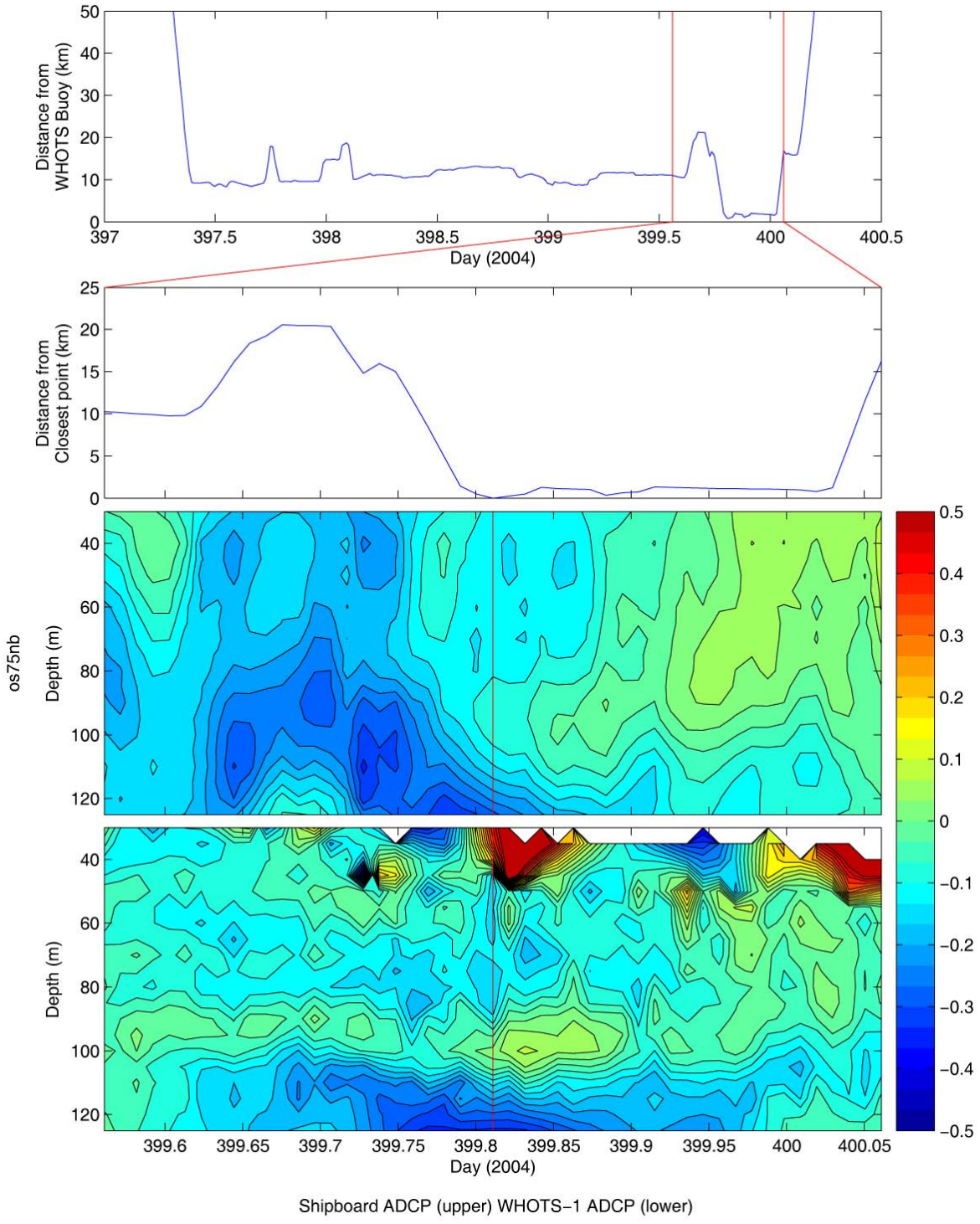

Figure 6-81 Distance of the ship from the WHOTS buoy using ARGOS position data for the duration of the cruise HOT-167 (top panel). [The red lines indicate a six-hour period either side of the closest point of approach.] Distance from the closest point of approach over the 12-hour period (second panel). North velocity component (m s^{-1}) from the Ocean Surveyor narrow band 75 KHz shipboard ADCP (third panel) compared with north velocity component from the moored ADCP from the WHOTS-1 deployment for the same time (lower panel).

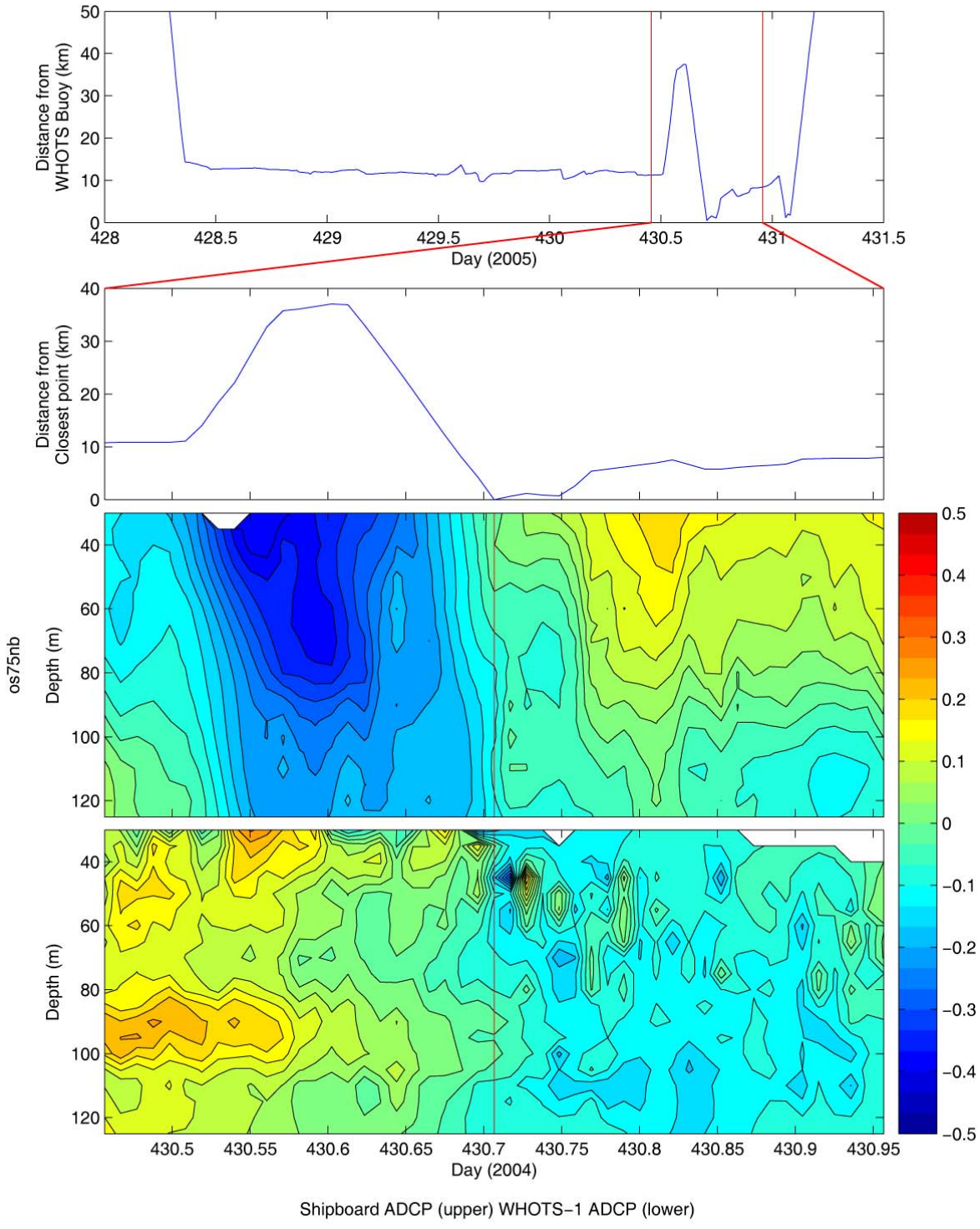

Figure 6-82 Distance of the ship from the WHOTS buoy using ARGOS position data for the duration of the cruise HOT-168 (top panel). [The red lines indicate a six-hour period either side of the closest point of approach.] Distance from the closest point of approach over the 12-hour period (second panel). East velocity component (m s^{-1}) from the Ocean Surveyor narrow band 75 KHz shipboard ADCP (third panel) compared with east velocity component from the moored ADCP from the WHOTS-1 deployment for the same time (lower panel).

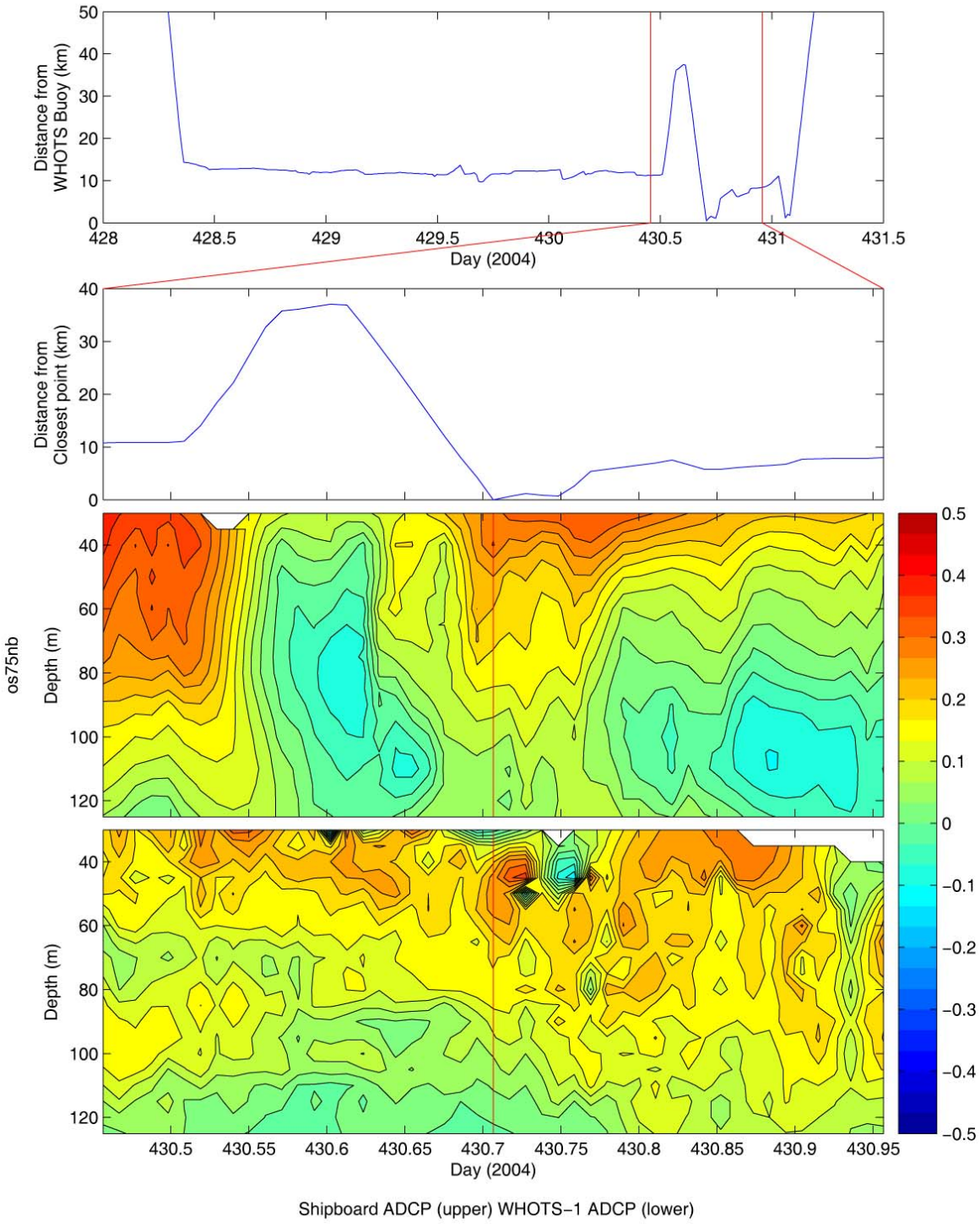

Figure 6-83 Distance of the ship from the WHOTS buoy using ARGOS position data for the duration of the cruise HOT-168 (top panel). [The red lines indicate a six-hour period either side of the closest point of approach.] Distance from the closest point of approach over the 12-hour period (second panel). North velocity component (m s^{-1}) from the Ocean Surveyor narrow band 75 KHz shipboard ADCP (third panel) compared with north velocity component from the moored ADCP from the WHOTS-1 deployment for the same time (lower panel).

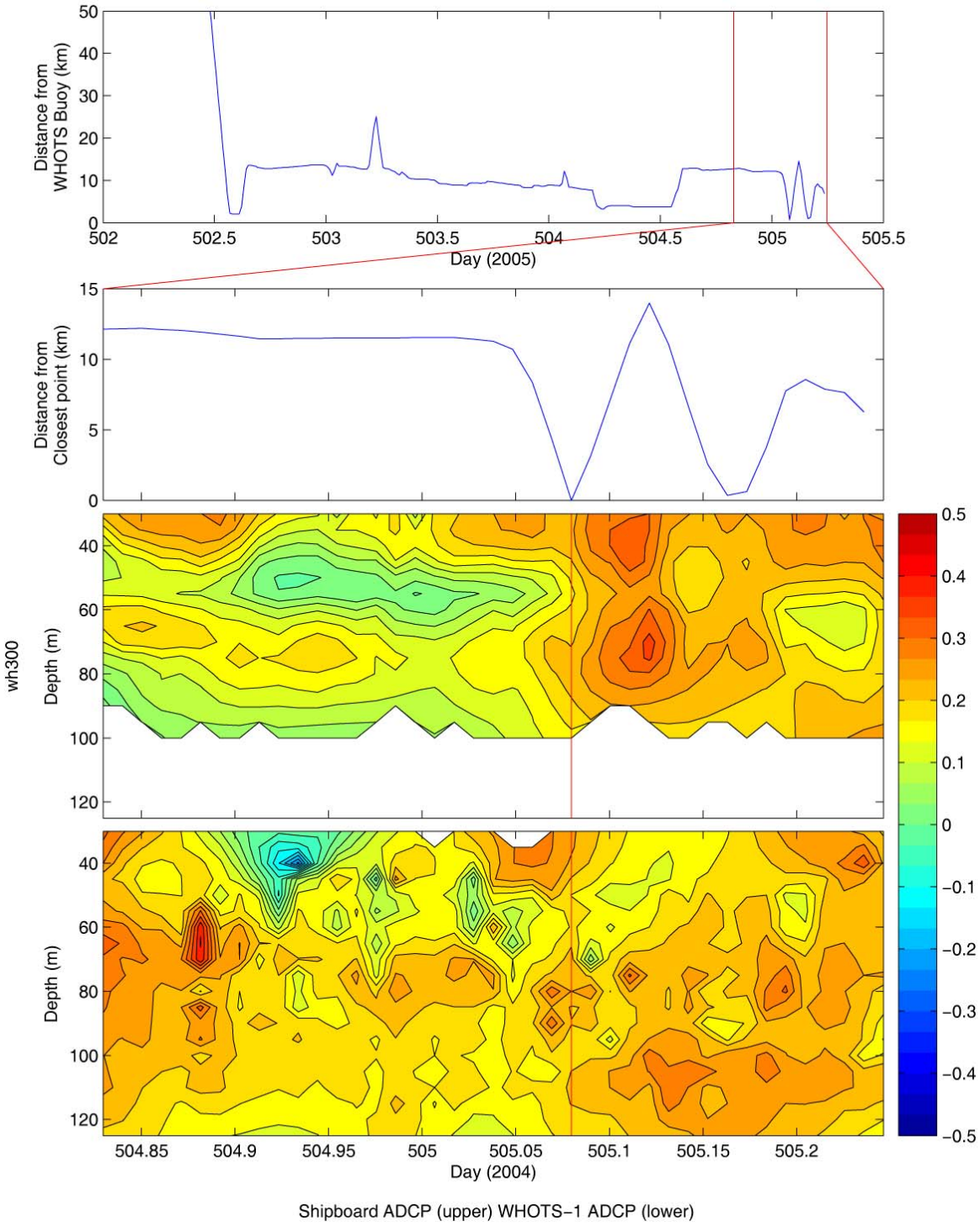

Figure 6-84 Distance of the ship from the WHOTS buoy using ARGOS position data for the duration of the cruise HOT-169 (top panel). [The red lines indicate a six-hour period either side of the closest point of approach.] Distance from the closest point of approach over the 12-hour period (second panel). East velocity component (m s^{-1}) from the Workhorse 300 KHz shipboard ADCP (third panel) compared with east velocity component from the moored ADCP from the WHOTS-1 deployment for the same time (lower panel).

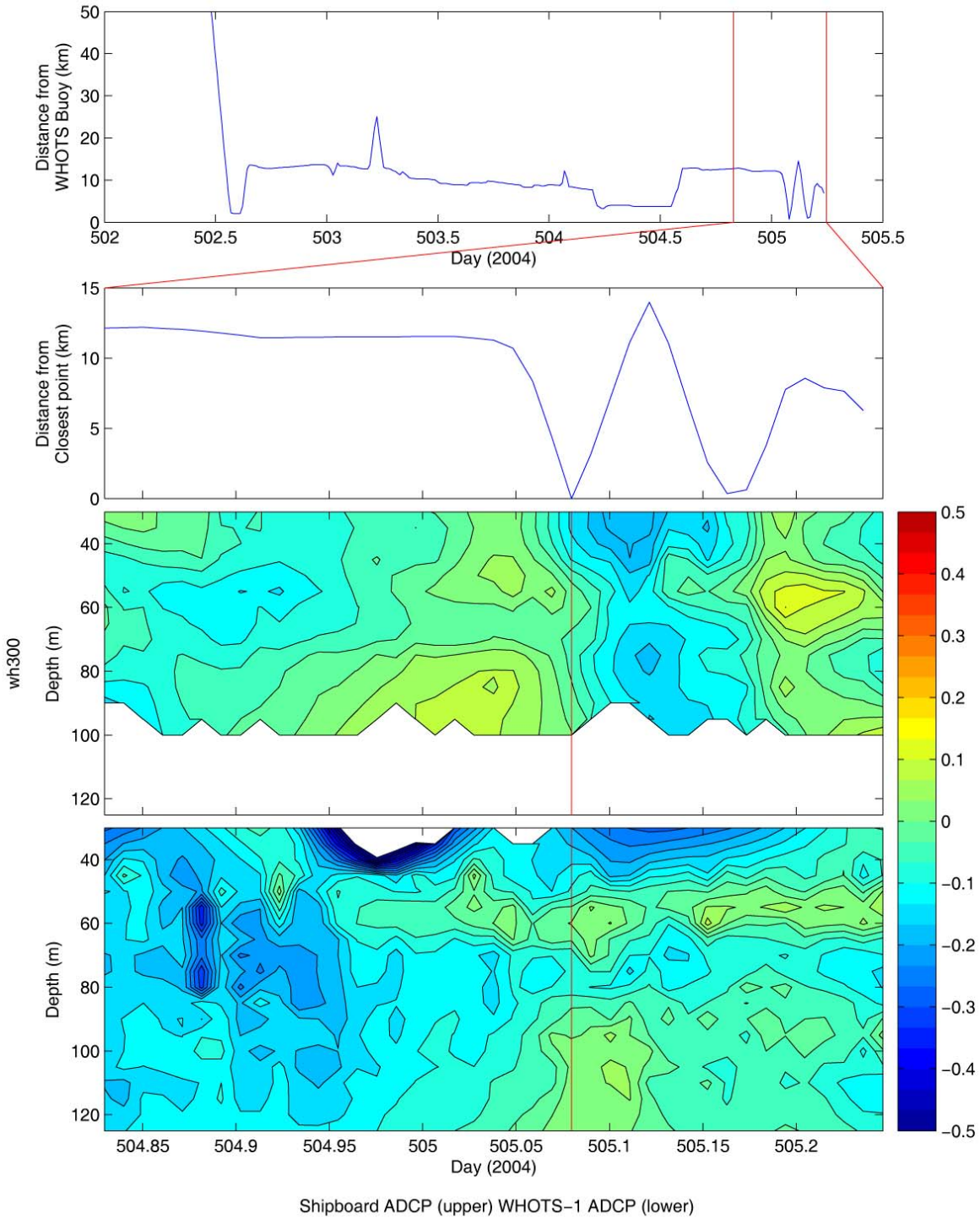

Figure 6-85 Distance of the ship from the WHOTS buoy using ARGOS position data for the duration of the cruise HOT-169 (top panel). [The red lines indicate a six-hour period either side of the closest point of approach.] Distance from the closest point of approach over the 12-hour period (second panel). North velocity component (m s^{-1}) from the Workhorse 300 KHz shipboard ADCP (third panel) compared with north velocity component from the moored ADCP from the WHOTS-1 deployment for the same time (lower panel).

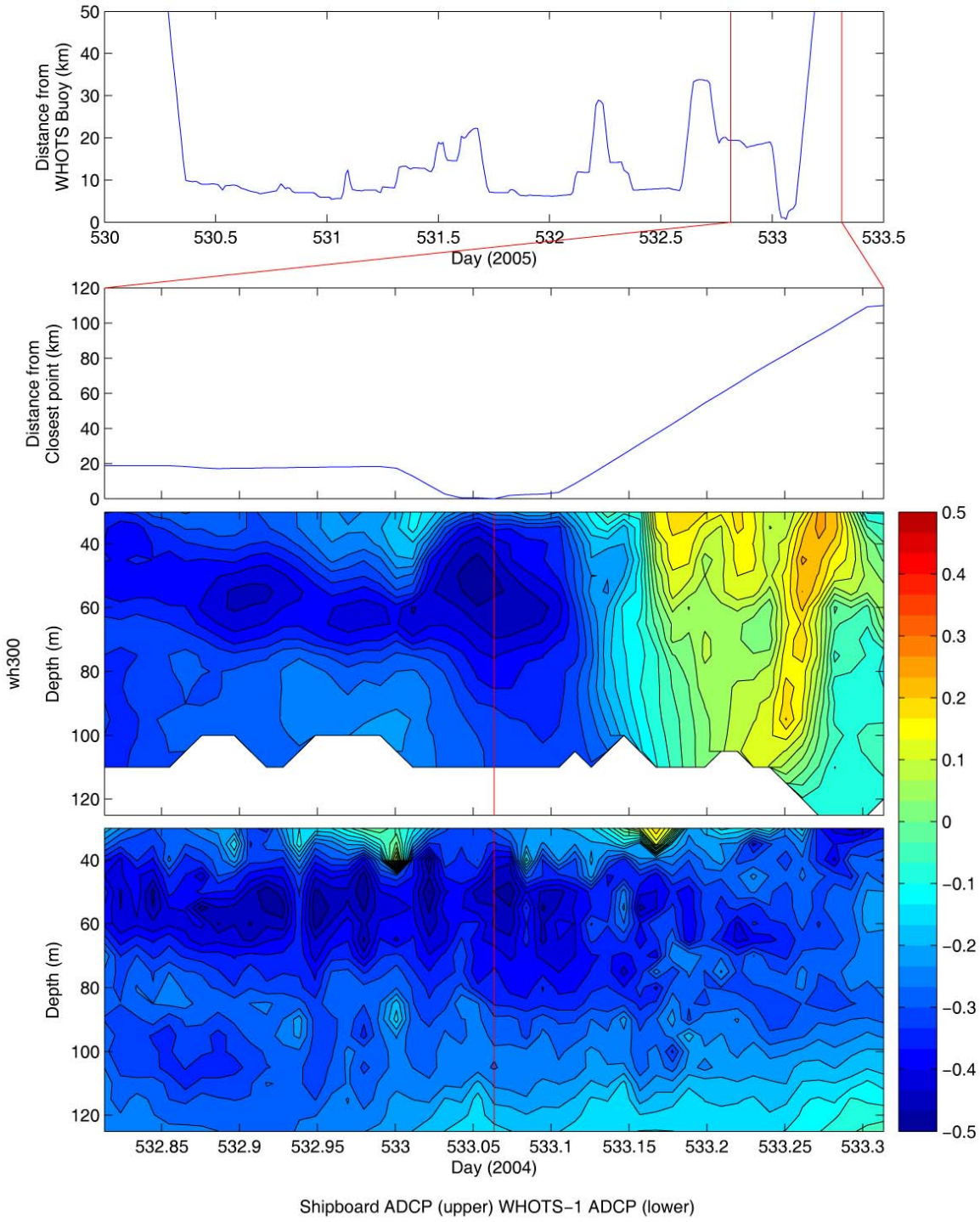

Figure 6-86 Distance of the ship from the WHOTS buoy using ARGOS position data for the duration of the cruise HOT-170 (top panel). [The red lines indicate a six-hour period either side of the closest point of approach.] Distance from the closest point of approach over the 12-hour period (second panel). East velocity component (m s^{-1}) from the Workhorse 300 KHz shipboard ADCP (third panel) compared with east velocity component from the moored ADCP from the WHOTS-1 deployment for the same time (lower panel).

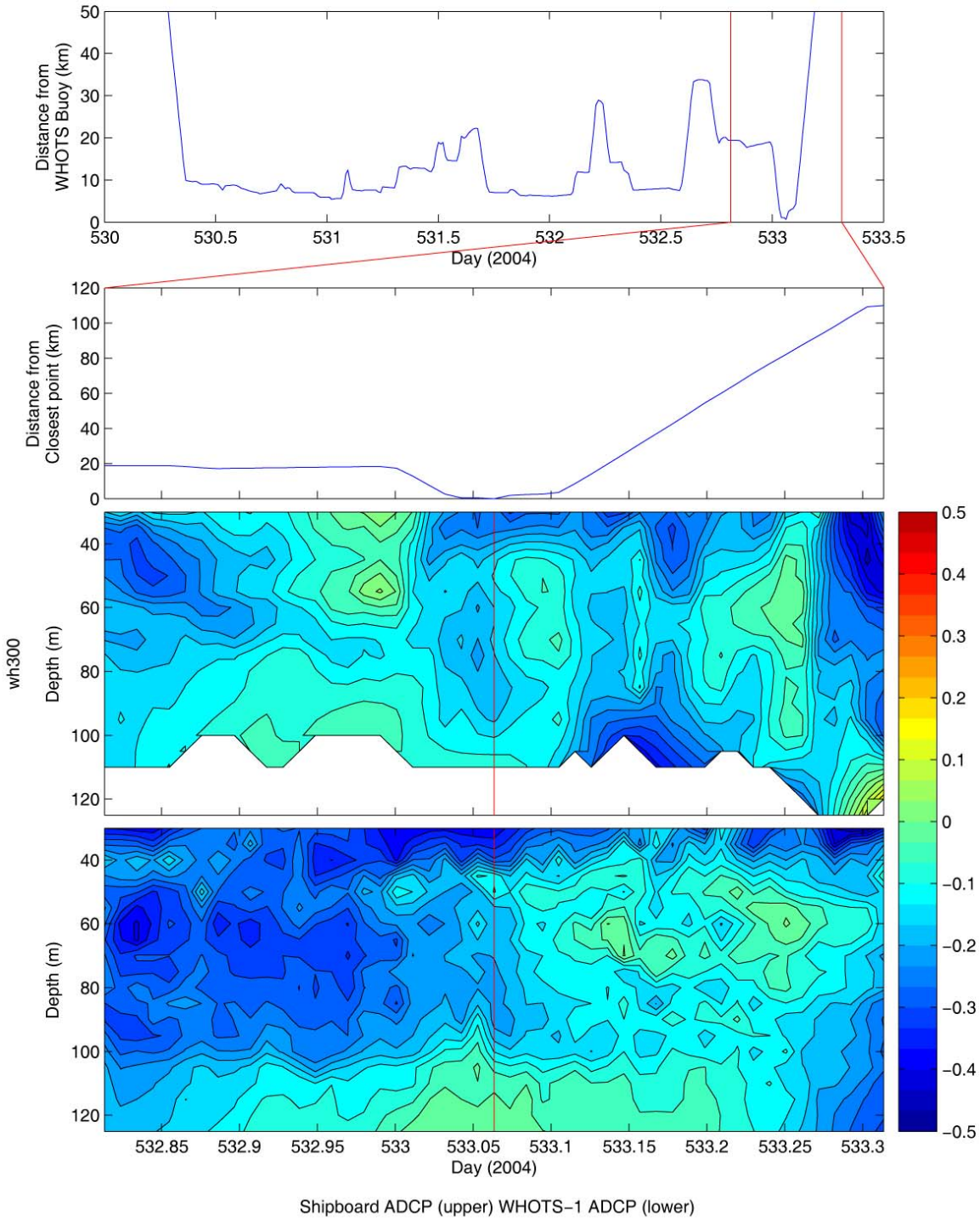

Figure 6-87 Distance of the ship from the WHOTS buoy using ARGOS position data for the duration of the cruise HOT-170 (top panel). [The red lines indicate a six-hour period either side of the closest point of approach.] Distance from the closest point of approach over the 12-hour period (second panel). North velocity component (m s^{-1}) from the Workhorse 300 KHz shipboard ADCP (third panel) compared with north velocity component from the moored ADCP from the WHOTS-1 deployment for the same time (lower panel).

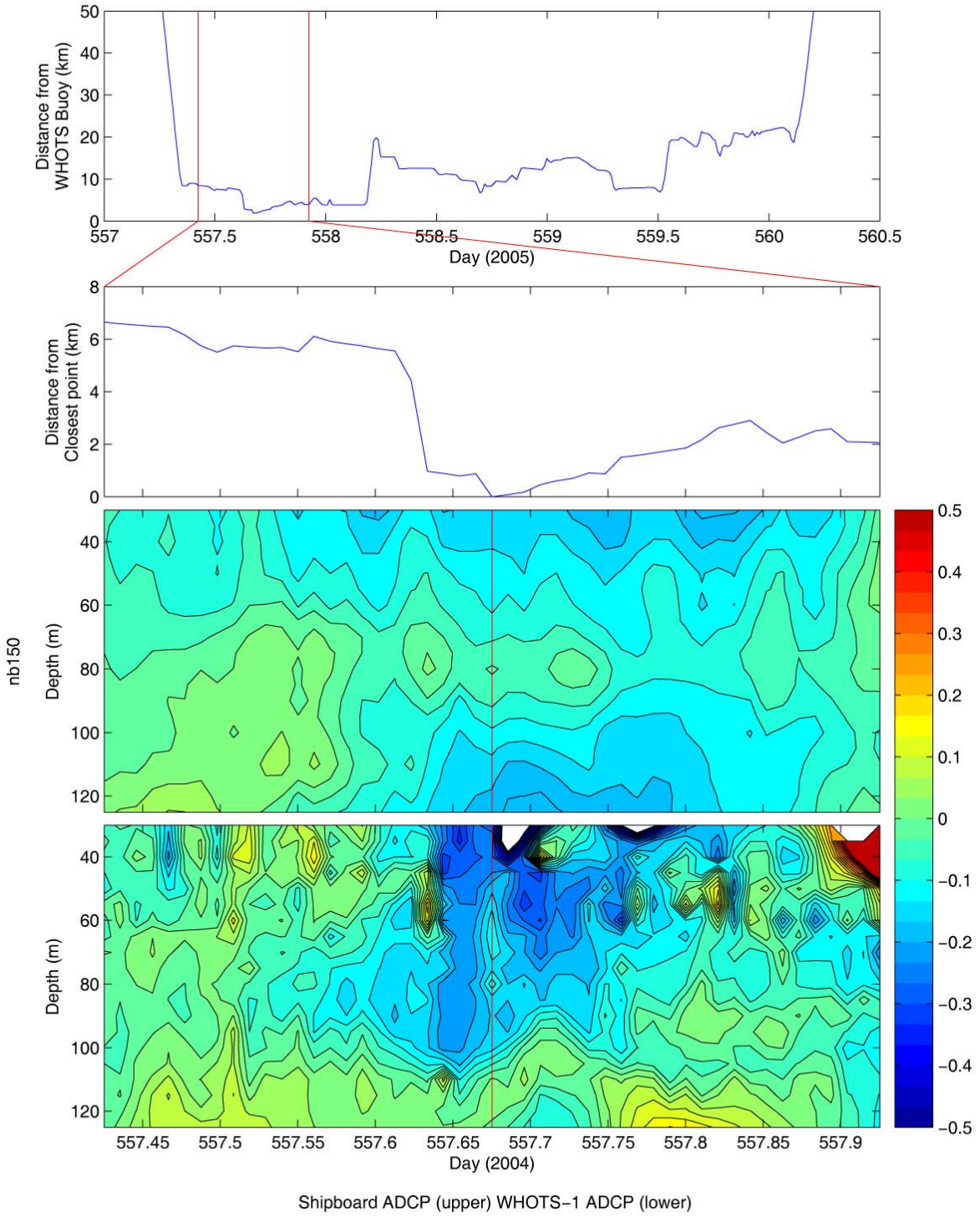

Figure 6-88 Distance of the ship from the WHOTS buoy using ARGOS position data for the duration of the cruise HOT-171 (top panel). [The red lines indicate a six-hour period either side of the closest point of approach.] Distance from the closest point of approach over the 12-hour period (second panel). East velocity component (m s^{-1}) from the narrow band 150 KHz shipboard ADCP (third panel) compared with east velocity component from the moored ADCP from the WHOTS-1 deployment for the same time (lower panel).

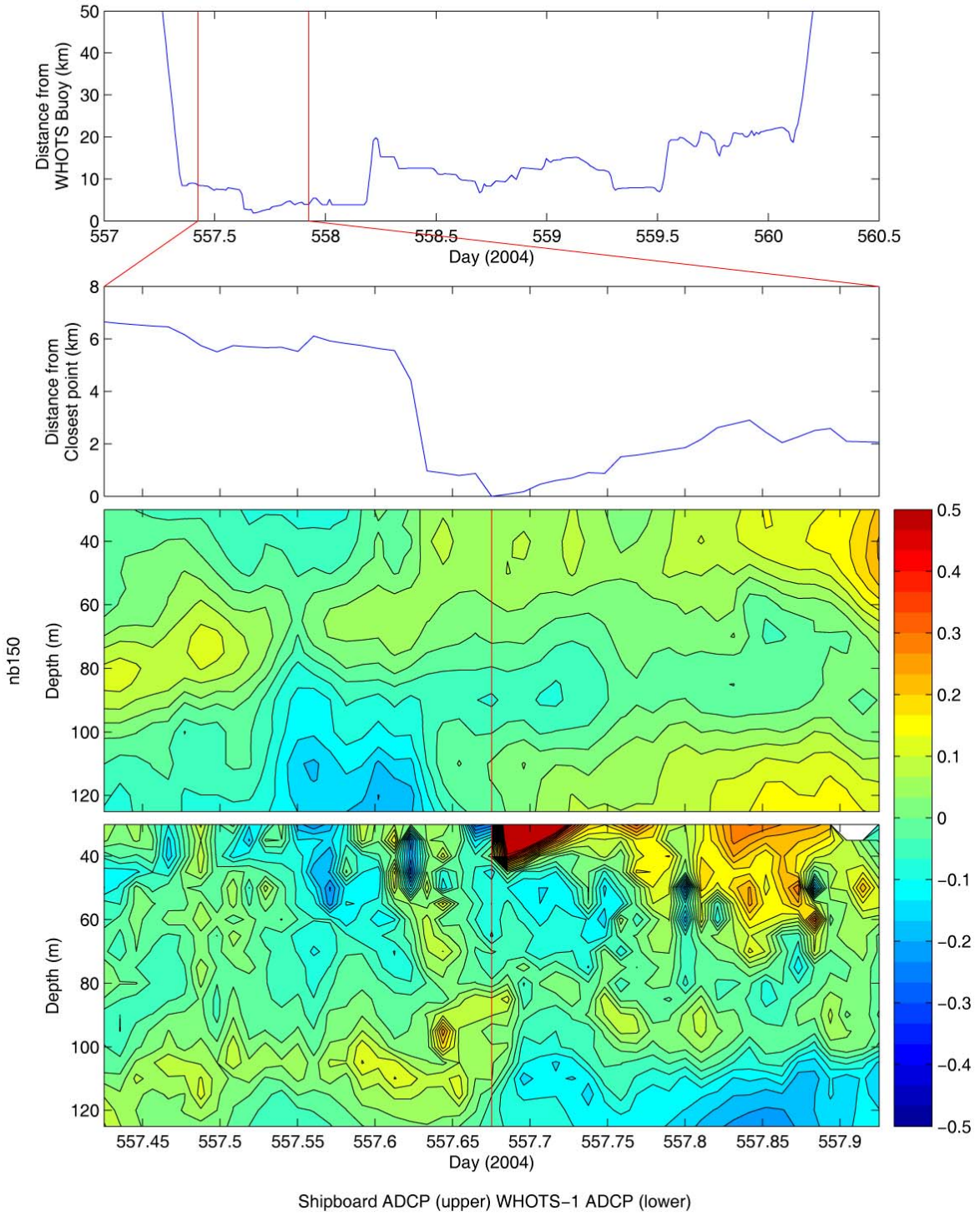

Figure 6-89 Distance of the ship from the WHOTS buoy using ARGOS position data for the duration of the cruise HOT-171 (top panel). [The red lines indicate a six-hour period either side of the closest point of approach.] Distance from the closest point of approach over the 12-hour period (second panel). North velocity component (m s^{-1}) from the narrow band 150 KHz shipboard ADCP (third panel) compared with north velocity component from the moored ADCP from the WHOTS-1 deployment for the same time (lower panel).

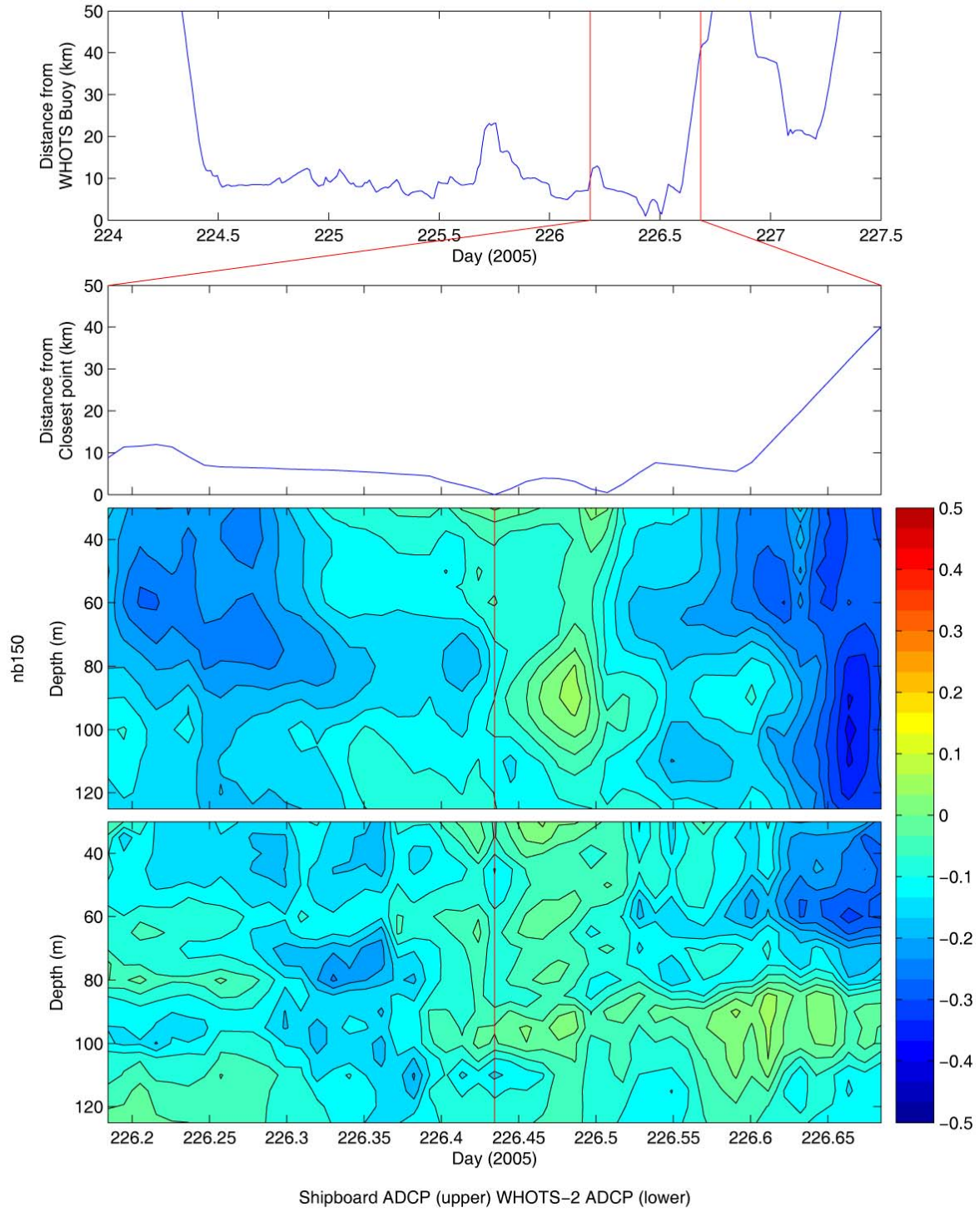

Figure 6-90 Distance of the ship from the WHOTS buoy using ARGOS position data for the duration of the cruise HOT-172 (top panel). [The red lines indicate a six-hour period either side of the closest point of approach.] Distance from the closest point of approach over the 12-hour period (second panel). East velocity component (m s^{-1}) from the Workhorse 300 KHz shipboard ADCP (third panel) compared with east velocity component from the moored ADCP from the WHOTS-2 deployment for the same time (lower panel).

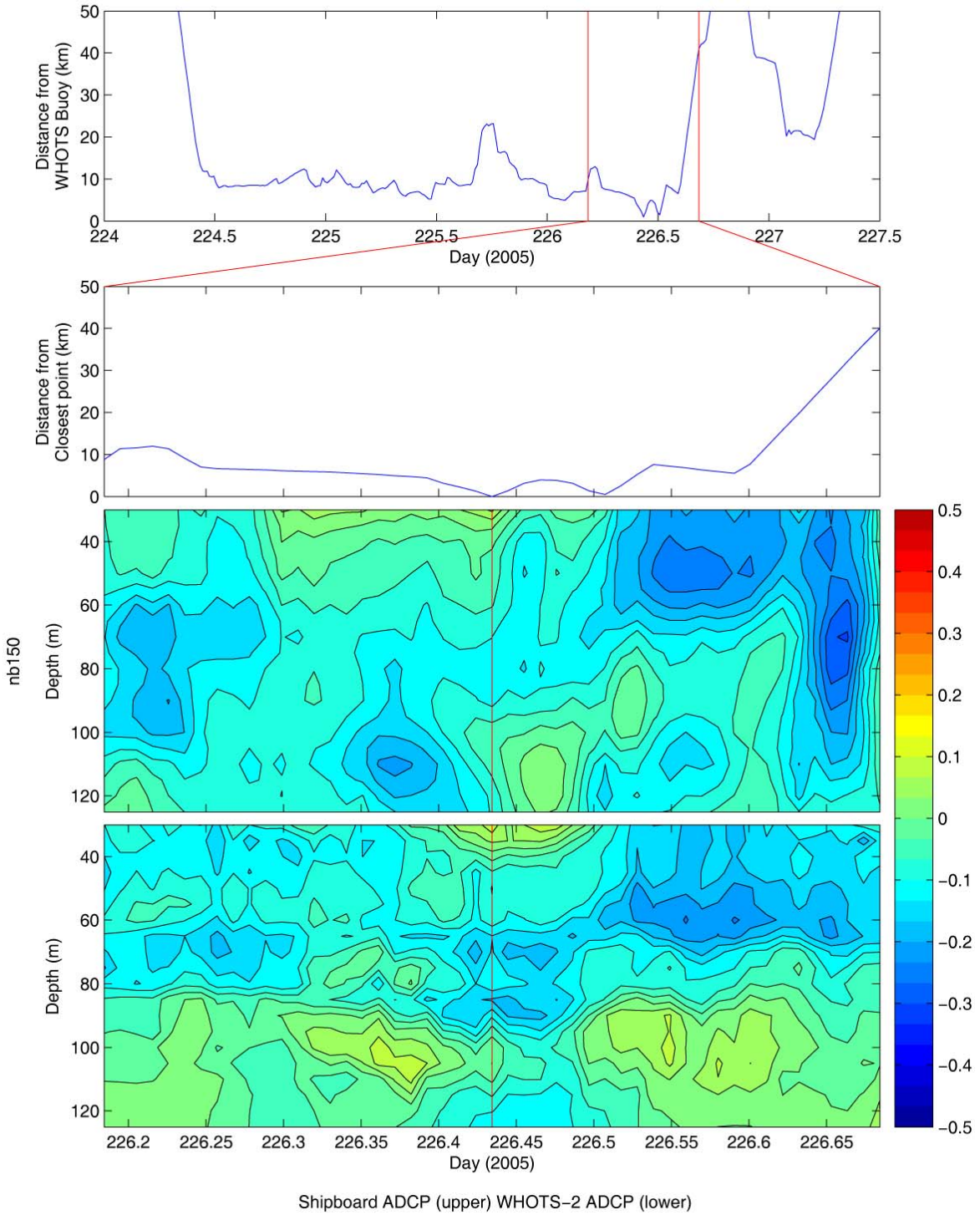

Figure 6-91 Distance of the ship from the WHOTS buoy using ARGOS position data for the duration of the cruise HOT-172 (top panel). [The red lines indicate a six-hour period either side of the closest point of approach.] Distance from the closest point of approach over the 12-hour period (second panel). North velocity component (m s^{-1}) from the Workhorse 300 KHz shipboard ADCP (third panel) compared with north velocity component from the moored ADCP from the WHOTS-2 deployment for the same time (lower panel).

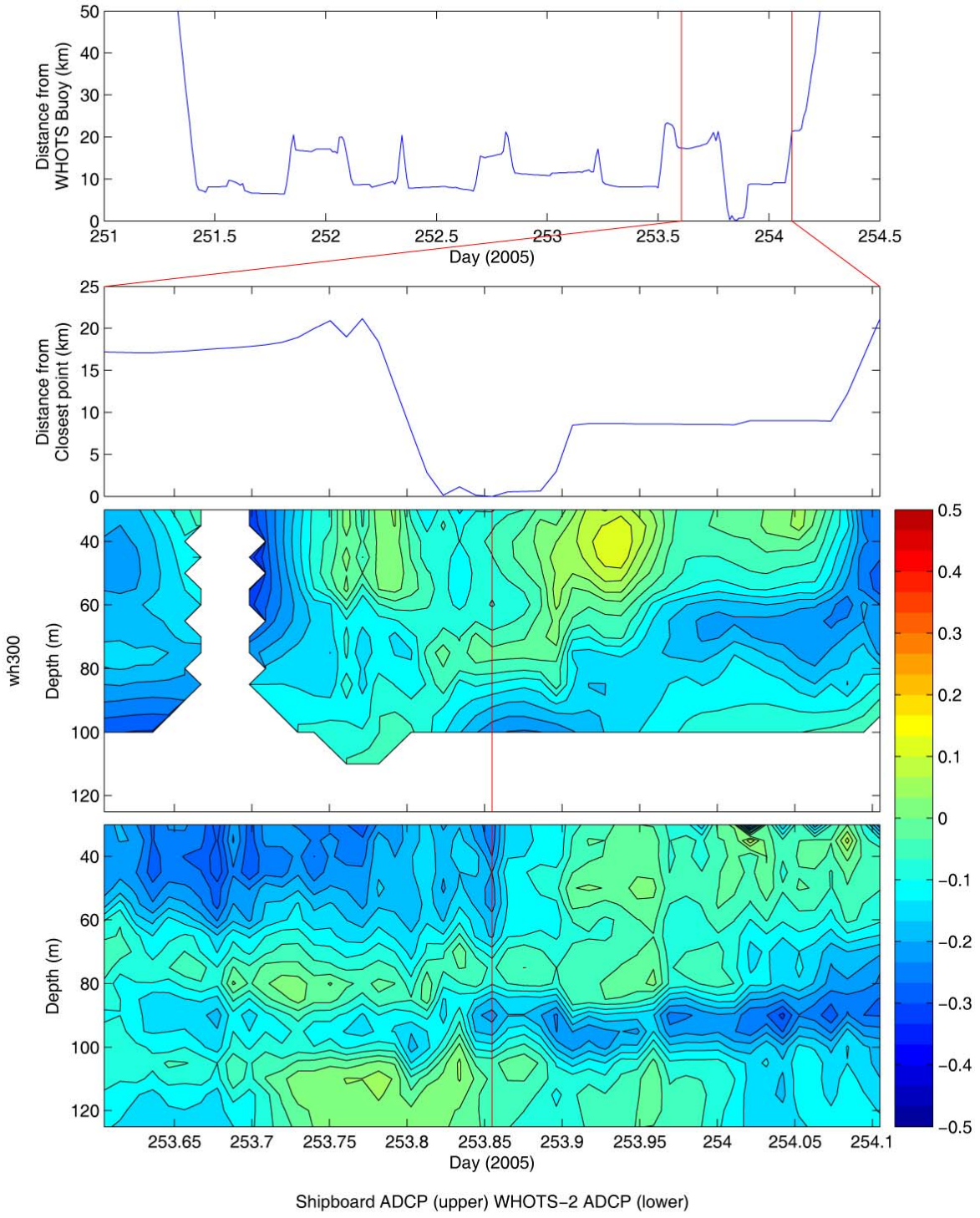

Figure 6-92 Distance of the ship from the WHOTS buoy using ARGOS position data for the duration of the cruise HOT-173 (top panel). [The red lines indicate a six-hour period either side of the closest point of approach.] Distance from the closest point of approach over the 12-hour period (second panel). East velocity component (m s^{-1}) from the Workhorse 300 KHz shipboard ADCP (third panel) compared with east velocity component from the moored ADCP from the WHOTS-2 deployment for the same time (lower panel).

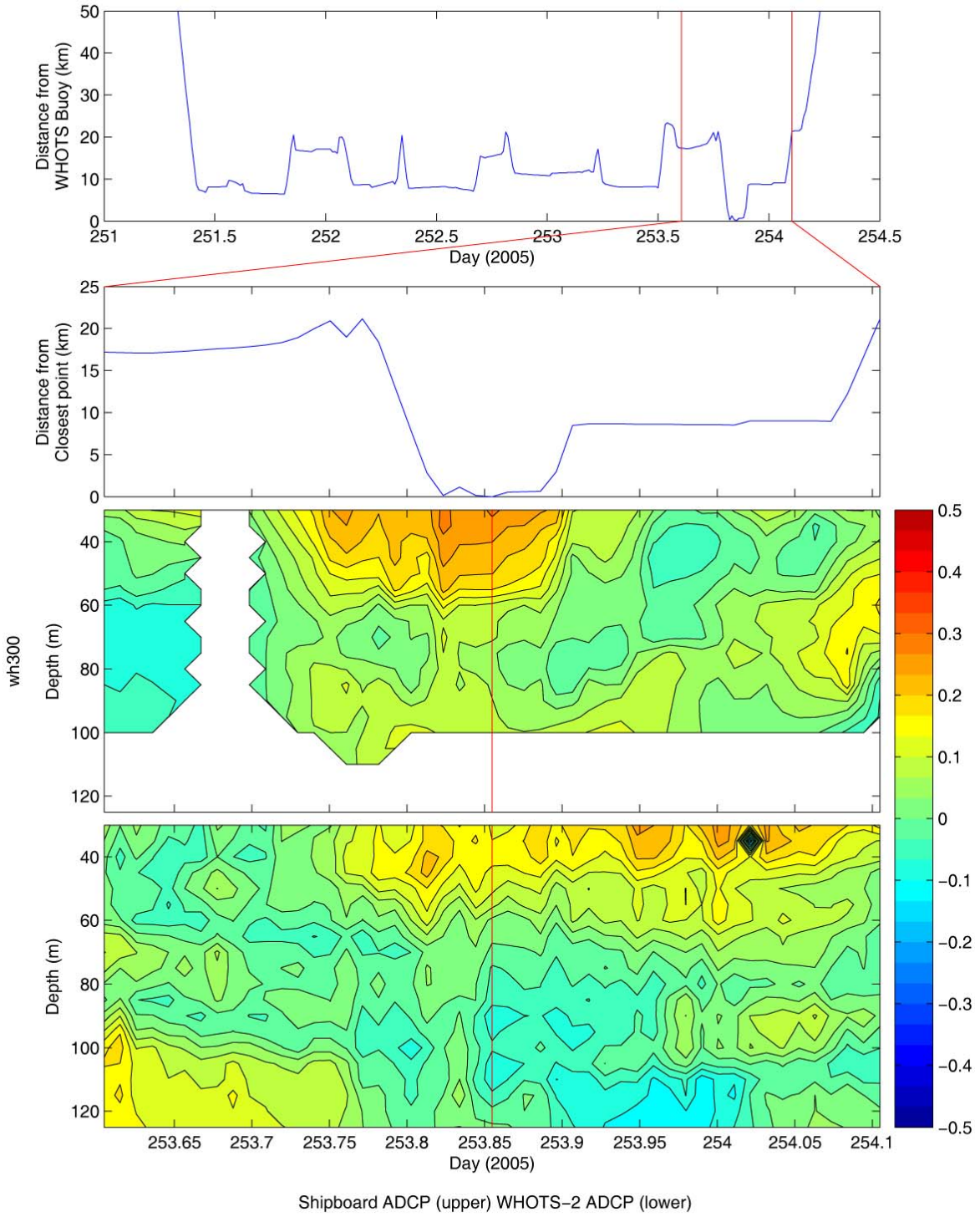

Figure 6-93 Distance of the ship from the WHOTS buoy using ARGOS position data for the duration of the cruise HOT-173 (top panel). [The red lines indicate a six-hour period either side of the closest point of approach.] Distance from the closest point of approach over the 12-hour period (second panel). North velocity component (m s^{-1}) from the Workhorse 300 KHz shipboard ADCP (third panel) compared with north velocity component from the moored ADCP from the WHOTS-2 deployment for the same time (lower panel).

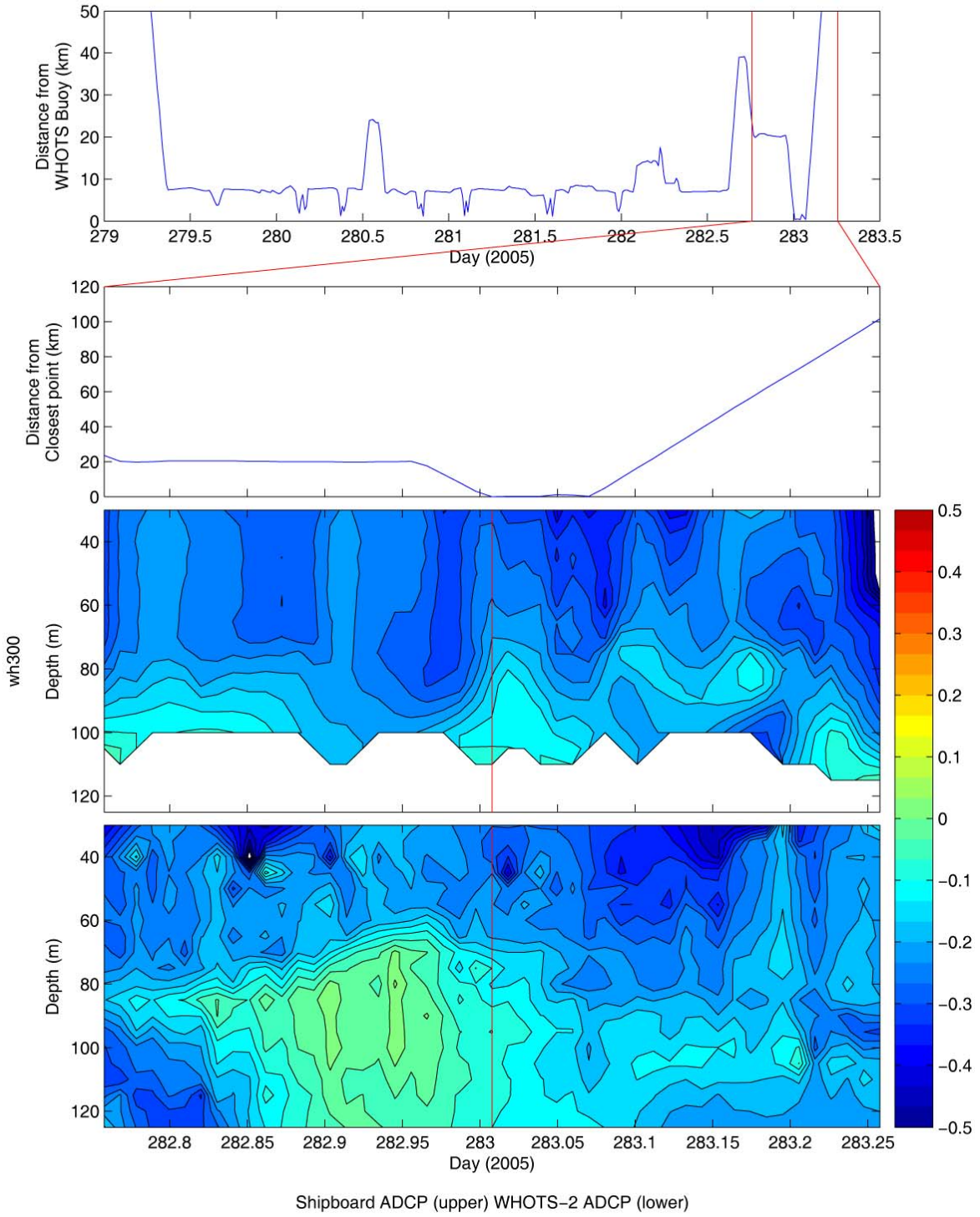

Figure 6-94 Distance of the ship from the WHOTS buoy using ARGOS position data for the duration of the cruise HOT-174 (top panel). [The red lines indicate a six-hour period either side of the closest point of approach.] Distance from the closest point of approach over the 12-hour period (second panel). East velocity component (m s^{-1}) from the Workhorse 300 KHz shipboard ADCP (third panel) compared with east velocity component from the moored ADCP from the WHOTS-2 deployment for the same time (lower panel).

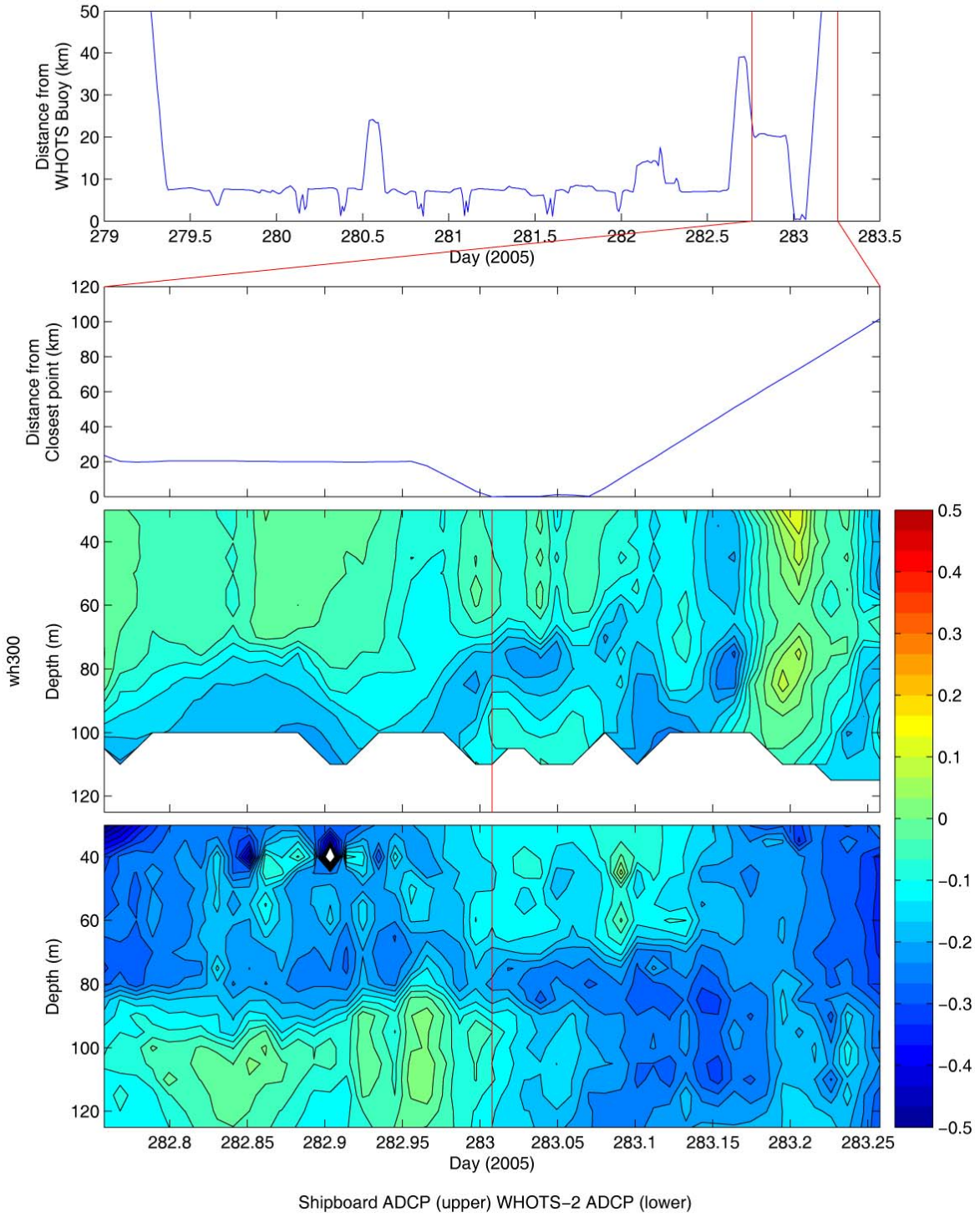

Figure 6-95 Distance of the ship from the WHOTS buoy using ARGOS position data for the duration of the cruise HOT-174 (top panel). [The red lines indicate a six-hour period either side of the closest point of approach.] Distance from the closest point of approach over the 12-hour period (second panel). North velocity component (m s^{-1}) from the Workhorse 300 KHz shipboard ADCP (third panel) compared with north velocity component from the moored ADCP from the WHOTS-2 deployment for the same time (lower panel).

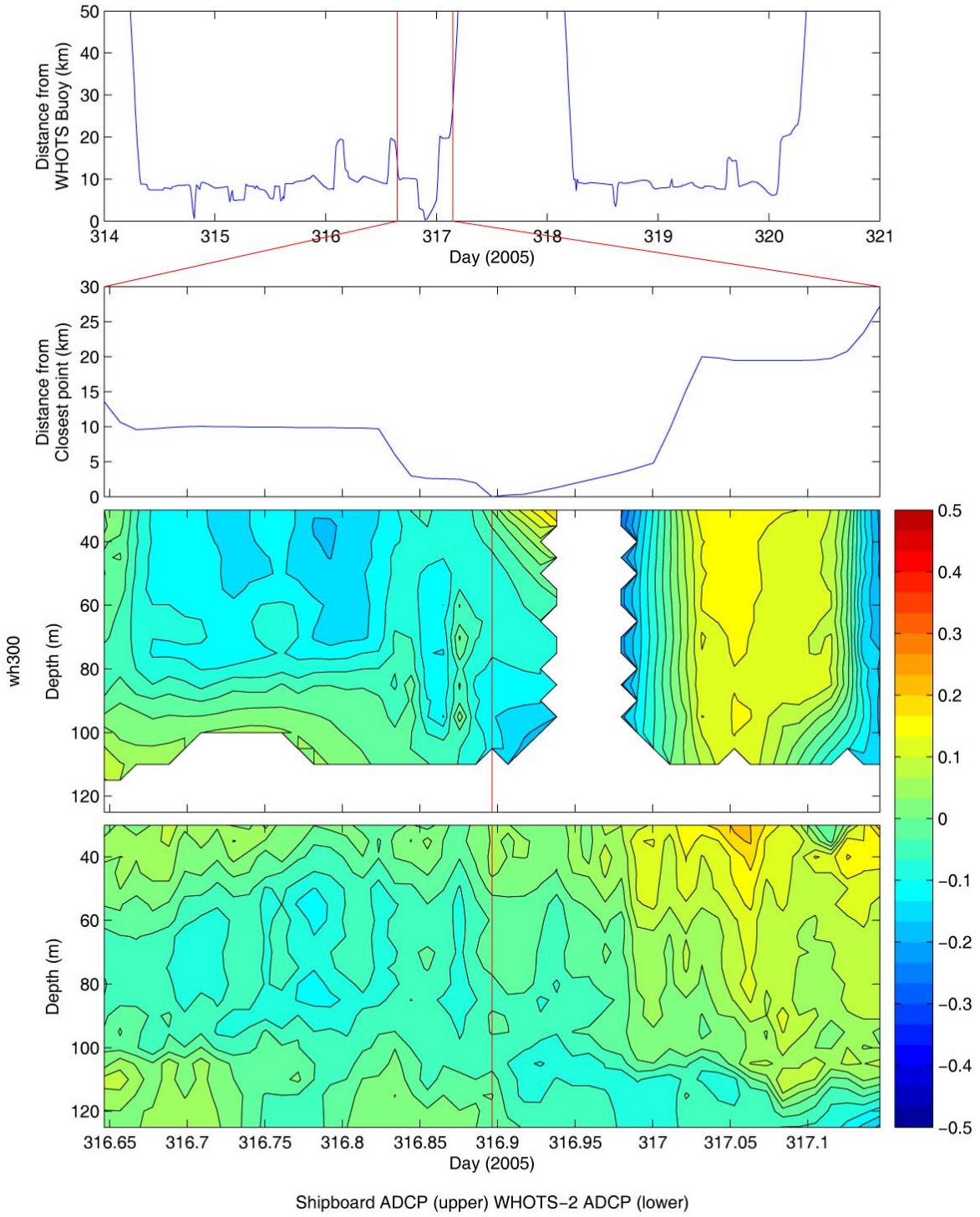

Figure 6-96. Distance of the ship from the WHOTS buoy using ARGOS position data for the duration of the cruise HOT-175 (top panel). [The red lines indicate a six-hour period either side of the closest point of approach.] Distance from the closest point of approach over the 12-hour period (second panel). East velocity component (m s^{-1}) from the Workhorse 300 KHz shipboard ADCP (third panel) compared with east velocity component from the moored ADCP from the WHOTS-2 deployment for the same time (lower panel).

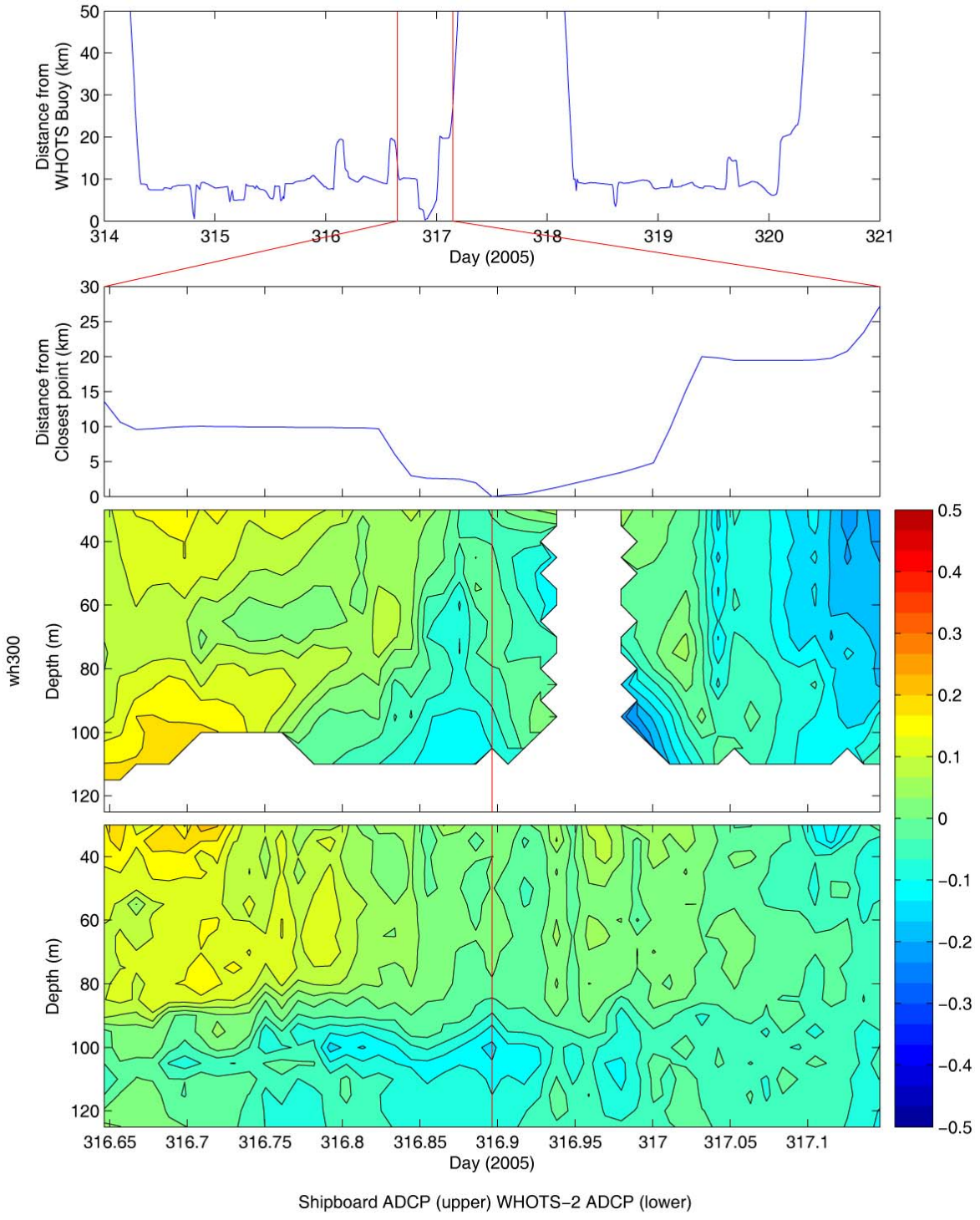

Figure 6-97. Distance of the ship from the WHOTS buoy using ARGOS position data for the duration of the cruise HOT-175 (top panel). [The red lines indicate a six-hour period either side of the closest point of approach.] Distance from the closest point of approach over the 12-hour period (second panel). North velocity component (m s^{-1}) from the Workhorse 300 KHz shipboard ADCP (third panel) compared with north velocity component from the moored ADCP from the WHOTS-2 deployment for the same time (lower panel).

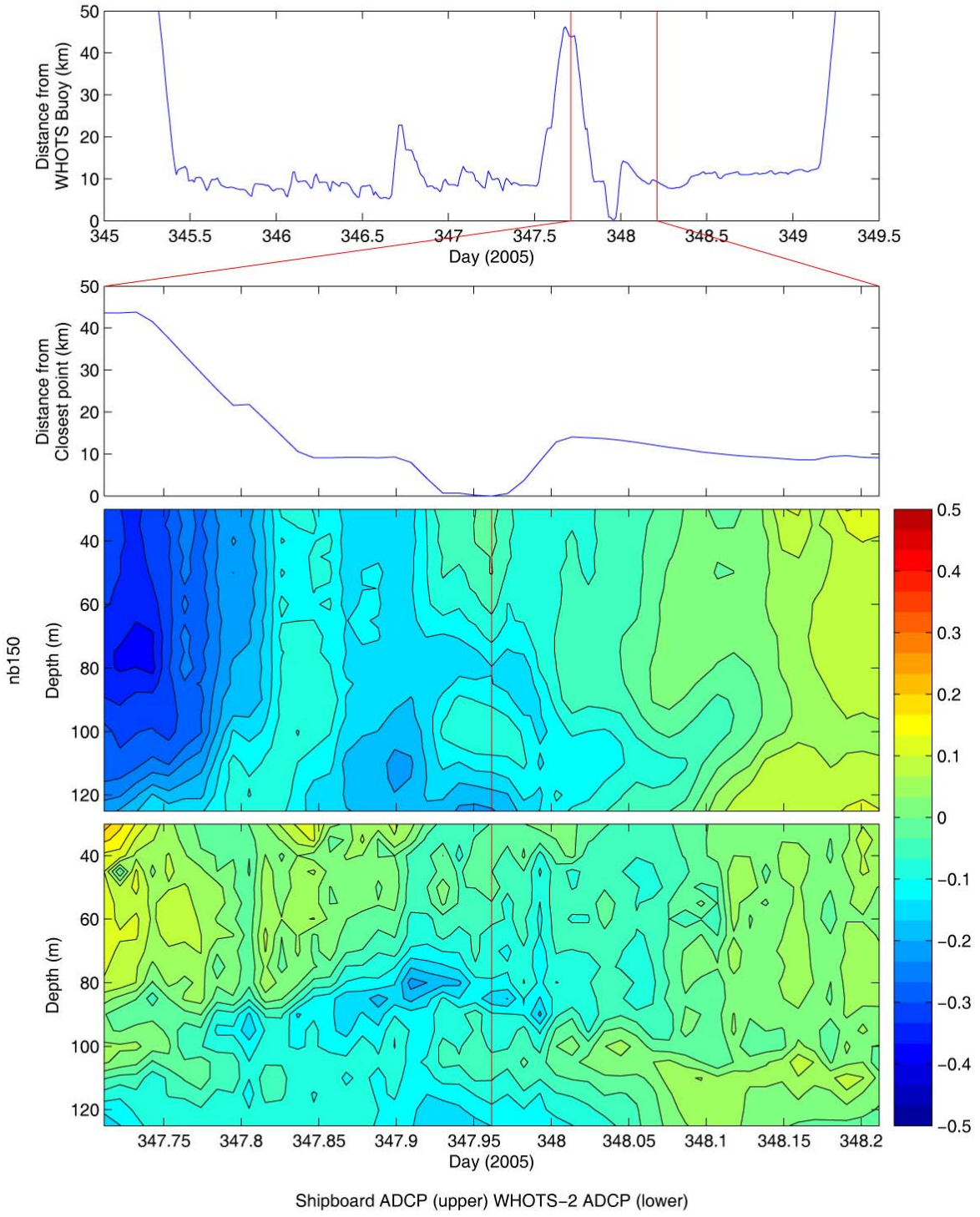

Figure 6-98. Distance of the ship from the WHOTS buoy using ARGOS position data for the duration of the cruise HOT-176 (top panel). [The red lines indicate a six-hour period either side of the closest point of approach.] Distance from the closest point of approach over the 12-hour period (second panel). East velocity component (m s^{-1}) from the Workhorse 300 KHz shipboard ADCP (third panel) compared with east velocity component from the moored ADCP from the WHOTS-2 deployment for the same time (lower panel).

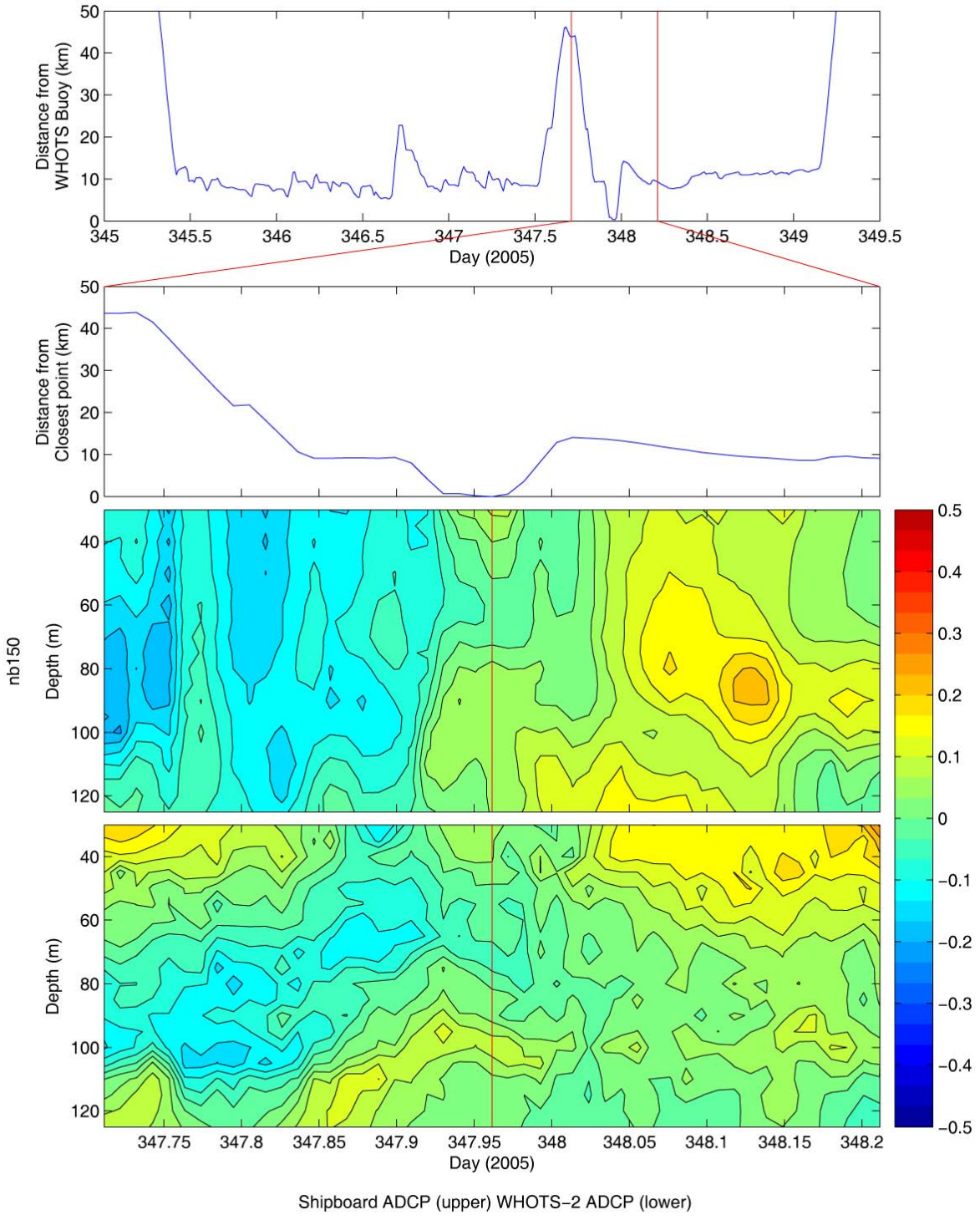

Figure 6-99. Distance of the ship from the WHOTS buoy using ARGOS position data for the duration of the cruise HOT-176 (top panel). [The red lines indicate a six-hour period either side of the closest point of approach.] Distance from the closest point of approach over the 12-hour period (second panel). North velocity component (m s^{-1}) from the Workhorse 300 KHz shipboard ADCP (third panel) compared with north velocity component from the moored ADCP from the WHOTS-2 deployment for the same time (lower panel).

F. Next Generation Vector Measuring Current Meter data (NGVM)

Timeseries of daily mean horizontal velocity components for the NGVM current meters deployed during WHOTS-1 and WHOTS-2 at 10 m and 30 m depth are presented in Figure 6-100.

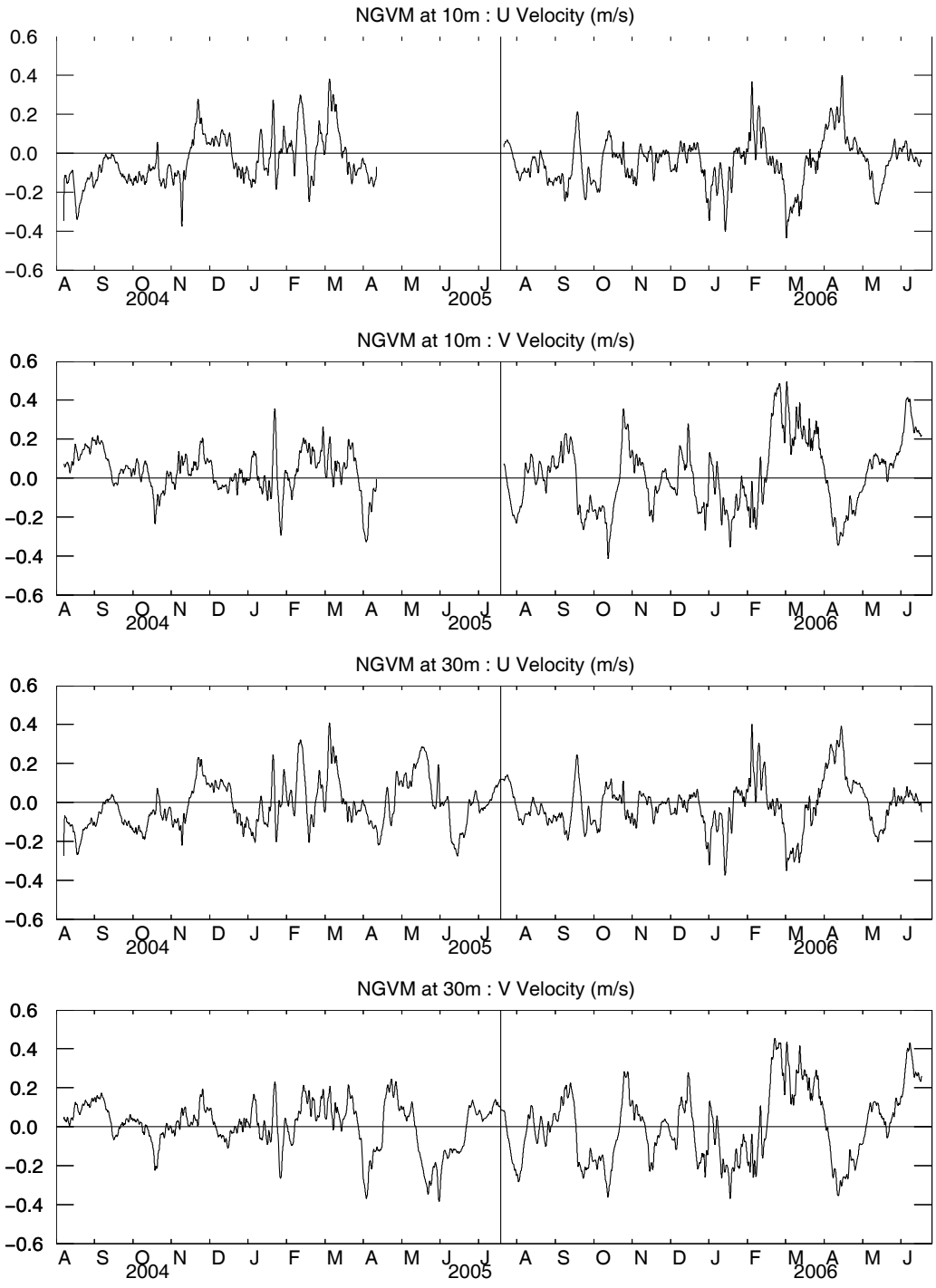

Figure 6-100 Horizontal velocity data (m/s) during WHOTS-1 and WHOTS-2 from the NGVMs at 10 m depth (first and second panel) and at 30 m depth (third and fourth panel).

G. GPS data

Timeseries of latitude and longitude of the WHOTS-1 and WHOTS-2 buoys from GPS data are presented in Figure 6-101 and Figure 6-102 respectively, and spectra of the two series are shown in Figure 6-103 and Figure 6-104.

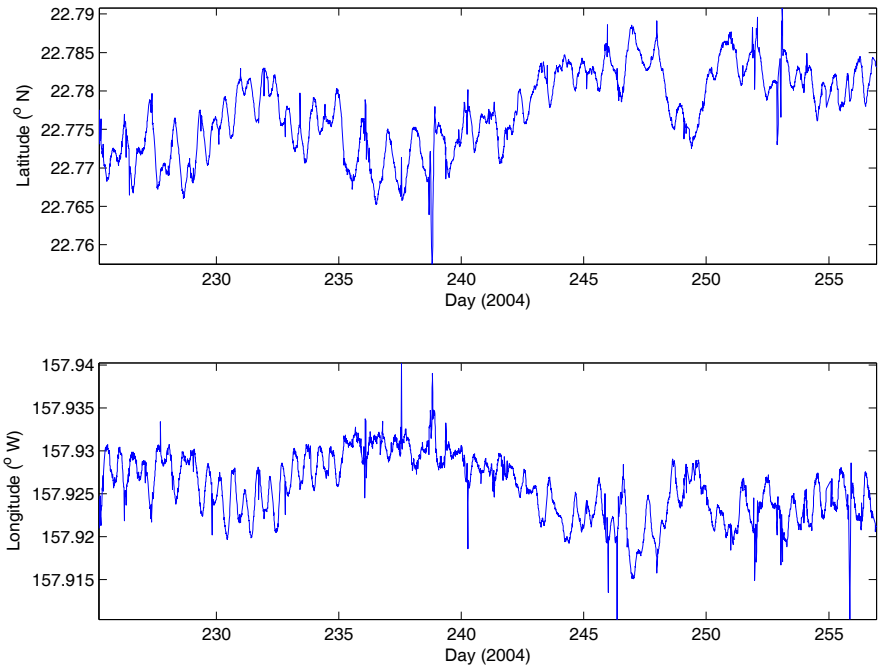

Figure 6-101 GPS Latitude (upper panel) and longitude (lower panel) time series from the WHOTS-1 deployment.

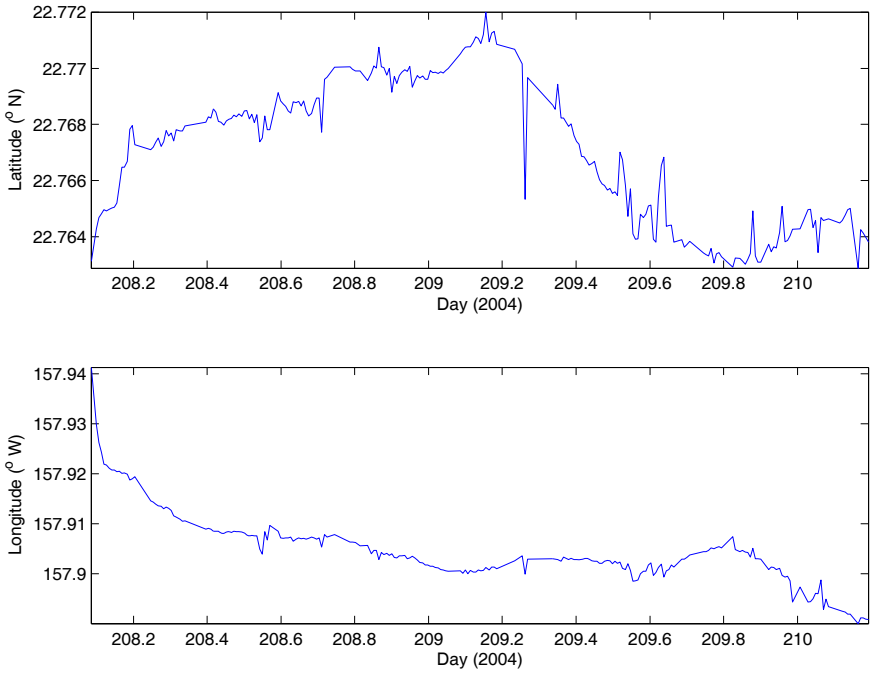

Figure 6-102 GPS Latitude (upper panel) and longitude (lower panel) time series from the WHOTS-2 deployment.

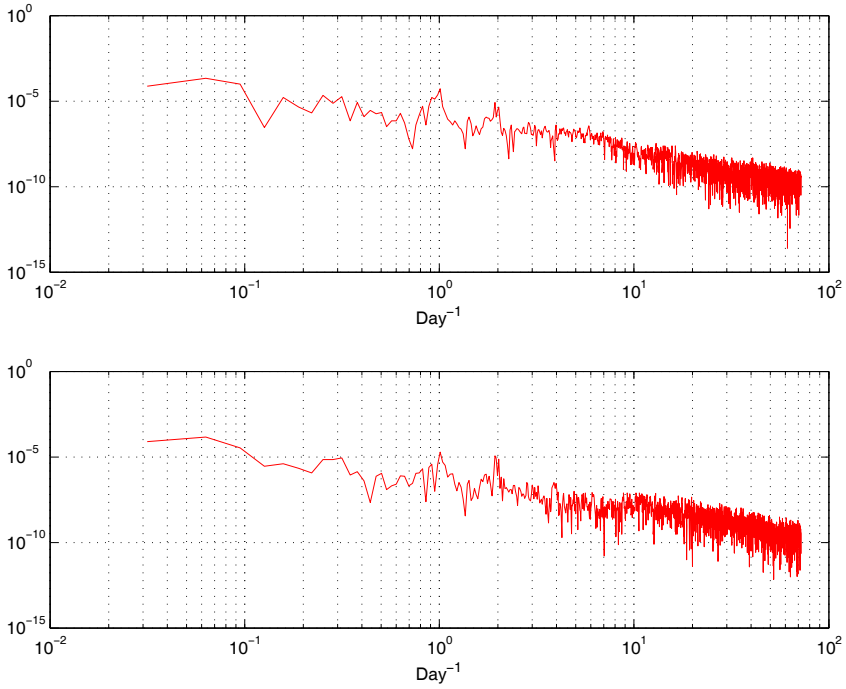

Figure 6-103. Power spectrum of latitude (upper panel) and longitude (lower panel) for the WHOTS-1 deployment.

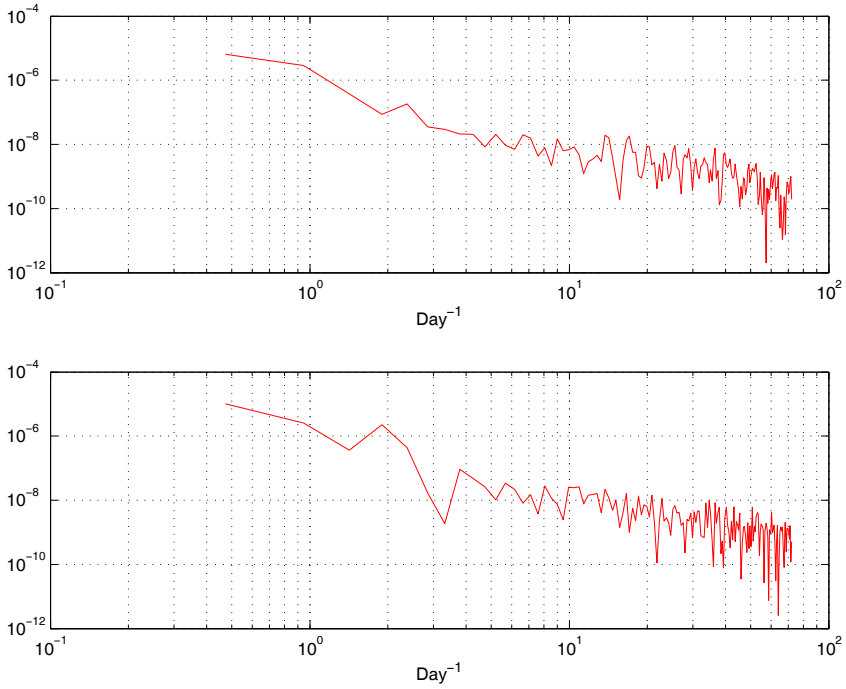

Figure 6-104. Power spectrum of latitude (upper panel) and longitude (lower panel) for the WHOTS-2 deployment.

H. Mooring Motion

The position of the mooring with respect to its anchor was determined from the ARGOS positions as shown in Section 5.D. Additional information of the mooring motion was provided by the MicroCATs pressures as shown in Section 5.A.2, and by the ADCP data of pitch, roll and heading, shown in this section.

Figure 6-105 shows the ADCP data of the instrument's tilt (a combination of the pitch and roll), plotted against the buoy's distance from its anchor (derived from ARGOS positions), for both WHOTS deployments. The red line in the plot is a quadratic fit to the median tilt calculated every 0.2 km distance bins. The figure shows that during both deployments, the ADCP tilt increased as the distance from the anchor increased. This tilting was caused by the deviation of the mooring line from its vertical position as it was pulled by the anchor. The tilting of the line also caused the rising of the instruments attached to the line, as indicated by the decrease in the MicroCATs' measured pressure (Figures 5.3 and 5.4, Section 5.A.2).

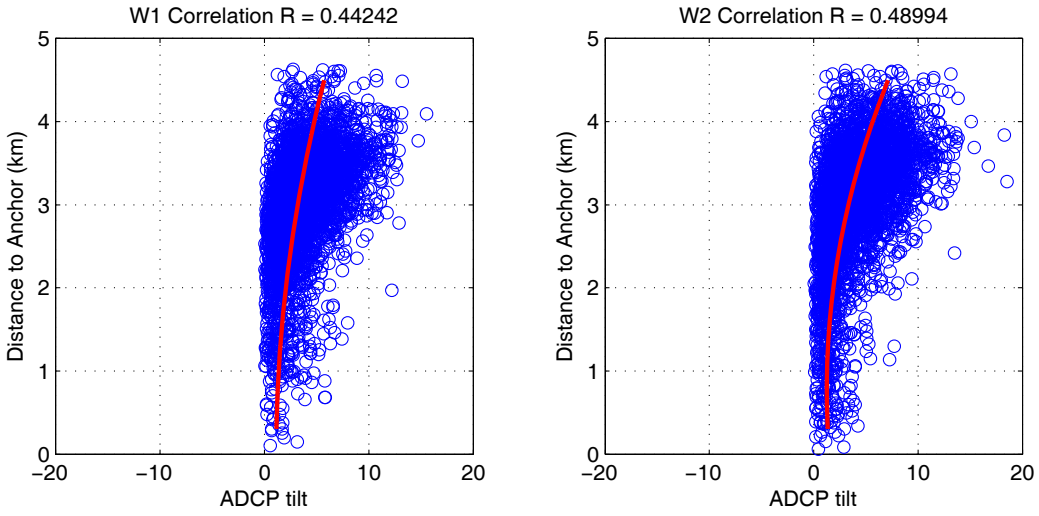

Figure 6-105. Scatter plots of ADCP tilt and distance of the buoy to its anchor for WHOTS-1 (left panel), and WHOTS-2 deployments (right panel, blue circles). The red line is a quadratic fit to the median tilt calculated every 0.2 km distance bins.

7. References

Firing, E., 1991. Acoustic Doppler Current Profiling measurements and navigation. In *WOCE Hydrographic Operations and Methods.* WOCE Operations Manual, WHP Office Report WHPO 91-1,WOCE Report No. 68/91, 144pp.

Fujieki et al., 2006. HOT-2005 report

Kara et al, 2000

Larson, N. and A.M. Pederson. 1996. Temperature measurements in flowing water: Viscous heating of sensor tips. 1st International Group for Hydraulic Efficiency Measurements (IGHEM) Meeting, Montreal, Canada, June 1996.

Lueck, R. G., 1990: Thermal inertia of conductivity cells: Theory. Journal of Atmospheric and Oceanic Technology, 7, 741-755.

Lueck, R. G. and Picklo, J. J., 1990: Thermal inertia of conductivity cells: Observations with a Sea-Bird cell. Journal of Atmospheric and Oceanic Technology, 7, 756-768.

Owens, W. B. and R. C. Millard, 1985: A new algorithm for CTD oxygen calibration. Journal of Physical Oceanography, 15, 621-631.

RD Instruments, 1996: Acoustic Current Doppler Profilers. Principles of Operation: A Practical Primer. Second Edition for Broadband ADCPs. 54 pp.

Santiago-Mandujano, F., L. Tupas, C. Nosse, D. Hebel, L. Fujieki, R. Lukas, D. Karl, 1999: Hawaii Ocean Time-series Data Report 10, 1998, School of Ocean and Earth Science and Technology, University of Hawaii, 99-5, 246 pp. In: R. Lukas and D. Karl, 1999. Hawaii Ocean Time-series. A Decade of Interdisciplinary Oceanography. SOEST. University of Hawaii CD-ROM.

Tupas, L., F. Santiago-Mandujano, D. Hebel, C. Nosse, L. Fujieki, E. Firing, R. Lukas, D. Karl, 1997: Hawaii Ocean Time-series Data Report 8, 1996, School of Ocean and Earth Science and Technology, University of Hawaii, 97-7, 296 pp.

UNESCO. 1981. Tenth Report of the Joint Panel on Oceanographic Tables and Standards. UNESCO Technical Papers in Marine Science, No. 36, UNESCO, Paris.

Plueddemann, A.J., R.A. Weller, R. Lukas, J. Lord, P.R. Bouchard, and M.A. Walsh, 2006, WHOI Hawaii Ocean Timeseries Station (WHOTS): WHOTS-2 Mooring Turnaround Cruise Repor**t,** Woods Hole Oceanographic Institution, Technical Report WHOI-2006-08, 68 pp.

Whelan S., R. Weller, R. Lukas, F. Bradley, J. Lord, J. Smith, F. Bahr, P. Lethaby, J. Snyder, 2007: WHOI Hawaii Ocean Timeseries Station (WHOTS): WHOTS-3 Mooring Turnaround

Cruise Report. Technical Report. Woods Hole Oceanographic Institution, WHOI-2007-03, 103 pp.

8. Appendices

A. Appendix 1: WHOTS-1 ADCP Configuration

File Size 37,717,943 bytes

Data Structure BB/WH/OS
Ensemble Length 748 bytes
Data Types 0000 0080 0100 0200 0300 0400

Firmware Version 16.21

System Frequency 307.2 kHz
Convex
Sensor Configuration #1
Transducer Head Attached TRUE
Orientation UP
Beam Angle 20 Degrees
Transducer 4 Beam Janus

Real Data

CPU Serial Number: 63 00 00 03 87 A5 E4 09

High Power (CQ) 0
Trigger (CX) 0

False Target(WA) 70 counts
Band Width (WB) 0
Cor. Thres. (WC) 64 counts
Err Thres. (WE) 2000 mm/s
Blank (WF) 1.76 m
Min PGood (WG) 0
Ref Layer (WL) 1, 5 first bin, last bin
Mode (WM) 1
Bins (WN) 30
Pings/Ens (WP) 40
Bin Size (WS) 4.00 m

Head Align (EA) 0.00 degrees
Head Bias (EB) 10.25 degrees
Coord Xform (EX) 11111 Earth Coordinates Using Tilts, 3 Beam Solutions, and Bin Mapping
Sens Source (EZ) 1111101 cdhprst
Sens Avail 0011101 cdhprst

Time/Ping (TP) 00:04.00

Hardware 4 Beams
Lag 53 elements
Code Reps. 9
Lag Length 0.49 m
Xmt Length 4.40 m
1st Bin 6.21 m

BT Pings/Ens (BP) 0
BT Ens Delay (BD) 0
BT Cor.Thres. (BC) 0 counts
BT Eval. Thres. (BA) 0 counts
BT PG Thres. (BG) 0
BT Mode (BM) 0
BT Err Thres. (BE) 0 mm/s
BT Max Range (BX) 0 dm

First Ensemble 00000001 04/08/10 00:00:00.00
Last Ensemble 00050414 05/07/26 02:10:00.00
Extra Data in File 8,271 bytes
NVRAM Data Set TRUE

B. Appendix 2: WHOTS-2 ADCP Configuration

File Size 35,981,087 bytes

Data Structure BB/WH/OS
Ensemble Length 748 bytes
Data Types 0000 0080 0100 0200 0300 0400

Firmware Version 16.21

System Frequency 307.2 kHz
Convex
Sensor Configuration #1
Transducer Head Attached TRUE
Orientation UP
Beam Angle 20 Degrees
Transducer 4 Beam Janus

Real Data

CPU Serial Number: 63 00 00 03 87 A5 E4 09

High Power (CQ) 0
Trigger (CX) 0

False Target(WA) 50 counts
Band Width (WB) 0
Cor. Thres. (WC) 64 counts
Err Thres. (WE) 2000 mm/s
Blank (WF) 1.76 m
Min PGood (WG) 0
Ref Layer (WL) 1, 5 first bin, last bin
Mode (WM) 1
Bins (WN) 30
Pings/Ens (WP) 40
Bin Size (WS) 4.00 m

Head Align (EA) 0.00 degrees

Head Bias   (EB) 0.00 degrees
Coord Xform (EX) 11111 Earth Coordinates Using Tilts, 3 Beam Solutions, and Bin Mapping
Sens Source (EZ) 1111111 cdhprst
Sens Avail   0011101 cdhprst

Time/Ping   (TP) 00:15.00

Hardware   4 Beams
Lag   53 elements
Code Reps. 9
Lag Length 0.50 m
Xmt Length 4.43 m
1st Bin   6.23 m

BT Pings/Ens   (BP) 0
BT Ens Delay   (BD) 0
BT Cor.Thres.   (BC) 0 counts
BT Eval. Thres. (BA) 0 counts
BT PG Thres.   (BG) 0
BT Mode   (BM) 0
BT Err Thres.   (BE) 0 mm/s
BT Max Range   (BX) 0 dm

First Ensemble 00000001 05/07/27 03:50:00.00
Last Ensemble 00048092 06/06/26 03:00:00.00
Extra Data in File 8,271 bytes
NVRAM Data Set TRUE

C. Appendix 3: WHOTS-1 NGVM report

WHOI NGVM deployment on WHOTS 1
Lara Hutto, Upper Ocean Processes Group, WHOI

1. Overview

Two WHOI Next Generation Vector Measuring Current Meters (NGVMs) were deployed on the first setting of the Hawaii Ocean Reference Station moorings (WHOTS 1) in support of Dr. Roger Lukas of the University of Hawaii. The Upper Ocean Processes Group (UOP) at WHOI prepared these instruments prior to deployment, and processed the data after recovery. This is a brief report on the preparation of the instruments, on the data processing, and on the data recovered. Data can be downloaded by accessing the following FTP site:

hostname: ftp.whoi.edu
username: anonymous
password: user's email address
ftp> cd pub/users/lhutto/WHOTS1

2. Pre-deployment and post-recovery procedures

Prior to deployment, the temperature pods were calibrated in the UOP calibration lab on April 15, 2004. VMTPOD 012 had a fit of ±0.0098 °C, and VMTPOD 019 had a fit of ±0.00588 °C. In addition, the current meters' compasses were checked. NGVM 012 was found to have an

average offset of 2.3 degrees, and NGVM 019 was found to have an average offset of 0.4 degrees.

The current meters came on deck in good condition with minimal fouling and no signs of damage. Figures 1 and 2 show the fouling present on the NGVMs after recovery.

Figure 1. Close-up of fouling present on NGVM 012 after recovery.

Figure 2. Close-up of fouling on NGVM 019 after recovery.

The accuracy of the time base of the data records was checked by applying data spikes at recorded times and checking the logged time versus the actual time. These spikes for NGVMs are quick spins of the propeller sensors amidst a period when the propellers are rubber banded to keep them from rotating. Data spikes were completed prior to deployment and after recovery. The timing spikes were shown to be aligned, and no time correction was needed for these

instruments.

3. Processing

In processing the current meter data a magnetic deviation of 10.1833 degrees has been applied to provide direction relative to true north.

NGVM 012 (at 10 m) had a short record, and failed on April 18, 2004. A complete diagnosis for this failure has not yet been determined, but a low voltage was measured when the instrument was recovered. NGVM 019 (at 30 m) recorded for the entire deployment period. Table 1 shows the start and stop times for the raw records, deployment and recovery times, and times the processed file was truncated to. The file is truncated to slightly after deployment time, to allow for the time it takes for the mooring anchor to settle.

Table 1. NGVM Record Times.

Raw File Start and Stop Times	05-Aug-2004 20:29:00 18-Apr-2005 05:15:00
Deployment and Recovery Times	13-Aug-2004 02:40 25-Jul-2005 17:15
Processed File Start and Stop Times	13-Aug-2004 03:40:00 18-Apr-2005 05:15:00 (NGVM 012) 25-Jul-2005 17:15:00

4. Results

Figure 3 shows the two sets of current meter data compared, as well as temperature data from the two current meters and the SST instrument compared. No data quality issues are apparent. Differences are believed to be due to shallow warming events and stratification.

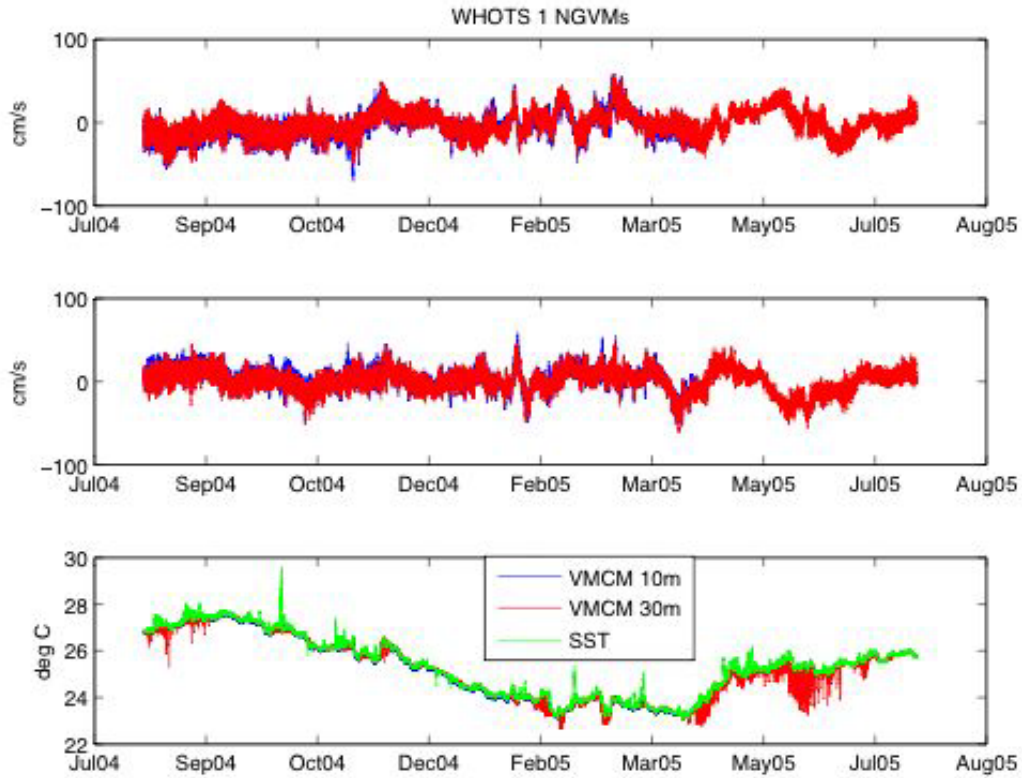

Figure 3. WHOTS 1 NGVM data overview.

The progressive vector diagram for the 10 and 30 m NGVMs are plotted in Figure 4. Note that some of the difference is due to the different record length.

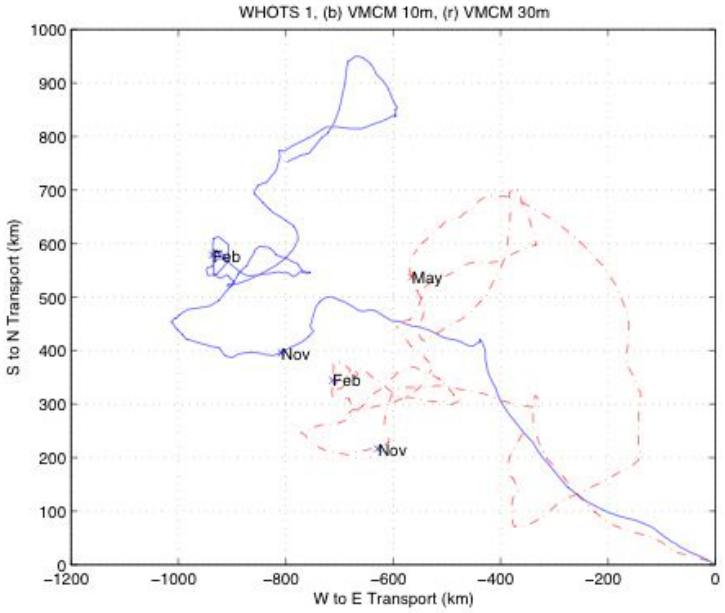

Figure 4. Progressive Vector Diagram.

The 10 m mean current is stronger to the NW than that at 30 m. We believe the difference to be real, evidence of wind-driven surface flow. In support of that, the monthly mean wind vectors have been overplotted with 1-day averages every 7 days on a progressive vector diagram of the difference velocity (U(10 m) - U(30 m)) in Figure 5.

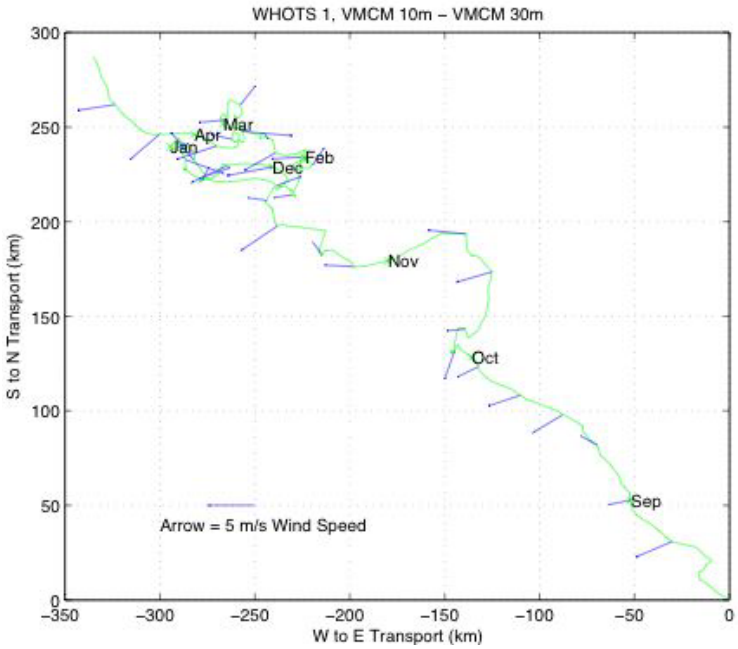

Figure 5. Progressive vector diagram with winds.

4. Further information
For any further information please contact Lara Hutto at lhutto@whoi.edu or (508) 566-9248.

D. Appendix 4: Waimea Buoy

Waimea buoy data:

Most recent location:
21° 40.36' N 158° 6.95' W (21.6727 N -158.1158 W)
"approximately 5 miles W of Sunset Beach"

Instrument description: Datawell directional buoy

Most recent water depth (MLLW):
200 m (656 ft, 109 fm)

Measured parameters: wave energy, wave direction, sea temperature
NDBC identifier: 51201

Data available from Coastal Data Information Program (CDIP) web site:
http://cdip.ucsd.edu/?units=metric&tz=UTC&pub=public&map_stati=1,2,3
Station ID: 106

Buoy maintained by UH Sea Level Center.